AD-A067 547 MCDONNELL DOUGLAS ASTRONAUTICS CO ST LOUIS MO F/G 17/9
EXPLORATORY DEVELOPMENT OF RESONANT METAL RADOMES.(U)
JUL 78 W R BUSHELLE, L C HOOTS F33615-76-C-5157
UNCLASSIFIED AFML-TR-78-106 NL

1 OF 3
ADA
067547

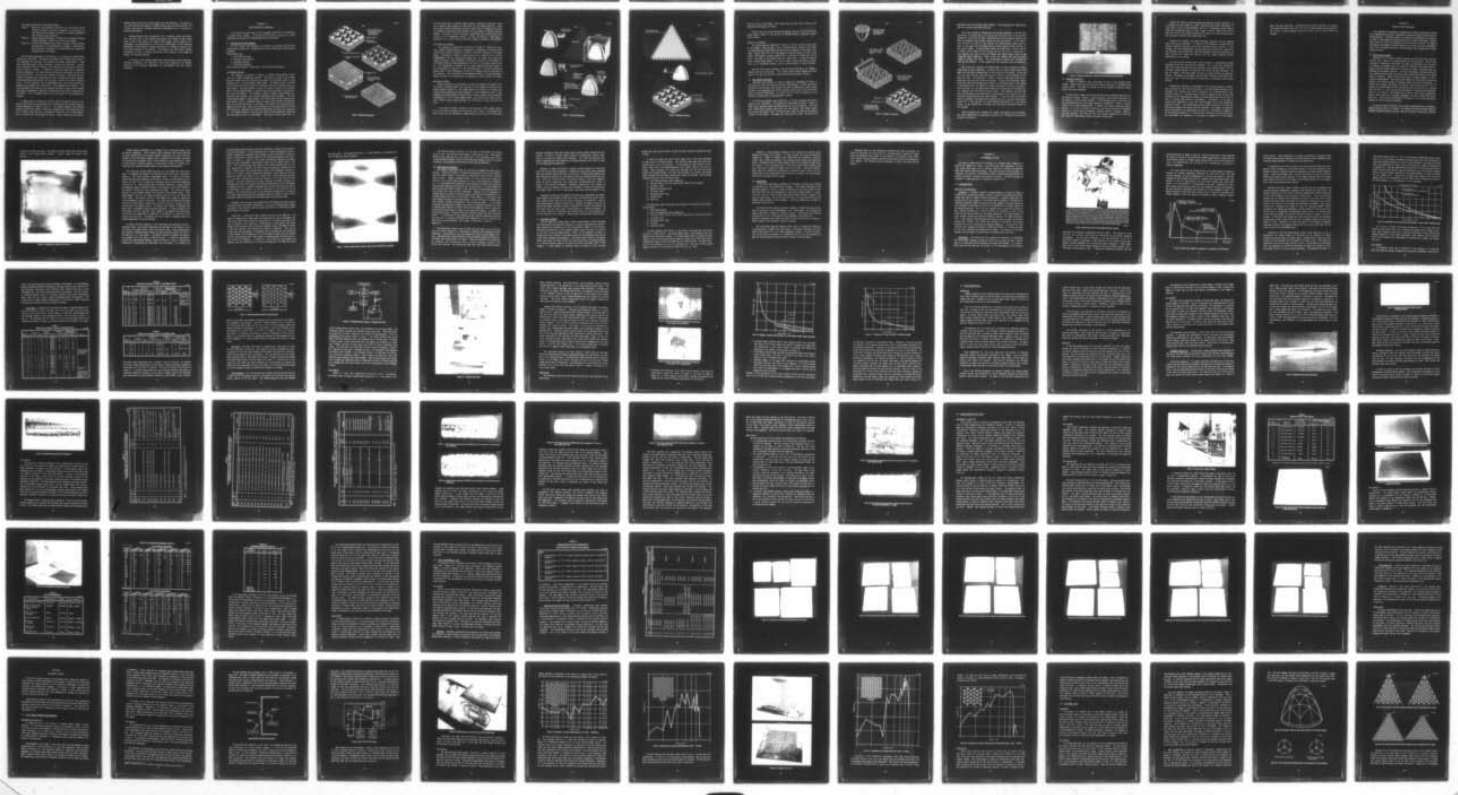

AFML-TR-78-106

LEVEL II

EXPLORATORY DEVELOPMENT OF RESONANT METAL RADOMES

MCDONNELL DOUGLAS ASTRONAUTICS COMPANY-ST. LOUIS DIVISION
St. Louis, Missouri 63166
(314) 232-0232

JULY 1978

FINAL REPORT

1 JUNE 1976 – 31 MARCH 1978

AIR FORCE MATERIALS LABORATORY
AIR FORCE WRIGHT AERONAUTICAL LABORATORIES
AIR FORCE SYSTEMS COMMAND
WRIGHT PATTERSON AIR FORCE BASE, OHIO 45433

NOTICE

When Government drawings,, specifications, or other data are used for any purpose other than in connection with a definitely related Government procurement operation, the United States Government thereby incurs no responsibility nor any obligation whatsoever; and the fact that the government may have formulated, furnished, or in any way supplied the said drawings, specifications, or other data, is not to be regarded by implication or otherwise as in any manner licensing the holder or any other person or corporation, or conveying any rights or permission to manufacture, use, or sell any patented invention that may in any way be related thereto.

This technical report has been reviewed and is approved for publication.

Robert M. Van Vliet

ROBERT M. VANVLIET, Project Engineer
Laser Hardened Materials Branch
Electromagnetic Materials Division

Gary L. Denman

GARY L. DENMAN, Program Manager
Laser Hardened Materials Branch
Electromagnetic Materials Division

FOR THE COMMANDER

R. E. Brocklehurst

ROBERT E. BROCKLEHURST
Chief
Electromagnetic Materials Division

"If your address has changed, if you wish to be removed from our mailing list, or if the addressee is no longer employed by your organization, please notify AFML/LPJ, W-PAFB, OH 45433 to help us maintain a current mailing list."

Copies of this report should not be returned unless return is required by security considerations, contractual obligations, or notice on a specific document.

AIR FORCE/56780/2 April 1979 — 200

Unclassified

SECURITY CLASSIFICATION OF THIS PAGE (When Data Entered)

REPORT DOCUMENTATION PAGE

READ INSTRUCTIONS BEFORE COMPLETING FORM

1. REPORT NUMBER: AFML-TR-78-106	2. GOVT ACCESSION NO.
3. RECIPIENT'S CATALOG NUMBER: Rept.	
4. TITLE (and Subtitle): EXPLORATORY DEVELOPMENT OF RESONANT METAL RADOMES.	5. TYPE OF REPORT & PERIOD COVERED: Final 1 Jun 76-31 Mar 78
	6. PERFORMING ORG. REPORT NUMBER
7. AUTHOR(s): William R. Bushelle, MDAC-St. Louis L. Clyde Hoots, Brunswick Corp.	8. CONTRACT OR GRANT NUMBER(s): F33615-76-C-5157
9. PERFORMING ORGANIZATION NAME AND ADDRESS: McDonnell Douglas Astronautics Company-St. Louis P.O. Box 516 St. Louis, Missouri 63166	10. PROGRAM ELEMENT, PROJECT, TASK AREA & WORK UNIT NUMBERS: 7371 01-57
11. CONTROLLING OFFICE NAME AND ADDRESS: Air Force Materials Laboratory (LPJ) Wright-Patterson AFB, Ohio 45433	12. REPORT DATE: July 1978 13. NUMBER OF PAGES: 218
14. MONITORING AGENCY NAME & ADDRESS (if different from Controlling Office): 219p.	15. SECURITY CLASS. (of this report): Unclassified 15a. DECLASSIFICATION/DOWNGRADING SCHEDULE

16. DISTRIBUTION STATEMENT (of this Report)
Approved for public release; distribution unlimited.

17. DISTRIBUTION STATEMENT (of the abstract entered in Block 20, if different from Report)

62102F

18. SUPPLEMENTARY NOTES

19. KEY WORDS (Continue on reverse side if necessary and identify by block number)
Resonant Metal Radome, radome, metallic radome, slotted metallic radome, antenna window, lightning strike protection, rain erosion, precipitation static, radome fabrication, photofabrication, phototransparency

20. ABSTRACT (Continue on reverse side if necessary and identify by block number)

The results of an exploratory development program conducted for the Air Force Materials Laboratory to define, develop, and demonstrate a slotted metal coating for radomes are reported. In this program a number of approaches for fabricating a metallic radome were defined. Of these approaches, three were developed and evaluated.

The evaluation considered environmental resistance, electrical performance and economic factors. The following environmental tests were performed which

Cover

DD FORM 1 JAN 73 1473 EDITION OF 1 NOV 65 IS OBSOLETE

Unclassified

SECURITY CLASSIFICATION OF THIS PAGE (When Data Entered)

ABSTRACT (continued)

demonstrate the feasibility of building a flightworthy resonant metal radome: lightning and rain erosion resistance, precipitation static reduction, temperature/humidity/altitude cycling, corrosion and solvent resistance, and sunshine exposure.

Flat panels were fabricated and tested for microwave performance. Transmission efficiencies of 87% were achieved without a rain erosion coating and 84% with the rain erosion coating. Results indicate that optimization of the wall design may yield better performance than achieved in this program. A hybrid fabrication method utilizing two of the approaches developed was selected for fabricating two demonstration radomes. The overall average transmission efficiency of the demonstration radomes was 77% at resonance (8.875 GHz). There was a 2.8 dB increase in the sidelobe levels for the H-plane and a 5.3 dB increase for the E-plane over the free-space levels for the antenna alone. Maximum boresight errors at resonance were 7 to 10 milliradians.

The electrical performance of the demonstration radomes agreed well with the results of the flat-panel tests. Average transmission of the two radomes was equal (to within approximately 3%) to that of the flat panel which incorporated the same slot pattern used on the radomes, at all three test frequencies. This degree of conformance indicates that the compromises necessary to adapt a periodic array to a double curved radome can be tolerated. Ninety percent overall average transmission is seen as readily achievable with an optimized design.

Additional work is recommended in the area of improved analytical methods for the design of resonant metal radomes as well as continued effort in the refinement of fabrication methods which are not constrained to the utilization of existing radome substrates.

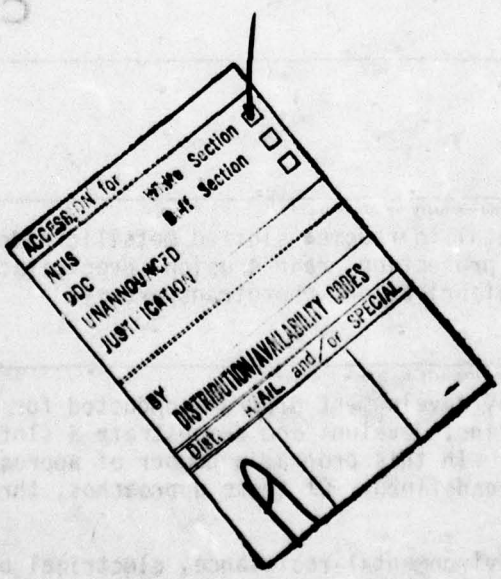

PREFACE

This final report summarizes the work performed under Contract F33615-76-C-5157 "Exploratory Development of Resonant Metal Radomes," from 1 June 1976 through 31 March 1978.

The program was conducted by the McDonnell Douglas Astronautics Company-St. Louis, St. Louis, Missouri and the Brunswick Corporation, Marion, Virginia (under subcontract) and was initiated under Project Number 7371. The work was administered under the technical direction of Mr. Robert M. Van Vliet AFML/LPO, Electromagnetic Materials Division, Air Force Materials Laboratory, Air Force Systems Command, Wright Patterson Air Force Base, Ohio, 45433. The program at the McDonnell Douglas Astronautics Company-St. Louis (MDAC-St. Louis) was under the supervision of Mr. William R. Bushelle, Program Manager.

The authors wish to acknowledge the efforts of the following personnel who contributed to the successful completion of this program: Mr. G. F. Schmitt of the Air Force Materials Laboratory for conducting the rain erosion testing; Prof. B. A. Munk of the Ohio State University ElectroScience Laboratory for consultation and guidance in the area of electrical design; Messrs. C. R. Scott, J. Z. Catron and the laboratory personnel of the Brunswick Corporation for laboratory support; Messrs. J. M. Bennett, D. L. Boaz, D. Favignano, W. D.Fortenberry and R. B. Thomas of the McDonnell Douglas Electronics Company for preparing phototransparencies and for photofabrication of specimens; Messrs. H. M. Kesser, E. Malakelis, M. B. Munsell and E. H. Shulte of the McDonnell Aircraft Company for laboratory support.

The authors also wish to acknowledge the efforts of the following MDAC-St. Louis personnel: Messrs. J. D. Lee, W. E. Mathews, D. B. Pickett, and T. R. Berkel for laboratory support; Ms. D. Y. Wilson and Mrs. S. A. Schoen for administration; Messrs. A. R. Brown and D. L. Kummer for functional management and technical consultation, Mr. D. C. Ruhmann for critically reviewing the text, and Mr. B. H. Emmons for coordinating preparation of this report.

TABLE OF CONTENTS

LIST OF ILLUSTRATIONS

LIST OF ILLUSTRATIONS (Continued)

LIST OF ILLUSTRATIONS (Continued)

LIST OF ILLUSTRATIONS (Continued)

LIST OF TABLES

SECTION I

INTRODUCTION AND SUMMARY

Although the concept of resonant metal radomes is not new, there has been renewed interest in their study because of their potential for overcoming disadvantages inherent in conventional radomes, such as susceptibility to lightning damage and static charge build-up. Also, a resonant metal radome offers electromagnetic pulse (EMP)/electromagnetic interference (EMI) attenuation. Finally, the resonant metal radome concept affords the radome designer a new set of design options not available with conventional radomes. For example, the potential exists that metallic radome designs may be a solution to the radome problems associated with hypersonic flight, such as rain erosion and thermal shock, or the solution to future design requirements such as laser hardening and IR signature reduction. All of this translates to improved survivability and penetration capability for military aircraft and missiles, and improved safety for all aircraft.

The resonant metal radome concept was most successfully demonstrated by E. L. Pelton of Ohio State University (OSU), in a study funded by the Air Force Avionics Laboratory (Reference 1). This study showed that excellent electrical performance was achievable from resonant metal surfaces in a conical shape. Pelton employed a periodic slotted metallic surface of novel design, developed by extending the work of Munk and Mentzer (References 2 through 5). The OSU radome was constructed of thin copper clad circuit board material and did not address the difficulties associated with building a flightworthy radome. Fabrication of a slotted metal surface on a compound curvature or the problems of obtaining adequate adhesion of the metal coating to a substrate of sufficient strength to resist the rigorous environments encountered in flight were not addressed in the OSU study.

The solution of these problems was the logical next step in the development of a resonant metal radome and was the objective of this program.

The program consisted of three major phases:

Phase I - Materials and Processes Selection and Evaluation, which included a study of materials, processes, and approaches for fabrication of the radomes in addition to process development and specimen level evaluation.

Phase II - Coating System Development, in which the selected system was further developed, refined, and electrically tested.

Phase III - Scale-Up and Demonstration, which included process scale-up and fabrication of two demonstration radomes. Additionally, the electrical performance of the demonstration radomes was characterized in this phase.

Four distinct approaches for fabrication of a flightworthy resonant metal radome were identified. Preliminary development work revealed that three of the approaches had potential for meeting the program requirements. These three approaches were further developed, refined, and evaluated. Testing, which simulated flight environments, was conducted to characterize the performance of metallic radomes. In addition, these tests were used to determine material parameters, i.e., metal and erosion coating thicknesses for this program specifically. The testing conducted included: lightning and rain erosion resistance tests, precipitation static susceptibility tests, temperature/humidity/altitude cycling, and corrosion, solvent and sunshine exposure tests. At the completion of the development work and testing program an approach was selected for fabrication of the demonstration radomes. Flat panel specimens were made by the selected fabrication method and microwave performance measurements conducted to characterize electrical performance of the panels. This information was used in the design of the demonstration radomes.

A radome used on a modern jet aircraft which has both military and commercial applications, was selected to be covered with the slotted metallic coating developed in Phases I and II. The radome selected, the Lockheed Jetstar (C-140) nose radome, utilizes an A-sandwich type wall construction and has a rounded shape that was a challenge to metallize. Two of these demonstration radomes were fabricated and tested. Power transmission efficiency,

antenna pattern distortion, and boresight error were measured. The results of this work indicate that metallic radomes exhibit good near-term potential for aircraft applications, although additional development work is required to optimize performance.

Average one-way power transmission (all incidence angles) was nearly 78%, and while this is not optimum performance, the radomes do work (radar range is 95% of the range of the unmetallized radome), and the potential for improvement was demonstrated in other tests accomplished in this program. Performance of 85% overall average transmission is probably achievable with only minor redesign of the coating. The potential for 90% overall average transmission is seen as readily achievable, with redesign of the radome to account for the metal coating.

In addition, the radomes demonstrated precipitation static reduction, lightning resistance, and significant out-of-band attenuation for EMP/EMI protection, while meeting requirements for environmental and rain erosion resistance.

SECTION II

IDENTIFICATION OF APPROACHES

This section describes each of four approaches identified for fabricating a resonant metal radome. In addition, preliminary evaluation of these approaches and selection of coating materials are discussed.

2.1 DESCRIPTION OF EACH APPROACH

For this study, four methods for providing an adherent and uniform slotted metal coating for a representative aircraft radome were identified and evaluated.

These methods were:

- o Electroform Approach
- o Plate and Etch Approach
- o Wallpaper Approach
- o Raised Slot Approach

Each of these approaches is described in the following paragraphs.

ELECTROFORM APPROACH

This approach, illustrated in Figure 1, involves electroforming a metal shell in a female planographic mandrel. The mandrel is made of metal which has been etched with the required slot pattern to some depth short of etch through, and is in the required radome shape. The etched pattern is filled with a dielectric material such as a silicone or Teflon to prevent plating in those areas. The metal mandrel is made of a metal dissimilar to the metal which is to be electroformed, in order to achieve easy release of the electroform from the mandrel. For instance, nickel or copper electroformed on a stainless steel mandrel can be easily separated from the mandrel. The completed female mandrel is then placed in the plating bath and the interior surface plated, using a conformal anode to assure even current distribution. When the correct thickness is attained, the mandrel and electroform are removed from the bath. Metal will not deposit on the areas which are filled with dielectric, therefore the completed electroform has the slots formed in it. The radome substrate is now laid up inside the electroformed slotted dome while the dome is still in the mandrel. The epoxy or other binder flows in

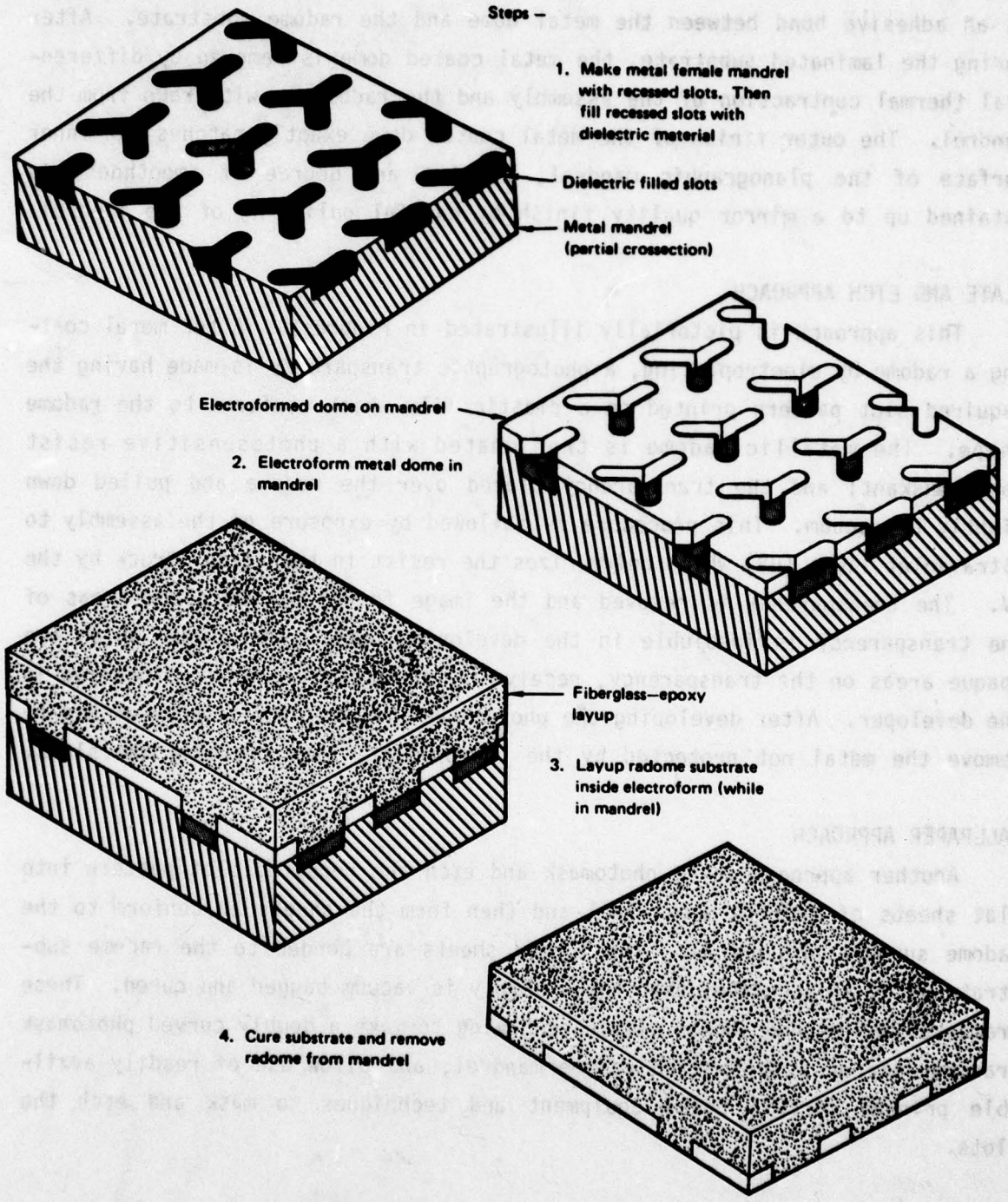

Figure 1 Electroform approach

and fills the slots in the metal dome providing a mechanical interlock as well as an adhesive bond between the metal dome and the radome substrate. After curing the laminated substrate, the metal coated dome is removed by differential thermal contraction of the assembly and the radome is withdrawn from the mandrel. The outer finish of the metal coated dome exactly matches the inner surface of the planographic mandrel, so that any degree of smoothness is obtained up to a mirror quality finish by careful polishing of the mandrel.

PLATE AND ETCH APPROACH

This approach is pictorially illustrated in Figure 2. After metal coating a radome by electroplating, a photographic transparency is made having the required slot pattern printed on a plastic film which conforms to the radome shape. The metallic radome is then coated with a photosensitive resist (photomaskant) and the transparency placed over the radome and pulled down tightly by vacuum. This procedure is followed by exposure of the assembly to ultraviolet light (UV) which polymerizes the resist in the areas struck by the UV. The transparency is removed and the image formed by the clear areas of the transparency is insoluble in the developing bath. The slots, which are opaque areas on the transparency, receive no UV exposure and are dissolved in the developer. After developing the photomasked radome, it is spray-etched to remove the metal not protected by the photoresist, thus creating the slots.

WALLPAPER APPROACH

Another approach is to photomask and etch the required slot pattern into flat sheets of ductile metal foil and then form the sheets to conform to the radome surface (Figure 3). The formed sheets are bonded to the radome substrate using an adhesive, then the assembly is vacuum bagged and cured. These premasked and etched sheets eliminate having to make a doubly curved photomask transparency or a full sized radome mandrel, and allow use of readily available printed circuit board equipment and techniques to mask and etch the slots.

If the sheets are small, relative to the curvature of the radome, distortion of the slots by forming will be minimal, and in fact, it was demonstrated that forming was not required for sheets which are applied to the areas away

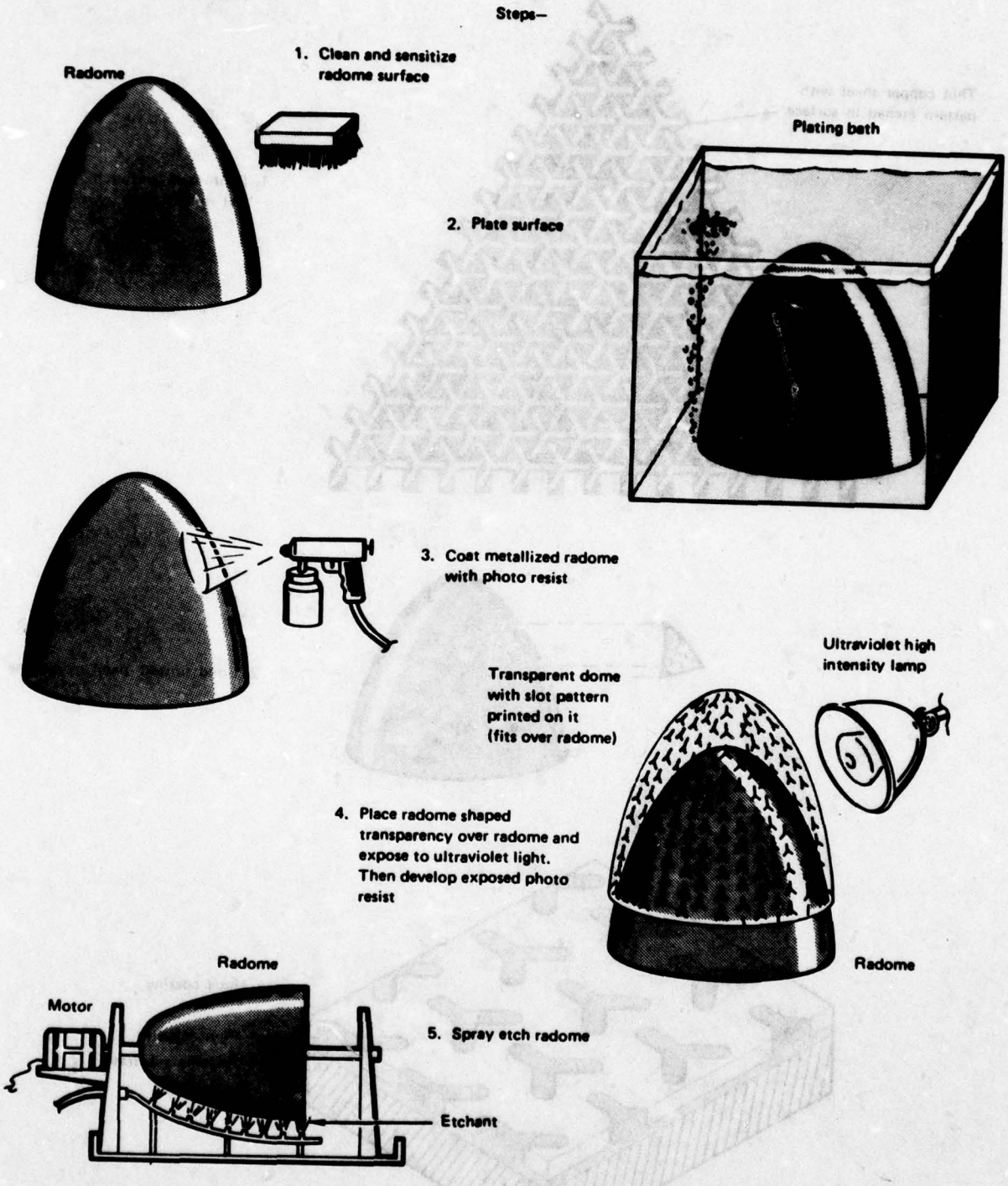

Figure 2 Plate & etch approach

Steps –

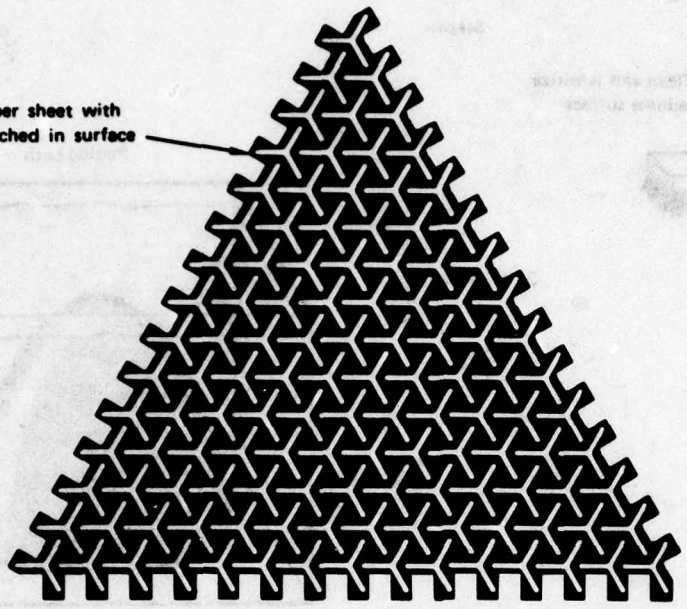

1. Photomask and etch flat metal sheets

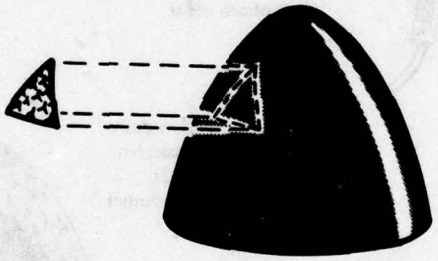

2. Bond slotted metal to radome

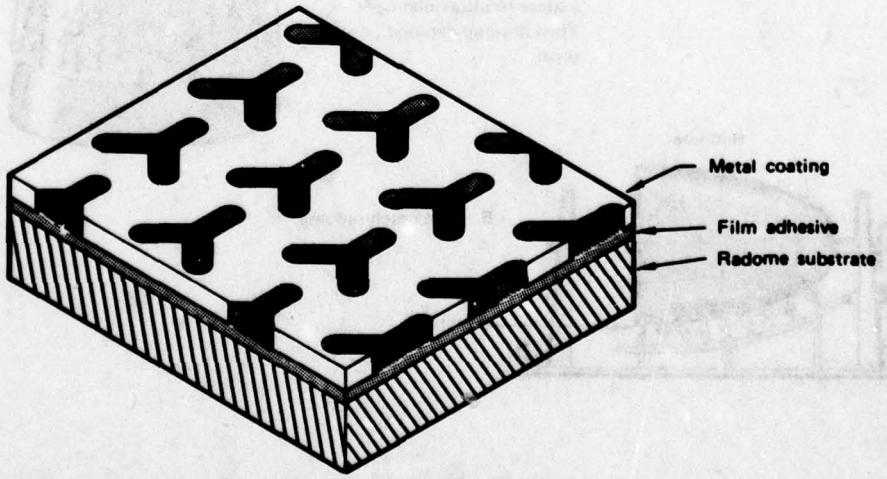

Figure 3 Wallpaper approach

from the nose of the radome, since these areas are very nearly singly curved (therefore developable) surfaces.

Because the slots are etched before bonding, the slots are filled by the epoxy adhesive when it flows during the bonding process, yielding a smooth outer surface.

RAISED SLOT APPROACH

The fourth approach, depicted in Figure 4, involves casting raised slots on the radome's outer surface. This is accomplished by laying up the radome in a female master mandrel which has the slots as recesses in the mandrel surface. Excess resin will fill the recesses during the layup and form raised slots. The mandrel is made to come apart in sections to release the laid-up part. The tops of the raised slots are coated with a "stop-off" material which resists being plated. The entire radome surface can then be plated, first by an electroless method, then by electroplating to build thickness.

When the metal deposit becomes flush with the raised slots, the radome is removed from the plating bath. This yields a metal coated radome with slots which are filled with dielectric and are flush with the metal surface.

2.2 PRELIMINARY EVALUATION

Specimens were prepared of each of these four approaches in order to evaluate their worth and identify potential difficulties. In this preliminary evaluation, the processes that would be involved in fabricating a metal radome by each of the approaches were further defined, and as many of the fabrication steps as possible identified. As a result of this initial evaluation, it was decided to pursue three of the approaches further.

To prove the concepts, small (typically 6 x 6 inch) specimens were fabricated in the laboratory. To examine the electroform approach, a sheet of thin, flat, stainless steel was photoetched with the slot pattern. The slots were filled with silicone rubber which was then cured. This simple mandrel was plated with nickel, and a fiberglass-epoxy layup was made on the exposed surface of the nickel. The epoxy was cured and the nickel electroform was

Steps –

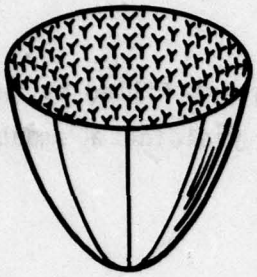

1. Prepare split or rubber-lined female mandrel with recessed slots on interior surface

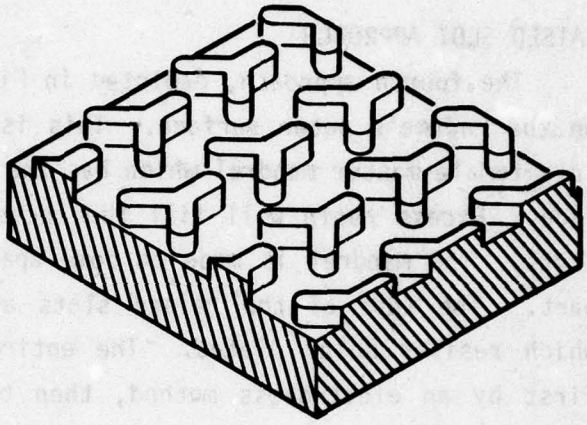

2. Layup radome in mandrel. Excess resin will form raised slots on radome surface.

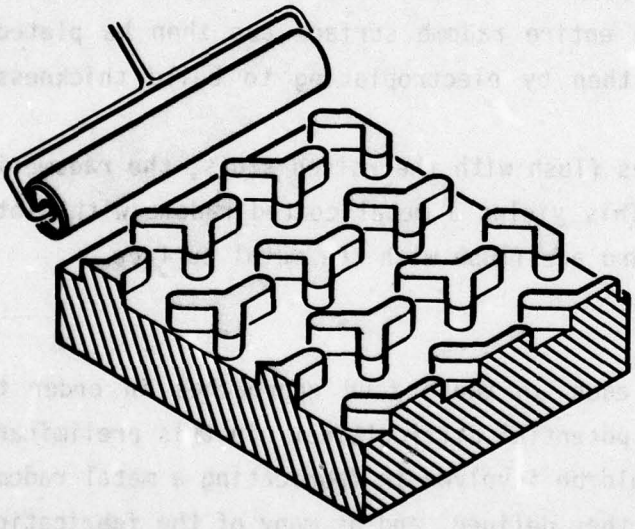

3. Clean and sensitize radome surface. Then coat tops of slots with stop off to prevent plating there

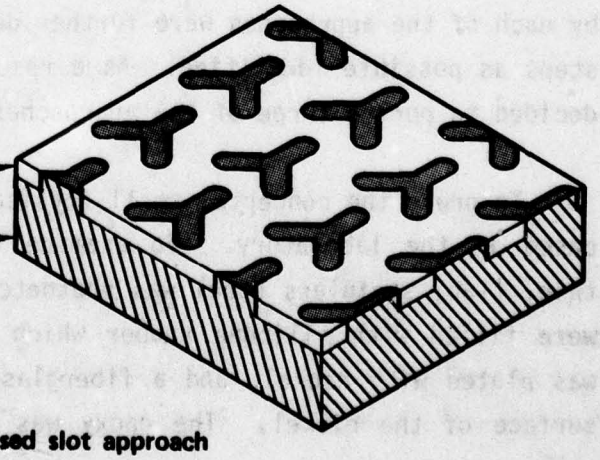

4. Electroless plate radome to make surface conductive. Then electroplate to make plating flush with slot tops

Figure 4 Raised slot approach

separated from the stainless steel mandrel. The resulting part demonstrated that this approach was worth pursuing.

Since the problems of plating and etching were addressed in the next two approaches discussed here, preliminary evaluation of the plate and etch approach by itself was not made. Demonstration of the wallpaper approach was made by photomasking thin copper sheets with the slot pattern. At the time of this evaluation it was not clear whether the centerloading element would be used, so the copper foil was masked and not etched, which allowed retention of the center element. The photomasked copper was formed over a typical section of double curved radome surface by hand, and with the aid of a vacuum bag. A film adhesive was used to bond the masked and formed copper sheet to the fiberglass epoxy substrate. After curing the adhesive the part was spray etched to produce the slots. The centerloading elements were now held in place by the adhesive. It was judged that this approach also had potential.

The raised slot approach was demonstrated in these preliminary evaluations using a ceramic substrate. A plaster mold of a small radome section was made, with the slots as depressions in the surface of the plaster. Silica was slip cast into this mold, and after the part "set up," it was removed from the mold and fired. The fired part is shown in Figure 5 where the raised slots, which were cast into the surface can be seen. The part was electroless copper plated and then electroplated with copper to a thickness equal to the height of the raised slots. No stopoff, to prevent plating on the slots, was used in this evaluation, so the copper which plated on the slots had to be sanded off. This technique was also tried on plastic parts. Some problems arose with the mold release agents, which were used to allow removal of the plastic part from the mold, interfering with the plating process. It was felt that this problem could be overcome, but because this approach was not a coating technique as called for in the contract, but would require fabrication of a new radome design, it was decided not to pursue this fabrication technique further in this program.

Three approaches were selected for further development and the development work accomplished is described in Section 3.0, following the discussion on material selection.

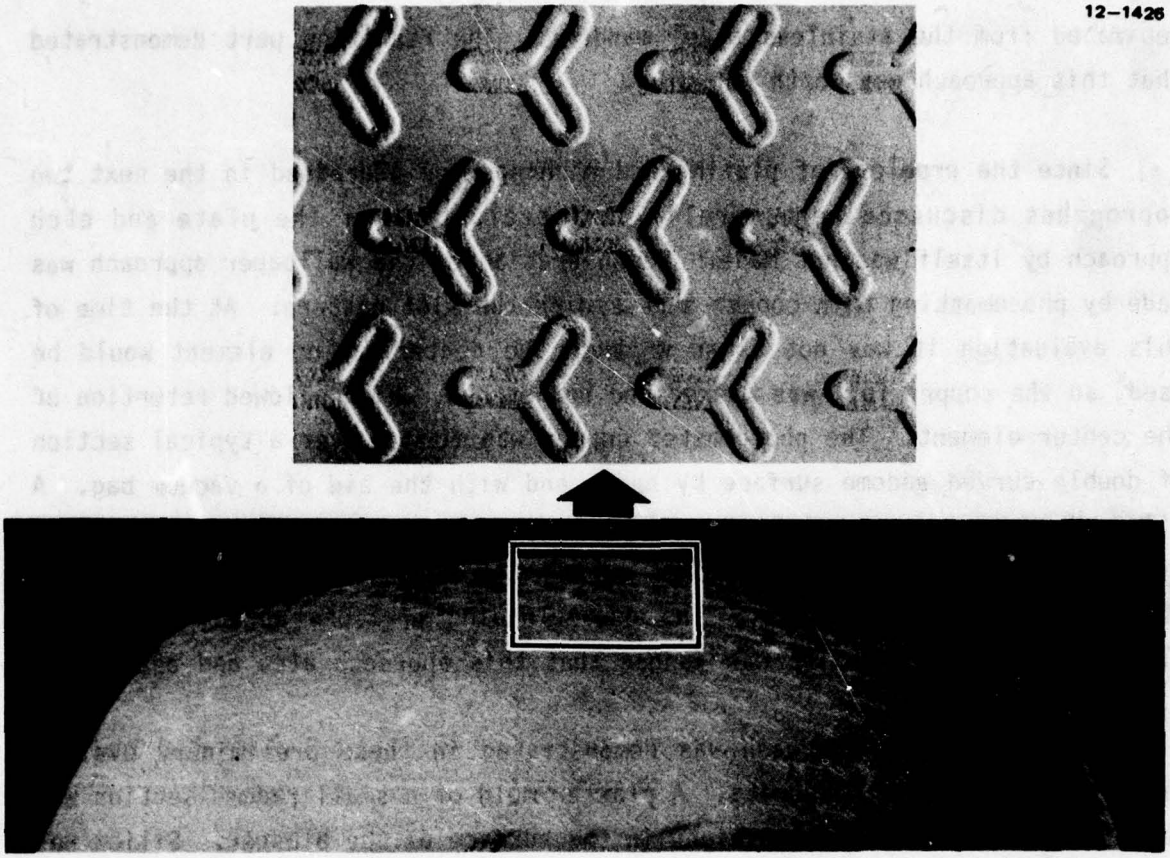

Figure 5 Raised slots slipcast on a doubly curved fused silica radome section

2.3 MATERIAL SELECTION

A number of materials were considered for use in the resonant metal radome. Radome substrates are typically epoxy, polyester, or polyimide with E-glass fibers. The metallic coating can be any conductive material, making metals the prime candidates.

Of the metals, copper and nickel were the prime candidate materials for the metallic coating. Nickel is easily applied, using either electroless or electrolytic or both plating methods. Electroforming nickel is possible and the electroformed parts have good mechanical properties. Nickel is easily etched, and as Weaver demonstrated, is highly rain erosion resistant (Reference 6). It is also resistant to corrosion, and from an electrical standpoint nickel is a viable coating candidate, although inferior to copper. However, for thin coatings, less than 50 mils, the surface conductivity of the slot wall does not significantly affect microwave transmission.

Copper like nickel is easily etched and plated by several processes. It is possible to etch copper to closer tolerances than nickel (Reference 7). Like nickel it can be electroformed, and it is an excellent choice from an electrical performance point of view. Copper is easily formed, and while it does not have the rain erosion resistance of nickel, it is more erosion resistant than most currently used radome materials.

Compatibility between the radome substrate material and the proposed metal coating was considered. Principally, the difference in coefficient of thermal expansion between coating and substrate was of concern. It was thought, and later demonstrated, that by keeping the coating thin relative to the substrate and by achieving a good bond between coating and substrate, the metal coating will expand and contract with the radome substrate without delamination of the coating.

The rain erosion coating used in this program is a polyurethane system developed by the Air Force and Olin Chemical. It is a two part system sold under the trade name Astrocoat and conforms to MIL-C-83231, Types I and II. The Type I system consists of primer and rain erosion resistant basecoat. The Type II system is the same except the Type II system receives an antistatic topcoat. Throughout this program, only the Type I coating (no antistatic topcoat) was used, since the metallic coating acts to eliminate static charge buildup.

Polyurethane represents an advancement in the state-of-the-art in elastomeric coatings for rain erosion resistance. Like the standard neoprene, polyurethanes will provide rain erosion protection to reinforced plastic substrates at Mach 1.5. They have been utilized on radomes similar to the C-140 (selected as the demonstration radome), and have shown good service life, as well as allowing good electrical performance. The material can be used at steady state conditions up to 175°F with allowable short term temperature exposure to 350°F. This polyurethane system affords protection far above the previously standard rain erosion coating, neoprene. For example, the specification requirements for polyurethane coatings is a resistance to damage for 120 minutes when exposed to a 1 inch per hour rainfield at 500 miles per hour. The requirement for neoprenes is a resistance to damage of 8 to 10 minutes

under the same conditions. Polyurethane rain erosion coatings are successfully being utilized on the F-14, F-4, and F-5 nose radomes and are applied in the field to replace neoprene coatings on the F-111 and earlier model F-4 radomes.

SECTION III

COATING SYSTEM DEVELOPMENT

Four methods for providing an adherent and uniform slotted metal coating for a representative aircraft radome were identified and described in the preceding section. Preliminary work to evaluate the processes and materials involved in each approach indicated that the first three approaches: electroform, plate and etch, and wallpaper, had the greatest potential for meeting the program requirements and major emphasis was placed upon their development. The following paragraphs describe the development work accomplished on these three approaches.

3.1 ELECTROFORM APPROACH

Manufacture of a metal radome specimen by the electroform approach requires that a mandrel be made, upon which to form the part. Since we were principally considering using nickel or copper as the material for the metallic coating, the mandrel had to be made of a material upon which nickel or copper could be electro deposited but would not adhere. Stainless steel was selected as the mandrel material. Initially one scheme involved etching the slot pattern on flat plates and forming these etched flat plates to the radome shape in sections. These sections would then be seamed together to form a complete radome mandrel. One concern was whether the slots would be distorted enough in the forming process to adversly affect electrical performance. To address this concern, two sheets of 0.090 inch thick stainless steel (13 x 16 inches) were photoetched with the slot pattern. One sheet was 321 S.S. and the other was 304 S.S., since we were also interested in comparing etch characteristics of two alloys. The sheets were cleaned, passivated, masked with Kodak's KMER photoresist, exposed, developed, and spray etched with ferric chloride. There were no noticeable differences in etch characteristics between the 304 and the 321 stainless.

In order to form the panels into a contour representative of a radome, a section was cut from an F-4 radome. The section was taken from the region of greatest compound curvature and was used as the pattern from which a kirksite

stretch form block was made. The etched stainless sheets were then stretch formed to that radome section contour. Figure 6 shows the mandrel after forming.

12-1277

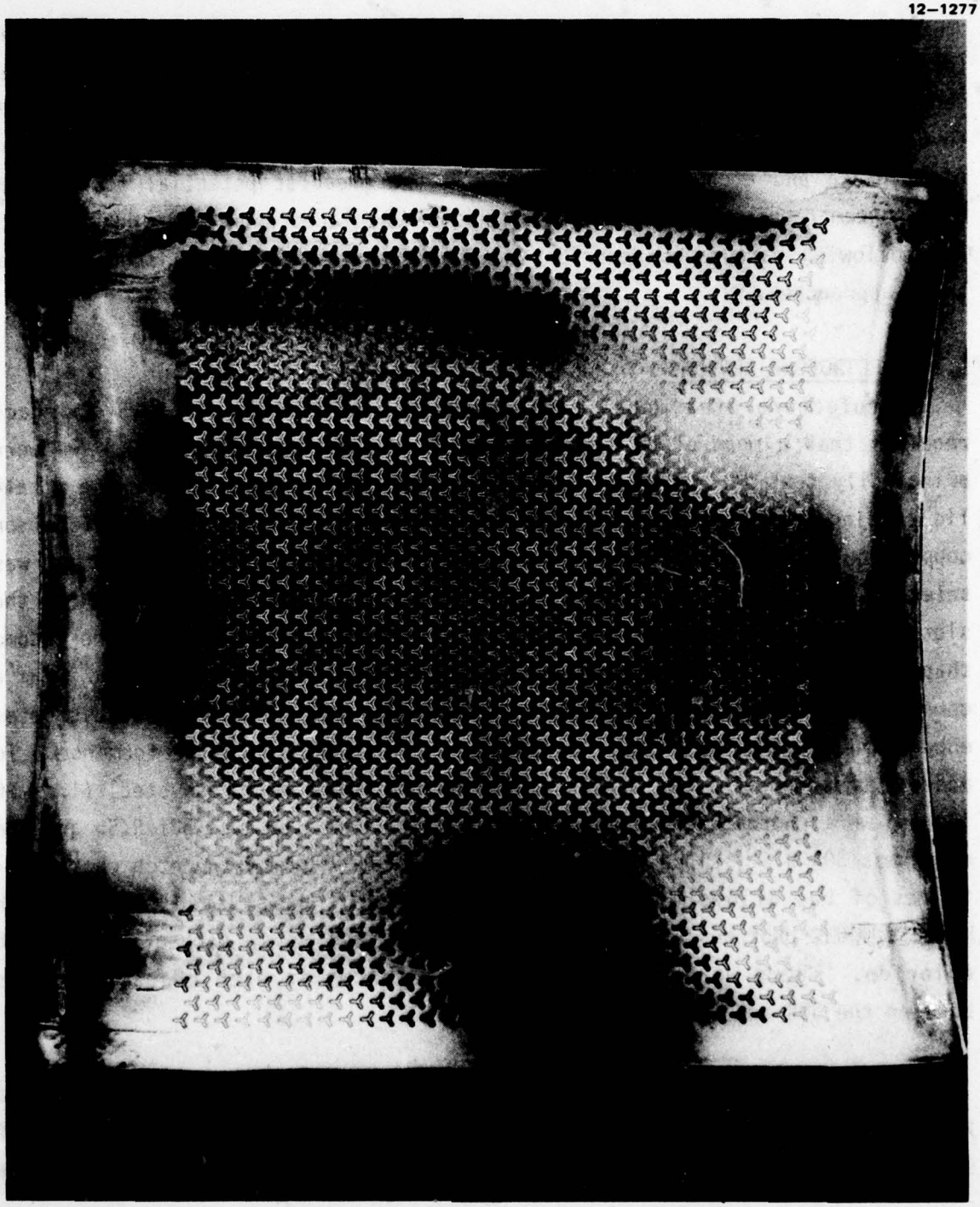

Figure 6 Planographic mandrel after forming

Before forming, dimensions of a diagonal row of slots were taken, using an optical comparator. After forming, these dimensions were again measured and then compared with the original element dimensions and it was found that "growth" of the individual elements due to stretching of the metal was found to be within the tolerances given in the statement of work ($\pm$0.02 cm). Based on these results, patching together a slotted metal surface is feasible, provided that the interface between panels can be handled satisfactorily.

The slots were etched 0.008 inch deep into the 0.090 inch thick stainless. To complete the mandrel the slots had to be filled with a dielectric material. The filler material requirements were: (1) that it be easily applied and have good adherence to stainless, (2) that it have chemical resistance, (3) that it be an electrical insulator, and (4) that epoxy adhesives not bond to it. After trying several different materials, a spray applied fluorocarbon, Dupont's 958-207 Telfon-S, was selected as the filler material. The mandrel surface was vapor degreased and baked. The Teflon was spray applied to the preheated mandrel and partially cured between coats. After approximately five mils of coating thickness was built up, the Teflon was final cured. The slotted surface of the mandrel was sanded to remove the Teflon everywhere except in the slots. The surface was polished and the edges and back of the mandrel masked with Turco 525 chem mill maskant so that plating would not deposit there. The mandrel was cleaned in detergent and water until a waterbreak free surface was attained. To insure release of the electroform from the stainless steel mandrel, the mandrel was passivated. Passivation was accomplished by immersion of the mandrel in a 50% nitric acid solution for one hour. The mandrel was then rinsed in deionized water and placed immediately in the plating bath.

To obtain uniform thickness of the electroform and minimize pitting, a conformal anode, a plexiglas frame about the perimeter of the mandrel, and a relatively low current density while plating were used. After electroforming was complete, fiberglass-epoxy layups were made and cured inside the electroform while still in the mandrel. The mandrel provides stiffness and shape to the assembly until the layup is made and cured. In addition, the mandrel locates the centerloading elements, when that design is used. Problems were encountered in separating the electroform from the mandrel. For example, the

fiberglass-epoxy would separate from the electroform, instead of the electroform from the mandrel. It was determined that it would be necessary to use an adhesive between the fiberglass-epoxy prepreg and the electroform in order to achieve a good bond. Several adhesives and cleaning procedures were evaluated. At first, a matrix of four metal preparation techniques and three adhesives were evaluated. Electroformed nickel was the metal used in the tests. The resulting bonds were good but an accurate determination of the best combination of adhesive and metal surface preparation method was not made. A more careful test was required to make a valid judgement, therefore a matrix of six metal surface preparation techniques, three adhesives, and two metals (Cu and Ni) was drawn up for a second test. These specimens were made in a lap shear configuration and were tested on an Instron tensile test machine. The best combination of peel strength and shear strength was obtained with an AF 147 supported film adhesive manufactured by the 3M Company in conjunction with a cleaning procedure which involves pickling the surface of the metal to be bonded in a nitric hydrofluoric acid solution for 20 seconds. This technique was used in the successful fabrication of a large (9 x 13 inch) doubly-curved process development specimen (shown in Figure 7) and provided a good bond between the fiberglass-epoxy and the electroform.

Specimens like the one just described were fabricated with equal success using both nickel and copper electroforms. A prepreg fiberglass-epoxy system was used for the substrate and the system was cured in an autoclave at 350°F and 50 psig for two hours.

There was a problem with small bubbles occuring in the adhesive. The amount of bubbling was reduced when the vacuum pump was left on throughout the cure cycle rather than venting the vacuum bag as is normally done when pressure is applied to the autoclave. Additionally, it was thought that slower warmup of the autoclave would allow more complete flow of the adhesive before a cure was achieved, thus reducing the amount of bubbling. This too was tried, with some improvement in evidence, but the problem was not eliminated. It was thought that unsupported AF 147 film adhesive might solve the problem since it was suspected that voids might be introduced when the scrim cloth is put in the film adhesive. In addition a scrim cloth was used between the adhesive and the electroform to allow any entrapped air to bleed out during

the cure cycle. This method worked well, in that bubbling in the adhesive of the finished part was eliminated.

12-1278

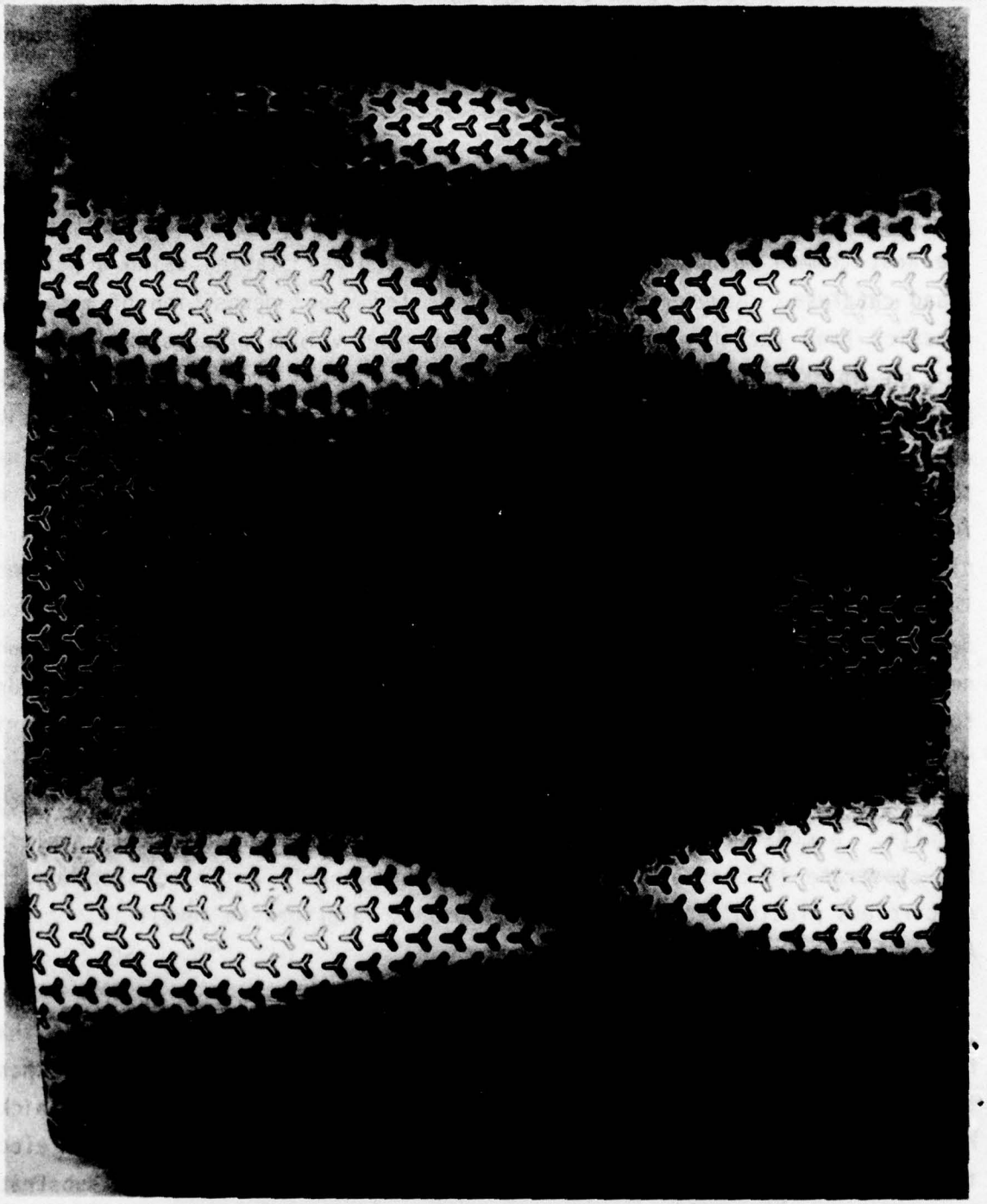

Figure 7 Nickel coated radome section, made using the electroform approach

The Teflon dielectric used to fill the slots in the mandrel was showing signs of wear, and required refurbishment, after several uses. Some experimentation was conducted with cure cycles but little improvement was noticed. It was discovered however, that if the Teflon were allowed to age for a couple of months, its resistance to deterioration was greatly enhanced.

3.2 PLATE AND ETCH APPROACH

The method investigated here for coating the radome with metal was by plating. Plating of plastics is normally accomplished by one of two methods. The most common method in use today is electroless plating using a paladium based catalyst. However, economic methods for vapor deposition of metals on plastics have recently been developed for high volume production (Reference 8). We investigated both techniques and encountered problems which made the plate and etch approach unattractive for our application. For most commercial applications the plastic plated is ABS (Acrylonitrile-Butadiene-Styrene) and the plating techniques are well developed. However for the substrates of interest here, principally fiberglass-epoxy, most metallizing experience is in plating through the holes of multilayer circuit boards. In trying to plate large smooth surfaces on fiberglass-epoxy, it was difficult to achieve good peel strength although appearance of the plating was good. It was found necessary to mechanically roughen the surface of substrate materials in order to achieve good adhesion no matter which plating method was used. Light grit blasting with glass beads at about 15 psig gave good results. In addition to vacuum metallizing, a Shipley electroless plating system was used with good results. A modification of the Shipley process involved chemically swelling the substrate in Shipley conditioner 1200 immediately prior to starting the electroless plating sequence. This process is described in detail in Appendix A.

The electroless deposit was in every case very thin, i.e., less than half a mil thick, because it is impractical to deposit thick coatings by these techniques. Electroplating was used therefore to build up the metal thickness. Specimens were always prepared using electroless copper and then electroplated with either nickel or copper. Since the surface of the substrate was roughened, and electroplating tends to enhance roughness, sanding of the surface was required. This sanding was done after sufficient metal thickness

had been attained so that the sanding could be done without exposing the substrate. To obtain a surface smooth enough for photomasking, several iterations of plating and sanding were necessary. The resulting specimens were good in appearance but were expensive to prepare because of the labor involved in the sanding/plating operation.

Because of these difficulties, another plating method was identified which did not have these drawbacks. A method was found which worked extremely well and involves dipping the part to be plated in Plybond brand adhesive and then electroless plating onto the adhesive using the Enthone electroless process. After 25 to 50 millionths of an inch of copper is built up, enough to make the surface conductive, the surface was electroplated with nickel or copper to the desired thickness. Specimens prepared for this program by Ethone, using this method, exhibited peel strengths in excess of 30 pounds per inch width, which is 2 to 3 times better than other plating methods tried.

Specimens prepared by the methods described were photomasked and etched. Three commercially available systems were used to photomask the various specimens, Dupont Riston 218R dry film resist, Waycoat, and Kodak KPR. Each of these photomaskants worked satisfactorily, although the Waycoat could not be seen on the copper specimens, making it impossible to inspect and touchup, and the Riston does not lend itself to application on a compound curvature. In all cases, etching of specimens was accomplished in a spray etcher with ferric chloride as an etchant. Results were consistently satisfactory.

3.3 WALLPAPER APPROACH

Much of what was learned about cleaning and bonding in work performed while developing the electroform approach, is directly applicable to the wallpaper approach and therefore will not be discussed in detail in this section. The copper selected was a fully annealed copper (alloy 110) which is available in foil and is easily formed by hand. Since, in this approach, the metal is etched while flat, etching of the copper panels was accomplished using routine circuit board methods and equipment. The Dupont Riston 218R dry film photoresist was found to be well suited for this application, principally because it is easily applied, requires no drying or curing, and needs little if any touchup. If some touchup is required, there is plenty of color contrast

between the part and the resist so that the areas requiring touchup are easy to spot.

In order to process the thin (5 mil) copper foil it was found necessary to tape the foil to backup boards. Once securely taped down, the resist was applied using a dry film laminator. It was exposed to high intensity ultraviolet light with the phototransparency held tightly against the part by vacuum. After exposing, the resist was developed and the part was spray etched until etched through. The resist was stripped in a solvent, the etched copper removed from the backup boards and cleaned for bonding. The cleaning procedure consists of the following steps:

1. hot tricloroethelyne vapor degreasing
2. alkaline bath, using Turco proprietary alkaline rust remover
3. tap water rinse
4. ammonium persulfate bath
5. tap water rinse
6. deionized water rinse
7. alcohol bath
8. blow dry

The fiberglass epoxy substrates were prepared for bonding by the following procedure:

1. glass bead peening
2. hot tricloroethelyne vapor degreasing
3. alkaline bath, using Turco 4215S proprietary alkaline solution
4. tap water rinse
5. deionized water rinse
6. blow dry
7. oven dry (120°F)

The film adhesive (3M's AF147) is positioned on the substrate and rolled out with a Teflon roller. The etched copper sheet is positioned on the film adhesive and rolled down tightly. A silicone rubber sheet is placed over the copper to seal off the slots against adhesive flowing out of the slots, while allowing the slots to fill with adhesive for a smooth finish. The other function of the silicone is to act as a release ply. The part is then vacuum bagged and cured in an autoclave at 350°F, 50 psia for 1 hour.

Inherent in the wallpaper approach is the necessity of having joints between the copper foil panels. In order to make the joints electrically conductive a number of methods were identified and evaluated, including: solder tapes, conductive epoxies, silk screened solder creams, and conductive paints. Although several of these methods could be satisfactorily applied to the radome, it was discovered that if the joints were butted tightly, they were electrically conductive without the aid of solder. Resistance measurements made with a Wheatstone bridge were no different across a butt joint on a bonded panel versus measurements from one point to another, the same distance apart within the same piece of copper.

3.4 CONCLUSIONS

Of the three approaches developed, the wallpaper approach was selected for fabrication of the demonstration radomes. The primary advantage of the wallpaper approach is that it allows utilization of existing printed circuit board facilities for the manufacture of the slotted copper sheets. In addition the slots are resin filled after bonding which proved to enhance rain erosion resistance. One of the difficulties involved was making joints between panels without losing elements. How this problem was overcome is discussed in Section 5.0.

The plate and etch approach requires a number of conditioning and plating baths of sufficient size to accommodate a full sized radome. For instance the process described in Appendix A requires 9 tanks. This process also required fabrication of a full sized doubly curved photomask, fabrication of a specially designed spray etcher and hand filling of the slots to achieve a smooth surface, after the metal coating is etched.

The electroform approach probably lends itself to commercial production of resonant metal radomes more than either of the other approaches, but does require fabrication of a full sized planographic mandrel. The cost of such a tool could easily be absorbed in a production run, but was too expensive to make for the manufacture of the two parts required in this program.

Specimens made by the techniques discussed here were fabricated and tested to determine the suitability of a slotted metallic radome for flight. These environmental tests helped in the selection of materials, metal thickness, erosion coating thickness, and fabrication method used on the demonstration radomes. The following section discusses in detail the tests and the results.

SECTION IV

ENVIRONMENTAL TESTING

In order to demonstrate the advantages of a resonant metal radome and to qualify the radomes for flight, a series of tests were conducted. In addition, these tests were used to evaluate fabrication methods and determine metal and erosion coating thickness. The tests covered in this section are: lightning, rain erosion, precipitation static, temperature/humidity/altitude cycling, corrosion, sunshine, and solvent resistance. Electrical evaluation of metallic radome specimens is discussed in Section 5.0.

4.1 LIGHTNING TESTS

OBJECTIVE AND BACKGROUND

Objective - A dramatic example of radome damage as a result of lightning strikes to an unprotected radome is shown in Figure 8 and graphically demonstrates the need for radome lightning protection. Lightning tests were conducted during this program to determine the thickness of slotted metal required to provide lightning protection for the radome. This test series was also designed to determine the effect of polyurethane rain erosion coating on the damage mechanisms. The first test sequence was to determine the range of metal coating thicknesses in which we should be interested, as well as the effect of the erosion coating on the damage mechanism. The second sequence of tests further refined the coating parameters required for lightning protection. Since plating, electroforming, and etching costs increase as the metal coating gets thicker, this effort was directed at minimizing the coating thickness while still providing the required protection. The third and final lightning test sequence consisted of lightning strikes on a witness specimen of the final configuration demonstration radome. The results of the third sequence are discussed in the section on the demonstration articles.

Background - The testing for this program was conducted in conformance with MIL-B-5087B; however, we would be remiss not to point out that a new MIL spec is in preparation which obsoletes the present MIL-B-5087B. It is anticipated that the new spec will be similar in its requirements to the recently

12-1263

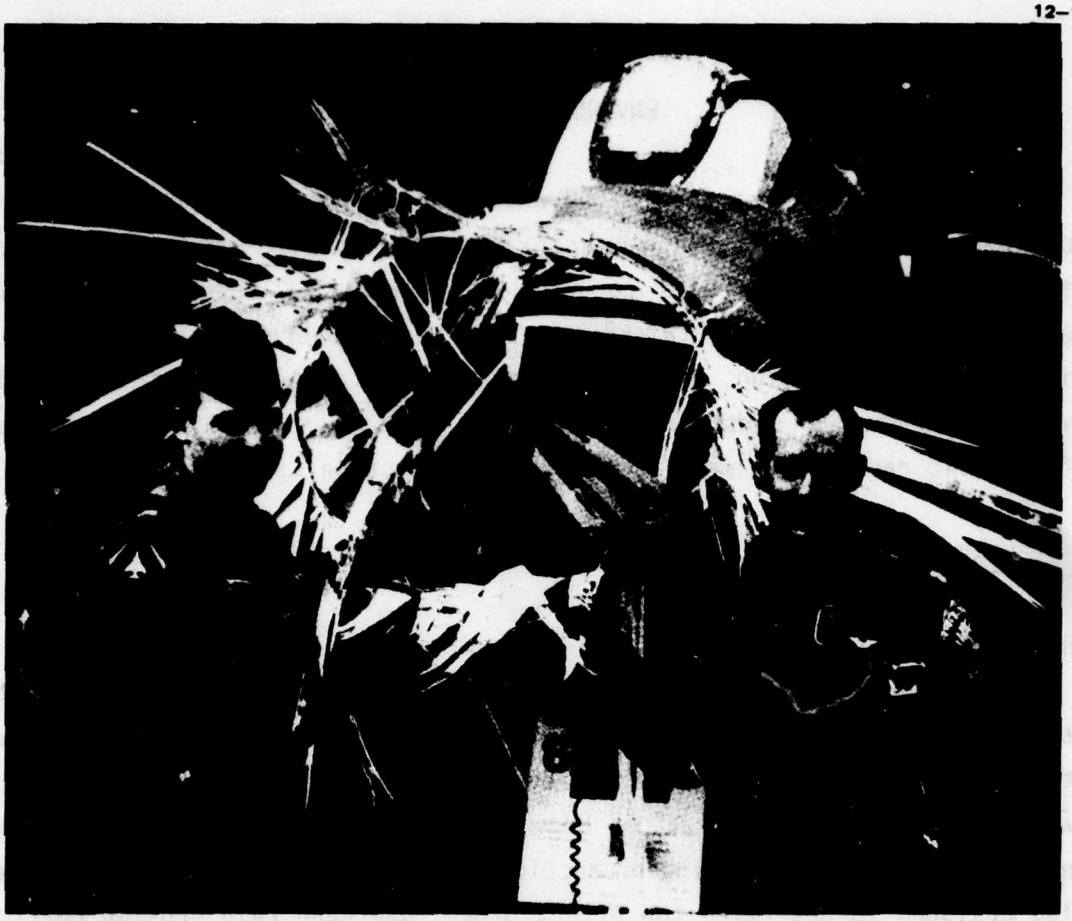

The RF-4C in the photo was being flown by Capt. Robin Lake, Pilot, and Lt. Denny Watkins, Navigator of the 86th TFW on a routine mission when they sustained substantial damage due to a dual lightning strike. All primary flight instruments were lost after the second strike and the attitude and vertical velocity indicators were fluctuating wildly. After declaring an emergency and taking the necessary precautionary measures, the crew, aided by another RF-4C, made a successful landing. This incident occurred in Europe during April 1970 and the weather conditions at the time of the incident were ceiling 1200 foot overcast, visibility 2 miles, and temperature 6°C. Through the superb airmanship of the crew, a total aircraft loss was averted. (U.S. AIR FORCE PHOTO) Ref.

GP78-0382-15

Figure 8 RF-4C after direct natural lightning strike to radome

published SAE Aerospace Recommended Practice (ARP). The purpose of this revision is to reflect a more realistic simulation of the natural lightning environment. The principle difference in the specifications, as far as a metallized radome is concerned, is the inclusion in the revision of an intermediate current component and a continuing current component. These components pose a more severe threat because of the high charge transfer over a relatively long period of time. A simplified combination waveform from the

new specification is shown in Figure 9. The first high peak current component by itself is similar to the present MIL-B-5087B specification, except that the new waveform specifies a higher energy content (I^2dt) than the old specification. MIL-B-5087B does not provide for the intermediate, continuing or restrike components.

It is well known from the extensive work on the development of protective coatings for advanced composites (Reference 9), that the initial high peak current component is easily accommodated on a large area surface by a few mils thickness of high conductivity coating. However, the high charge content components in the new specification can burn holes through even thick metal plates if all the waveform is concentrated at one spot. Whereas the initial peak current pulse carries no more than 3-5 coulombs of charge, the intermediate and continuing components may transfer up to 200 coulombs or more. The damage produced by the high peak current pulse is typically associated with intense magnetic fields and explosive vaporization where inadequate conduc-

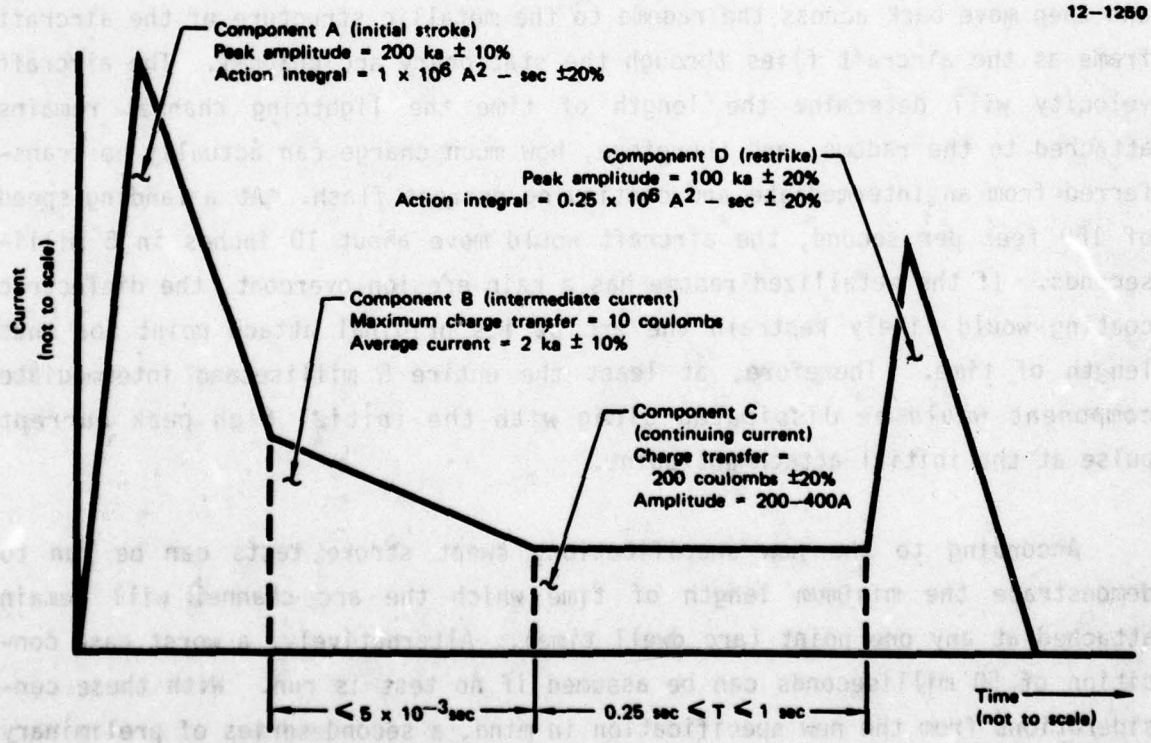

Figure 9 Current test waveform components for evaluation of direct effects

tivity exists. These mechanisms are almost insignificant on exposed large area metal coatings when compared to the high charge transfer components whose principle damage mechanism is thermal burning and erosion.

To demonstrate the relative severity of the high peak current and intermediate current components, preliminary evaluation tests were conducted at the McDonnell Douglas Lightning Simulation Laboratory on copper coated fiberglass panels. These tests showed that a 145 kA pulse twice as wide as the MIL-B-5087B pulse failed to burn through a 67 mil copper coating, while an intermediate current pulse of 3 kA for about 5 milliseconds burned a 1.5 cm diameter hole in the same thickness metal coating.

Although the total charge transfer specified for the intermediate and continuing current components is enough to burn through even thick plates, the dynamic interaction of the aircraft with the lightning arc channel should act to limit the damage at any particular attach point. For a nose mounted radome, the arc channel can be expected to attach to the nose of the radome and then move back across the radome to the metallic structure of the aircraft frame as the aircraft flies through the stationary arc channel. The aircraft velocity will determine the length of time the lightning channel remains attached to the radome, and therefore, how much charge can actually be transferred from an intermediate and continuing current flash. At a landing speed of 160 feet per second, the aircraft would move about 10 inches in 5 milliseconds. If the metallized radome has a rain erosion overcoat, the dielectric coating would likely restrain the arc at its original attach point for that length of time. Therefore, at least the entire 5 millisecond intermediate component would be dissipated along with the initial high peak current pulse at the initial attachment point.

According to the new specification, swept stroke tests can be run to demonstrate the minimum length of time which the arc channel will remain attached at any one point (arc dwell time). Alternatively, a worst case condition of 50 milliseconds can be assumed if no test is run. With these considerations from the new specification in mind, a second series of preliminary tests was conducted on different thicknesses of copper foil bonded to fiberglass-epoxy using 3 different current waveforms. The waveforms included a) a

high peak current pulse, b) a full 5 millisecond intermediate current pulse, and c) a 5 millisecond intermediate current pulse plus 50 milliseconds of continuing current transfer at a rate of about 400 amps. The results of these tests are summarized in Figure 10 and illustrated in Figures B-1 through B-4 of Appendix B. The data demonstrate conclusively that the new specification poses the more severe threat, requiring thicknesses up to 18 mils for uncoated metals, and even thicker coatings for overcoated systems, in order to achieve the zero damage level. These tests do demonstrate however, that the extra damage done by the intermediate and continuing current waveform only adds to the metal damage; i.e., the substrate is still protected.

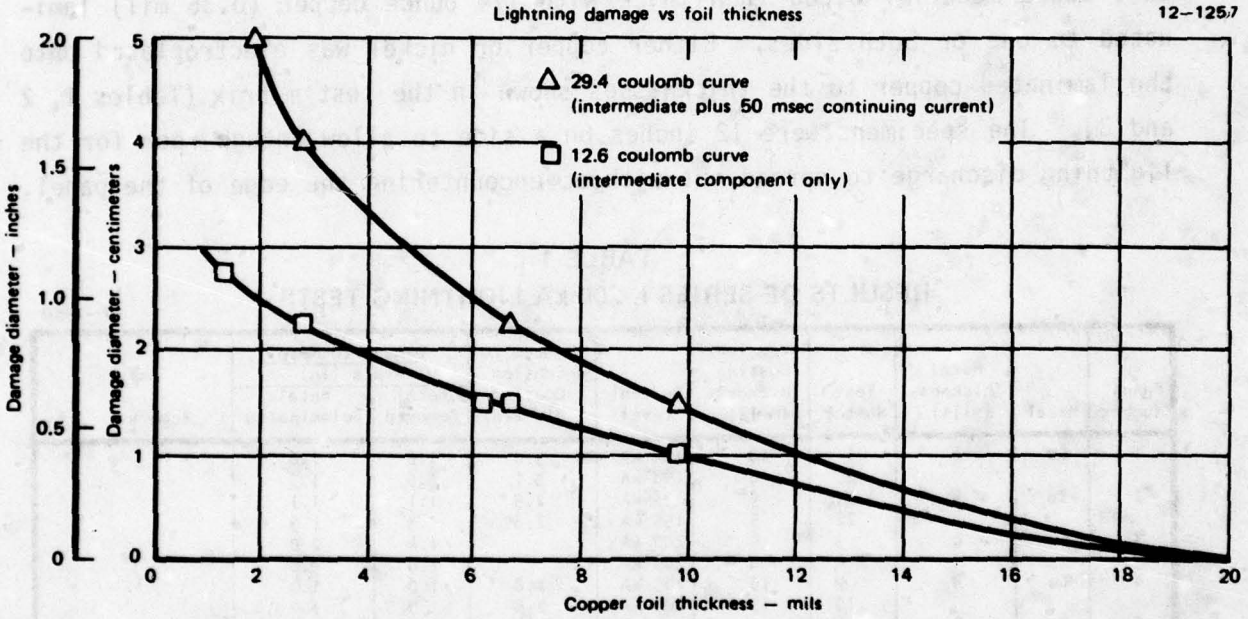

Figure 10 Intermediate and continuing current damage to copper coated fiberglass panels

As a result of these preliminary evaluations, it was clear that the objective here should not be to eliminate the possibility of damage from a worst case lightning strike, but to find that thickness of metal, which gives maximum protection to the radome substrate, radar antenna, and the aircraft itself, while meeting the requirements of fabricability, weight, and reasonable cost.

TEST METHOD

In evaluation tests such as required in this program, it is important that the lightning current waveshape be accurately repeatable from test to

test or the resulting data may be erroneous or misleading. At the McDonnell Douglas Lightning Simulation Laboratory, the peak current, pulse width and I^2t are accurately controlled, thus minimizing data scatter from test to test (Reference 10). The actual testing was done in two phases. The first series, to identify specific areas of interest, tested various metal thicknesses, metal types and rain erosion coating thicknesses with two waveforms. The second series allowed further investigation of variations in metal thickness and type while holding the other parameters constant.

Test Panels - Lightning test specimens were made on epoxy-fiberglass circuit board material 0.060 inch thick with 1/4 ounce copper (0.35 mil) laminated to one or both sides. Either copper or nickel was electroplated onto the laminated copper to the thicknesses shown in the test matrix (Tables 1, 2 and 3). The specimens were 12 inches on a side to allow enough room for the lightning discharge to spread out without encountering the edge of the panel.

TABLE 1
RESULTS OF SERIES I, 200 kA LIGHTNING TESTS

12-1450

Panel Number	Metal	Metal Thickness (mils)	Test Number	Erosion Coating Thickness (mils)	Current Level	Damage to Erosion Coating ~ dia (in)	Damage to Metal ~ dia (in)		Remarks
							Metal Removed	Metal Delaminated	
1	Cu	4	1	10	198 kA	3.0	1.6	1.6	
			2	10	198 kA	3.1	1.5	1.5	
2	Cu	4	21	5	195 kA	2.9	1.1	1.1	
			22	5	195 kA	2.8	1.3	1.3	
3	Cu	4	3	0	200 kA		1.4	2.0	
			4	0	200 kA		1.0	1.6	
4	Cu	8	9	15	205 kA	2.8	1.0	1.0	
			10	15	200 kA	2.6	1.0	1.0	
5	Cu	8	7	7	205 kA	2.4	0.5	0.7	
			8	7	205 kA	2.3	0.5	0.7	
6	Cu	8	17	0	190 kA		*	1.0	Localized Erosion of Surface Metal
			18	0	195 kA		*	0.9	*Center Pieces Were Removed
7	Cu	12	11	15	200 kA	2.7	0.7	0.7	
			12	15	200 kA	2.5	0.6	0.6	
8	Cu	12	13	6	205 kA	2.6	0.6	0.6	
			14	6	200 kA	2.3	0.5	0.5	
9	Cu	12	19	0	195 kA		*	1.2	
			20	0	190 kA		*	0.9	
10	Ni	4	5	0	200 kA		0.0	2.0	
			6	0	205 kA		0.7	2.2	
11	Ni	8	15	0	205 kA		0.0	1.0	
			16	0	205 kA		0.0	0.7	
12	Ni	12	23	0	190 kA		0.0	0.0	Minor Surface Erosion
			24	0	195 kA		0.0	0.0	
13	Cu	4			150 kA 200 kA				Preliminary Test Punctured Substrate. (Polyurethane Foam Backed)

TABLE 2
RESULTS OF SERIES II, 200 kA LIGHTNING TESTS

12-1449

Panel Number	Metal	Metal Thickness (mils)	Erosion Coating Thickness (mils)	Current Level	Damage to Erosion Coating ~ dia (in)	Damage to Metal ~ dia (in)		Remarks
						Metal Removed	Metal Delaminated	
14	Cu	0.35	12	200 kA				Edge Effects Predominant
15	Cu	0.35	12	200 kA				" "
16	Cu	0.35	12	205 kA	7.50	7.50	9.00	Slight Edge Effects
17	Cu	0.7	12	200 kA				Edge Effects Predominant
18	Cu	0.7	12	205 kA	4.50	4.75	6.00	
19	Cu	0.7	12	200 kA	4.50	4.50	6.00	
20	Cu	1.4	12	200 kA	2.50	2.50	3.50	
21	Cu	1.4	12	200 kA	2.75	2.75	3.25	
23	Cu	2.8	12	200 kA	1.75	1.75	2.00	
24	Cu	2.8	12	200 kA	1.50	1.50	2.00	
26	Ni	0.7	12	200 kA	7.00	6.50	8.00	
27	Ni	0.7	12	200 kA	8.00	7.00	8.50	
29	Ni	1.4	12	200 kA	7.00	6.00	7.50	
31	Ni	1.4	12	200 kA	6.25	5.25	7.50	
32	Ni	2.8	12	200 kA	5.00	5.00	7.00	
33	Ni	2.8	12	200 kA	5.00	5.00	7.00	

TABLE 3
RESULTS OF SERIES I, 50 kA LIGHTNING TESTS

12-1446

Panel Number	Metal	Metal Thickness (mils)	Test Number	Erosion Coating Thickness (mils)	Current Level	Damage to Erosion Coating ~dia (in)	Damage to Metal ~ dia (in)	
							Metal Removed	Metal Delaminated
3	Cu	4	E	0	52 kA		0	Very Slight
	Cu	4	F	0	51 kA		0	" "
5	Cu	8	C	7	52 kA	0.5	0	Minor Erosion
	Cu	8	D	7	51 kA	0.5	0	" "
1	Cu	4	A	10	50 kA	0.6	0.25	0.25
	Cu	4	B	10	50 kA	0.9	0.25	0.25

The panels were photoetched with a periodic array of tripolar slot elements which were loaded (centerpiece) for the Series I testing and were unloaded (no centerpiece) for the Series II testing. The two slot designs are pictured in Figure 11. To evaluate the effects of a rain erosion coating on the degree of lightning protection afforded by this type of radome, some of the specimens were overcoated with polyurethane conforming to MIL-C-83231, Type I coating.

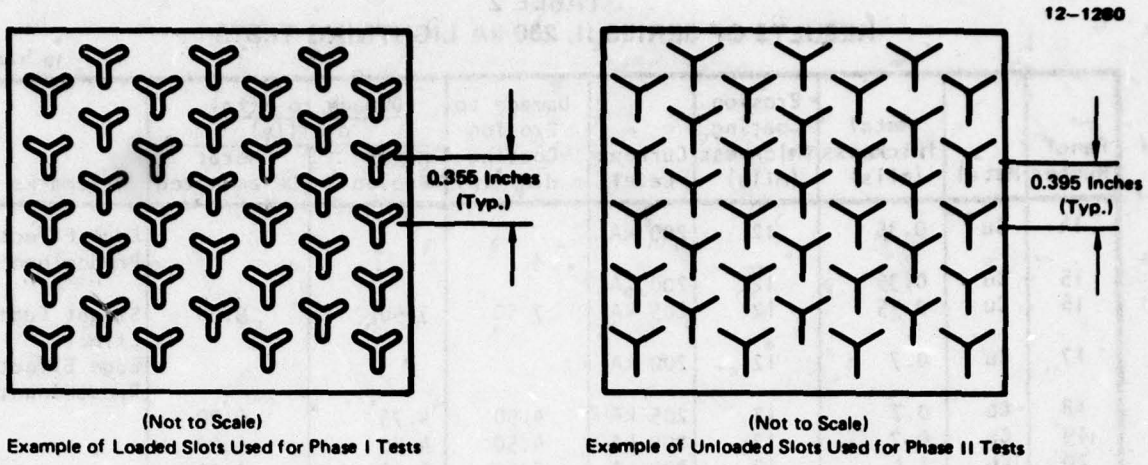

Figure 11 Slot Configurations Used for Lightning Tests

Edges of the panels were masked to provide an area of bare metal for electrical grounding of the panels. The Type I coating consists of 1 to 2 mils of Olin Astrocoat 8200 primer and 10 to 13 mils of Olin Astrocoat 8000 rain erosion resistant polyurethane. For the Series I tests the thickness of the polyurethane was varied from 5 to 15 mils, as shown in Table 3, to evaluate the effect on lightning resistance of various thicknesses of the coating. Some of the coatings differ in appearance because the polyurethane was not fully pigmented. It is not believed that this affected the results of these tests.

Test Setup - The basic test setup is schematically illustrated in Figure 12 and is pictured in Figure 13. This setup was the same throughout the testing except for the test panel holding fixture which was modified to provide a ground on two opposite sides of the panel. This was necessary for the thinner metal coatings used in the second test series, in order to center the damage and reduce edge effects noted on panels 14, 15 and 17. Additionally, it was found that the 0.060 inch panel thickness was not sufficient to contain the explosive forces generated at the strike point, so all test panels were backed by 1/4 inch phenolic sheet to simulate the strength of a radome.

Test Procedure - The test specimen was clamped into the appropriate test fixture and the discharge probe was positioned one inch above the desired strike location on the test panel. The lightning generator was then charged

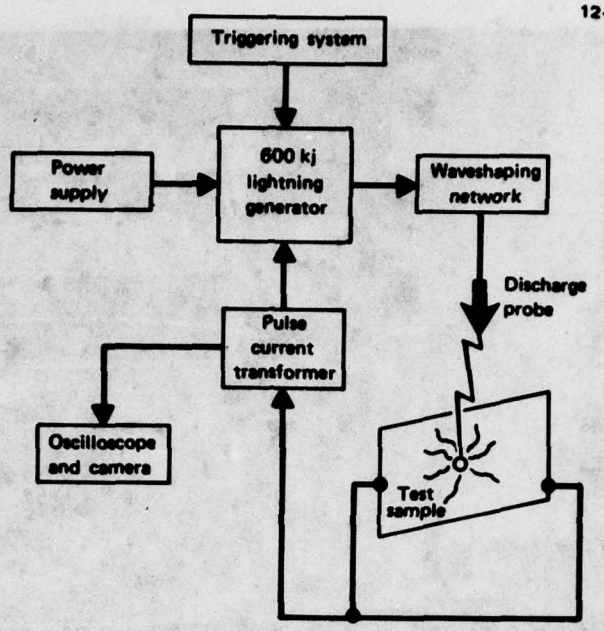

Figure 12 Simplified block diagram of lightning test setup

to the predetermined voltage level, and discharged into the test sample. The lightning current waveform was recorded during each test. After each test, the panel was visually inspected for damage and photographed. Prior to photographing the panels tested in Series I, the carbon residue left on the panels from the lightning strikes was removed with an alcohol swab. On Series I panels, after it was ascertained that the damage was confined to a small area, another location on each panel was struck to obtain additional data points. The tests were run on the 600 kilojoule lightning generator. Most of the lightning strikes were a 200,000 amp peak, 23 microsecond wide waveform conforming to MIL-C-5087B. This intensity strike is in the upper 1% of naturally occurring lightning strikes. Most strikes are below this level and therefore would produce less severe damage. Some selected panels were struck with a 50,000 amp lightning strike to determine the metal thickness required for no damage with this level strike, one of the requirements of the statement of work.

TEST RESULTS

Tables 1, 2, and 3 are a compilation of the test results. As expected, the thicker metal coatings provided more protection, i.e., less damage to the

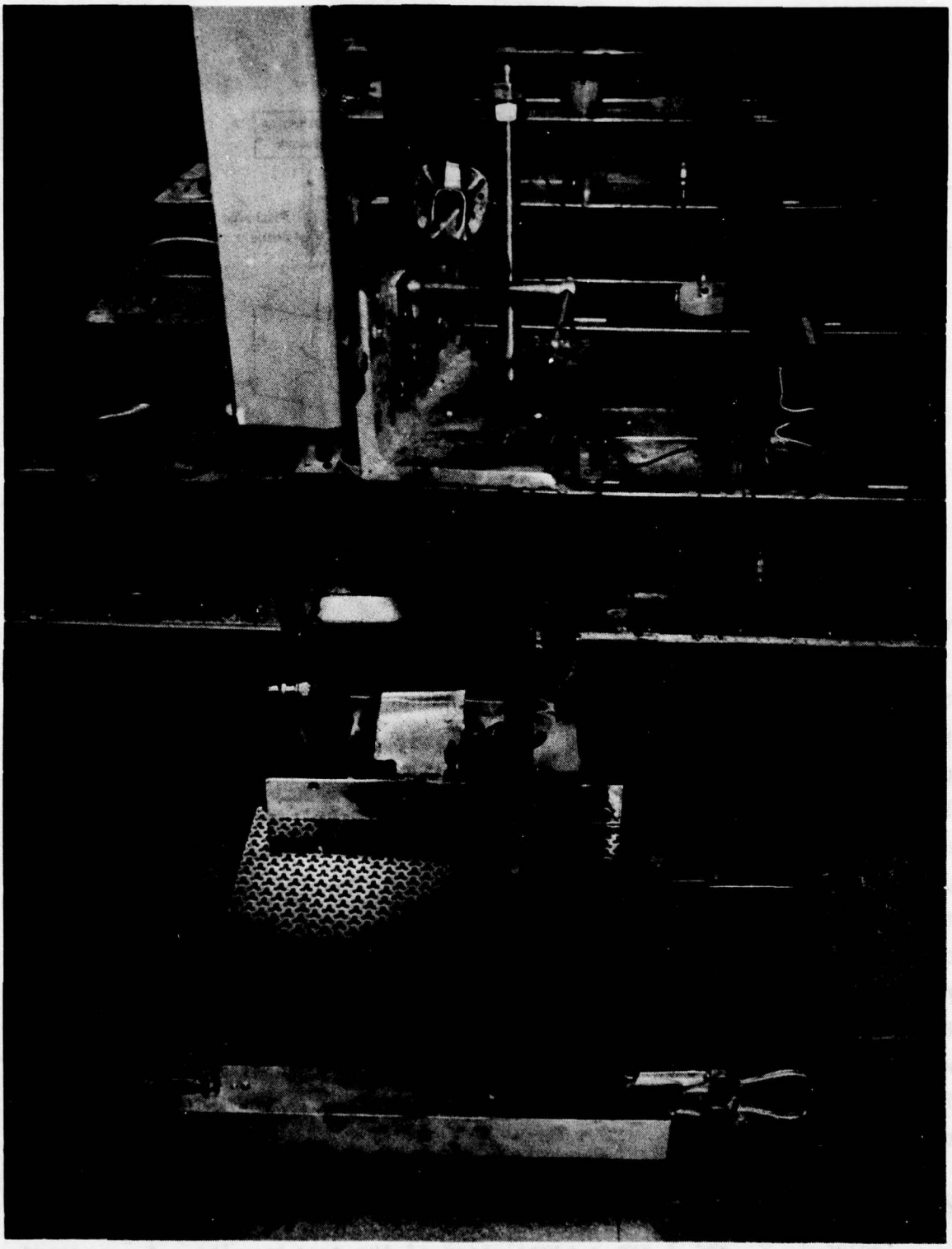

Figure 13 Lightning test setup

metal coating occurred. Not surprisingly, the polyurethane erosion coating caused more metal to be removed due to its charge concentrating effect. The thick nickel coated specimens were slightly more resistant to delamination than were the copper. The 200,000 amp strike, 1 cm damage criteria mentioned in the statement of work is met by the 12 mil nickel coated panel without erosion coating (thick nickel plated specimens were not tested with erosion coatings). The 12 mil copper plated panel with 6 mil erosion coating very nearly met this criteria (1.2 cm damage).

Damage from a 200 kA strike on a 12 mil copper plated panel (no polyurethane) is shown in Figure 14. The dark area around the strike is a carbon deposit which is easily wiped away with a rag and alcohol. The bright spot is the area over which the charge spread, producing minor surface erosion and delaminating a few of the slot centerloading pieces. Figure 15 shows damage to a copper panel of the same thickness by the same intensity lightning strike, however, in this case the panel was overcoated with 15 mils of polyurethane rain erosion coating. The energy of the strike was confined to a smaller area, evaporating the metal there, but producing no damage to the adjacent metal. The rain erosion coating, which can be seen peeled back from the strike area, was separated in that region but is easily repairable. (The carbon deposited on this specimen has been wiped away.) Also, per the contract statement of work, some panels were struck with a 50,000 amp lightning strike to determine the metal thickness required for no damage with this level strike. The 8 mil thick copper with a 7 mil erosion coating meets the 50,000 amp strike, no damage criteria mentioned in the statement of work.

The significant result of all this testing is that in none of the cases where the substrate had strength approximating that of a real radome, did damage to the substrate occur. This means that after taking a severe lightning strike to the radome, an aircraft equipped with even a thinly metal coated radome would remain flightworthy. Some degradation in radar capability can be expected, even if only the polyurethane coating is removed or charred, as is true of any radome.

CONCLUSIONS

The following conclusions were drawn from the test data obtained during these tests.

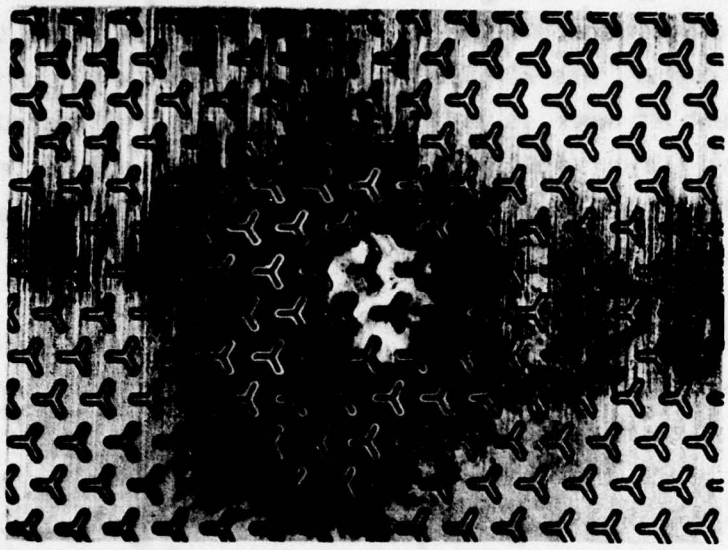

Figure 14 Post test photograph of lightning strike specimen 12 mil copper, no polyurethane

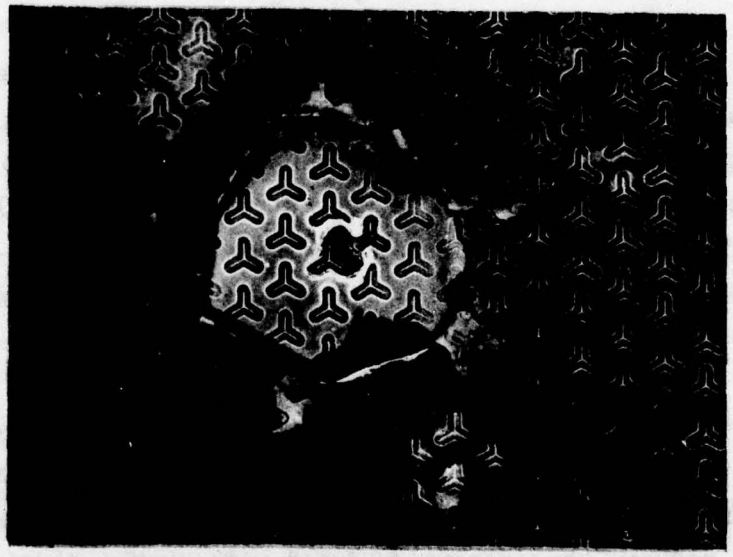

Figure 15 Post test photograph of lightning strike specimen 12 mil copper, 15 mil polyurethane

- Increasing the thickness of the metal coating beyond 4 mils does not significantly reduce the amount of damage to the metal as shown in Figure 16. It does, however, significantly increase the weight of the radome as well as the difficulty and expense of fabrication.

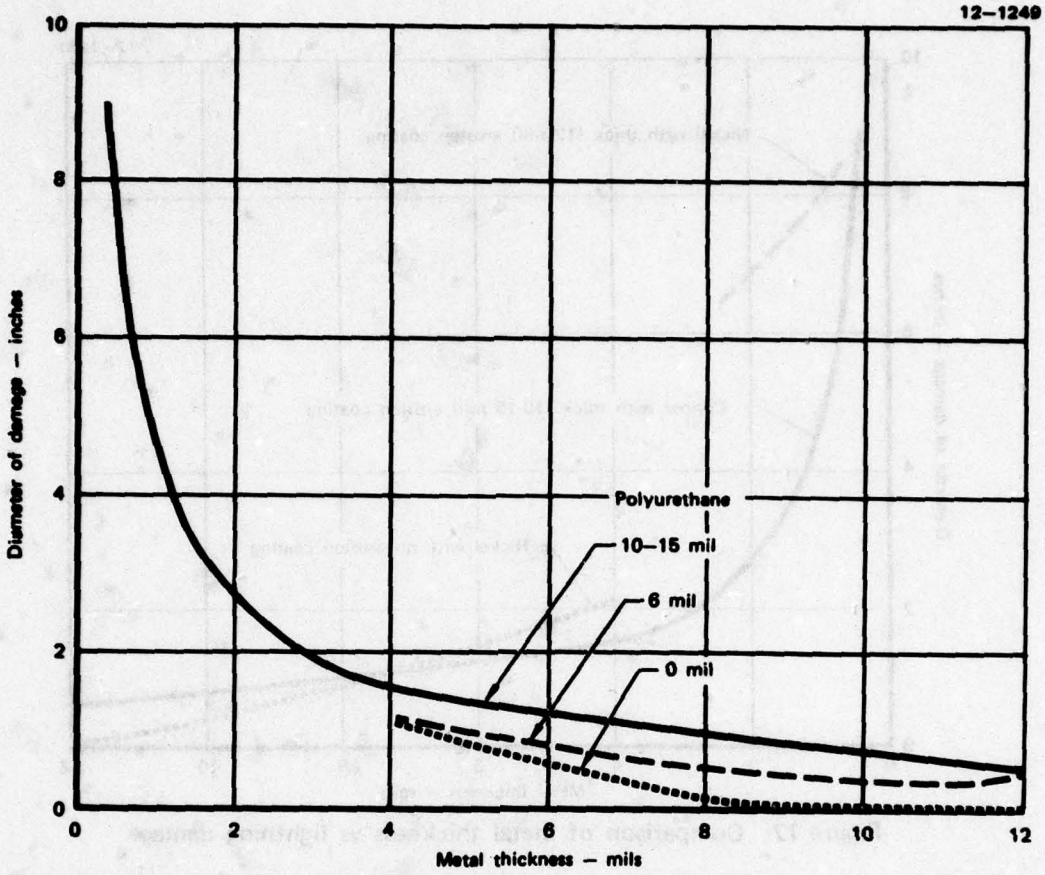

Figure 16 Damage vs slotted metal thickness for polyurethane coated copper specimens

- o Uncoated copper performs better than uncoated nickel until the metal gets about 8 mils thick, where the superior strength and higher melting temperature of the nickel begins to overcome the conductivity advantage of the copper as can be seen in Figure 17.
- o Polyurethane coated copper performs significantly better than polyurethane coated nickel (all data is for metal less than 3 mils thick). Figure 17 also illustrates this point.
- o Although damage to the metal does increase as polyurethane coating thickness increases, the effect is not dramatic. It can be extrapolated from the data that 12 mil copper with a 20 mil erosion coating will meet the requirements (1 cm damage with 200 kA strike and no damage with 50 kA strike).

However, it was decided by the Air Force project officer and this contractor that a 12 mil thick metal coating would be unnecessarily difficult and costly

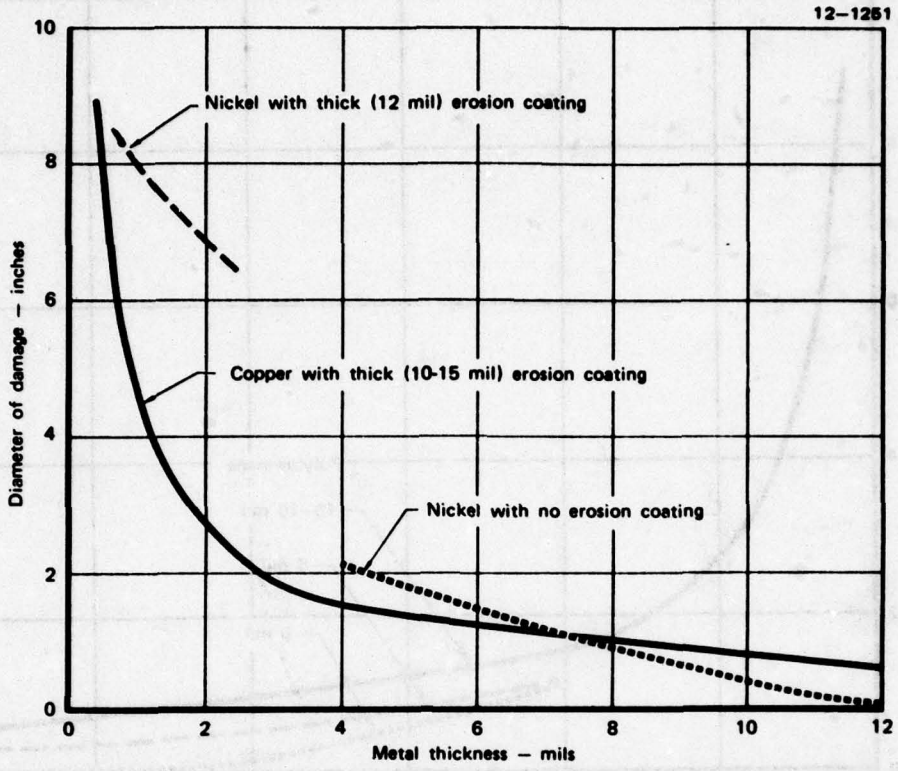

Figure 17 Comparison of metal thickness vs lightning damage

to fabricate, and might be unacceptably heavy. Therefore, a decision was made to baseline a 5 mil copper coating with a 20 mil polyurethane overcoating for rain erosion protection. Thickness of the polyurethane coating was determined by the rain erosion tests which were conducted as a part of this program. The 5 mil metal thickness was decided upon after analysis of the data revealed it to be a near optimum thickness when balancing fabricability, cost, weight, electrical performance, and lightning protection. A look at Figure 16, which is a summary of the test data for copper clad panels, and compares damage spot size with copper thickness for panels with varying erosion coating thicknesses, discloses that the zero damage level is approached nearly asymptotically for panels with thick (10 mil) erosion coatings. There is a knee in the curve near 4 or 5 mils which indicates that this point provides a maximum of protection with a minimum of metal, which is equivalent to minimum fabrication difficulty, cost and weight. Copper was chosen over nickel because for thicknesses under 8 mils it suffered less damage than the nickel (Figure 17).

4.2 RAIN EROSION TESTS

BACKGROUND

Radomes, because of their forward location on the aircraft and because of their high incidence angles to the airstream, are particularly susceptible to damage from rain. Exposure to rain in high speed flight results in failure of the radome material by one or more mechanisms.

One of the failure mechanisms is an erosion action which acts on the surface, and is caused by the rain drop breaking up on impact and flowing laterally across the surface at velocities many times greater than the velocity of impact. As these lateral water jets move across the surface, they strike minor surface irregularities, cracking them at their bases. Successive drop impacts deepen and widen these cracks until they start to run together and the material between the cracks is lost.

The mechanism of rain erosion may be different for different materials, finishes, and constructions. For instance, from the preceding discussion, it could be concluded that a perfectly smooth surface would be ideal to prevent erosion damage by the mechanism mentioned above. However, tests run on the AFML whirling arm by J. H. Weaver and reported in Reference 11 indicate that a roughened nickel surface offered superior rain erosion resistance. His explanation is that the very rough surface tends to break up the drop before impact, reducing radial flow and its resulting damaging effects.

Tests (Reference 12), have also shown that void content in laminated substrates affects the erosion resistance of the radome. Low void content composite materials withstand longer exposure times before failure than composites with higher void content. High quality substrates are therefore important to good rain erosion resistance probably because their higher strength makes them resistant to the direct effects of droplet impact.

One of the failure mechanisms of greatest interest for a metal coated radome involves the difference in sonic impedance between the substrate material and the metal coating. The impact of the rain drop impinging on the

radome surface sends a shock pulse through the coating into the substrate. When the shock pulse reaches the coating/substrate interface, a part of the shock is transmitted into the substrate and part is reflected due to the imperfect energy transfer resulting from the impedance mismatch between materials. The transmitted pulse creates a compression stress as it moves through the coating, while at the coating substrate interface, the reflected portion of the pulse creates a tensile stress. Therefore, a material which is very strong in compression may fail in tension at this interface.

The thickness and impedance of the metal coating can influence its erosion performance because they control the period and amplitude of the stress-wave oscillations. From the stress wave point of view, one would want a coating which has (1) impedance close to that of the substrate because that minimizes the amplitude of the oscillations, and (2) significant thickness, because that minimizes the number of oscillations.

The fatigue resistance of the coating is a prime determinant of its erosion resistance. Ductile metals such as nickel or copper, or tough polymers such as polyurethane, have better fatigue resistance than fiberglass-epoxy and increase the erosion resistance of fiberglass radomes.

OBJECTIVE

It has been demonstrated that thin metal coatings (20 mils) can greatly enhance the erosion resistance of plastic laminates (Reference 11). However, on a metal radome the metal coating must have the required slots for RF transmission. The slots expose the substrate directly to droplet impact and it was anticipated that the substrate would fail at this point. Another concern was that stress concentration might occur in the region of the slots which could result in failure initiation in that region at lower load levels than in other regions. Potentially, the most serious concern was the initiation of delamination or debonding at the edge of the cutout, since the modulus of the metal coating is considerably higher than that of the substructure. This difference in modulus results in in-plane strain incompatibility causing a high shear stress at the bond interface.

The objective of this testing was to help produce a resonant metal radome which is sufficiently resistant to rain erosion damage so that a significant number of flight hours can be flown before refurbishment of the radome is required.

TEST METHOD

The tests were conducted at Wright Patterson AFB under the direction of George Schmitt of the AFML. The Air Force Materials Laboratory Mach 1.2 Rain Erosion Test Apparatus was used for the testing. This apparatus is a whirling arm rig consisting of an eight foot diameter rotor, rotating in a horizontal plane under an eight foot diameter pipe-ring, which has hypodermic needles positioned to spray water droplets on the specimens mounted at the rotor tips. The hypodermic needles are sized to give a 1.8 mm (diameter) drop size. The rain field simulates a 1 inch/hour rainfall and the tip speed of the rotor was 500 mph for all of the tests. A closed circuit television camera with stroboscopic lighting of the rotor tips allows observation of the specimens while they are being tested.

The specimens were exposed, in most cases until failure initiation occurred. A specimen was considered to have failed when the polyurethane coating was penetrated or lost adhesion. In some cases, when the specimens failed quickly, they were allowed to run beyond failure initiation. These cases occurred only in the first test series. Three series of tests were performed, with a total of 42 specimens being evaluated.

Specimen Preparation - Slotted metal radome specimens were prepared for testing on the AFML Whirling Arm Rain Erosion Test Facility using techniques like those being evaluated for use in fabricating the full scale radomes.

Electroform Approach - To prepare specimens representative of the electroform and bond fabrication technique required that a planographic mandrel be prepared in the airfoil shape used on the AFML Whirling Arm. To accomplish this, a tool was made whose outside contour is the same as the outside contour of the required leading edge airfoil. An 0.090 inch thick 321 stainless steel panel was etched with the tripolar center loaded slot element to a depth of

0.008 inch. This panel was then formed around the tool just described, yielding a female mandrel whose inside contour is the same as the outside contour desired on the test specimen. The depressions previously etched were then filled with Teflon, creating the planographic mandrel needed to make a slotted electroform. The completed mandrel is pictured in Figure 18. The mandrel was then processed using the electroform approach as described in Section 3.1. A conformal anode, also pictured in Figure 18, was used while depositing the electroform to insure a uniform deposit. Prefabricated fiberglass-epoxy substrates were bonded into the electroform lined mandrel with AF 147 film adhesive, vacuum bagged and cured in an autoclave. The resulting parts, Figure 19, were overcoated with MIL-C-83231, Type I polyurethane by Brunswick. The Type I coating consists of 1 to 2 mils of Olin Astrocoat 8200 primer and 10 to 13 mils of Olin Astrocoat 8000 rain erosion resistant polyurethane. For this investigation, the thickness of the polyurethane was varied from 12 to 20 mils.

12-1273

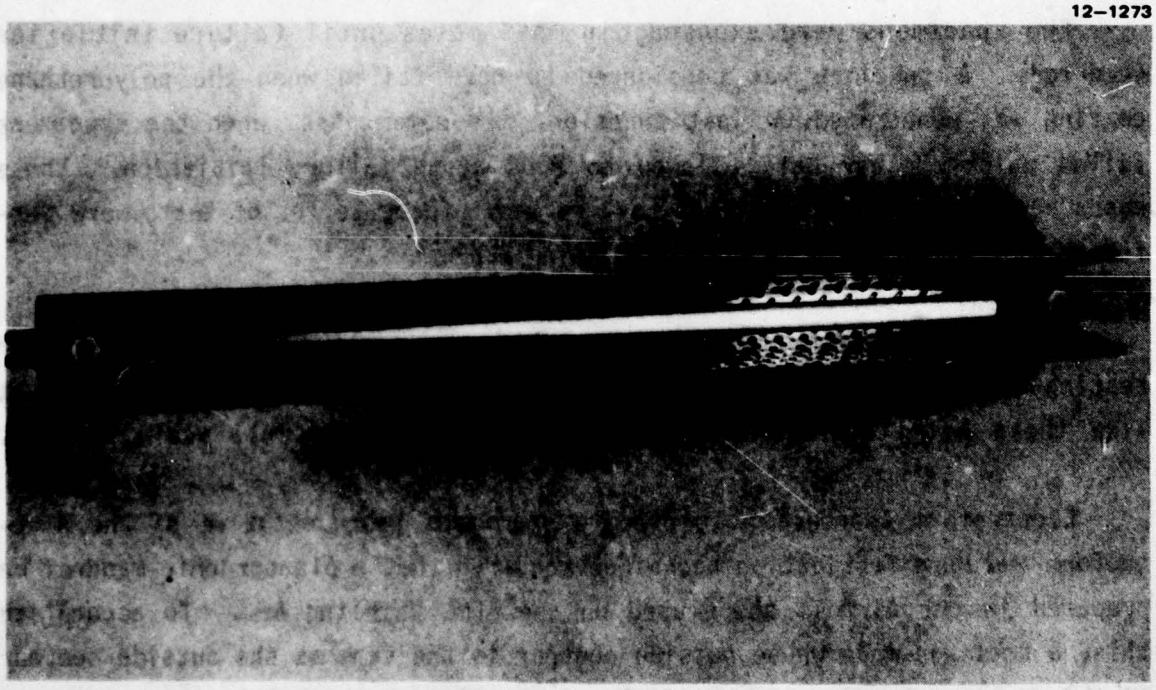

Figure 18 Mandrel for rain erosion specimens

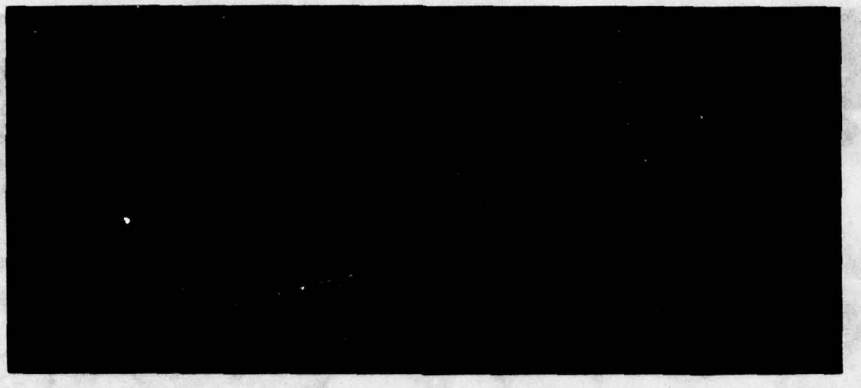

Figure 19 Electroformed nickel, bonded to epoxy fiberglass substrate

Plate and Etch - Specimens of this approach were prepared as described in the previous discussion on the plate and etch approach. Fiberglass epoxy airfoil leading edge blanks, manufactured by Brunswick to AFML specifications were plated using methods described in Section 3.2, i.e., electroless plated, electroplated, sanded smooth and so on until the desired thickness and smoothness were attained. The plated specimens were photomasked, exposed, developed and then etched. In order to etch the airfoil shaped specimens uniformly, a fixture was designed and built to adapt a Chemcut circuit board spray-etch machine to the task. The fixture held several airfoils stationary on the conveyor while rotating them between the upper and lower spray nozzles. Specimens requiring the rain erosion coating were then sent to Brunswick where the polyurethane coating was applied.

Wallpaper Approach - The two film adhesives used for fabricating rain erosion specimens using this approach were 3M company's AF126-2 and AF147. The adhesive was cut to size, laid over the airfoil, and the metal foil formed over the top. In some instances, the metal foil was photomasked with the centerloaded slot pattern and then vacuum bagged and cured. After curing, the specimens were spray etched.

To make the airfoils with the unloaded slot pattern, the metal foil was photomasked and etched before bonding. This allowed the film adhesive to flow and fill the slots while curing, as shown in Figure 20, providing a smooth surface over which to apply the rain erosion coating.

12-1302

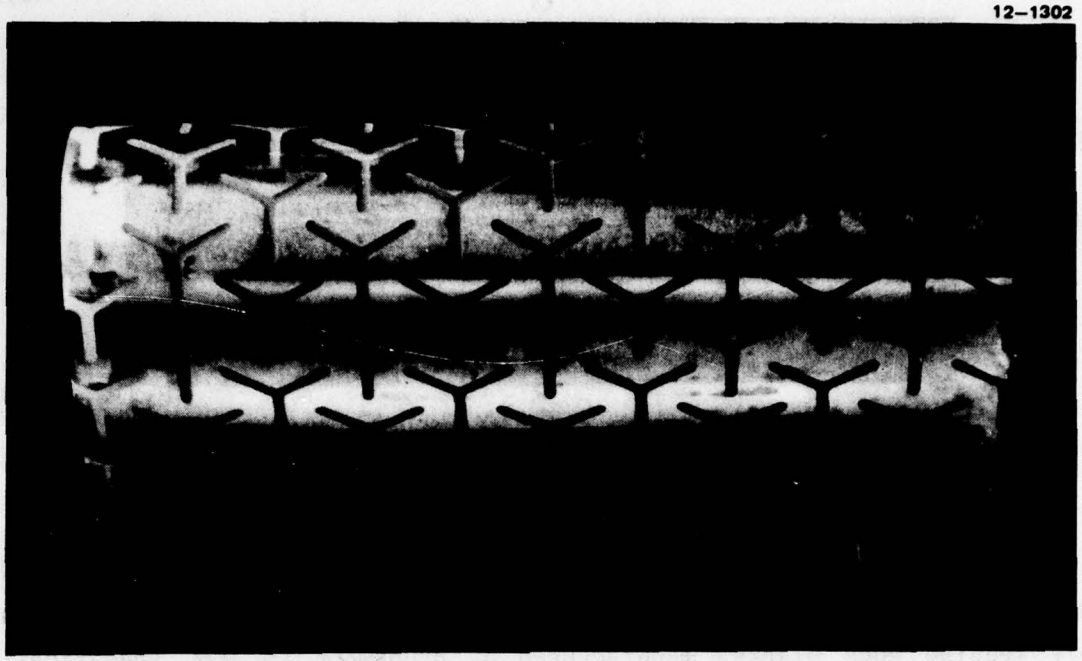

Figure 20 Bonded copper specimen with filled slots.

TEST RESULTS

The test data is shown in Appendix C and is summarized in Tables 4, 5 and 6. In the first test series the loaded slot pattern was utilized (Figure 11). These specimens, in general, did not fare well. In this series, some of the specimens were run without a polyurethane coating and loss of the center load ing elements occurred in less than two minutes. Erosion of the substrate occurred in the region of the slots as the test continued (Figure 21) and delamination and peening of the metal coating occurred in the bonded copper specimens (Figure 22). The electroformed nickel specimens performed the best, the electroformed copper second best, and the bonded copper the poorest, probably due to the softness of the copper foil used. The specimens which were coated with 12 mils of polyurethane received significantly less damage than did the uncoated specimens, although in the 5 minute exposure, which all specimens received, failure of the coating had been initiated (Figure 23).

The second series of tests was more successful. Since loss of the center loading elements was a primary failure mode, and since we expected to be able to use a slot design which has no center loading element on the demonstration

TABLE 4
RAIN EROSION DATA FROM THE FIRST TEST SERIES 500 mph, 1 INCH/HOUR SIMULATED RAINFALL (1.8 mm dia DROPS)

12-1480

AFML No.	MDAC No.		Time to Failure (min)	Comments
7556	1	14 mils Plated Nickel	5.0	Y-elements gone, slight laminate erosion
7557	2	11 mils Plated Nickel	5.0	Y-elememts gone, laminate erosion, layer-off of top coat of nickel
7558	3	12 mils Plated Nickel/12 mils MIL-C-83231 Polyurethane	5.0	Erosion failure of urethane at Y-element, metal wire protruding from coating
7559	4	12 mils Plated Nickel/12 mils MIL-C-83231 Polyurethane	5.0	Erosion failure of urethane at Y-element
7560	6	3 mils Plated Copper/12 mils MIL-C-83231 Polyurethane	5.0	Erosion failure initiated at Y-element
7561	8	12 mils Plated Copper/12 mils MIL-C-83231 Polyurethane	5.0	Erosion failure initiated at Y-element
7562	7	13 mils Plated Copper	5.0	Y-elements gone at 2.0 min, laminate erosion
7563	9	9 mils Plated Copper	5.0	Y-elements gone at 1.5 min, laminate erosion, adhesion loss of copper
7564	5	5 mils Bonded Copper/12 mils MIL-C-83231 Polyurethane	5.3	Erosion failure of urethane at Y-elements copper foil peened beneath coating.
7565	10	5 mils Bonded Copper/12 mils MIL-C-83231 Polyurethane	5.0	No coating failures, peening of copper beneath
7566	11	5 mils Bonded Copper	5.3	Peening of leading edge area, erosion of slots, laminate erosion, incipient adhesion loss
7567	12	5 mils Bonded Copper	5.0	See 7566 above

NOTES: 1 All specimens were Y-shaped elements with centerloading pieces.
2 Substrates were fiberglass-epoxy laminates.

TABLE 5
RAIN EROSION DATA FROM THE SECOND TEST SERIES 500 mph, 1 INCH/HOUR SIMULATED RAINFALL (1.8 mm dia DROPS)

12-1481

AFML No.	MDAC No.		Time to Failure (min)	Comments
7755	1	8 mils Plated Copper/12 mils MIL-C-83231 Polyurethane	25.0	Erosion failure
7756	3	7 mils Plated Copper/12 mils MIL-C-83231 Polyurethane	60.0	Erosion failure
7757	2	8 mils Plated Copper/20 mils MIL-C-83231 Polyurethane	90.0	Erosion failure
7758	4	7 mils Plated Copper/20 mils MIL-C-63231 Polyurethane	75.0	Erosion failure
7759	5	15 mils Plated Nickel/12 mils MIL-C-83231 Polyurethane	10.0	Erosion failure
7760	6	9 mils Plated Nickel/12 mils MIL-C-83231 Polyurethane	40.0	Erosion failure
7761	7	13 mils Plated Nickel/12 mils MIL-C-83231 Polyurethane	7.0	Erosion failure
7762	8	11 mils Plated Nickel/12 mils MIL-C-83231 Polyurethane	33.0	Erosion failure
7763	9	10 mils Plated Nickel (no slots)/12 mils Polyurethane	170.8	Erosion pit
7764	10	2 mils Bonded Nickel/12 mils MIL-C-83231 Polyurethane	87.1	Erosion failure
7765	11	2 mils Bonded Nickel/12 mils MIL-C-83231 Polyurethane	83.7	Erosion failure
7766	12	5 mils Bonded Copper/12 mils MIL-C-83231 Polyurethane	90.0	Erosion failure
7767	13	5 mils Bonded Copper/12 mils MIL-C-83231 Polyurethane	95.4	Erosion failure
*7768	14	2 mils Electroformed Nickel/12 mils MIL-C-83231 Polyurethane (with centerloaded slot)	6.6	Erosion failure
*7769	15	2 mils Electroformed Nickel/12 mils MIL-C-83231 Polyurethane (with centerloaded slot)	12.0	Erosion failure

NOTES: 1 All specimens except those noted (*) were simple Y-shaped elements without centerloading pieces.
2 Substrates were fiberglass-epoxy laminates.

TABLE 6
RAIN EROSION DATA FROM THE THIRD, FOURTH, AND FIFTH TEST SERIES
500 MPH, 1 INCH/HOUR SIMULATED RAINFALL (1.8 MM DIA DROPS)

12-1442

AFML No.	MDAC No.	DESCRIPTION	TIME TO FAILURE (MIN.)	COMMENTS
8139	21	5 mils bonded copper/20 mils MIL-C-83231 Polyurethane (unsupported adhesive)	82.0	Erosion Failure
8140	22	5 mils bonded copper/20 mils MIL-C-83231 Polyurethane (overcured film adhesive)	60.0	Erosion Failure
8141	23	"	80.0	Erosion Failure
8142	24	"	82.0	Erosion Failure
8143	25	"	75.5	Erosion Failure
8144	26	5 mils bonded copper/20 mils MIL-C-83231 Polyurethane	146.5	Erosion Failure
8145	27	"	121.5	Erosion Failure
8146	28	"	130.0	Erosion Failure
8147	29	"	78.0	Erosion Failure
8305	30	5 mils bonded copper/20 mils MIL-C-83231 Polyurethane	16.3	Intercoating Failure of the Polyurethane
8306	31	"	16.3	"
8307	32	"	21.7	"
8308	33	"	21.7	"
8609	30	5 mils bonded copper/16 mils MIL-C-83231 Polyurethane	17.5	Erosion Failure then Adhesion Loss
8610	31	"	45.0*	"
8611	32	"	17.5	Erosion Failure
8612	33	"	60.0*	Erosion Failure then Adhesion Loss

*Failure was in a location difficult to spot on the TV monitor; failure probably occurred between 30 and 45 minutes.

NOTES: (1) All specimens were simple Y-shaped elements without centerloading pieces.
(2) Substrates were fiberglass - epoxy laminates.

12-1296

Figure 21 Electroplated copper specimen (#7563) after 5 min exposure to 1 inch per hour rain at 500 mph

12-1297

Figure 22 Bonded copper specimen (#7566) after 5 min exposure to 1 inch per hour rain at 500 mph

radomes, new specimens were fabricated without these loading elements. These specimens were of nickel and copper electroplate, and of nickel and copper bonded construction. It was thought that the edges of the slots and the center loading elements, because they protrude, are preferentially attacked by the raindrops. Therefore the wallpaper approach was modified so that the slots in the bonded metal would be filled with excess adhesive during the bonding process (Figure 20). This gave the airfoil specimens a smooth surface i.e., no protrusions. This smooth surface also takes a uniform coat of poly-

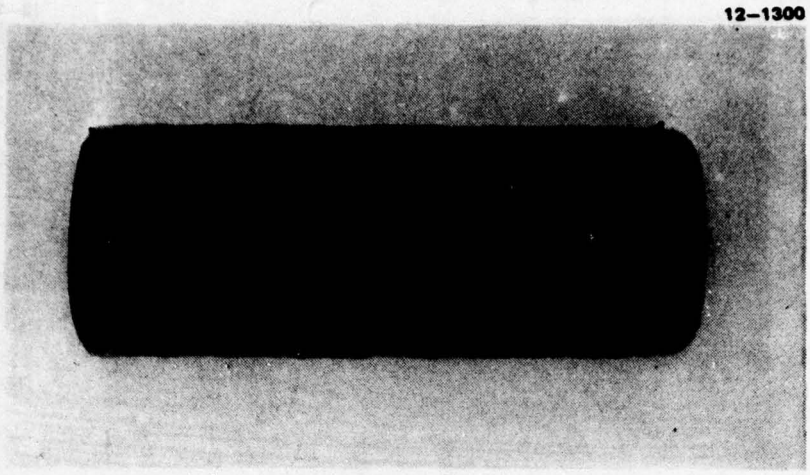

Figure 23 Rain erosion specimen (#7564) after 5 min. exposure to 1 in. per hr. rain at 500 mph (1.5X)

urethane, unlike the recessed slotted surface where the polyurethane tends to thin out at the slot edges and on the tops of the loading elements. Additional rain erosion test specimens were also fabricated using the electroform and bond approach (Figure 19). These specimens had the center loading element mechanically interlocked with excess adhesive as well as adhesively bonded to the substrate. All specimens were polyurethane coated. The smoother surfaced specimens with the unloaded elements performed reasonably well and specimens prepared by the wallpaper approach using 5 mil bonded copper and 12 mil polyurethane lasted for over 90 minutes before the polyurethane started to fail (Figure 24). One specimen was tested which had a metal coating with no slots and a polyurethane overcoat. It lasted 170 minutes with just an indication of an erosion pit, verifying that early failure of specimens was a result of the presence of the slots. Table 5 summarizes the results of the second test series.

For the third test series nine specimens were prepared, one using an unsupported film adhesive (AF147U), four using a supported film adhesive (AF147) which were cured well beyond the optimum cure time and four others which also used a supported film adhesive but were cured at the optimum time and temperature. All specimens used an unloaded (no centerpiece) slot design in 5 mil thick copper. A summary of the results of this third test series is presented in Table 6.

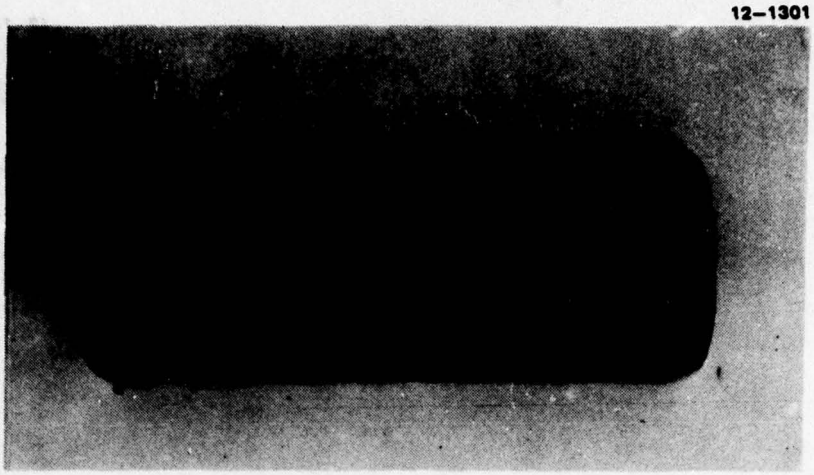

Figure 24 Rain erosion specimen (#7767) after 95 min. exposure to 1 in. per hr. rain at 500 mph (1.5X)

The first specimen with unsupported film adhesive (#21) failed in 82 minutes. The second group of specimens which were over cured (#22 through 25), failed in 60, 80, 82 and 75.5 minutes, respectively. The next group (#26 through 29), which were optimally cured, lasted 146.5, 121.5, 130 and 78 minutes, respectively. It is not known why #29 failed prematurely, since there were no noticeable differences between the last four specimens. One possible explanation is that the polyurethane erosion coating may have had a bubble in it. Our goal in this program was to achieve erosion resistance equivalent to current conventional radomes which is specified to be 120 minutes exposure without damage. It is believed that this last group of specimens meets that goal. Four other specimens were prepared and tested. The results (summarized in Table 6) were not good, and are attributible to problems with the polyurethane coating. The failure was between layers of the polyurethane coating. These same specimens were stripped and recoated. This second coating did not have a good appearance, therefore, it was stripped, and a third coating application made. The specimens were retested and failed. Upon closer examination it was discovered that the solvent used to strip the coating had attacked the epoxy of the airfoil substrate leaving it with a white resin starved appearance. We believe that the substrate and the bond to the metal was probably weakened by repeated exposure to the solvent thus contributing to the early failure of the specimens. Additionally, in this and the previous test, the failures all occurred at the edges of the specimens

where the clamps hold the specimen to the whirling arm. This may be because the coating system (adhesive/metal/20 mil polyurethane) was so thick that it was pinched under the clamp, introducing a strain in the coating adjacent to the clamp. This region, already weakened, failed rapidly when exposed to droplet impact. Specimens 8609 thru 8612 are simply specimens 8305 thru 8308 recoated and renumbered. Time did not permit these last tests to be repeated.

CONCLUSIONS

Several conclusions can be reached from examination of the data:

- o The slotted metal coating alone is not sufficient to protect the substrate from damage. The rain attacks the substrate where it is exposed; at the slots, as seen in Figure 25. The rain also takes advantage of the edge exposure of the metal/substrate interface at the slot to separate the metal from the substrate.
- o The center loading element of the Y slot is particularly susceptible to separation. It was also the focal point for the failure of the polyurethane coating (Figure 26) probably because the spray applied coating tends to runoff high spots (like the centerpiece) before the polyurethane sets up.
- o The smoothness of the outer surface of the polyurethane seems to be a primary determinant in the time to failure. The fewer bumps in the surface, caused by unevenness in the specimen underneath, the longer the time to failure of the coating. This might be, at least in part, the result of thinner polyurethane on high spots and edges, because the polyurethane, while wet tends to runoff, as mentioned above.
- o The thickness and type of metal have little effect on the time to failure as long as there are slots in the surface, because the rain attacks the slot.
- o A thicker polyurethane coating, offers more protection based on a comparison between 12 and 20 mil coatings on otherwise identical specimens, e.g., specimens 7755 through 7758. These tests show that a 20 mil polyurethane coating coupled with epoxy filled slots (to obtain a smooth surface) provides the rain erosion protection necessary for our demonstration radomes.

12-1295

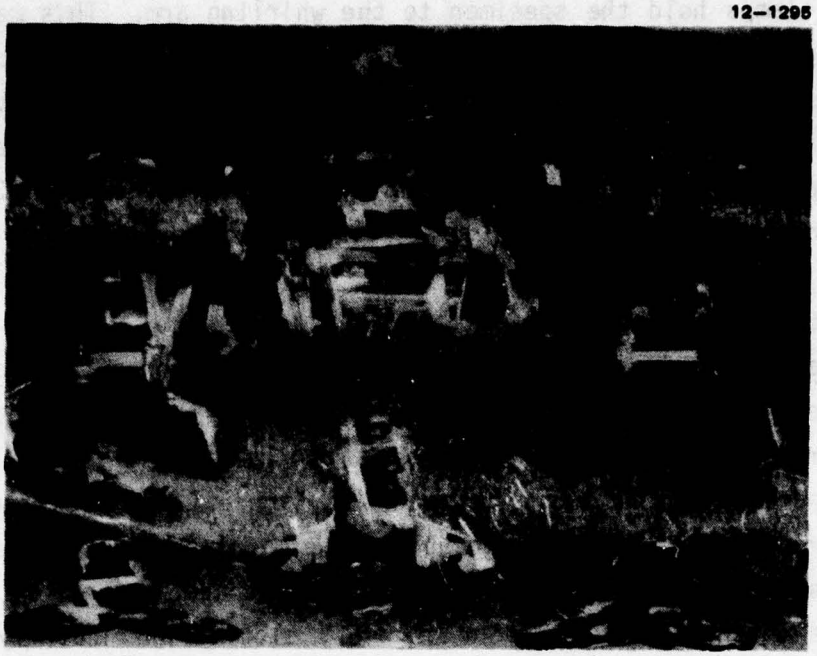

Figure 25 Electroplated copper specimen after 5 min exposure to A 1 inch per hour rain at 500 mph (5X)

12-1298

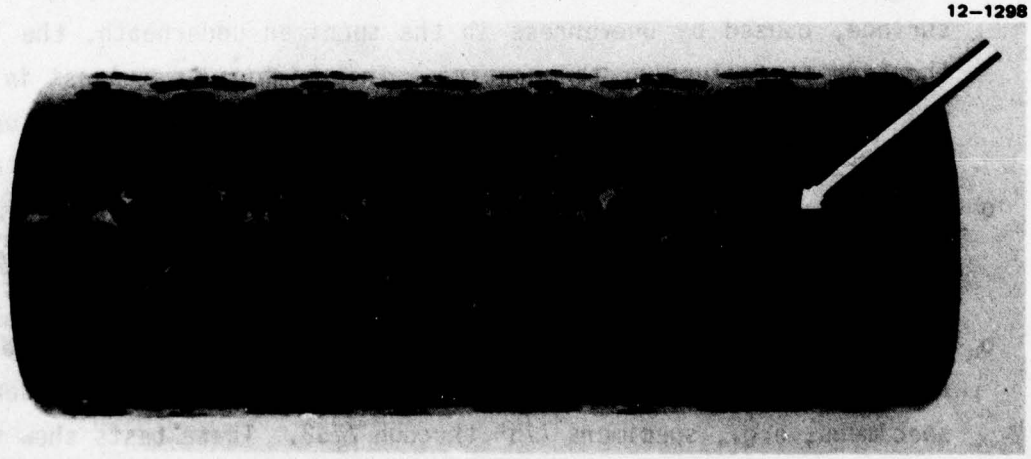

Figure 26 Polyurethane coated specimen. Failure initiation occured on center loading element. (# 7558)

4.3 PRECIPITATION STATIC TESTS

BACKGROUND & OBJECTIVE

Precipitation static (P-static) has plagued aircraft since the introduction of radio communication and navigation systems. P-static is generated when the electrostatic potential acquired by an aircraft surface, through triboelectric charging by particulate matter in the atmosphere (rain, ice crystals, dust, sand or nuclear debris), becomes high enough that sparking, streamering, or corona occurs, thereby producing broadband radio frequency (RF) noise. This vehicle generated noise, although principally viewed as a low frequency phenomena, has a continuous spectrum that can extend into the gigahertz range. Because P-static noise can interfere with the operation of onboard electronics equipment, it is desirable to eliminate this noise, if possible. Since the radome is a primary contributor to the P-static problem and there is always electronic equipment in and around a radome, a reduction or elimination of radome associated P-static is especially desirable. In addition, the severity of the problem is often a function of the distance between the P-static source and the equipment or antenna being interfered with. Again, radome associated P-static can be the most troublesome. Since the surface of a metal coated radome is highly conductive and since the metal coating is grounded to the airframe, accumulated charge is drained from the radome before the electromotive potential necessary to generate P-static builds up.

The grounded metal radome will not be a source of P-static interference because static charge is conducted away as rapidly as it accumulates. However, the presence of a thick (10-20 mil) dielectric (polyurethane) rain erosion coating raised the question of whether sufficient charge could build up on the surface of the coating to cause P-static. The objective then, of these tests was to evaluate the effectiveness of a polyurethane coated metal radome in reducing P-static. It was expected that at some polyurethane thickness, the coating would have sufficient resistance so that all of the charge building up on the panel surface could not bleed through to the copper coating where it could be conducted away, therefore there would be RF noise associated with very thick rain erosion coatings. This in fact, proved to be the case. However, the coating thickness at which that occurred was well

beyond the thickness used for rain erosion protection, i.e., greater than 20 mils.

TEST METHOD

The P-static blown-dust simulator was employed to statically charge the specimens under test. The P-static simulator generates a stream of high velocity (to 400 knots) dust particles that impact the test article causing triboelectric charging of its surface. The flux, velocity, angle of impingement and diameter of particle stream are adjusted to obtain the desired charging rate. Dry high pressure nitrogen gas, generated from a 15,000 gallon LN_2 tank, was used as the accelerating medium. This results in very uniform charging and RF noise generation. The simulator is equipped with a filtered exhaust system to minimize the possibility of the formation of a cloud of charged particles while operating. The field intensities of the radiated emissions were determined by a full compliment of calibrated EMI measuring equipment.

TEST DESCRIPTION

The charging rate was adjusted to 20 amps per ft^2 on an aluminum Panel which is about one-half the worst case charging rate observed on conventional aircraft in flight. The impact area of the particle stream was 5 square inches. These parameters were used for all radiated noise measurements conducted during this test. The test setup is shown in Figure 27.

The test articles were 12 X 12 X 16 inch panels. The two substrate materials used were fiberglass-epoxy and fiberglass-polyimide. Most panels had a slotted metal coating and all panels had a MIL-C-83231, Type I polyurethane rain erosion coating which is available in either black or white. The coating was applied in various thicknesses (and colors because of availability), per Table 7. The Type I coating used here does not have an anti-static topcoat. In all, ten panels were tested. The erosion coating thickness specified is the thickness at the center of the panel as determined by micrometer measurements. The thickness of the heavy coatings (Panels A through E) on a particular panel varied over the surface of the panel by as much as 15%, generally being thicker at the center. The thinner coatings (Panels I through V) were more uniform in thickness. Typical panels are shown in Figure 28 through 30.

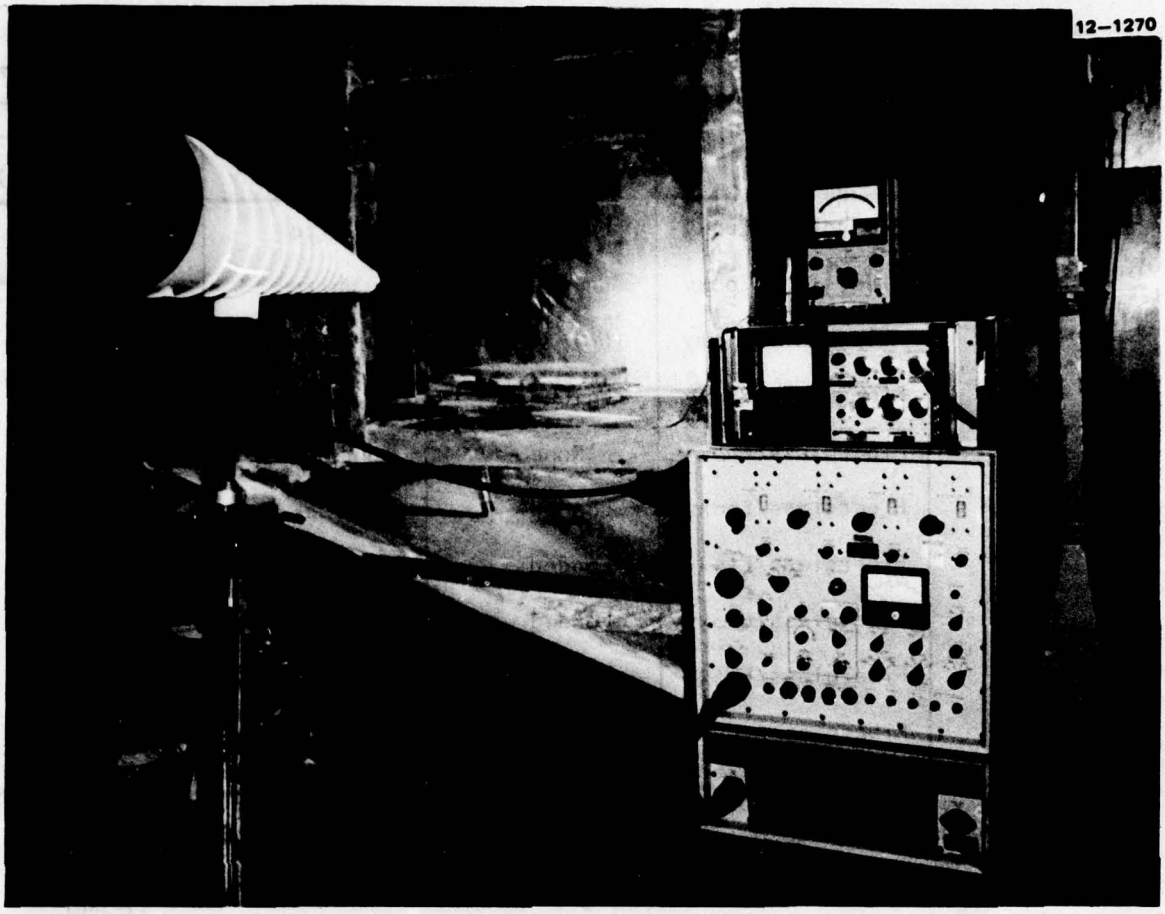

Figure 27 Blown dust p-static simulator

A conductive border was placed around the edges of the panels which did not have a slotted metal coating. A microammeter was used to monitor the charging currents by grounding this conductive border through the microammeter and recording its output on a strip chart recorder. On the panels having a slotted metal coating the microammeter probe was connected directly to the metal coating. A conductive border was also placed around these panels and was grounded. Figure 31 shows a panel, with the slotted metal coating, installed in the Blown Dust Simulator.

Field intensity measurements of the radiated-emissions were conducted at three frequencies per decade from 100 kHz to 10 GHz. Peak values, rather than average values were measured in accordance with MIL-STD-461A, and the distance from the test article to the antenna was standardized at one meter. The EMI measuring equipment that was used is listed in Table 8.

TABLE 7
DESCRIPTION OF TEST PANELS

12-1478

Panel Designation	Substrate Material	Tripolar Slotted Metal Coating Type	Rain Erosion Coating	
			Pigmentation	Thickness At Center (mils)
I	Fiberglass/Epoxy	Unloaded	White	5
II	Fiberglass/Epoxy	Unloaded	White	11
III	Fiberglass/Epoxy	Unloaded	White	15
IV	Fiberglass/Epoxy	Unloaded	White	22
V	Fiberglass/Epoxy	None	White	17
A	Fiberglass/Epoxy	Loaded*	Black	27
B	Fiberglass/Epoxy	Loaded	Black	53
C	Fiberglass/Epoxy	Loaded	Black	67
D	Fiberglass/Epoxy	None	Black	29
E	Fiberglass/ Polyimide	None	Black	34

*Capacitively loaded (conductive propeller within each tripolar slot)

12-1360

Figure 28 P-static test panel with black polyurethane erosion coating and slotted metal coating

12-1351

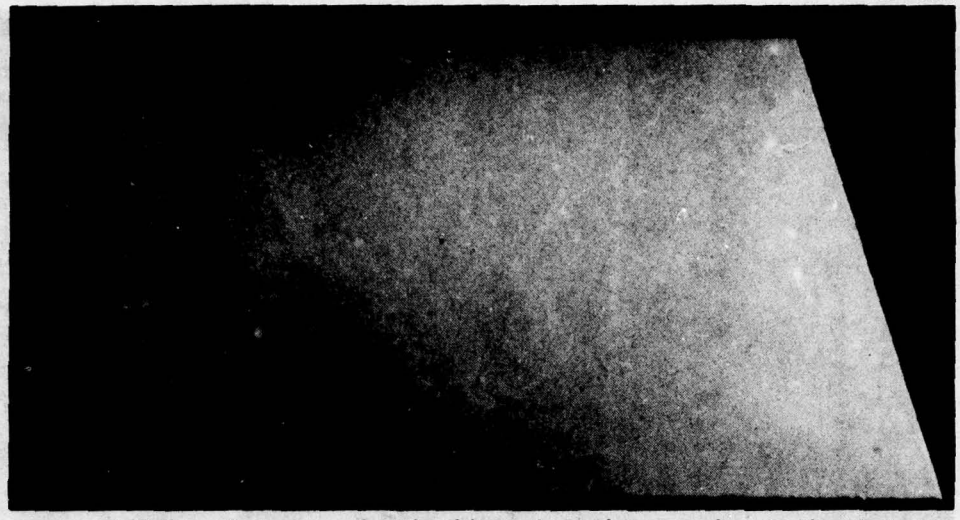

Figure 29 P-static test panel with white polyurethane erosion coating, but no slotted metal coating

12-1352

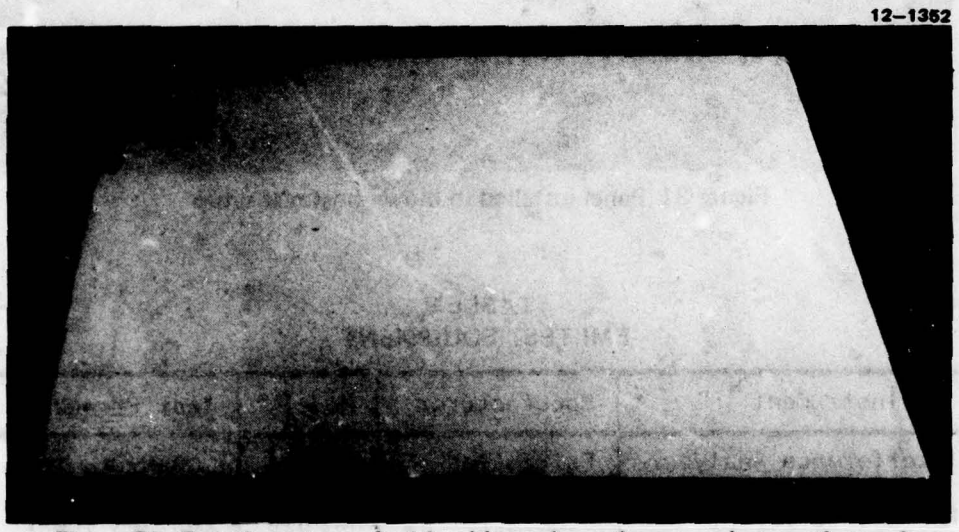

Figure 30 P-static test panel with white polyurethane erosion coating and slotted metal coating

TEST RESULTS

The RF noise and charging currents measured are given in Tables 9 and 10, respectively. For slotted metal coated panels with polyurethane erosion coatings up to a thickness of 22 mils (Panels I through V), no noise above ambient was detected at any frequencies except 200 and 500 kHz. However, noise considerably above ambient was measured from 100 kHz emanating from Panel V, the panel without a slotted metal coating. The noise level from Panel V at 200 to 500 kHz was at least 19 dB greater than the slotted metal coated panels I through IV.

12-1349

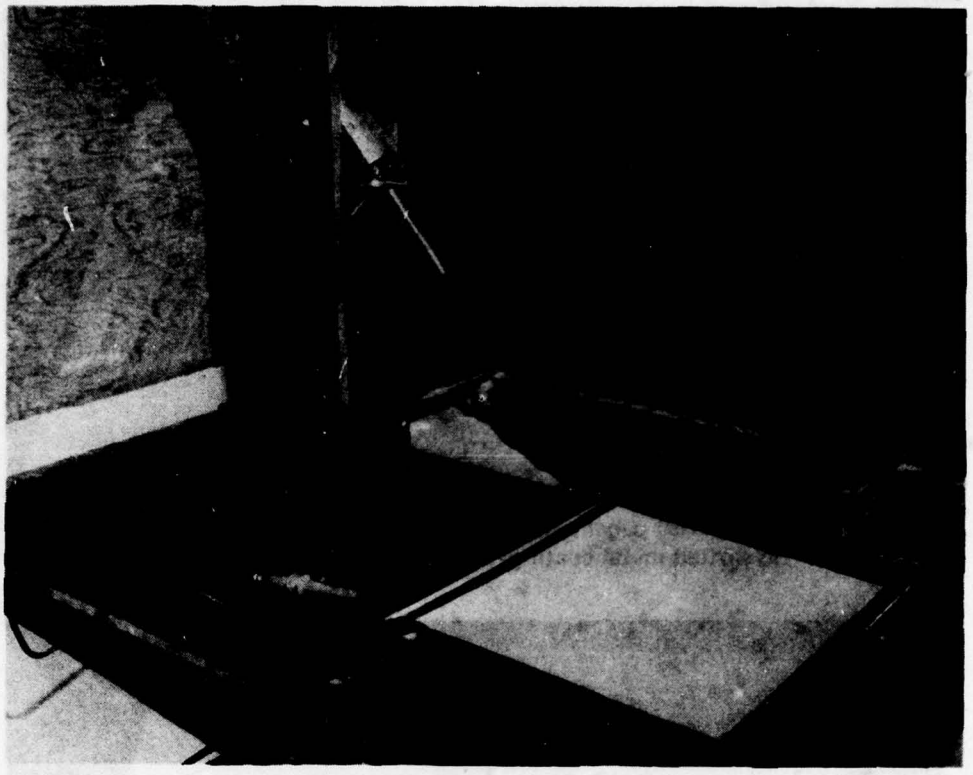

Figure 31 Panel installed in blown dust test setup

TABLE 8
EMI TEST EQUIPMENT

12-1447

Instrument	Manufacturer	Model	Test Frequency
Interference Analyzer	Fairchild	EMC-25	100kHz to 1GHz
Radio Interference Field Intensity Meter	Stoddart	NM-62B	2GHz to 10GHz
Remote Vertical Antenna	Singer	VR-105	100kHz
Vertical Antenna	Empire	VA-105	200kHz to 20MHz
Bi-Conical Antenna	Fairchild	BIA-25	50MHz to 200 MHz
Spiral Cone Antenna	Fairchild	LCA-25	500MHz to 1GHz
Broadband Horn	Sylvania	AN-10	2GHz to 10GHz

TABLE 9 RF NOISE MEASUREMENT RESULTS

Frequency (Hz)	Field Intensity (dBμV/m/MHz)									
	Panel I		Panel II		Panel III		Panel IV		Panel V	
	Ambient	Test	Ambient	Test	Ambient	Test	Ambient	Test	Ambient	Test
100K	121	*	135	*	132	*	129	*	133	140
200K	101.5	112.5	115.5	*	110.5	115.5	109.5	115.5	109.5	136.5
500K	103	*	101	*	102	106	103	*	99	125
1M	101.5	*	101.5	*	102.5	*	105.5	*	100.5	124.5
2M	87.5	*	86.5	*	84.5	*	83.5	*	84.5	105.5
5M	82.5	*	83.5	*	82.5	*	86.5	*	82.5	106.5
10M	76	*	79	*	77	*	82	*	76	99
20M	60	*	66	*	57	*	63	*	58	74
50M	52.5	*	57.5	*	59.5	*	61.5	*	52.5	65.5
100M	45	*	55	*	46	*	50	*	47	55
200M	57	*	54	*	50	*	56	*	55	*
500M	52	*	52	*	57	*	62	*	67	*
1G	55.5	*	50.5	*	49.5	*	49.5	*	51.5	*
2G	27	*	27	*	25	*	25	*	27	*
5G	41	*	40	*	41	*	41	*	40	*
10G	43	*	43	*	46	*	40	*	41	*

Frequency (Hz)	Field Intensity (dBμV/m/MHz)									
	Panel A		Panel B		Panel C		Panel D		Panel E	
	Ambient	Test	Ambient	Test	Ambient	Test	Ambient	Test	Ambient	Test
100K	123	*	125	135	123	139	108	163	121	173
200K	97.5	117.5	97.5	134.5	97.5	135.5	88.5	162.5	97.5	164.5
500K	117	*	106	123	114	129	104	152	119	153
1M	104.5	*	106.5	117.5	102.5	122.5	112.5	137.5	104.5	129.5
2M	100.5	*	92.5	111.5	97.5	116.5	97.5	122.5	95.5	121.5
5M	72.5	82.5	68.5	105.5	70.5	110.5	68.5	105.5	70.5	102.5
10M	77	96	75	110	77	120	72	106	77	111
20M	59	72	59	84	59	85	60	70	58	71
50M	47.5	61.5	37.5	111.5	46.5	101.5	43.5	*	29.5	*
100M	45	66	47	104	46	100	52	*	40	*
200M	50	72	60	108	49	94	53	*	43	*
500M	49	74	56	111	49	103	48	*	55	*
1G	52.5	77.5	60.5	91.5	52.5	82.5	50.5	*	60.5	*
2G	-	-	-	-	-	-	-	-	-	-
5G	-	-	-	-	-	-	-	-	-	-
10G	-	-	-	-	-	-	-	-	-	-

*No RF noise above ambient level detected.

TABLE 10
CHARGING CURRENT RESULTS

12-1448

Panel Designation	μamps	μamps/ft^2
I	-11.1	-320
II	-10.1	-291
III	-12.2	-351
IV	-11.0	-317
V	- 1.6	- 46
A	- 9.4	-271
B	-10.6	-306
C	- 9.3	-268
D	- 1.0	- 29
E	- 1.3	- 37
Aluminum (Reference Material)	- 0.7	- 20

For polyurethane coatings of 27 mils and greater, noise was measured above the ambient levels in proportion to the polyurethane thickness, i.e., the thicker the polyurethane the more noise generated. Panels A, B, C, with slotted metal coatings, had erosion coating thickness of 27, 53, and 67 mils, respectively. Panels D and E, which did not have slotted metal coatings, had erosion coating thickness of 29 and 34 mils, respectively. Panel A showed some noise reduction below 5 MHz while Panels B and C exhibited noise above ambient over the frequency range of 100 kHz to 1 GHz. The noise levels were below those of Panels D and E until a frequency of about 5 MHz, where they unexplainably became higher than the unmetallized panels (D&E). It would appear that when the polyurethane coating gets very thick, like that on Panels B and C, the nature of the substrate becomes less important than that of the coating. The pigmentation of the erosion coating on Panels A through E and the slot pattern in the metal coating on Panels A through C were not the same as that used on Panels I through V, however it is not believed that these variables explain the increase in noise measured on these heavily coated panels.

The fiberglass-polyimide panel (E) exhibited noise characteristics similar to the fiberglass-epoxy panel (D). The scale-up in panel size from the 6 X 6 inch panels used in earlier tests (Reference 13) to the 12 X 12 inch panels used in these tests did not increase the RF noise level. The charging currents measured on all of the panels were negative, indicating a negative polarity charge buildup on the panels. It was found that the measured charging current on the panels with slotted metal coatings was several times greater than that on the panels without metal coatings. It was determined that the current path on the metal coated panels was down through the erosion coating to the metal coating rather than across the surface of the erosion coating to the grounded border, as was true in the case of the panels with no metal coating. The relative voltage levels required for current to leak through the coating, versus flashing across the surface, can be approximated by assuming a dielectric strength of 700 volts/mil for polyurethane coatings and a flashover level of 23 kV/inch (Reference 14). On this basis the surface voltage would be limited to 15.4 kV for a 22 mil coating over grounded metal, whereas the voltage required to flashover about 4 inches of surface to the conductive border would be on the order of 112 kV. Since the charging mechanism is basically a surface phenomenon and the surfaces are essentially the same, it is felt that a similar amount of triboelectric charging is occuring in both cases. The higher surface voltage of the nonmetallized panels undoubtedly plays a role in the lower charging current measured on them. The surplus of negative charge on the surface could be reattaching to impinging particles at a much higher rate than at the lower voltages. Another possible explanation is that a significant amount of the charge on the nonmetallized panels is bleeding off as corona and not being measured by the probe.

CONCLUSIONS

A slotted metallic coating on a dielectric radome eliminates the generation of precipitation static. It was also shown that a metallic coating continues to inhibit generation of P-static even when over coated with a polyurethane rain erosion coating, up to a thickness of about 22 mils. Beyond that thickness, charge which has accumulated on the surface of the polyurethane finds it increasingly difficult to bleed through the polyurethane to the metallic coating underneath. These tests indicate that the upper limit of coating thickness from the P-static standpoint is in the 25 mil range. Since

the polyurethane erosion coating used on the demonstration articles for this program, or any radome will be less than that, there should be no P-static problem with a resonant metal radome. By comparison the P-static noise levels were high for the polyimide and epoxy fiberglass panels which had no metal coatings.

4.4 OTHER ENVIRONMENTAL TESTS

Environmental tests to determine the extent to which radomes of the resonant metal concept will withstand more conventional environmental hazards common to aircraft components were conducted. These tests were conducted in conformance with MIL-STD-810 and consisted of those tests commonly found in aircraft radome specifications, i.e., sunshine, temperature/humidity/altitude, and fluid immersion. In addition, an accelerated corrosion test was performed to determine if the polyurethane rain erosion coating will protect the metal from corrosion.

TEST METHOD

A total of 25 slotted metal specimens, described in Table 11, were evaluated per the matrix shown in Table 12. The "plate and etch," "wallpaper" and "electroform" approaches were tested. Nickel and copper slotted metal coated specimens were prepared of each approach, except for the wallpaper approach, where copper specimens only, were tested. All specimens were coated with 12 mils of MIL-C-83231 (black) polyurethane rain erosion coating, since that coating will be required for rain erosion protection. Figure 32 shows a typical group of specimens before testing. At the end of each exposure, the coatings were examined for detrimental effects such as blistering, peeling, cracking, crazing, and softening. Then they were adhesion tested by the dry tape method, which is the standard coating adhesion test used to determine the adhesion of finish systems used on aircraft. The specimens, after exposure are pictured in Figures 33-37. The metallic coating and substrates were examined, after removal of a patch of polyurethane coating, to determine environmental effects on them, if any. The tests were as follows:

Sunshine - Specimens representing each approach (five total) were exposed for 100 hours to high intensity ultraviolet light as described in MIL-STD-810, Method 505, Procedure I, using a Schoeffel 26 kW Xenon arc lamp as the source

TABLE 11

DESCRIPTION OF THE FIVE GROUPS OF SLOTTED METAL RADOME TEST SAMPLES

12-1439

Group	
A	Curved pieces, 4.5" x 5", copper coated on convex sides by electroform approach.
B	Curved pieces, 4" x 5", nickel coated on convex sides by electroform approach.
C	Curved pieces, 6" x 7", copper coated on convex sides by plate and etch approach.
D	Curved pieces, 6" x 7", nickel coated on convex sides by plate and etch approach.
E	Curved pieces, 8" x 8", copper coated on convex sides by wallpaper approach.

of radiation. The surface temperature of the coating during the sunshine exposure was 200-220°F, as measured with a thermocouple. Only the convex side of each specimen was irradiated with the lamp. The polyurethane coating on all of the specimens was crazed, softened, and blistered as a result of the exposure. The tape adhesion test resulted in coating failure in the area of the blisters, and the adhesion failure was between the primer and the polyurethane coating, not between the metal and the primer (Figure 33).

Temperature/Humidity/Altitude - Specimens representing each approach (five total) were cycled per method 518.1, MIL-STD-810. Method 518.1 requires cycling from standard ambient conditions to an altitude of 50,000 feet and a temperature of -54°C, return to ambient with 95 percent relative humidity, increasing temperature to +65°C maintaining 95 percent relative humidity, and a slow decrease in temperature back to ambient with 95 percent relative humidity. The specimens were cycled 4 times. During the humidity segment of the second cycle there was an equipment failure resulting in a 16 hour delay in completing that cycle. However, the problem was corrected and the test completed. The polyurethane coating on two of the specimens had blistered slightly. This is not unusual for the MIL-C-83231 polyurethane coating; it

TABLE 12

TABLE xx ENVIRONMENTAL EXPOSURES AND TEST RESULTS

12-1479

Spec. No.	Environmental Exposure	Coating Condition After Exposure	Adhesion Test (PS 13500)	Substrate Protection Provided by Coating During Environmental Exposure
A1	Sunshine	Severely crazed. One large blister	Failed at blister	Complete
B1	Sunshine	Severely crazed. Three blisters	Failed at blisters	
C1	Sunshine	Severely crazed. One medium blister	Failed at blister	
D1	Sunshine	Severely grazed. One large blister	Failer at blister	
E1	Sunshine	Severely crazed. No blisters	Passed	
A2	Salt Spray	Not Affected	Passed	Complete
B2	Salt Spray	Not Affected	Passed	
C2	Salt Spray	Not Affected	Passed	
D2	Salt Spray	Not Affected	Passed	
E2	Salt Spray	Not Affected	Passed	
A3	Temp-hum-alt	Slight softening	Passed	Complete
B3	Temp-hum-alt	Slight softening	Passed	
C3	Temp-hum-alt	Slight softening	Passed	
C3	Temp-hum-alt	Slight softening. Three small blisters on concave side but disappeared later	Passed	
E3	Temp-hum-alt	Slight softening. Six small blisters on convex side, but disappeared later	Passed	
A4	4 hrs in JP-4 fuel	Slight softening	Passed	Complete
B4	4 hrs in JP-4 fuel	Slight softening	Passed	
C4	4 hrs in JP-4 fuel	Slight softening	Passed	
D4	4 hrs in JP-4 fuel	Slight softening	Passed	
E4	4 hrs in JP-4 fuel	Slight softening	Passed	
A5	4 hrs in MIL-H-5606	Slight softening	Passed	Complete
B5	4 hrs in MIL-H-5606	Slight softening	Passed	
C5	4 hrs in MIL-H-5606	Slight softening	Passed	
D5	4 hrs in MIL-H-5606	Slight softening	Passed	
E5	4 hrs in MIL-H-5606	Slight softening	Passed	

12-1286

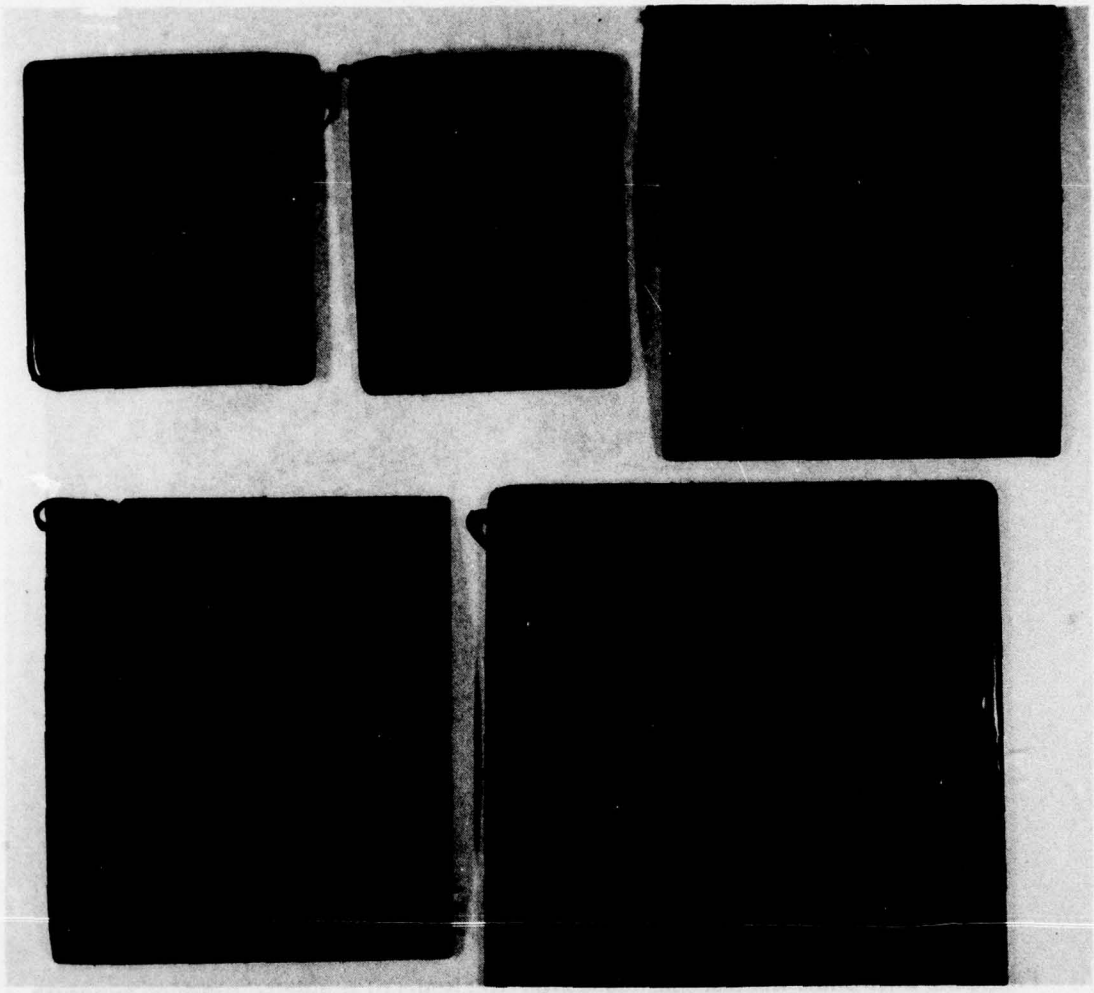

Figure 32 Typical environmental test specimens before exposure

Figure 33 Environmental test specimens after 100 hours of simulated sunshine exposure

12–1283

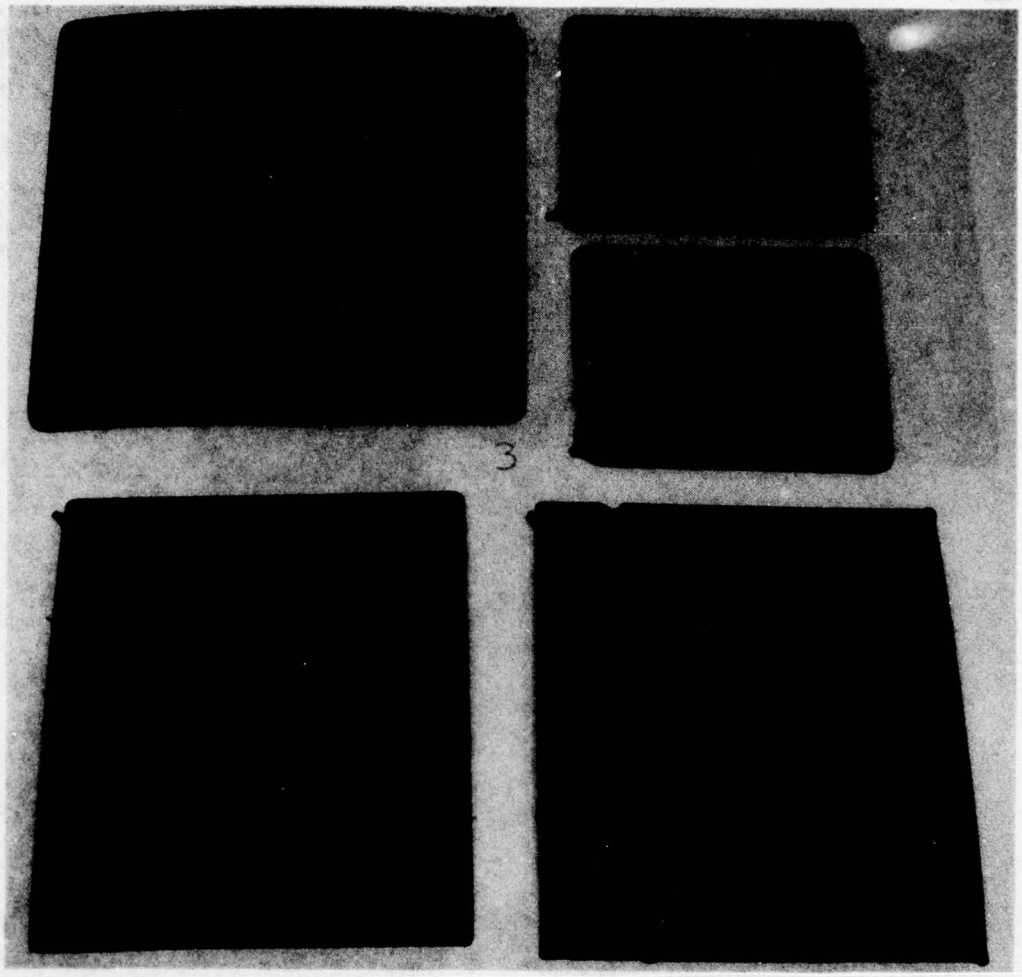

Figure 34 Environmental test specimens after exposure to temperature/humidity/altitude cycling

12–1282

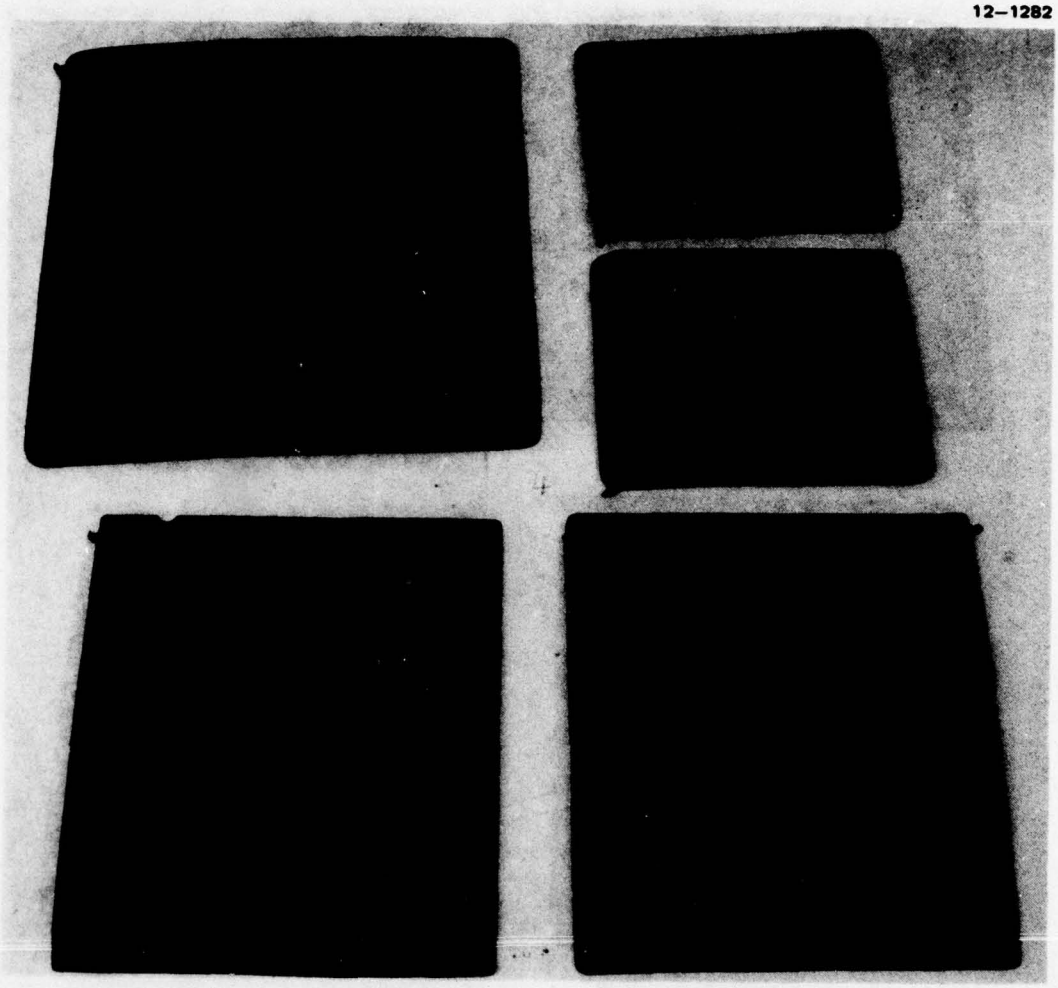

Figure 35 Environmental test specimens after 4 hours immersion in JP-4 fuel

12-1281

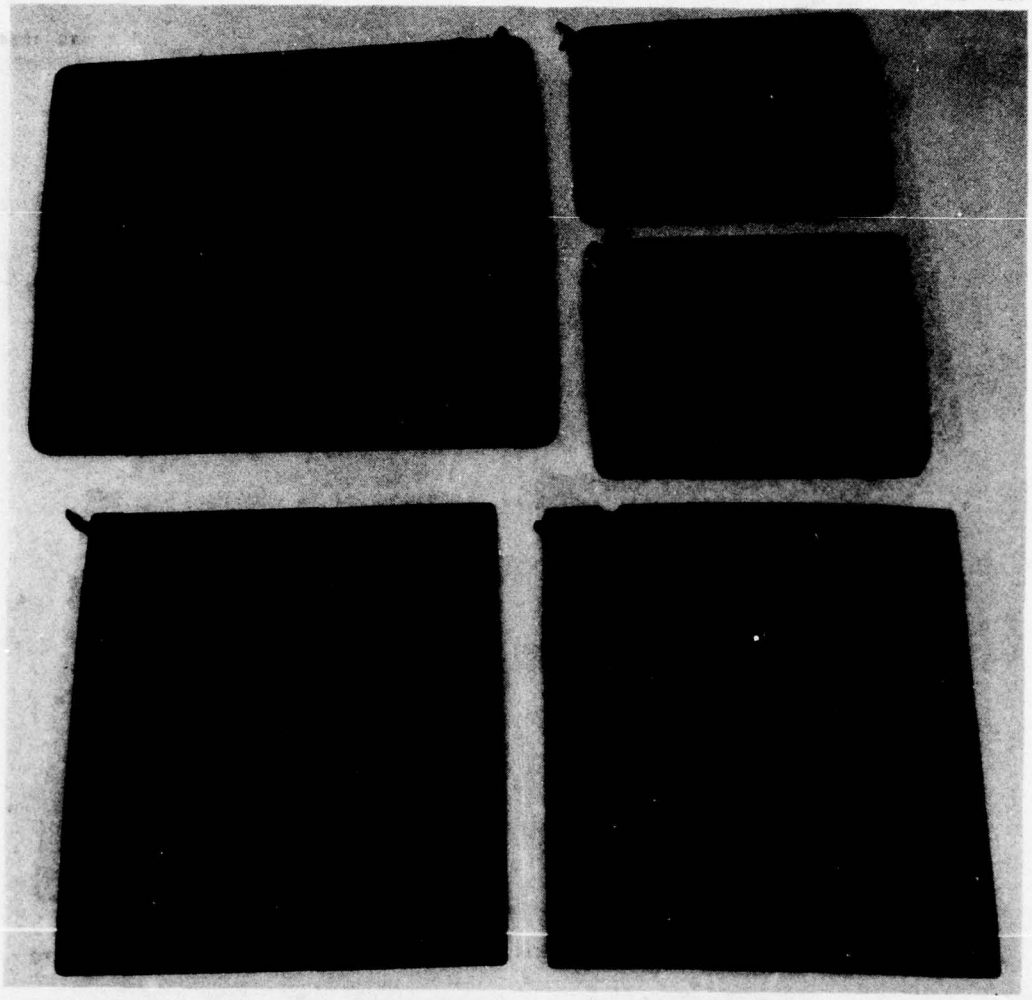

Figure 36 Environmental test specimens after 4 hours immersion in MIL-H-5606 hydraulic fluid

12–1284

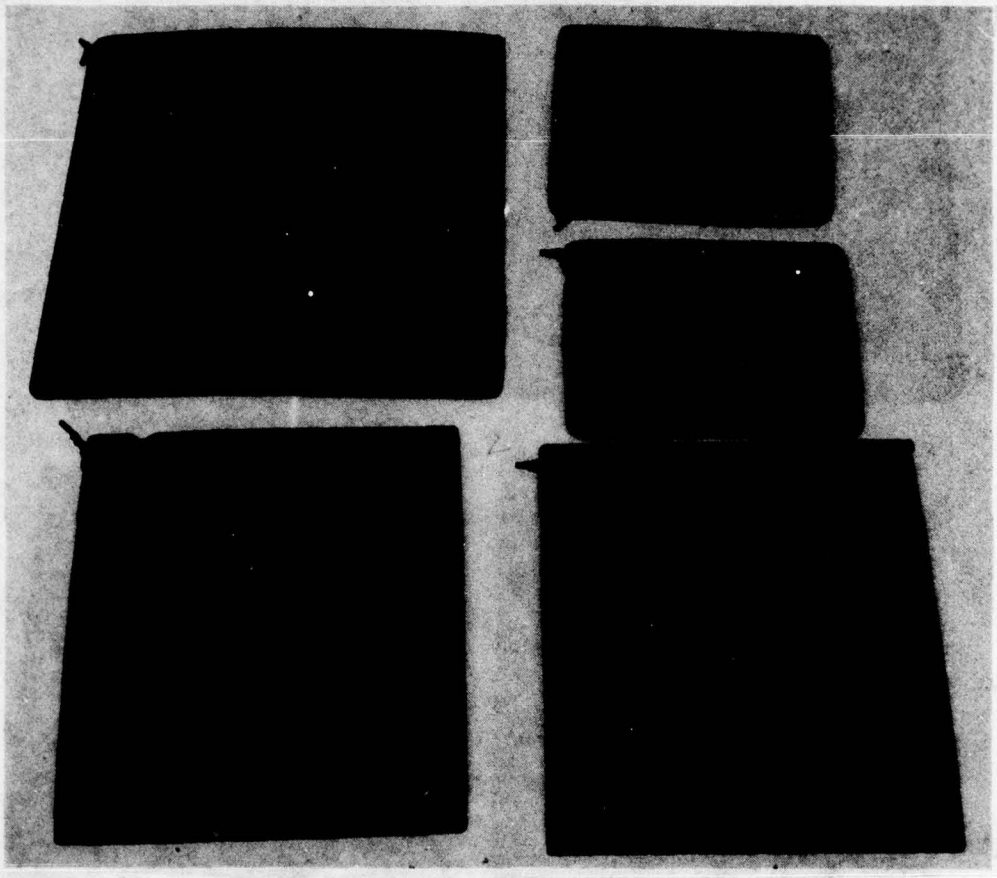

Figure 37 Environmental test specimens after 240 hours of 5% salt spray exposure

has been observed during testing of full sized radomes by Brunswick on many occasions, and is believed to be caused by minute pin holes introduced during application of the coating. Like the sunshine test results, the blistering is a characteristic of the polyurethane coating, not the slotted metal coating or radome substrate. The blisters disappeared after a short period of ambient storage and the coating passed the adhesion test (Figure 34).

Fluid Immersion - These tests were conducted in accordance with MIL-R-7705B which requires four hours immersion in fluids common to the operation and maintenance of the aircraft. Five specimens representing each configuration were tested at room temperature in jet fuel (JP-4) and hydraulic fluid (MIL-H-5606C) for the required four hours. Immersion of the specimens in the two fluids resulted only in slight softening of the polyurethane coating (Figures 35 and 36). The coating passed the adhesion test.

Corrosion - Because of the unique construction of the resonant metal radome when compared with conventional radomes, an accelerated corrosion test was conducted on specimens of each approach. Salt fog tests were performed in accordance with method 509.1, Procedure I, of MIL-STD-810 which calls for 240 hours of exposure to 5 percent salt fog spray. No adverse effects to the coatings or the specimens were noted and the coatings passed the adhesion test (Figure 37).

CONCLUSIONS

The above environmental tests show that a metallized radome made by any of the methods being considered will resist exposure to adverse environments encountered by aircraft. In all of the tests, the fiberglass-epoxy substrate, the slotted metal coating, and the bond between the two were all unaffected by the exposure. The polyurethane rain erosion coating, the only thing affected by the tests, is easily repaired or replaced and would only have required replacement after the sunshine exposure. Our testing was obviously severe since this coating has been in service for years and the effects noted in this test have not occurred in the field. There was no difference in the results between the copper and the nickel specimens.

SECTION V

ELECTRICAL TESTING

Since the ultimate success of the resonant metal radome will depend to a great extent on the RF performance of the concept, a major part of the program addressed the characterization of the electrical performance of metallized specimens and demonstration radomes. The results of tests conducted with slotted metallic specimens are reported in detail in this section and the results obtained with the full scale demonstration radomes are discussed in the next section (Section 6.0).

The electrical design of the demonstration articles for this program was performed by the Ohio State University ElectroScience Laboratory (OSU) under a separate contract with the Air Force Avionics Laboratory. The specifics of the design are detailed in Reference 15 and discussed briefly in this section (paragraph 5.2).

5.1 OUT OF BAND ATTENUATION MEASUREMENTS

BACKGROUND AND OBJECTIVE

An important part of the interest in resonant metal radomes is their potential for providing protection against electromagnetic pulse, and for filtering out other electromagnetic interference such as precipitation static. These advantages are in large part a function of out of band attenuation. Tests were conducted therefore to measure the amount of attenuation provided by slotted metallic specimens, at frequencies apart from the resonant frequency of the specimen.

Electromagnetic Pulse (EMP) is the large burst of electromagnetic energy associated with a nuclear explosion in or near the atmosphere. EMP can cause severe disruption of, and sometimes damage to, electrical and electronic equipment at distances where other weapon effects such as nuclear radiation, blast, thermal effects, dust, debris, and biological effects are all absent. This energy has characteristic frequencies which are for the most part below

10 megahertz. Since virtually all airborne radars operate above 1000 megahertz, a narrow band radome which only transmits energy at or near the operating frequency of the radar could reasonably be expected to filter out much of the energy associated with EMP. The response of a system, an aircraft for instance, to EMP is dependent upon not only the response of the individual component parts of the system, but upon the response of the complete aircraft configuration. It is reasonable, however, to assume that a system whose individual component parts are not EMP hardened will not itself be hard. Therefore, we were interested in evaluating resonant metal radome material in a component level test setup since it is not within the scope of this program to evaluate the entire radome/ aircraft assembly.

Like EMP, radio frequency (RF) noise associated with precipitation static,* although extending into the gigahertz range, is principally a low frequency phenomena. Therefore, it is possible to filter out this type of noise with a bandpass filter. The following tests demonstrate that the resonant metal radome configuration acts very much like a bandpass filter, and that it is an effective method for shielding the avionics bay located aft of the radome.

TEST METHOD

The attenuation of out of band frequencies was measured on one singly coated specimen and one doubly coated specimen (biplanar array). The attenuation measurements were performed over the frequency range of 100 kHz to 12 GHz. This frequency range was selected to provide the necessary attenuation information to both EMP frequencies and the frequencies associated with P-static. The attenuation measurements from 100 kHz to 1 GHz were performed using MIL-STD-285 techniques. Measurements above 1 GHz were performed using MIL-STD-1377 techniques.

MIL-STD-285 is a requirements and verification specification for shielded enclosures. Testing per MIL-STD-285 utilizes a shield room in which one wall of the room is modified to incorporate the article being tested. By transmitting energy from inside the room and measuring the energy penetrating the article under test, the article's shielding effectiveness can be determined.

*Refer to Section 4.3 for further discussion of precipitation static.

The MIL-STD-285 type procedure used in these tests is illustrated in Figure 38. The power transfer between the two antennas is measured in two configurations, first in free space and then with the slotted metal radome specimen being tested, placed between the antennas. The difference in received power, expressed in dB, for the two measurements (keeping the transmitted power constant) is the shielding effectiveness of the test specimen. At each test frequency the receiving antenna is physically oriented for maximum receiver indication.

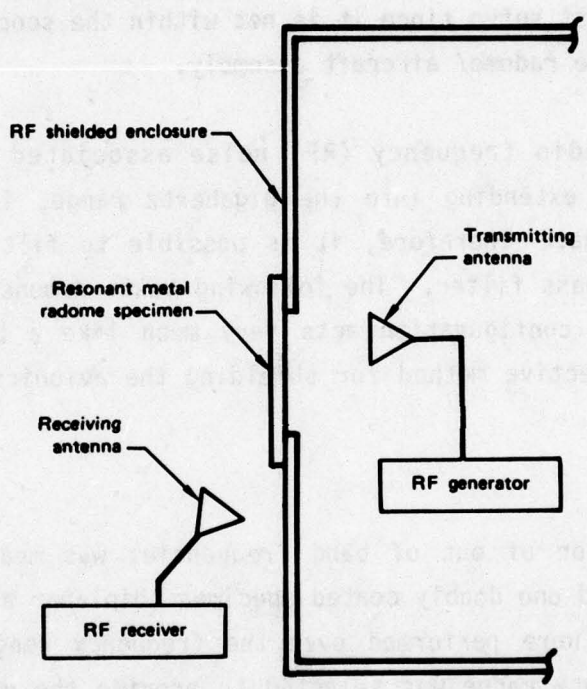

Figure 38 MIL-STD-285 type test setup

The MIL-STD-1337 procedure is not used at low frequencies because of the size limitations of the test cabinet; however, it is the new and preferred method of testing and, therefore, was used in these tests for the frequencies above 1 GHz. In this procedure, illustrated schematically in Figure 39 and pictured in Figure 40, the metal radome specimen was mounted on one wall of a small enclosure. This enclosure was then placed in a larger test cabinet. The shielding effectiveness is determined by injecting RF power into the test cabinet and measuring the received power on an antenna internal to the small

enclosure. The transmitting antenna is placed around three walls of the test cabinet and electrically isolated from the walls. The receiving antenna runs the length of the smaller enclosure and is electrically bonded to the device at each end, with a center tap connected to the receiver. The power received by the internal antenna is measured with and without a reference discontinuity placed in the small enclosure. The reference discontinuity is a two-foot length of wire that penetrates the device (one foot internal and one foot external). The discontinuity couples energy into the device, and is used as the zero shielding reference. With a constant input power, the difference in received powers (with and without the reference discontinuity) expressed in dB, is the shielding effectiveness of the device.

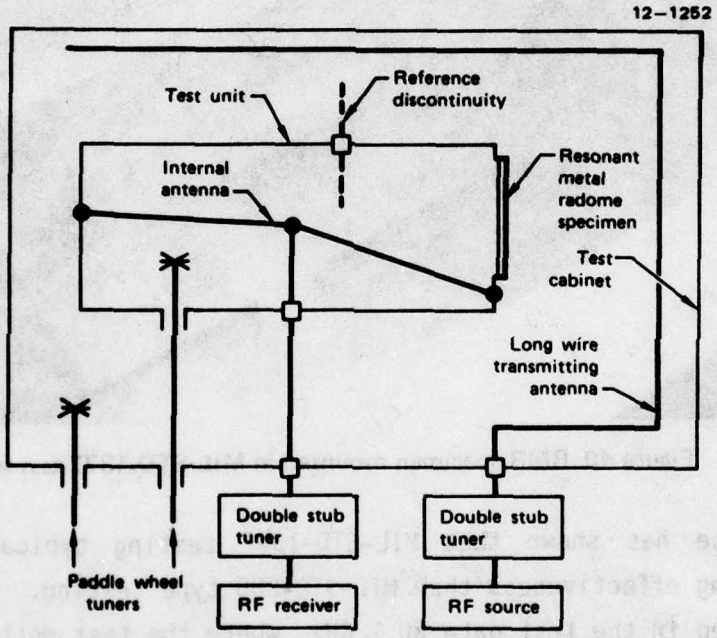

Figure 39 MIL-STD-1377 test setup

When making the two measurements, several tuning procedures are utilized to give a maximum receiver indication. Double stub tuners located on the input and output cables are used to obtain an impedance match at the particular test frequency. Paddlewheel tuners, which can be rotated and moved longitudinally, are used to orient the fields inside both the test cabinet and the enclosure under test for maximum receiver indication.

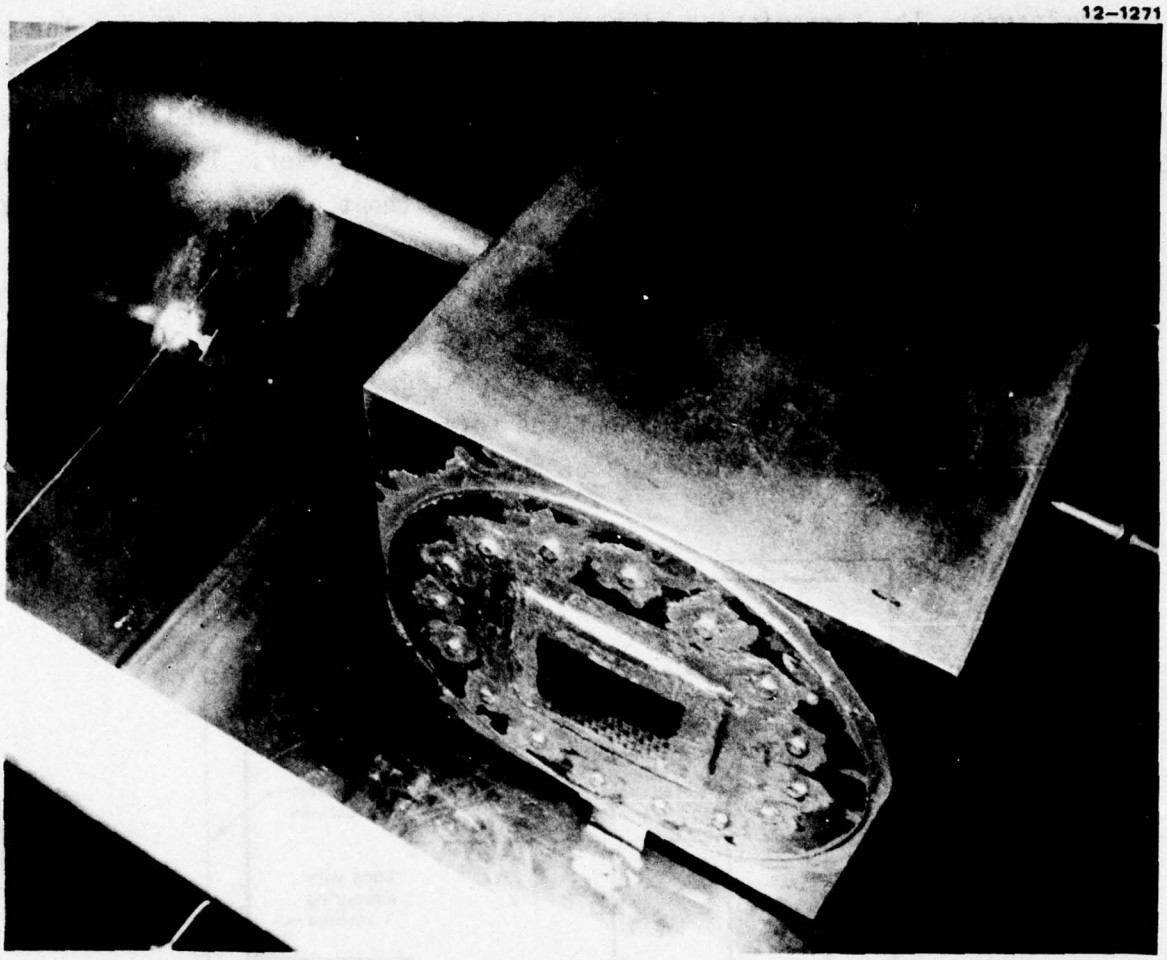

Figure 40 RMR specimen mounted in MIL-STD-1377 test setup

Experience has shown that MIL-STD-1377 testing typically indicates a lower shielding effectiveness than MIL-STD-285 type testing. Because of this, there is a step in the test data at 1 GHz, where the test method switches from MIL-STD-285 to MIL-STD-1377.

TEST RESULTS

Two configurations were tested. The first, a singly coated (8 x 8 inch) specimen with an 0.080 inch fiberglass-epoxy substrate, was tested using both the 285 and 1377 Military Standard methods to cover the entire range of frequencies, 100 kHz to 12 GHz. Attenuation measurements were made at 4 frequencies per decade from 100 kHz to 1 GHz and then every 0.5 GHz from 1 to 12 GHz. The results are plotted in Figures 41 and 42. The performance of the singly

coated specimen at resonance is the result of a design fault in the substrate and should not be interpreted as the optimum performance achievable.

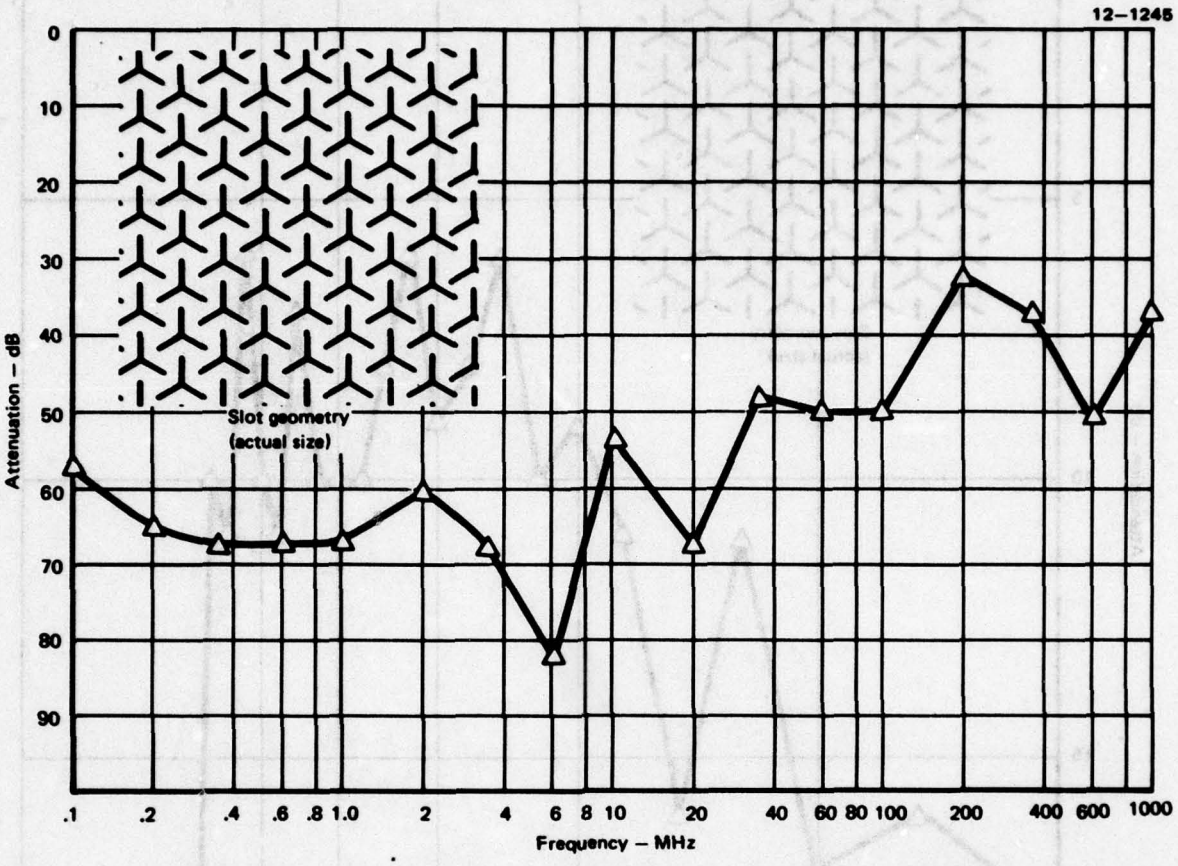

Figure 41 Attenuation of a singly coated specimen. (0.1 MHz – 1000 MHz)

The other configuration tested was the biplanar array pictured in Figure 43. This specimen consists of a foam core (dielectric constant of approximately 1.1) sandwiched between two 5 mil thick slotted copper panels. The biplanar array is of interest because of its potential to further reduce bandwidth over the singly coated specimens (Reference 16). Only the MIL-STD-1377 test was performed on the biplanar array because it was anticipated that the most significant changes in transmission would occur in the frequency range covered by this test. The results of this test are plotted in Figure 44. Additional data points were taken near the resonant frequency of the biplanar array to illustrate the sharp cutoff near the resonant frequency. Incidently, it is not necessary for the slot elements to be indexed one over the other, for the biplanar array to work, thereby facilitating the fabrication process.

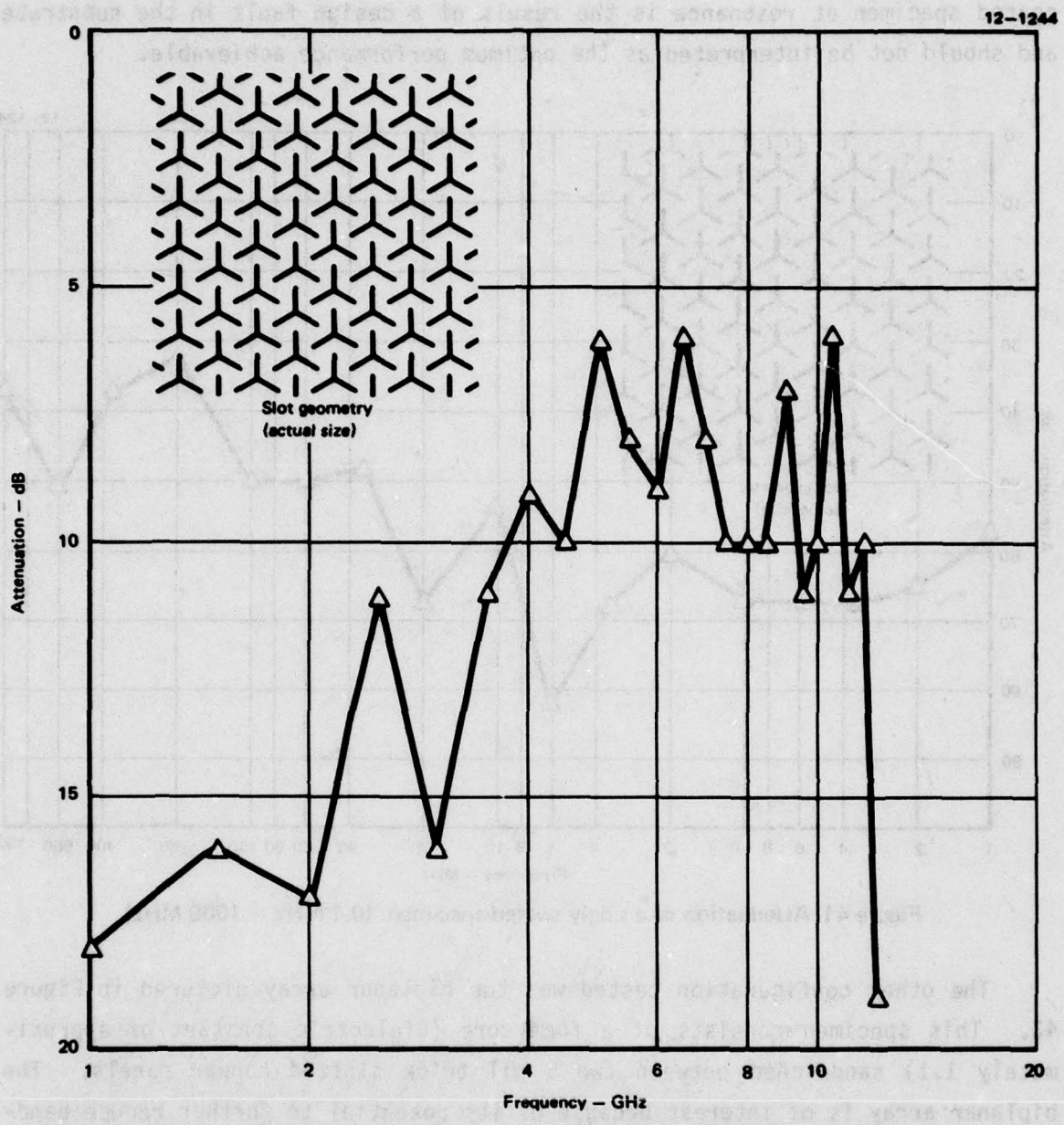

Figure 42 Attenuation of a singly coated specimen (1 GHz – 12 GHz)

A third configuration had been tested earlier and is included here for completeness. It was a 5 x 5 inch double curved specimen, made by the wallpaper technique and utilized the centerloaded slot element. The MIL-STD-1377 test was performed and the results are shown in Figure 45.

(a) Top view

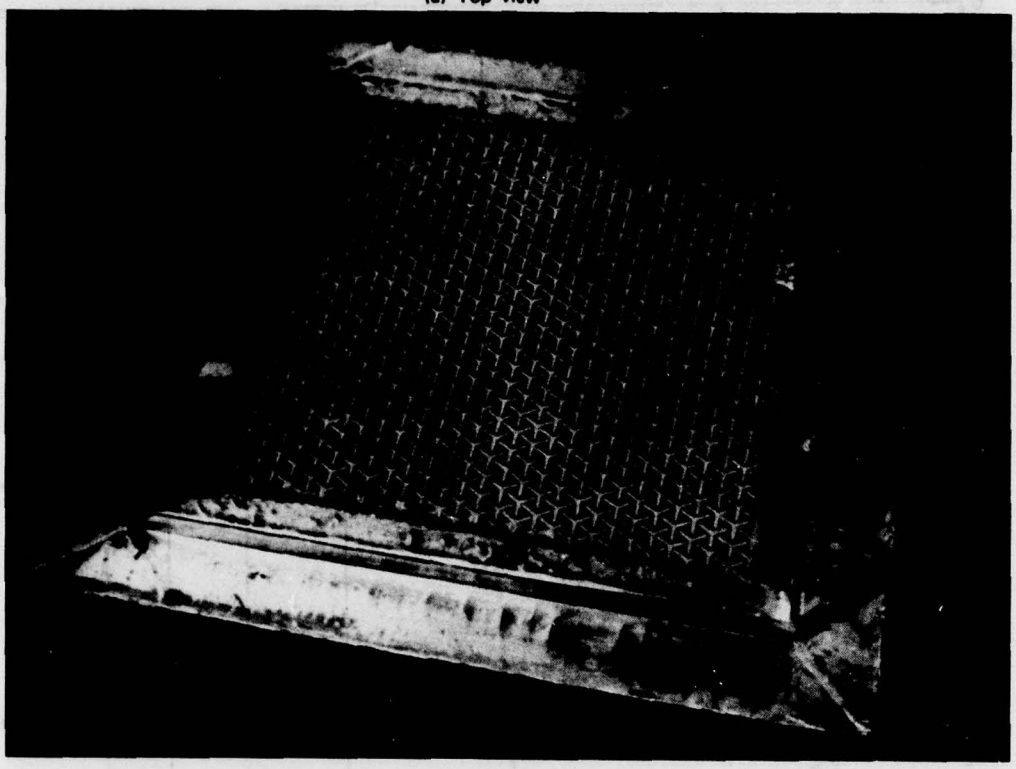

(b) Bottom view

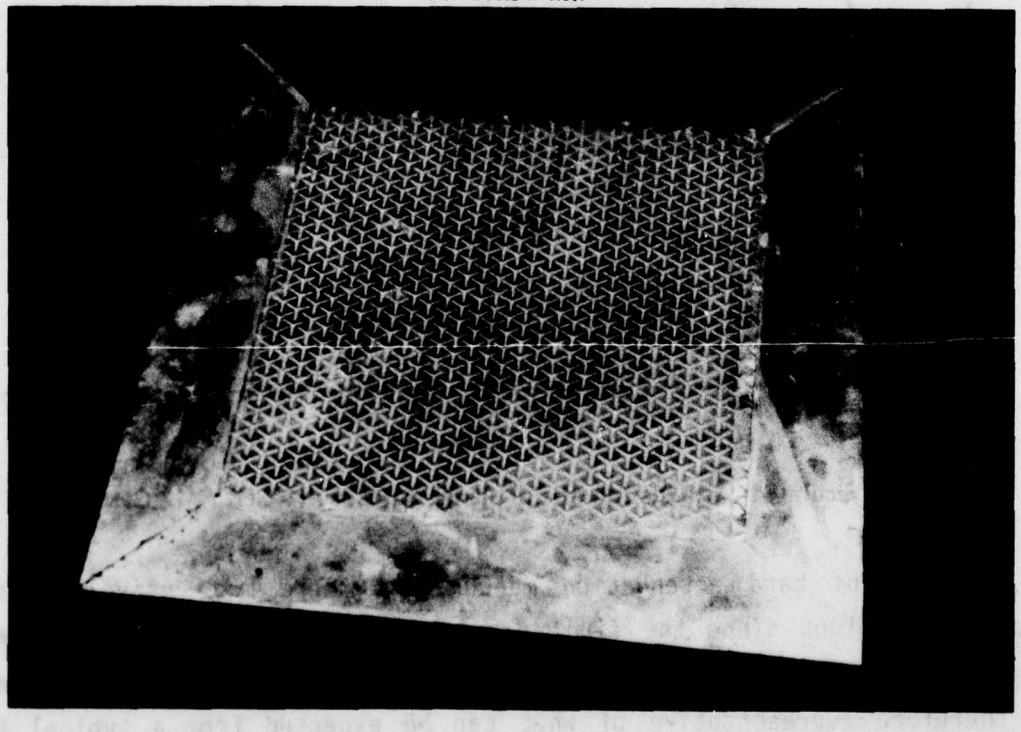

Figure 43 Biplanar slot array

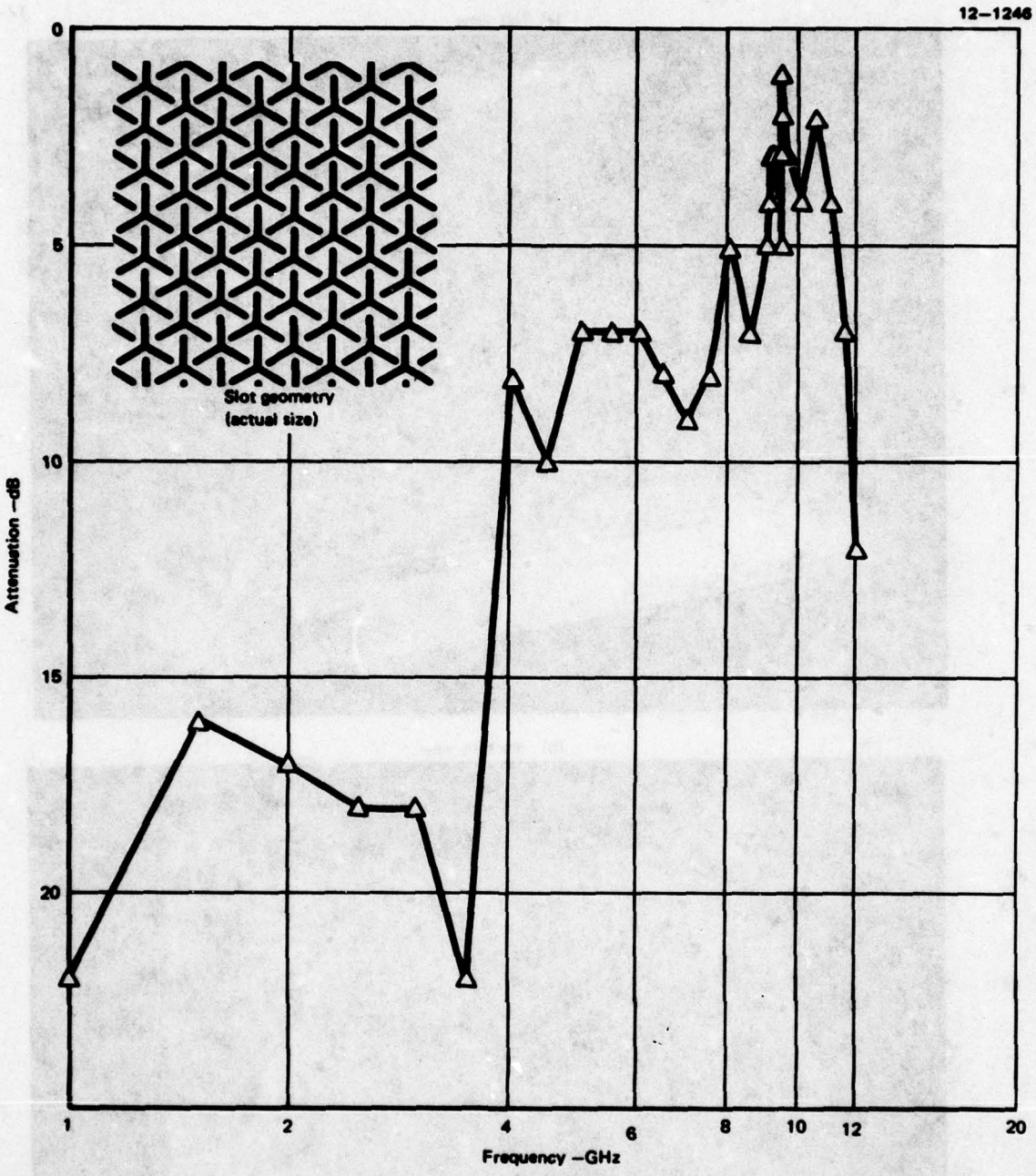

Figure 44 Attenuation of a bi-planar slot array (1 GHz – 12 GHz)

The out of band attenuation measurements were made using preliminary electrical designs since the final design was not available until after the attenuation measurements were completed. The results of these measurements are therefore representative of what can be expected from a typical X-band

design. In addition, this type of radome construction can be refined by design, to broaden or reduce bandwidth within certain limits. Reference 5 discusses this further.

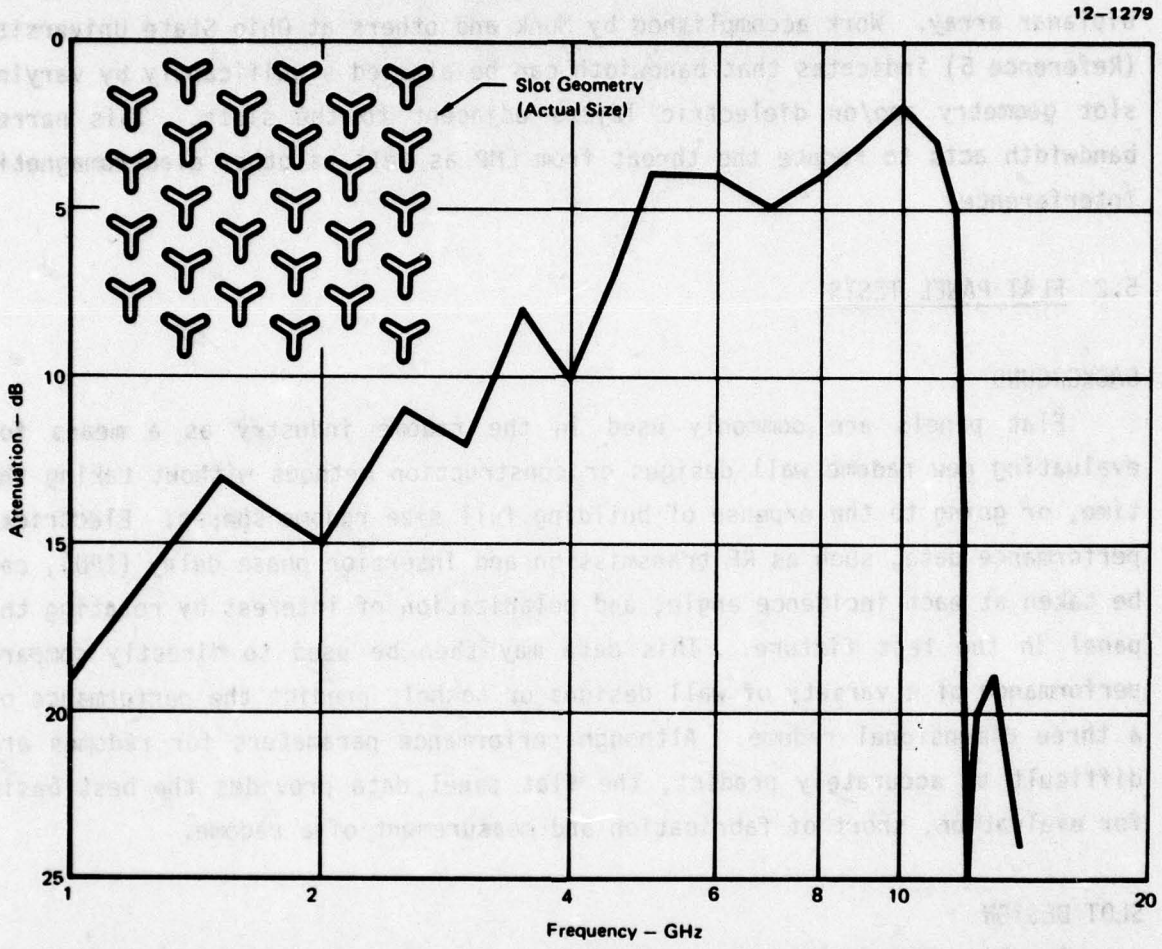

Figure 45 Attenuation of a singly coated specimen centerloaded design (1 GHz – 15 GHz)

CONCLUSIONS

These tests confirm the results of work done by others and demonstrate that the resonant metal radome does indeed act as a bandpass filter and that significant out-of-band attenuation can be achieved with a metal radome. This attenuation is especially pronounced at the lower frequencies where energy due to EMP and P-static is concentrated. A resonant metal radome would provide several orders of magnitude of protection (each 10 dB attenuation is an order of magnitude reduction in power or energy) to sen-

sitive electronic components located under the radome. With a standard non-metallic radome the total RF environment would impinge on the electronics, and appropriate protection would have to be incorporated into the housing and cable shielding. In addition, sharper cutoff is possible through use of the biplanar array. Work accomplished by Munk and others at Ohio State University (Reference 5) indicates that bandwidth can be altered significantly by varying slot geometry and/or dielectric layers adjacent to the slots. This narrow bandwidth acts to reduce the threat from EMP as well as other electromagnetic interference.

5.2 FLAT PANEL TESTS

BACKGROUND

Flat panels are commonly used in the radome industry as a means for evaluating new radome wall designs or construction methods without taking the time, or going to the expense of building full size radome shapes. Electrical performance data, such as RF transmission and insertion phase delay (IPD), can be taken at each incidence angle, and polarization of interest by rotating the panel in the test fixture. This data may then be used to directly compare performance of a variety of wall designs or to help predict the performance of a three dimensional radome. Although performance parameters for radomes are difficult to accurately predict, the flat panel data provides the best basis for evaluation, short of fabrication and measurement of a radome.

SLOT DESIGN

As already mentioned, the slot designs for this program were furnished by OSU under a parallel Air Force Avionics Laboratory project. The slot pattern was designed especially for application to the Lockheed Jetstar (C-140) radome chosen as the demonstration radome. Several patterns were considered early in the program, including the center loaded design shown in Figure 11. However, the loaded design was rejected because of the susceptibility of the center loading element to delamination during rain erosion and lightning testing. The advantage of the centerloaded element is that it is less sensitive to frequency shift at higher incidence angles. Since the Jetstar radome has a

low fineness ratio, the incidence angles in the Jetstar radome were not particularly high; therefore it was decided that an unloaded slot design could be used. It should be pointed out for future applications which have higher fineness ratios, that there are other methods for loading the slots which do not involve the somewhat troublesome center loading element. References 8 and 19 discuss these other methods.

The slot geometry and layout designed by OSU for the Jetstar radome is described in Reference 15 and discussed briefly in this paragraph. Since a double curved surface, like our radome, cannot be unfolded and laid out flat, i.e., is not a developable surface, it is impossible to arrange a perfectly periodic slotted array on its surface. However, a high degree of periodicity is desired for good electrical performance. It was necessary, therefore, to approximate the radome as a developable surface in order to lay out the slots in a near periodic arrangement. Since in this program the slots were arranged on a triangular grid, it was natural to approximate the radome shape with an arrangement of isosceles triangles. This approximation scheme is depicted in Figure 46. It was arrived at through several iterations of trial fittings, the object of which was to reduce the number of different types of triangles required. The triangles (all isosceles) are of four basic types, where the angle between the equal sides are 50, 56, 60 or 70 degrees. The lengths of the sides vary from two or three inches near the tip of the radome, to 8 or 10 inches near the back edge where the degree of double curvature is smaller. The grid angle (the slot elements were arranged on a triangular grid and the angle between the intersecting lines of that grid is referred to as the grid angle) of the slotted array is the same as the angle between the equal sides of the triangles, i.e., 50, 56, 60 or 70 degrees so that the triangles could be cut out along a row of slot elements.

Work accomplished at OSU and reported in Reference 1 demonstrated that the 120° tripolar slot element has good frequency stability with changes in angle of incidence, and has low cross polarization when the elements are arrayed in an equilateral grid. However, when the grid angle is skewed to the 50°, 56° or 70° grid angle just discussed, cross polarization and subsequent loss of transmission occurs. It is possible to compensate for this effect by altering the angle between the legs of the tripolar slot elements (Reference

15). The slot element used with the equilateral grid (60°) triangle is shown in Figure 47a, and the element which compensates for the skewed grid (50°, 56°, and 70°) triangles is shown in Figure 47b. The four slot patterns used on the four types of triangles are illustrated in Figures 48 and 49.

12-1275

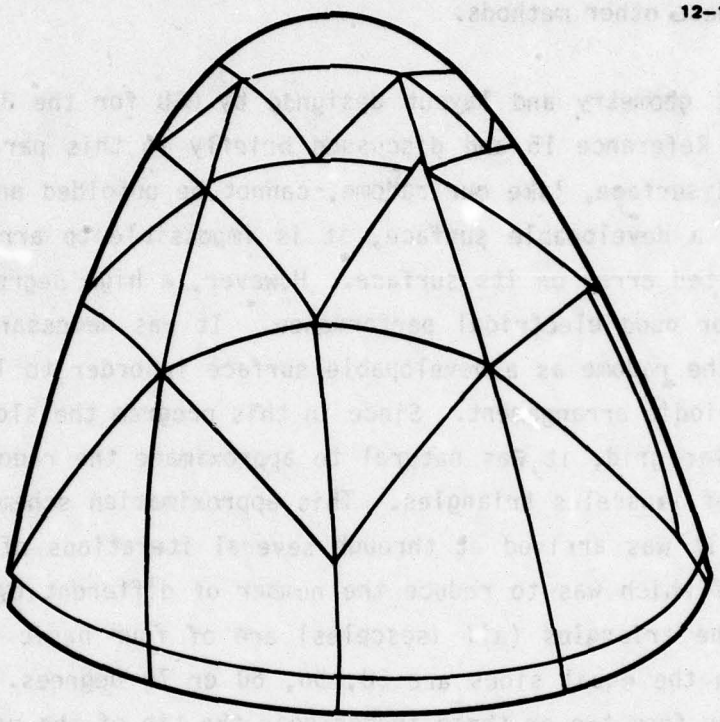

Figure 46 Flat pattern, single curvature approximation, of the Jetstar radome

12-1437

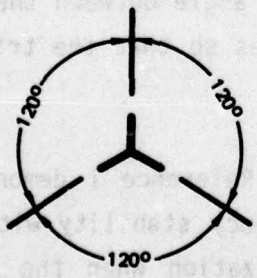

(a) Element used on the 60° triangles

(b) Element used on the 50°, 56°, and 70° triangles

Figure 47 The two slot element designs used for the flat panels and on the radomes

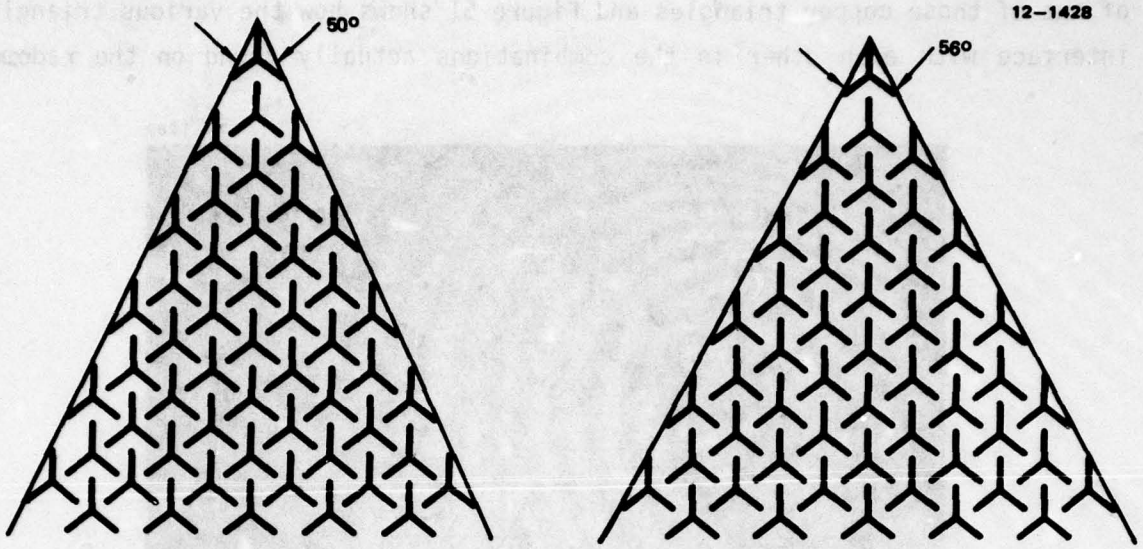

Figure 48 Slot patterns with 50° and 56° grid angles as used on the 50° and 56° triangles

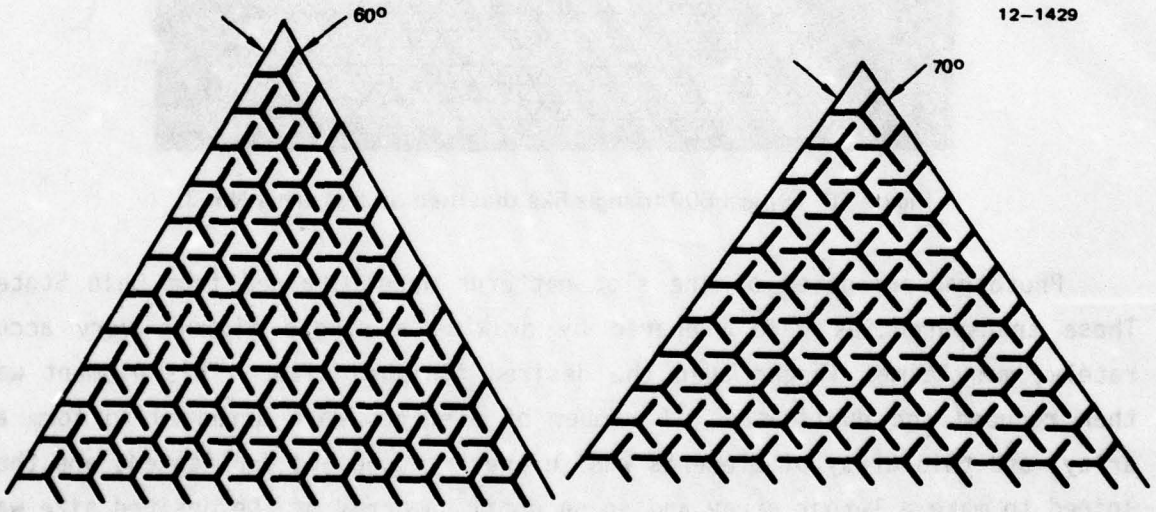

Figure 49 Slot patterns with 60° and 70° grid angles as used on the 60° and 70° triangles

Because of the slot density and resulting overlap of slot element legs it was necessary to cut the edges of the triangles in a zigzag or serrated fashion to avoid cutting across elements when cutting out the triangles. Since the wallpaper fabrication method was selected, it was natural to choose the slotted copper panels to be the same size and shape as the triangles described in the OSU report and shown in Figure 46. Figure 50 is a photograph

AD-A067 547 MCDONNELL DOUGLAS ASTRONAUTICS CO ST LOUIS MO F/G 17/9
EXPLORATORY DEVELOPMENT OF RESONANT METAL RADOMES.(U)
JUL 78 W R BUSHELLE, L C HOOTS F33615-76-C-5157
UNCLASSIFIED AFML-TR-78-106 NL

2 OF 3
ADA
067547

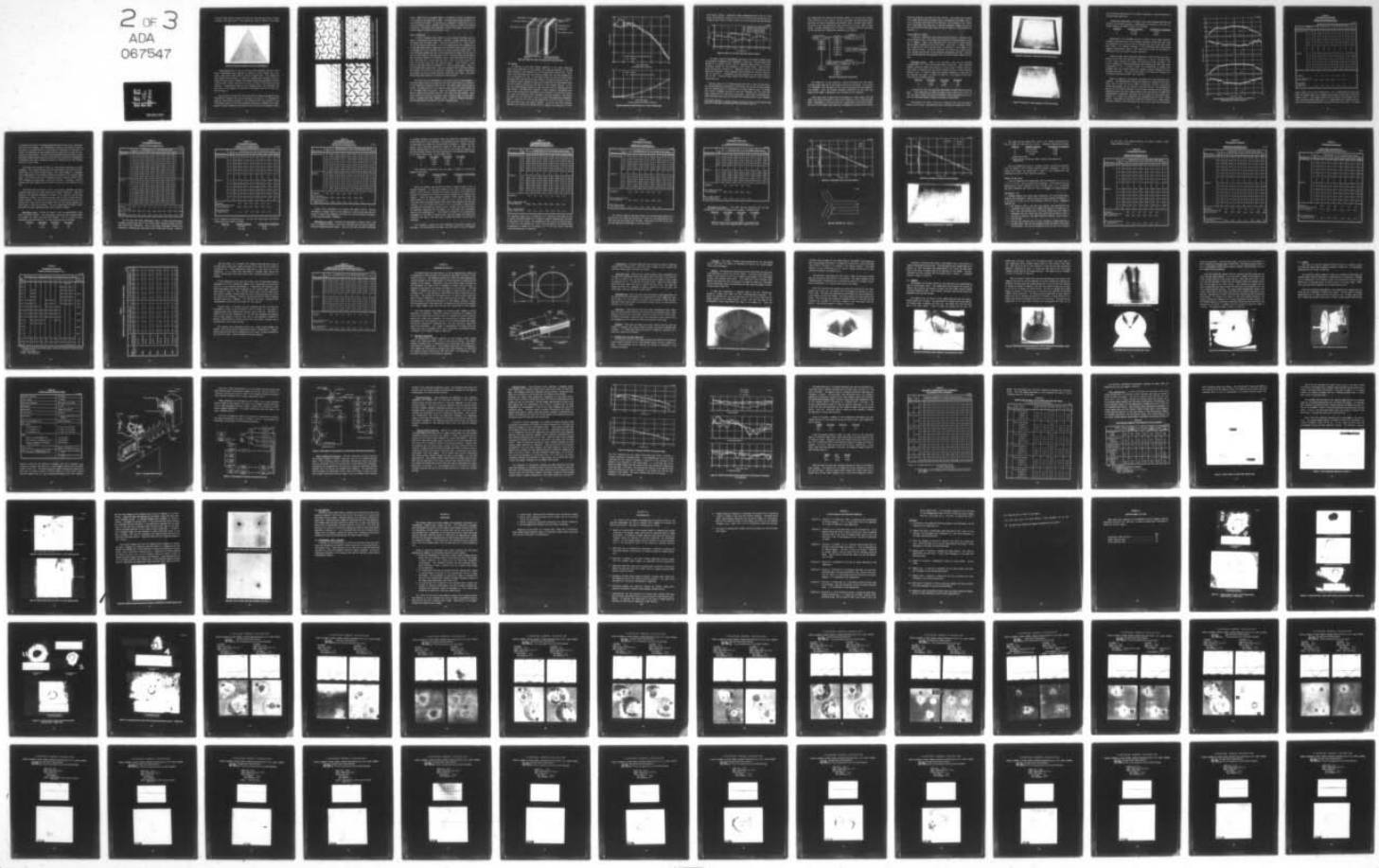

of one of those copper triangles and Figure 51 shows how the various triangles interface with each other in the combinations actually found on the radome.

12-1289

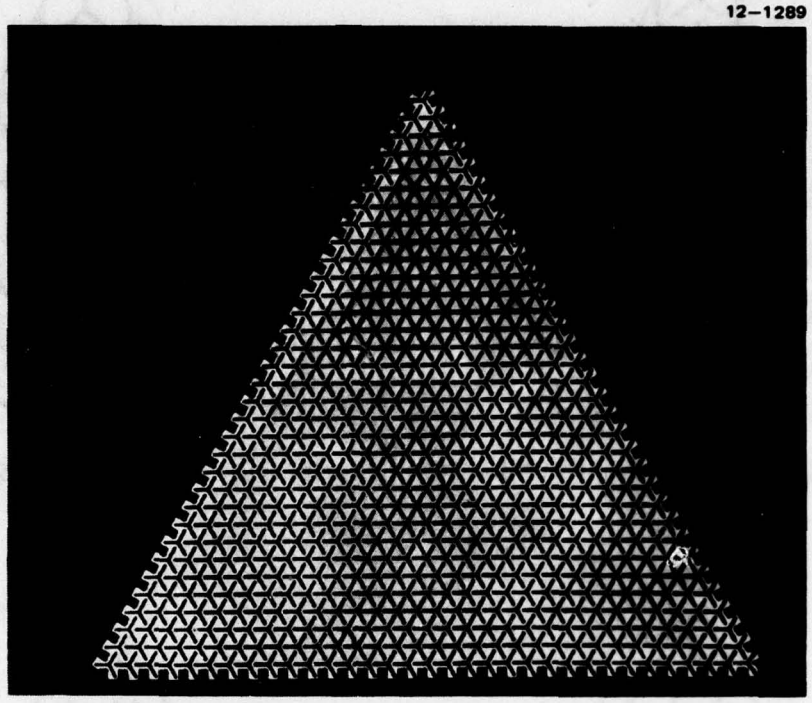

Figure 50 Typical 60° triangle like that used on test panel No. 3.

Phototransparencies of the slot patterns were obtained from Ohio State. These transparencies were prepared by drawing a single element very accurately, many times larger than the desired finished size. This element was then reduced and duplicated. A number of elements were arranged to form an array, and this array of elements was further reduced and duplicated, and then joined to make a larger array and so on until an array of the desired size was complete. Transparencies made by this technique were used throughout the early part of the program for fabrication development work and for the first two flat panels.

Starting with the third flat panel the metallic coating was applied using interlocking triangles like the one pictured in Figure 50. In attempting to make the interlocking triangles it was determined that the accuracy of the interelement spacing of the hand assembled artwork was inadequate for proper mating, although completely satisfactory from an electrical performance stand-

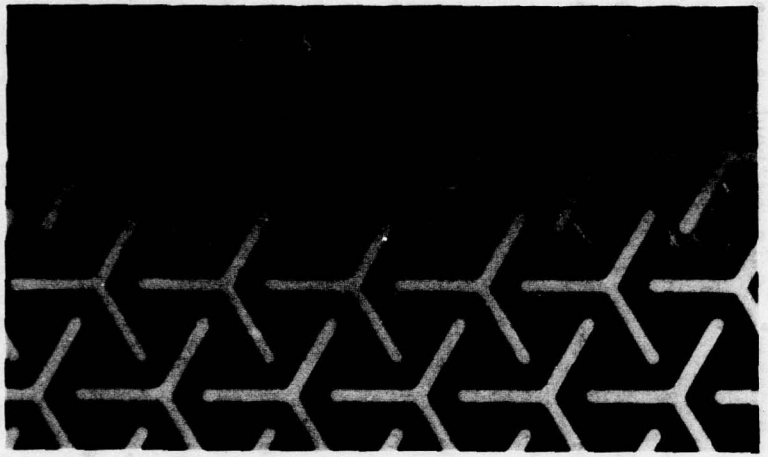

a.) 60° to 60° (or 70°) triangles, all three sides

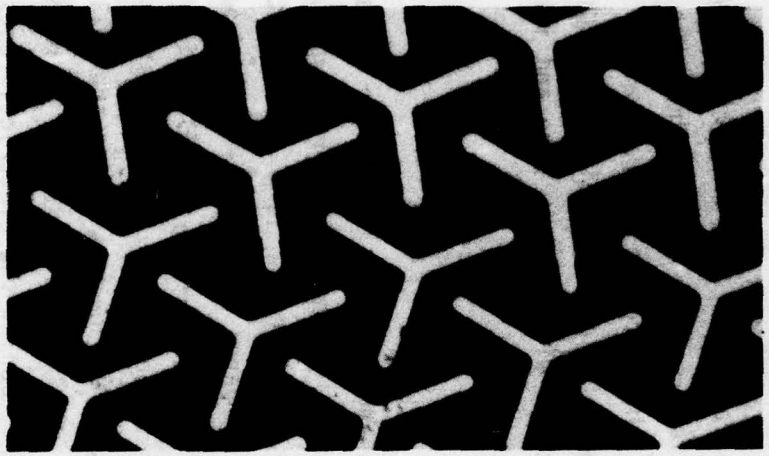

b.) 50° to 50° (or 56°) triangles, sides adjacent to the 50° (or 56°) angle

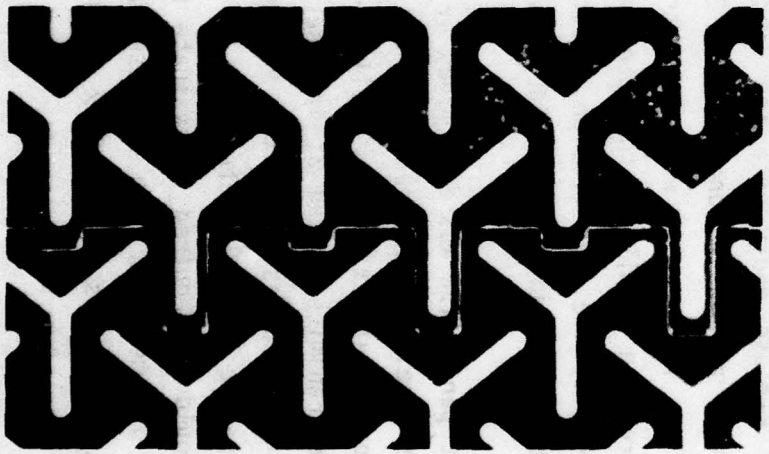

c.) 50° to 50° triangles, sides opposite to the 50° angle

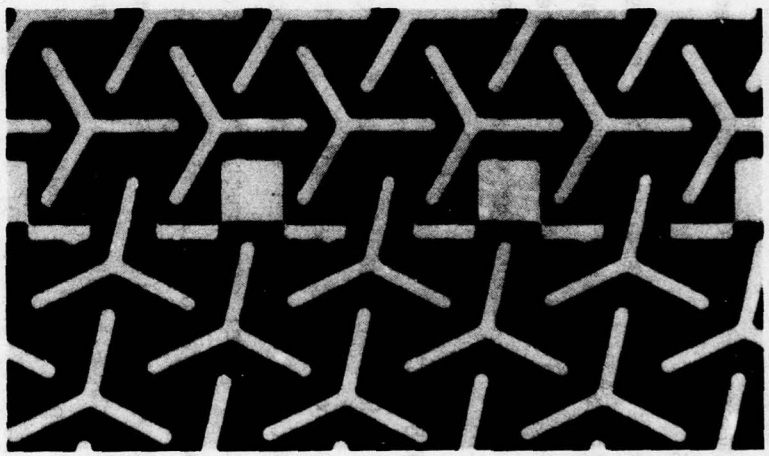

d.) 60° to 50° (or 56°) triangles, sides adjacent to the 50° or 56° angle

Figure 51 Detail of interfaces between various combinations of copper triangles, like those used on the flat panels and the radome.

point. Minor errors in assembly tended to be additive, and on a triangle with a long side it was impossible to make a uniform serrated edge without the cut line crossing an element. It was necessary, therefore, to generate all of the required artwork using a computer controlled plotter to obtain the required tolerances. The system used, generated artwork with element size and inter-element spacing tolerances within $\pm$0.001 inch.

PANEL CONSTRUCTION

In order to expedite panel fabrication and minimize the number of variables in evaluating the various metal coatings, a common substrate was used throughout the flat panel tests. Pictured in Figure 52 is a cross section of the test panel construction. It can be compared with the A-sandwich wall of the metallized Jetstar radome which uses two 33 mil epoxy E-glass skins and a honeycomb core plus the metal and rain erosion coating (Figure 63). The only difference between the wall of the demonstration radomes and the wall of the flat test panel is that the outer skin of the flat panel can be removed and replaced by another of a different design. During the electrical tests, a thin vacuum bag and a vacuum pump were used to hold the copper coated 21 mil plies of E-glass epoxy onto the substrate panel. Tests without a copper coating were made using one uncoated 21 mil ply of E-glass epoxy. Thus, all slot designs were tested with a substrate sandwich which could only possibly be different in 21 mils of the outer skin thickness, the adhesive which bonds the copper, or the rain erosion coating applied over the copper. By careful processing, these potential variables were held constant.

Test panel size was determined by preliminary electrical measurements on Plexiglas panels, which are stable and have well known electrical properties. It was found that a sample as small as 24" x 24" would support data accuracies of 2% in transmission and 3° in insertion phase delay at X-band frequencies for incidence angles up to 60°. Since the incidence angles "seen" in the Jetstar radome are no greater than 60°, this panel size was adopted. Larger panels would be required to evaluate higher incidence angles as are experienced in radomes with high fineness ratios. Figure 53 compares theoretical and measured results for the 24 x 24 inch Plexiglas panel.

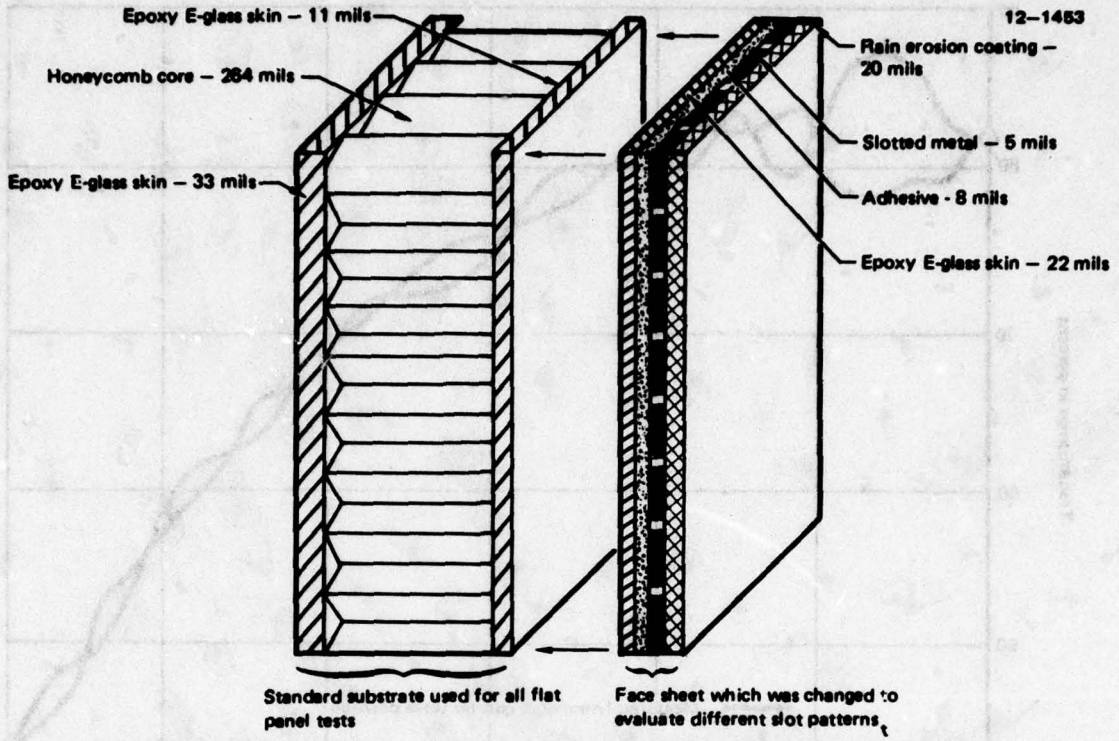

Figure 52 Construction detail of flat panels used for electrical testing

TEST METHOD

In addition to the usual factors important in flat panel electrical tests, the orientation of the tripolar slot required attention for the RMR panels because of the possibility of slot polarization sensitivity. Therefore, tests were made with the E-vector aligned with, and then perpendicular to, one reference slot leg. In all panels except one, the slots were aligned with each other over the entire test surface. In the one exception, Panel 11, an arbitrary panel reference direction was established and measurements made with the E-vector aligned with, and normal to, this chosen direction. In this way, the random pattern effects for the one panel could be compared with the other panels. The tests also included, in most instances, measurements both prior to and following the application of the protective rain erosion coating. This layer did effectively shift the panel's resonant frequency, and knowing the amount of this shift was of value in sizing slot elements for subsequent panels. Figure 54 is a plot of the transmission curves for Panels 3 and 4, with and without the rain erosion coating. It can be seen that resonance (darkened data points) was shifted nearly a gigahertz by application of the

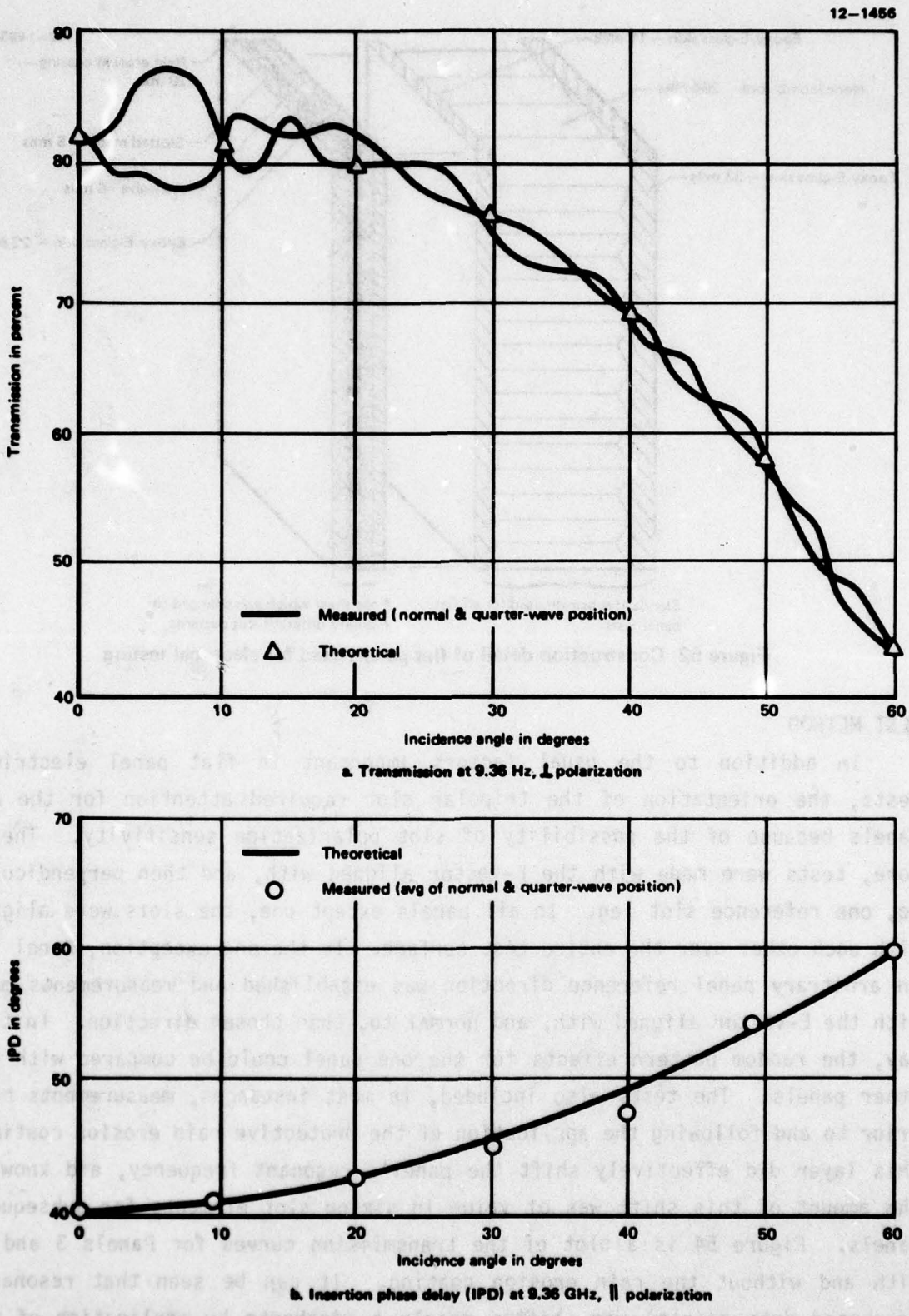

Figure 53 Measured vs theoretical results for reference plexiglas panel

rain erosion coating. Additional testing demonstrated that this is a non-linear relationship, where 10 mils of rain erosion coating results in a frequency shift nearly as great as 20 mils of rain erosion coating provides.

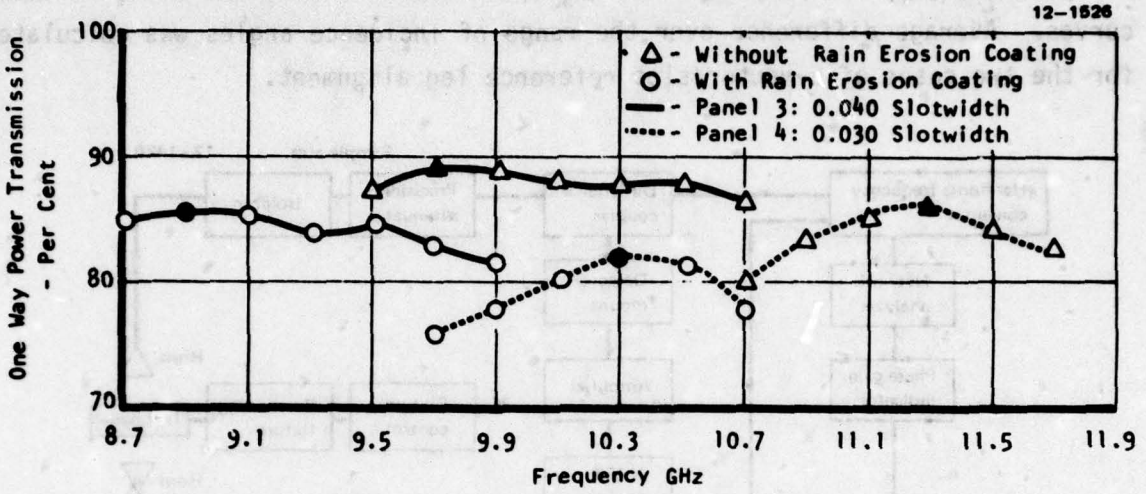

Figure 54 Effects of rain erosion coating on resonant frequency

Flat panel electrical measurements were made in an anechoic chamber using the equipment arrangement block diagrammed in Figure 55. The test panels were mounted on an azimuth fixture, and all incidence angles from 0° (or normal incidence) through 60° were measured in the azimuth plane. With the test horns horizontally polarized, $\theta_{\parallel}$ components (where θ is the angle of incidence) were measured. The $\theta_{\perp}$ components were recorded with vertical polarization of the horns. Transmission data was measured for continuous scans of -60° to +60°. Insertion phase delays (IPD's) were taken at fixed incidence angles every 10°.

Data was taken at all incidence angles from +60° to -60° for both parallel and perpendicular polarization of the horns, and for the E-vector aligned with and perpendicular to a reference leg of the tripolar slots. To change the E-vector alignment relative to the slot reference leg, the panel was simply rotated 90° (in the plane of the panel). Both normal and quarter-wave panel positions* were used for the above four parameter pairs. Data averaging

*The normal position is centered between the two test horns and the quarter wave position is displaced a quarter wave from the normal position.

was accomplished for positive and negative angles, for the two slot orientations relative to the E-vector, and for the normal and quarter-wave panel positions, to obtain transmission performance versus incidence angle curves. The parallel ($\theta_{\parallel}$) and perpendicular ($\theta_{\perp}$) polarization cases are shown in these curves. Average difference over the range of incidence angles was calculated for the two cases of E-vector/slot reference leg alignment.

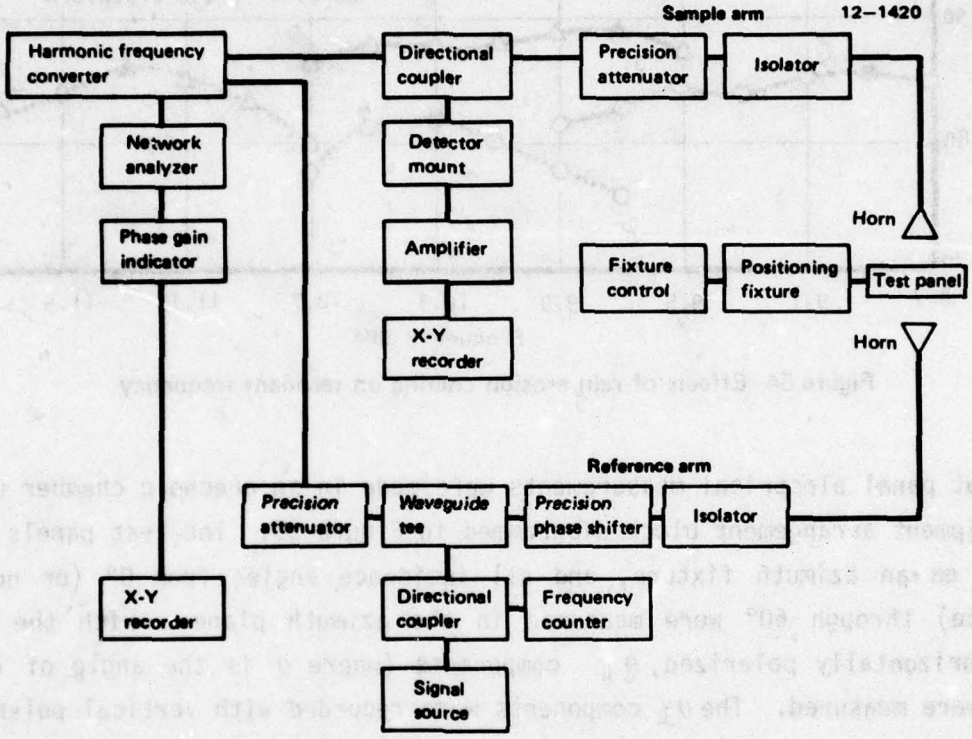

Figure 55 Test arrangement, flat panel tests

For simplicity in data evaluation, average performance over the entire incidence angle range and for both polarizations was calculated. This average is a reasonable first estimate of what could be expected from the demonstration radomes. Also, the resonant frequency determined for each panel was based on the highest transmission value attained by this averaging.

IPD's were taken by measuring the difference in signal phase, with the panel, and without the panel in place; this difference is the insertion phase delay. Measurement of the phase delay was accomplished by nulling the "reference arm of the bridge" (the lower set of components in Figure 55) using the

precision attenuator and precision phase shifter. The transmission reference is the power level without the panel, and is represented by the 100% transmission line on the graph paper used in recording. The attenuator in the "sample arm of the bridge" (the upper set of waveguide components shown in Figure 55) was used to calibrate the graph paper and verify linearity of the transmission readings.

TRANSMISSION TEST RESULTS

A total of 11 RMR panels were tested during the program. The panels were fabricated and tested in five groups and therefore are presented here by group and in sequence. Panel 1 was fabricated with a wide joint at its mid-height position which extended the full panel width. This joint, in effect, deleted one or more rows of slots from the array. In addition, a large number of the slots were distorted. The panel was found to be sensitive to positioning, thus creating inaccuracies in the measured transmission and IPD. Measured data was discarded and new specimens were fabricated without these deficiencies.

RMR Panels 2 and 3 - Panel 2 was fabricated, using the OSU furnished transparencies, as a single uninterrupted sheet (Figure 56). Panel 3 used the computer generated artwork and consists of 8-inch copper triangles with serrated edges interlocked over the entire surface to form a nearly perfectly periodic array. A single triangle was pictured previously in Figure 50 and the facesheet for Panel 3 is shown in Figure 57. Slot dimensions were measured with the following results:

Panel No.	Leg Length	Slot Width	Grid Angle
2	0.195"	0.038"	50°
3	0.186"	0.042"	60°

In addition to slot size, physical measurements of panel thicknesses were made. It was found that for these two panels, and in fact for all eleven of the flat panels tested, the physical dimensions never varied more than ± 1 mil from the dimensions shown in Figure 52, except as noted below.

One exception was Panel 2 which had an adhesive layer that was approximately 12 mils thick. Some RMR panels were intentionally sprayed with 16 mils

12-1288

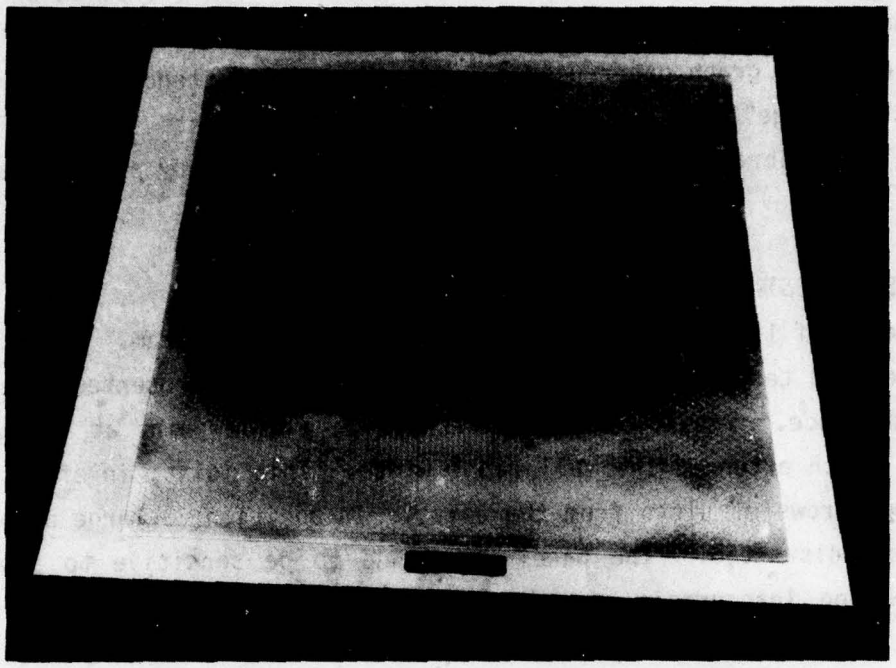

Figure 56 Test panel No. 2, 50° pattern, before erosion coating.

12-1290

Figure 57 Test panel No. 3 before application of the erosion coating.

of rain erosion coating and will be noted as appropriate under discussions of the particular panel sets.

Transmission measurements for Panels 2 and 3 were conducted both with and without rain erosion coating. Transmission at resonance, with the rain erosion coating, for Panels 2 and 3 is as follows:

Panel No.	Resonant Frequency	Transmission at Resonance
2	9.9 GHz	80.9%
3	9.9 GHz	86.4%

Additionally, the facesheet portion of Panels 2 and 3 were initially stacked on the wrong side of the A-sandwich substrate so that the total stack was unbalanced, i.e., an 11 mil skin on the back and a 55 mil skin next to the metal layer. The resonant frequency of the unbalanced panels was shifted downward significantly, which is not surprising in light of the effect on resonance of the rain erosion coating (Figure 54).

Figure 58 shows typical measured transmission curves for the four polarization/ slot orientation conditions (labeled a, b, c and d). The dual curves in this figure represent the normal and quarter-wave panel positions. The initial averaging of quarter-wave/normal panel position and left/right panel orientations (+ and - incidence angles) was accomplished by folding each recorded sheet and drawing through the apparent average transmission versus incidence angle plot. The specific data shown is for Panel 2 at 9.9 GHz, with rain erosion coating and proper layer stacking.

Table 13 summarizes transmission performance for each measured panel/ condition. The perpendicular polarization results are average for two conditions, such as cases (a) and (c) shown in Figure 58. Parallel polarization results are averages such as Figure 58, cases (b) and (d). This averaging of the two slot orientations relative to the E-vector provides the two customary components used in the usual radome analysis, and would suffice for predicting radome/antenna transmission scans which are the average for two antenna polarizations if a given slot orientation was maintained over the entire radome surface. They should also provide a good first estimate for a radome surface with many different slot orientations and array sizing such that the antenna

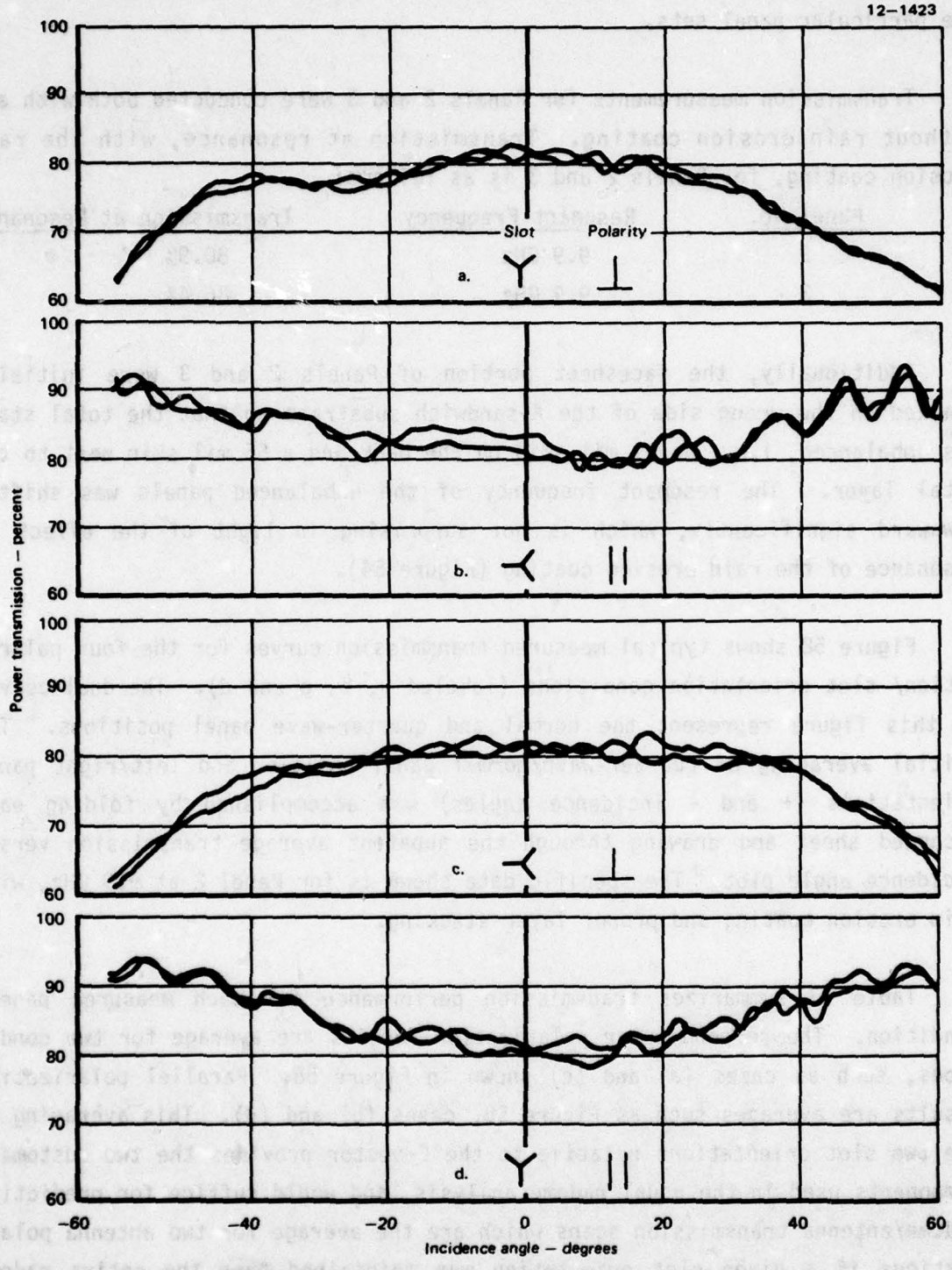

Figure 58 Measured transmission, RMR panel no. 2, 9.9 ghz, four polarization/slot orientation conditions

TABLE 13
TRANSMISSION RESPONSE

RESONANT METAL RADOME PANEL NO. 2 (50° SLOTS) WITH RAIN EROSION COATING

12-1444

Polarization	Freq. GHz	Transmission, %, For Incidence Angle (Deg.) 0	10	20	30	40	50	60	Avg.
Perpendicular	9.3	77.8	77.8	77.8	77.3	76.1	71.8	63.6	74.6
	9.5	80.3	79.6	78.6	77.6	75.3	71.8	63.3	75.2
	9.7	80.1	80.3	79.8	78.3	76.1	72.3	66.3	76.2
	9.9	81.5	81.0	80.0	78.5	76.3	71.3	65.0	76.2
	10.1	77.0	76.3	75.0	72.8	70.5	65.5	57.8	70.7
	10.3	74.6	73.9	72.9	70.6	67.4	61.9	54.1	67.9
Parallel	9.3	77.8	78.1	78.3	79.6	81.6	83.1	84.6	80.4
	9.5	80.3	80.8	81.8	83.2	85.2	87.2	89.0	83.9
	9.7	80.1	80.6	81.9	83.6	84.9	88.1	90.1	84.2
	9.9	81.5	81.8	82.5	84.5	86.8	90.0	92.3	85.6
	10.1	77.0	78.5	80.5	83.8	86.0	88.3	91.0	83.6
	10.3	74.6	75.8	78.1	81.8	84.6	87.3	89.6	81.7

Frequency:	9.3	9.5	9.7	9.9	10.1	10.3	
Avg. Transmission (%) 2 Polarizations:	77.5	79.6	80.2	80.9	77.2	74.8	
Avg., Polarization/Slot Sensitivity:	6.3	3.9	1.9	1.1	2.5	1.7	

always "sees" a mix of slot orientations. This is representative of the case where the antenna looks near a radome nose and sees a great deal of the total radome surface. High antenna offsets tend to localize the antenna field of view, and hence minimum transmission in a radome might not be predicted accurately by the average perpendicular and parallel polarization cases. As a means

to estimate this effect, an "average polarization/slot sensitivity" was determined for each frequency. This information is given at the bottom of Table 13 for Panel 2, and specifically is the average of differences in Figure 58, "a" versus "c" conditions for seven angles plus the Figure 58 "b" versus "d" conditions for seven angles. In view of the measurement accuracy (± 2% in transmission), average polarization/slot sensitivity less than 2% can reasonably be disregarded, thus Panel 2 exhibited virtually no sensitivity to slot orientation at 9.7 and 9.9 GHz.

Also shown at the bottom of Table 13 is the average transmission for each frequency. This average includes both the perpendicular and parallel polarization data at the seven indicated angles. This single number is a reasonable first approximation of the average transmission expected in the Jetstar radome shape. This single value versus frequency provides a means to define "resonant" frequency for each panel, in this case 9.9 GHz is indicated. Table 14 provides the final summary data for Panel 3, which was also resonant at 9.9 GHz.

The earlier data for Panels 2 and 3, as previously indicated, was inadvertently taken with the E-glass epoxy skins stacked incorrectly. Under that condition, the resonant frequencies of Panels 2 and 3 were 9.7 and 9.9 GHz, respectively, without rain erosion coating, and 8.7 and 8.9 GHz with rain erosion coating. This data and the fact that the stacking error was not discovered until later, led to the assumption that the slot design needed to be scaled down to raise the frequency. This was accomplished and Panels 3 and 4 were made with newly generated artwork having smaller elements.

RMR Panels 4 and 5 - Artwork for Panels 4 and 5 was generated by a computer controlled plotter. The interelement spacing was held constant while the element leg length and width were reduced. The rain erosion coating thicknesses were again 20 mils. The slot dimensions were as follows:

Panel No.	Leg Length	Slot Width	Grid Angle
4	0.174"	0.030"	60°
5	0.174"	0.028"	50°

TABLE 14
TRANSMISSION RESPONSE
(60° SLOTS) WITH RAIN EROSION COATING

12-1482

Polarization	Freq. GHz	Transmission, %, For Incidence Angle (Deg.)							
		0	10	20	30	40	50	60	Avg.
Perpendicular	8.7	74.8	73.3	71.5	70.3	67.8	65.0	61.0	69.1
	8.9	77.6	77.3	75.8	74.1	71.8	67.6	61.8	72.3
	9.1	79.1	79.1	78.6	77.4	75.9	72.1	66.1	75.5
	9.3	81.4	81.9	82.4	82.7	81.2	76.9	67.7	79.2
	9.5	81.9	82.2	82.4	82.3	81.2	77.4	68.7	79.4
	9.7	84.0	84.8	85.0	84.8	83.8	80.0	71.0	81.9
	9.9	86.8	86.8	86.5	86.5	86.0	82.5	73.3	84.1
	10.1	85.1	85.3	85.1	84.6	84.1	80.6	72.3	82.4
	10.3	87.0	86.7	85.7	84.2	83.2	80.5	71.5	82.7
	10.5	86.3	85.8	84.3	83.1	81.3	78.1	71.8	81.5
	10.7	82.9	82.7	81.7	80.2	78.7	74.4	67.4	78.3
Parallel	8.7	74.8	75.3	75.5	77.0	79.5	83.3	85.0	78.6
	8.9	77.6	78.6	79.4	80.4	81.9	85.1	87.6	81.5
	9.1	79.1	79.6	80.3	81.3	82.6	84.6	86.6	82.0
	9.3	81.4	81.6	81.6	82.6	84.6	86.1	86.9	83.5
	9.5	81.9	82.4	82.9	84.6	86.1	88.1	89.1	85.0
	9.7	84.0	84.5	84.8	85.8	87.5	89.8	90.5	86.7
	9.9	86.8	86.8	87.0	87.8	89.3	91.0	92.5	88.7
	10.1	85.1	85.4	85.6	85.6	86.6	89.4	91.6	87.0
	10.3	87.0	87.0	87.2	87.5	88.7	90.0	91.0	88.3
	10.5	86.3	86.3	86.1	87.3	88.6	89.8	90.3	87.8
	10.7	82.9	83.4	85.1	86.6	87.9	89.6	90.1	86.5

Frequency:	8.7	8.9	9.1	9.3	9.5	9.7	9.9	10.1	10.3	10.5	10.7
Avg. Transmission (%), 2 Pol:	73.9	76.9	78.8	81.4	82.2	84.3	86.4	84.7	85.5	84.7	82.4
Pol./Slot Sensitivity	2.0	2.0	3.0	1.6	3.0	4.9	3.8	2.8	2.8	2.4	1.8

As with the other panel measurement cases, a single polarization/slot alignment condition was used for an initial panel frequency survey to determine logical test frequencies. Due to time lapse, measurement accuracy with reference to Plexiglas was reverified prior to RMR panel testing. Tables 15

TABLE 15
TRANSMISSION RESPONSE
RESONANT METAL RADOME PANEL NO. 4 (60° SLOTS) WITH RAIN EROSION COATING

12-1462

Polarization	Freq. GHz	Transmission, %, For Incidence Angle (Deg.)							
		0	10	20	30	40	50	60	Avg.
Perpendicular	9.7	77.1	76.6	76.1	75.1	73.5	69.1	62.1	72.8
	9.9	80.8	80.1	78.6	77.8	75.6	71.8	64.3	75.6
	10.1	82.8	82.3	81.1	79.8	78.1	75.3	67.6	78.1
	10.3	82.5	82.0	81.3	79.5	77.5	75.0	68.5	78.0
	10.5	80.4	80.4	79.9	77.7	74.9	71.9	66.4	75.9
	10.7	77.4	76.9	75.9	73.7	70.7	67.4	61.9	72.0
Parallel	9.7	77.1	77.4	78.1	79.1	81.1	83.1	84.4	80.0
	9.9	80.8	80.6	80.6	81.0	82.8	84.8	86.1	82.4
	10.1	82.8	82.8	83.1	83.8	84.8	86.1	87.2	84.4
	10.3	82.5	82.3	82.8	84.5	85.8	87.3	88.0	84.7
	10.5	80.4	80.6	81.6	83.9	86.1	86.9	86.9	83.8
	10.7	77.4	78.4	79.6	81.9	84.6	85.4	85.9	81.9

Frequency	9.7	9.9	10.1	10.3	10.5	10.7
Avg. Transmission (%) 2 Polarizations:	76.4	79.0	81.3	81.4	79.9	77.0
Polarization/Slot Sensitivity:	1.7	1.8	1.4	0.8	0.8	1.4

and 16 summarize transmission data. For the final tests with rain erosion coating the results were as follows:

Panel No.	Resonant Frequency	Transmission at Resonance
4	10.3 GHz	81.4%
5	10.5 GHz	74.0%

TABLE 16
TRANSMISSION RESPONSE
RESONANT METAL RADOME PANEL NO. 5
(60° SLOTS) WITH RAIN EROSION COATING

12-1483

Polarization	Freq. GHz	Transmission, %, For Incidence Angle (Deg.)							
		0	10	20	30	40	50	60	Avg.
Perpendicular	9.9	65.3	65.1	64.1	62.3	60.1	57.6	53.6	61.2
	10.1	69.3	69.0	68.8	67.3	65.3	62.5	56.5	65.5
	10.3	71.9	72.1	72.1	70.9	69.1	66.6	60.9	69.1
	10.5	73.5	73.2	72.7	71.7	70.0	68.0	62.7	70.3
	10.7	73.9	73.4	72.4	70.7	68.4	64.9	59.7	69.1
	10.9	72.3	71.5	69.8	67.8	64.5	60.8	55.8	66.1
	11.1	66.5	65.5	64.0	60.5	56.8	52.5	47.5	59.0
Parallel	9.9	65.3	68.5	69.5	70.2	72.5	76.7	81.2	72.0
	10.1	69.3	69.5	70.5	72.0	73.8	76.5	79.8	73.1
	10.3	71.9	72.2	72.4	73.9	75.4	77.9	80.7	74.9
	10.5	73.5	74.0	75.2	77.0	79.0	81.0	83.2	77.6
	10.7	73.9	74.6	75.9	77.4	79.6	81.9	84.1	78.2
	10.9	72.3	74.0	76.3	79.0	82.0	85.0	87.3	79.4
	11.1	66.5	69.0	72.8	77.3	81.8	85.3	87.8	77.2
Frequency:	9.9	10.1	10.3	10.5	10.7	10.9	11.1		
Avg. Transmission (%), 2 Pol:	66.6	69.3	72.0	74.0	73.7	72.8	68.1		
Polarization/Slot Sensitivity:	11.6	8.8	6.3	4.6	1.6	2.1	1.9		

Panels 4 and 5 performed 5 to 7% poorer than Panels 2 and 3. This was attributed to stagger tuning of the radome wall, which occurs when the substrate is tuned at one frequency (9.375 GHz) and the slot pattern at another, in this case much higher, frequency.

RMR Panels 6, 7 and 8 - Following the measurement of Panels 4 and 5, the error in assemblying Panels 2 and 3 was discovered and verified by reassembling and remeasuring those panels. Also, at this time, the small difference

in resonant frequency for Panels 4 and 5 was tentatively attributed to the slight difference in slot leg width. The new panel set was therefore selected to investigate the effects of slot leg width on frequency. Towards this end, Panels 7 and 8 were made identically, except for slot leg width. The rain erosion coatings were 16 mils in lieu of 20 for this panel set because a 16 mil thick erosion coating was being considered for the demonstration radomes at the time of these tests. Slot parameters were:

Panel No.	Leg Length	Slot Width	Grid Angle
6	0.191"	0.033"	60°
7	0.192"	0.034"	50°
8	0.192"	0.047"	50°

Final measured transmission data are shown in Tables 17, 18 and 19. Summary results were:

Panel No.	Resonant Freqency	Transmission at Resonance
6	9.9 GHz	84.0%
7	9.9 GHz	80.3%
8	10.1 GHz	83.9%

Again, the greater slot leg width on Panel 8 caused an upward shift in resonant frequency. All data was reviewed at this point in the program and based on that review, a projection was made to predict the element size required for resonance at 9.375 GHz, the design frequency of our demonstration radomes. Figure 59 shows resonant frequency plotted against element leg length (center to tip distance) for Panels 4, 5, 6, 7 and 8. Only the last five panels were considered because these panels were prepared from the same artwork; i.e., the artwork for Panels 6 and 7 are merely a photographic enlargement of the artwork for Panels 4 and 5. Artwork for the earlier panels was generated separately and leg length, slot leg width, and interelement spacing vary independently. The artwork for Panel 8 is a photographic enlargement of the Panel 5 artwork except that the element leg widths were increased from .030 to .040 inch wide to examine the effect of leg width on frequency.

In an attempt to account for this difference in leg width, another plot was made. This time element leg length, from near edge to tip, was computed.

TABLE 17

TRANSMISSION RESPONSE

RESONANT METAL RADOME PANEL NO. 6
(60° SLOTS) WITH RAIN EROSION COATING

12-1534

Polarization	Freq. GHz	Transmission, %, For Incidence Angle (Deg.)							
		0	10	20	30	40	50	60	Avg.
Perpendicular	9.3	78.3	78.5	78.5	77.7	76.0	72.5	63.8	75.0
	9.5	80.9	81.2	81.9	80.9	78.4	74.7	65.9	77.7
	9.7	83.4	83.4	84.1	84.1	81.6	76.6	68.4	80.2
	9.9	83.9	83.9	83.4	82.9	80.6	75.6	66.6	79.6
	10.1	81.6	81.1	80.3	79.1	77.8	73.1	64.8	76.8
	10.3	80.0	79.5	79.0	77.2	74.4	69.0	61.7	74.4
	10.5	74.9	74.4	72.7	70.2	66.9	61.4	55.4	68.0
Parallel	9.3	78.3	79.0	80.3	81.8	83.5	85.3	86.0	82.0
	9.5	80.9	81.6	82.9	84.4	86.4	88.4	90.1	85.0
	9.7	83.4	83.7	84.4	86.4	88.2	89.7	89.9	86.5
	9.9	83.9	84.7	86.4	88.4	90.4	91.7	93.2	88.4
	10.1	81.6	82.9	85.1	88.1	90.1	92.1	93.4	87.6
	10.3	80.0	81.2	83.2	87.0	89.5	92.2	93.0	86.6
	10.5	74.9	76.4	80.1	84.4	89.4	92.1	93.1	84.3
Frequency:		9.3	9.5	9.7	9.9	10.1	10.3	10.5	
Avg. Transmission (%), 2 Polarizations:		78.5	81.4	83.4	84.0	82.2	80.5	76.2	
Avg., Polarization/ Slot Sensitivity:		1.8	1.5	1.4	1.9	1.6	1.8	1.5	

This distance, shown as L_2 in Figure 60, is a function of leg width as well as length, and when plotted, as in Figure 61, against frequency puts the Panel 8 data point on the curve. The projection of this curve to 9.375 GHz occurs at .2075 inch, the required L_2. This is the near edge to tip distance which corresponds to a center to tip distance (L_1) of .214 inch, which is the same as the extrapolation of Figure 59.

TABLE 18

TRANSMISSION RESPONSE

RESONANT METAL RADOME PANEL NO. 7
(50° SLOTS) WITH RAIN EROSION COATING

12-1533

Polarization	Freq. GHz	Transmission, %, For Incidence Angle (Deg.) 0	10	20	30	40	50	60	Avg.
Perpendicular	9.3	71.0	71.5	72.5	71.5	69.5	65.5	58.5	68.6
	9.5	74.4	74.9	75.1	74.6	73.1	69.4	61.9	71.9
	9.7	77.6	77.9	77.6	77.1	75.6	70.9	63.1	74.3
	9.9	80.6	80.6	79.9	78.6	76.1	71.4	63.9	75.9
	10.1	79.1	79.1	78.1	76.4	73.6	68.4	60.1	73.5
	10.3	77.3	76.8	75.3	73.1	69.3	64.1	56.8	70.4
Parallel	9.3	71.0	72.5	74.0	75.5	77.3	79.8	77.5	75.4
	9.5	74.4	74.9	75.7	77.2	79.2	81.2	83.7	78.0
	9.7	77.6	77.8	78.6	78.8	81.8	85.1	88.1	81.1
	9.9	80.6	81.3	82.6	84.1	86.1	88.1	90.3	84.7
	10.1	79.1	79.6	81.3	83.6	85.6	87.8	90.8	84.0
	10.3	77.3	78.6	79.8	81.8	84.3	86.8	90.1	82.7
Frequency:		9.3	9.5	9.7	9.9	10.1	10.3		
Avg. Transmission (%), 2 Polarizations:		72.0	75.0	77.7	80.3	78.8	76.6		
Avg. Polarization/ Slot Sensitivity:		9.1	7.3	4.9	2.0	0.9	2.2		

The original computer generated artwork was enlarged photographically to achieve this leg length and fabrication of parts for the demonstration articles using the new artwork was initiated. Additionally, the 56° and 70° artwork was generated and enlarged in the same fashion.

TABLE 19

TRANSMISSION RESPONSE

RESONANT METAL RADOME PANEL NO. 8
(50° DESIGN, WIDE SLOTS) WITH RAIN EROSION COATING

12-1532

Polarization	Freq. GHz	Transmission, %, For Incidence Angle (Deg.): 0	10	20	30	40	50	60	Avg.
Perpendicular	9.7	79.6	79.6	79.6	79.6	78.6	75.3	66.8	77.0
	9.9	83.0	83.0	82.5	82.2	81.2	77.7	69.0	79.8
	10.1	85.1	84.9	84.1	82.9	80.9	77.6	69.1	80.7
	10.3	84.3	83.8	82.8	81.6	79.8	75.8	69.3	79.6
	10.5	82.8	82.8	81.5	79.5	76.7	72.3	65.8	77.3
Parallel	9.7	79.6	79.9	80.1	81.4	83.6	85.9	87.6	82.6
	9.9	83.0	83.2	83.5	83.7	85.2	87.0	88.7	84.9
	10.1	85.1	85.3	86.1	86.8	87.2	88.7	90.2	87.1
	10.3	84.3	84.8	85.6	86.6	87.6	89.1	91.1	87.0
	10.5	82.8	84.0	85.3	87.0	89.0	90.8	92.0	87.3
Frequency:		9.7	9.9	10.1	10.3	10.5			
Avg. Transmission (%), Polarizations:		79.8	82.4	83.9	83.3	82.3			
Avg., Polarization/ Slot Sensitivity:		4.9	4.8	3.7	3.2	1.9			

RMR Panels 9, 10 and 11 - This panel set was fabricated with the same transparencies used on the demonstration radomes. Parameters were:

Panel No.	Leg Length	Slot Width	Grid Angle
9	0.214	0.035	60°
10	0.215	0.036	50°
11	0.215	0.036	*

*Various pieces of all four grid angles. Orientation was similar to that on the demonstration radomes (Figure 62).

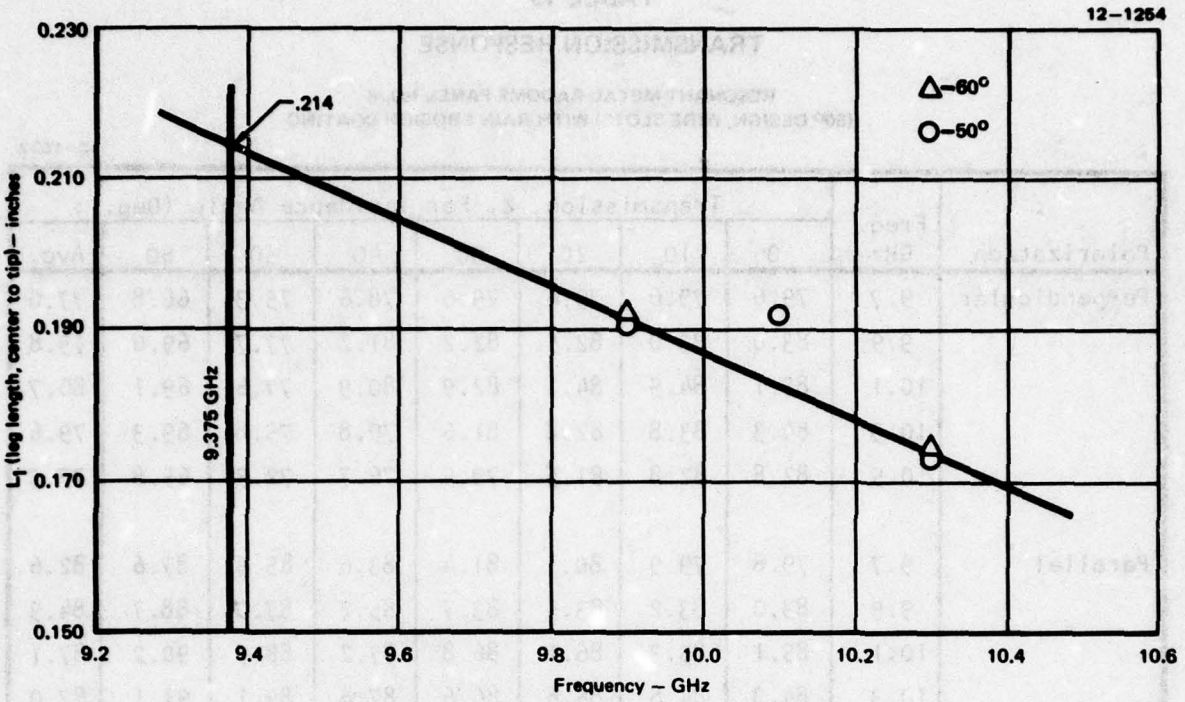

Figure 59 L_1 (leg length, center to tip) versus frequency

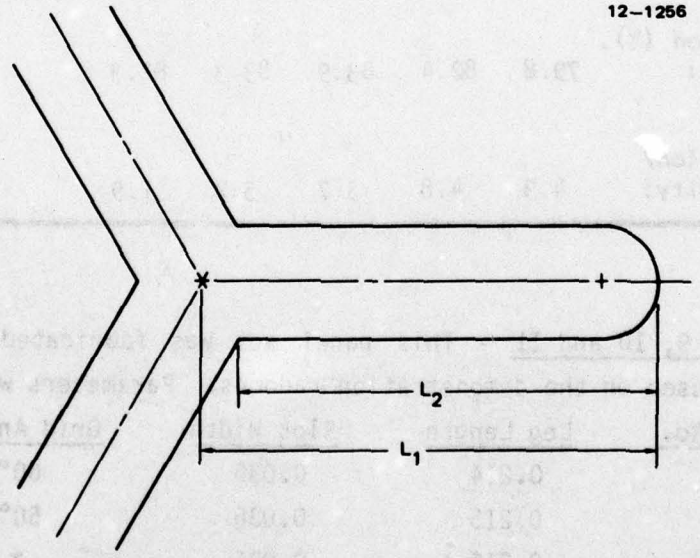

Figure 60 Definition of L_1 and L_2

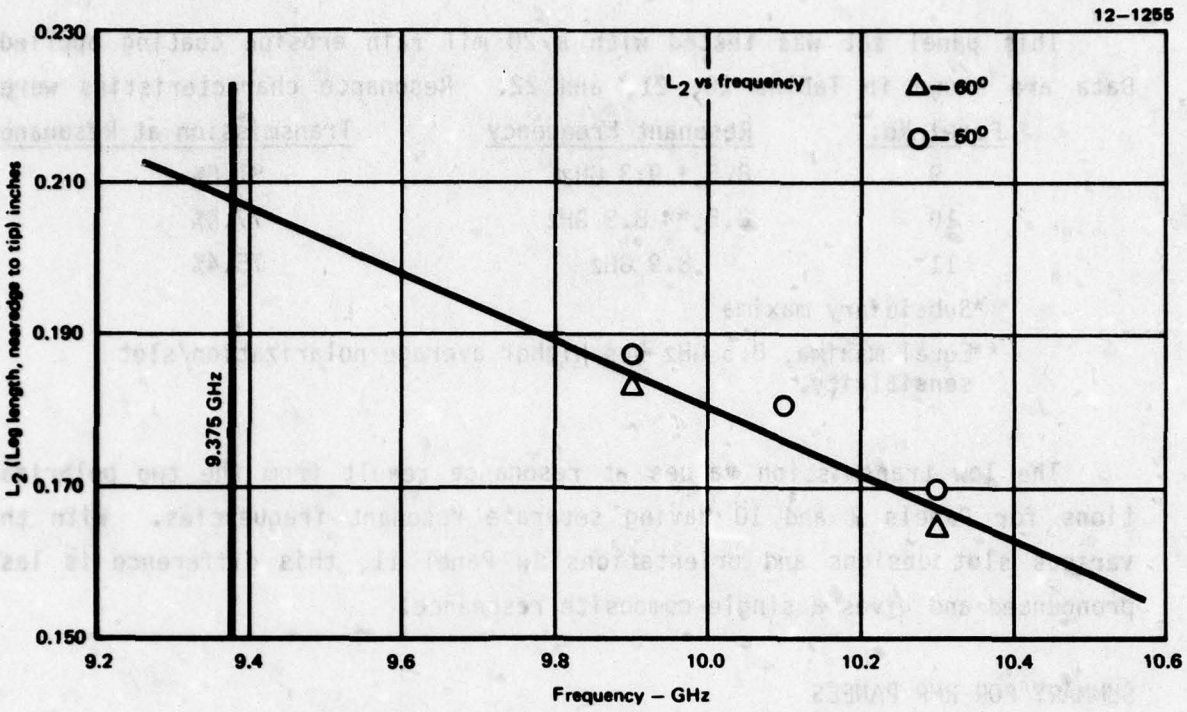

Figure 61 (L_2 leg length, near edge to tip) versus frequency

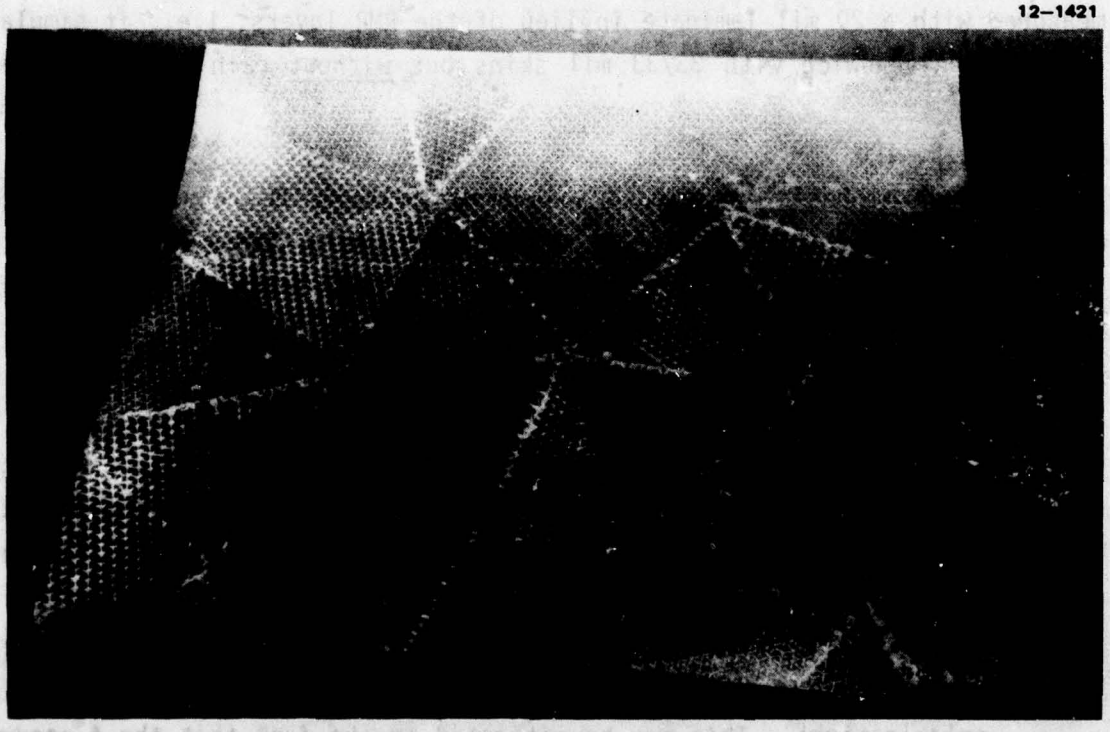

Figure 62 Flat panel number 11. face sheet

This panel set was tested with a 20 mil rain erosion coating applied. Data are shown in Tables 20, 21, and 22. Resonance characteristics were:

Panel No.	Resonant Frequency	Transmission at Resonance
9	8.5,* 9.3 GHz	81.0%
10	8.5,** 8.9 GHz	77.0%
11	8.9 GHz	75.4%

*Subsidiary maxima

**Equal maxima, 8.5 GHz has higher average polarization/slot sensitivity.

The low transmission values at resonance result from the two polarizations for Panels 9 and 10 having separate resonant frequencies. With the various slot designs and orientations in Panel 11, this difference is less pronounced and gives a single composite resonance.

SUMMARY FOR RMR PANELS

Table 23 summarizes the transmission data for RMR Panels 2, 3, 4, 5, 6, 7, 8, 9, 10 and 11, and the unmetallized A-sandwich. The A-sandwich data was measured with a 20 mil laminate in lieu of the RMR layers, i.e., it simulated the total A-sandwich with 33/33 mil skins but without rain erosion coating.

TEST RESULTS, IPD

Although emphasis was placed upon transmission, IPD results were determined at two frequencies. Table 24 shows the values obtained for Panels 6, 7, 9, 10 and 11, as well as for the A-sandwich (33/33 mil skins). Noteworthy features are:

- For Panels 6 and 7, the IPD's were smaller than observed for the A-sandwich alone except at the highest two angles of incidence at 9.7 GHz. Thus, the resonant metal slot arrays effectively have inductive impedances over this range. The other panels may be inductive, but if so, this is offset by the added dielectric material in the rain erosion coating.
- The net IPD variation over 0 to 60° incidence is higher with any of the RMR panels than for the A-sandwich alone for both E and H plane polarizations. This may be mitigated by the fact that the A-sandwich

did not have a rain erosion coating, but tends to predict larger radome boresight errors.

TABLE 20
TRANSMISSION RESPONSE

RESONANT METAL RADOME PANEL NO. 9 (60° SLOTS) WITH RAIN EROSION COATING 12-1464

Polarization	Freq. GHz	Transmission, %, For Incidence Angle (Deg.)							
		0	10	20	30	40	50	60	Avg.
Perpendicular	8.5	80.9	80.9	80.4	79.1	77.4	72.6	64.1	76.5
	8.7	81.5	81.5	81.5	80.7	79.0	74.5	62.7	77.3
	8.9	83.1	82.8	82.3	81.1	78.1	72.1	60.6	77.2
	9.1	83.5	83.5	83.8	82.5	78.3	70.5	60.3	77.5
	9.3	83.6	83.3	81.6	79.6	75.3	67.6	57.6	75.5
	9.5	78.5	77.3	75.6	73.6	69.6	61.6	51.1	69.6
Parallel	8.5	80.9	81.9	83.2	85.2	87.2	86.9	86.9	84.6
	8.7	81.5	81.5	81.7	82.7	83.5	83.5	83.0	82.5
	8.9	83.1	83.4	82.6	81.6	83.4	83.4	83.6	83.0
	9.1	83.5	83.5	83.3	83.0	84.0	85.5	86.3	84.2
	9.3	83.6	83.9	84.6	85.4	86.6	89.1	91.4	86.4
	9.5	78.3	78.6	81.1	83.3	87.1	89.8	92.3	84.4

Frequency:	8.5	8.7	8.9	9.1	9.3	9.5
Avg. Transmission (%) 2 Polarizations:	80.6	79.9	80.1	80.3	81.0	77.0
Avg. Polarization/Slot Sensitivity:	1.7	4.0	2.1	4.5	1.9	2.1

TABLE 21

TRANSMISSION RESPONSE

RESONANT METAL RADOME PANEL NO. 10
(50° SLOTS) WITH RAIN EROSION COATING

12-1458

Polarization	Freq. GHz	Transmission, %, For Incidence Angle (Deg.)							
		0	10	20	30	40	50	60	Avg.
Perpendicular	8.3	71.5	71.5	71.0	70.7	69.7	69.7	64.2	69.8
	8.5	76.4	76.9	76.4	76.6	76.1	73.9	68.9	75.0
	8.7	76.8	76.8	76.5	75.8	75.5	71.0	63.3	73.7
	8.9	77.5	77.5	76.2	74.7	73.7	70.0	62.2	73.1
	9.1	76.8	76.5	76.0	73.5	70.3	66.3	53.3	70.4
	9.3	72.5	73.2	73.2	71.2	66.5	59.2	50.2	66.6
	9.5	70.0	68.8	67.0	64.8	61.0	53.3	43.5	61.2
Parallel	8.3	71.5	71.2	71.7	74.2	78.0	81.2	87.5	76.5
	8.5	76.4	75.9	75.2	77.2	79.2	83.4	84.9	78.9
	8.7	76.8	77.0	76.3	76.5	80.3	84.0	85.0	79.4
	8.9	77.5	77.2	78.2	79.0	81.7	85.5	87.2	80.9
	9.1	76.8	77.5	78.8	79.8	82.0	85.8	89.0	81.4
	9.3	72.5	73.7	76.2	79.2	82.0	84.5	87.0	79.3
	9.5	70.0	71.0	73.3	76.0	78.5	82.3	86.3	76.8

Frequency	8.3	8.5	8.7	8.9	9.1	9.3	9.5
Avg. Transmission (%) 2 Polarizations:	73.2	77.0	76.6	77.0	75.9	73.0	69.0
Avg., Polarization/Slot Sensitivity:	14.0	9.3	5.5	3.1	2.8	6.6	7.4

TABLE 22

TRANSMISSION RESPONSE

RESONANT METAL RADOME PANEL NO. 11
(MIXED SLOT DESIGNS) WITH RAIN EROSION COATING

12-1463

Polarization	Freq. GHz	Transmission, %, For Incidence Angle (Deg.)							
		0	10	20	30	40	50	60	Avg.
Perpendicular	8.5	72.0	71.7	70.5	68.7	67.7	66.5	62.7	68.5
	8.7	74.9	73.9	72.4	70.4	68.4	65.7	53.0	68.4
	8.9	78.0	76.7	74.5	71.7	68.5	65.0	57.7	70.3
	9.1	77.3	77.3	76.8	72.3	67.0	61.8	55.0	69.6
	9.3	75.4	74.6	72.6	69.6	63.9	61.4	48.1	66.5
	9.5	74.5	73.3	70.8	67.0	61.8	53.5	41.0	63.1
Parallel	8.5	72.0	71.7	71.0	71.5	76.0	79.2	80.2	74.5
	8.7	74.9	74.6	74.6	74.6	76.4	79.9	81.6	76.7
	8.9	78.0	79.0	79.5	77.7	78.7	83.5	87.2	80.5
	9.1	77.3	78.5	79.5	80.0	80.8	83.0	87.0	80.9
	9.3	75.4	76.9	79.4	81.2	82.7	86.2	89.2	81.6
	9.5	74.5	75.0	77.3	80.5	83.3	87.3	89.8	81.1

Frequency:	8.5	8.7	8.9	9.1	9.3	9.5
Avg. Transmission (%), 2 Polarizations:	71.7	72.6	75.4	75.3	74.1	72.1
Avg., Polarization/ Slot Sensitivity:	5.9	4.0	3.5	2.5	2.9	3.1

TABLE 23

TRANSMISSION RESPONSE

SUMMARY FOR RMR AND A-SANDWICH PANELS

12-1484

Freq. (GHz)	Transmission, %, Average (0°-60°, ⊥ &, //Polarization), Panel No.:										
	2	3	4	5	6	7	8	9	10	11	A-Sandwich*
8.3									73.2		
8.5								80.6	77.0	71.7	
8.7		73.9						79.9	76.6	72.6	
8.9		76.9						80.1	77.0	75.4	95.2
9.1		78.8						80.9	75.9	75.3	
9.3	77.5	81.4			78.5	72.0		81.0	73.0	74.1	96.3
9.5	79.6	82.2			81.4	75.0		77.0	69.0	72.1	95.3
9.7	80.2	84.3	76.4		83.4	77.7	79.8				96.0
9.9	80.9	86.4	79.0	66.6	84.0	80.3	82.4				
10.1	77.2	84.7	81.3	69.3	82.2	78.8	83.9				95.8
10.3	74.8	85.5	81.4	72.0	80.5	76.6	83.3				
10.5		84.7	79.9	74.0			82.3				95.9
10.7		82.4	77.0	73.7							
10.9											94.6
11.1											
11.3											92.7
Slot	50°	60°	60°	50°	60°	50°	60°	60°	50°	Mixed	NA
LLM**	195	186	174	174	191	192	192	.214	.215	.215	NA
SWM***	38	42	30	28	33	34	47	.035	.036	.036	NA

* A-Sandwich used with all RMR layers, tested with 33/33 mil skins, no rain erosion coating.
** LLM = Leg Length Mils
*** SWM = Slot Width Mils

TABLE 24

INSERTION PHASE RESPONSE – RESONANT METAL RADOME PANELS

12–1440

Panel	Polarization	9.3 GHz, For Incidence (Deg) of:							9.7 GHz, For Incidence (Deg) of:						
		0	10	20	30	40	50	60	0	10	20	30	40	50	60
A-Sandwich	Perpendicular	33.3	33.4	34.3	36.0	38.7	42.9	49.3	35.8	36.8	38.0	39.7	42.5	46.5	52.8
	Parallel	33.3	33.1	32.2	32.2	31.2	32.7	36.2	35.8	35.2	34.9	34.2	34.5	34.9	37.6
RMR#6	Perpendicular	13.3	14.1	15.7	18.5	23.2	29.7	39.1	24.5	25.8	28.5	32.7	38.3	46.3	56.1
	Parallel	13.3	14.1	14.5	16.1	18.4	21.9	27.1	24.5	25.1	25.3	25.8	27.8	30.7	36.2
RMR#7	Perpendicular	10.3	10.9	12.6	15.9	20.8	28.0	37.4	24.2	25.4	28.5	33.6	39.7	48.5	59.1
	Parallel	10.3	11.0	12.1	13.6	16.3	20.1	26.0	24.2	24.0	23.9	24.3	26.7	29.5	35.1
RMR#9	Perpendicular	38.3	38.9	41.5	47.0	54.5	62.6	74.1	49.5	51.7	54.7	60.9	68.9	78.8	87.5
	Parallel	38.3	38.7	38.1	37.0	37.0	38.1	42.3	49.5	49.7	49.2	47.2	46.3	46.8	49.7
RMR#10	Perpendicular	39.0	39.7	42.2	48.2	56.8	65.2	73.8	50.0	50.8	56.9	63.4	72.0	81.0	89.0
	Parallel	39.0	39.8	40.0	40.7	41.4	41.9	43.0	50.0	50.0	49.4	48.0	48.0	49.5	50.0
RMR#11	Perpendicular	39.0	39.9	43.6	47.4	55.9	64.8	74.5	52.8	54.5	57.7	63.8	72.3	80.7	91.3
	Parallel	39.0	38.9	38.6	37.9	37.4	38.7	42.2	52.8	52.7	51.7	50.8	49.9	50.0	52.7

From the above, it is evident that radomes having the same design as the RMR panels would have larger boresight errors than the all dielectric A-sandwich wall. Since transmission efficiency is also less, this is not unexpected. It is likely that improvement of resonant metal designs for better transmission efficiency would yield improved performance in all respects.

At the completion of the flat panel tests, Panel 10 was bonded together permanently (in lieu of being held together with a vacuum bag as was the case with all of the previous measurements). Transmission and insertion phase delay measurements were made and compared to the original Panel 10 measurements given in Table 21. Out of 98 data points taken, 67 were within 2% of the original readings, 92 were within 4%, and of those which were not within 4%, 4 were at 60° incidence. Insertion phase delays were all within 3 degrees and most were within 2 degrees. This confirms that using a substrate with interchangeable skins gives valid electrical test results.

Biplanar Array - A biplanar array was assembled for test, utilizing the now bonded up Panel 10 and the metallic skin for Panel 11. Two plies of fiberglass-epoxy were removed from the back side of Panel 10. The Panel 11 metallic skin was then assembled to it, so that the A-sandwich was balanced with an equal number of plies on each side of the honeycomb in addition to having a slotted metallic surface on each side of the panel. Neither side of the panel had a rain erosion coating.

The biplanar array characteristically has a more narrow bandpass and sharper out of band cutoff as demonstrated by OSU in Reference 16. However, these characteristics were not pronounced on this panel. Average transmission was 71.3% at 9.3 GHz. Table 25 summarizes the test results.

TABLE 25
TRANSMISSION RESPONSE
RESONANT METAL RADOME PANEL NO. 10 & 11
BIPLANAR ARRAY WITHOUT RAIN EROSION COATING

12-2126

Polarization	Freq. GHz	Transmission, %, For Incidence Angle (Deg.)							
		0	10	20	30	40	50	60	Avg.
Perpendicular	8.3	64.9	63.4	60.4	53.4	45.4	35.4	24.7	49.7
	8.5	68.1	68.1	66.3	61.8	55.3	46.8	36.6	57.6
	8.7	70.3	70.0	68.8	65.8	61.0	55.3	44.0	62.2
	8.9	72.0	71.2	70.7	68.5	64.5	58.2	49.5	65.0
	9.1	70.0	69.8	68.5	67.3	62.8	56.3	47.0	63.1
	9.3	74.0	73.0	71.7	69.5	65.0	58.2	48.7	65.7
	9.5	70.0	69.3	66.8	63.8	59.0	52.5	44.5	61.0
Parallel	8.3	64.9	64.4	62.6	60.9	61.4	64.1	66.1	63.5
	8.5	68.1	67.6	67.4	66.6	67.6	69.1	71.6	68.3
	8.7	70.3	70.3	70.5	71.0	72.8	76.0	79.0	72.8
	8.9	72.0	71.2	69.7	71.5	74.7	78.2	78.2	73.6
	9.1	70.0	70.3	71.3	72.8	76.5	79.5	81.0	74.5
	9.3	74.0	73.7	74.0	76.5	79.2	80.2	81.0	76.9
	9.5	70.0	71.0	73.0	76.3	79.0	81.0	81.8	76.0
Frequency		8.3	8.5	8.7	8.9	9.1	9.3	9.5	
Avg. Transmission (%), 2 Polarizations:		56.6	63.0	67.5	69.3	68.8	71.3	68.5	
Avg., Polarization/ Slot Sensitivity:		12.5	6.9	3.5	2.8	2.8	3.9	1.3	

SECTION VI
DEMONSTRATION ARTICLES

The method chosen for metallization of the two demonstration radomes was a combination of the wallpaper and electroform approaches discussed in Sections 2.0 and 3.0. The wallpaper approach was chosen for these demonstration articles because of the minimum amount of tooling required to manufacture the radomes by this method. Additionally, the slot pattern layout developed by OSU (Reference 15) lends itself to assembly in pieces since the layout is composed of equilateral and isosceles triangles of various sizes. Since the number of triangles near the tip of the radome is large, and the size of the triangles small, it was decided to electroform the region around the nose as one piece. The nosecap was sufficiently small so that existing facilities were utilized to fabricate, i.e., form, expose and etch the tool. Aside from the advantage of simplifying fabrication of the radomes, building a doubly curved nosecap gave us the opportunity to demonstrate two fabrication methods on a single radome, within the time and cost constraints of the program.

The C-140 (Jetstar) Nose Radome is a relatively small radome in current production at Brunswick. Among the reasons for choosing this radome as an appropriate demonstration article were its compatibility with currently operational range test equipment, the availability of radome electrical performance data for comparison, the use of an available antenna with known, unclassified operational characteristics, and the relatively noncritical electrical performance. This radome is approximately 22 inches long by 34 inches wide, has an A-sandwich wall, and is fabricated using female tooling. A schematic of the radome is shown in Figure 63.

6.1 SUBSTRATE FABRICATION

The demonstration radome's substrate was the standard Jetstar radome without the lightning diverter strips or rain erosion coating. The Jetstar radome's A-sandwich wall is constructed with E-glass-epoxy face sheets and a nylon-phenolic honeycomb core. The A-sandwich substrates for the demonstration radomes were fabricated by standard hand layup procedures as controlled by Brunswick Process Specification BPS 754-121-001. The fabrication steps are briefly described in the following paragraphs.

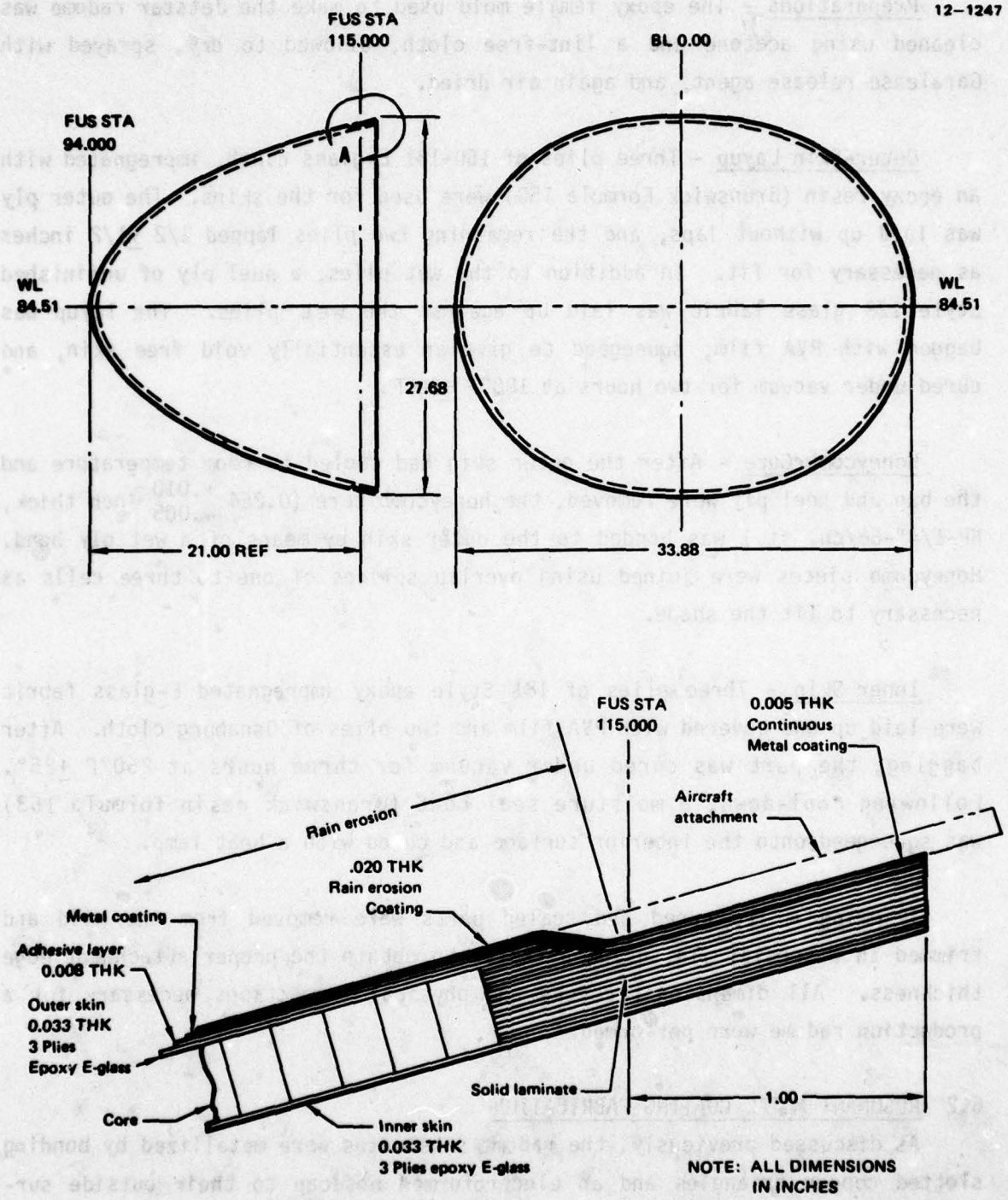

Figure 63 C-140 nose radome

Preparations - The epoxy female mold used to make the Jetstar radome was cleaned using acetone and a lint-free cloth, allowed to dry, sprayed with Garalease release agent, and again air dried.

Outer-Skin Layup - Three plies of 150-181 E-glass cloth, impregnated with an epoxy resin (Brunswick Formula 150) were used for the skins. The outer ply was laid up without laps, and the remaining two plies lapped 1/2 $\pm$1/2 inches as necessary for fit. In addition to the wet plies, a peel ply of unfinished Style 128 glass fabric was laid up against the wet plies. The layup was bagged with PVA film, squeegeed to give an essentially void free skin, and cured under vacuum for two hours at 180°F $\pm$20°F.

Honeycomb Core - After the outer skin had cooled to room temperature and the bag and peel ply were removed, the honeycomb core (0.264 $^{+.010}_{-.005}$ inch thick, NP-1/4"-6#/cu. ft.) was bonded to the outer skin by means of a wet ply bond. Honeycomb pieces were joined using overlap splices of one to three cells as necessary to fit the shape.

Inner Skin - Three plies of 181 Style epoxy impregnated E-glass fabric were laid up and covered with PVA film and two plies of Osnaburg cloth. After bagging, the part was cured under vacuum for three hours at 250°F $\pm$25°. Following cool-down, a moisture seal coat (Brunswick resin formula 163) was squeegeed onto the interior surface and cured with a heat lamp.

Trimming - The cured and sealed parts were removed from the mold and trimmed in a special jig, using a router to obtain the proper attachment edge thickness. All dimensional checks and physical inspections necessary for a production radome were performed.

6.2 RESONANT METAL COATING FABRICATION

As discussed previously, the radome substrates were metallized by bonding slotted copper triangles and an electroformed nosecap to their outside surfaces. The manufacture of the triangles and nosecap are described in the following paragraphs.

Triangles - The copper triangles were manufactured by the same method used to make the flat panels, as described in Section 5.0, using standard circuit board equipment.

Nosecap - The nosecap was manufactured by the electroform and bond technique described in Section 2.0 of this report. A stainless steel mandrel was formed to the contour of the first 6 inches of the radome tip by drop hammer forming using matched metal molds. This 0.020-inch thick stainless steel mandrel was etched with the slot pattern to a depth of 0.006 inch. The doubly curved transparency used for photoetching was fabricated from copper clad fiber glass-epoxy (Figure 64).

To make the transparency, a negative image of the slot pattern was etched on a copper clad 0.005 inch thick fiberglass-epoxy substrate. Triangles of appropriate size and shape were cut out of the substrate and seamed together on the radome mandrel in such a way that the shape of the transparency closely approximated the shape of the radome tip. After the

12-1422

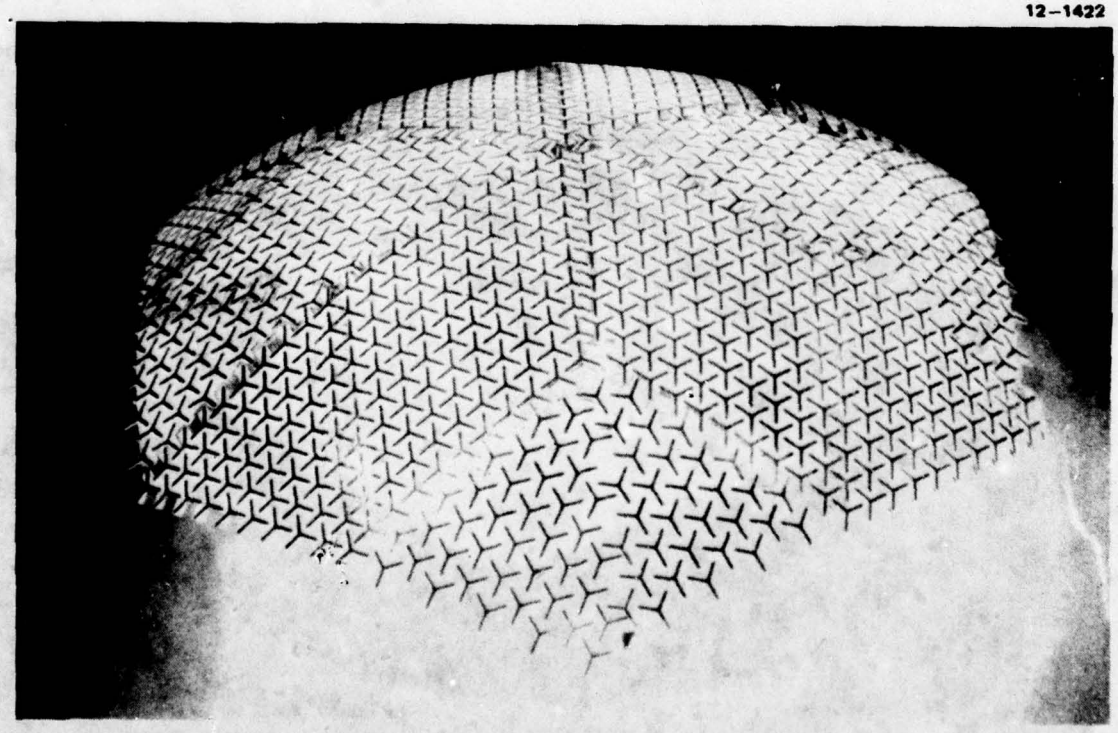

Figure 64 Doubly curved transparency used to image the resist for the nosecap mandrel

triangles were arranged, on the radome mandrel, the mandrel and transparency were vacuum bagged and heated to a temperature sufficient to soften the epoxy (about 250°F), allowing it to conform to the mandrel surface. The copper elements on the transparency do not distort thereby maintaining the most important dimension, the element size.

The completed transparency was then used to image the photoresist which had been previously spray applied to the mandrel. The copper elements on the fiberglass-epoxy transparency act as the emulsion would on a standard circuit board transparency, i.e., masking those areas to be etched.

After the stainless steel mandrel was coated with photoresist, the transparency was placed over the mandrel and the assembly was exposed to ultraviolet light. The resist was developed and the mandrel was spray etched until a slot depth of 0.006 was reached. The etched mandrel was spray coated with Teflon. The Teflon was then sanded off everywhere except in the slots and the stainless was polished to facilitate release of the electroform from the mandrel. The completed mandrel is shown in Figure 65.

12-1436

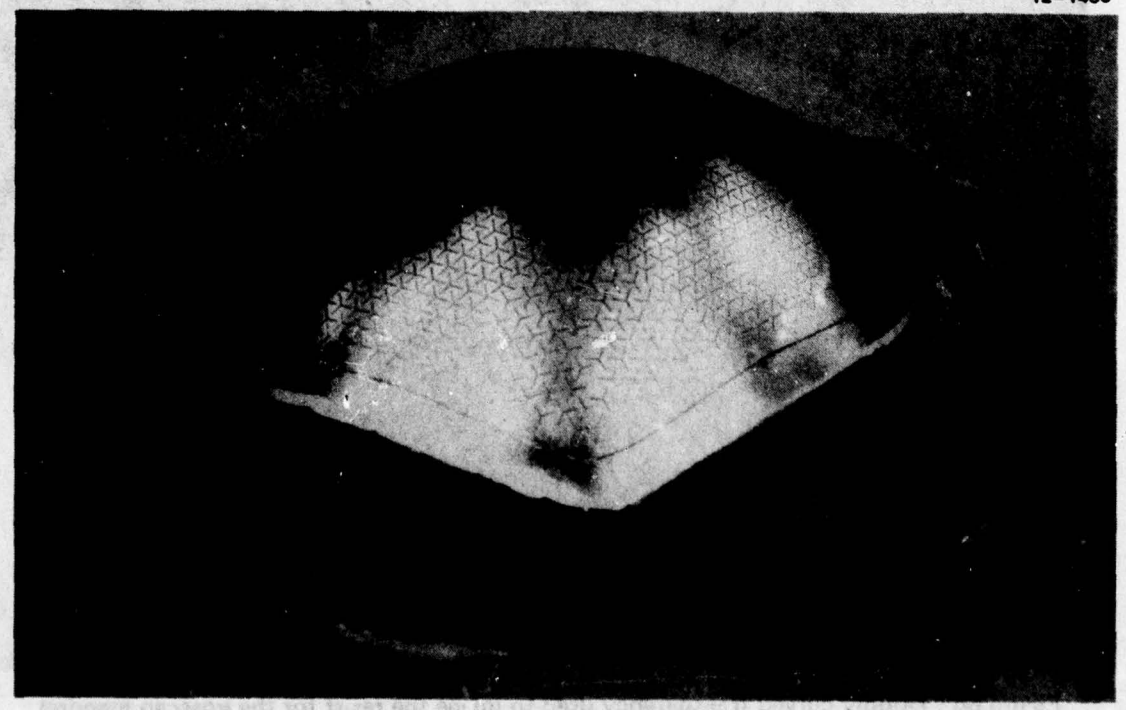

Figure 65 Mandrel for electroforming the radome nosecap

Electrical connections were made to the mandrel and it was placed in a copper pyrophosphate plating bath. The electroplating was accomplished at 35 amps/sq. ft. until the deposit was approximately 5 mils thick (the same thickness as the copper triangles used on the remainder of the radome). The electroformed part was released from the mandrel with a spatula. A completed nosecap is shown in Figure 66.

6.3 ASSEMBLY

The assembly of the metal coating to the substrates was accomplished by hand in the Brunswick plant. The radome shells were prepared for coating by lightly sand blasting the surface to remove the resin sheen without fraying the woven fiberglass cloth. After sanding, the shells were solvent wiped with cheesecloth wet with MEK solvent.

Film adhesive was cut and fit to the radome substrates and the electroformed nosecap set in place. The slotted metal triangles were butted against the nosecap edge to complete the first row. The second and third rows were done in the same fashion. Figure 67 shows the nosecap and the first and

12-1261

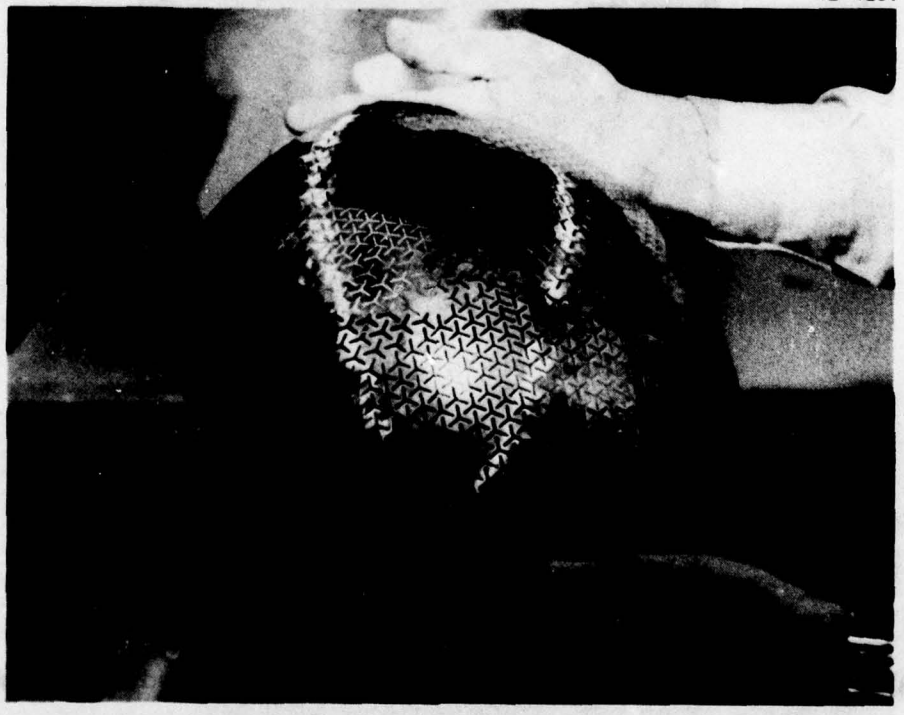

Figure 66 Electroformed copper nosecap for the demonstration radome

second rows in place. The AF 147 film adhesive used is not very tacky at room temperature which allowed repositioning of parts before final bonding. When the parts are in final position, a heat gun was used to warm the adhesive, increasing its tack. A roller was then used to roll the copper cladding tightly against the radome substrate. The radome with all triangles in place is pictured in Figure 68.

After the copper cladding was properly positioned and held firmly on the radome by the tack of the film adhesive, the entire assembly was covered by a conformal silicone rubber boot whose purpose was to seal off the slot openings to reduce the amount of adhesive flow over the surface during cure as well as to act as a release ply after curing. The entire assembly was vacuum bagged and placed in the mold used to fabricate the substrate, to hold the radomes' shape during cure. The vacuum bag was pumped down to apply approximately 14.7 psi of pressure and held for 20 minutes to allow venting of air pockets and the entire assembly was placed in an autoclave. The autoclave was pressurized to 35 psig (total pressure was approximately 50 psig, due to

12-1291

Figure 67 Demonstration radome, coated with AF 147 film adhesive and some triangles in place. (Details of joints can be seen in this picture.)

12–1431

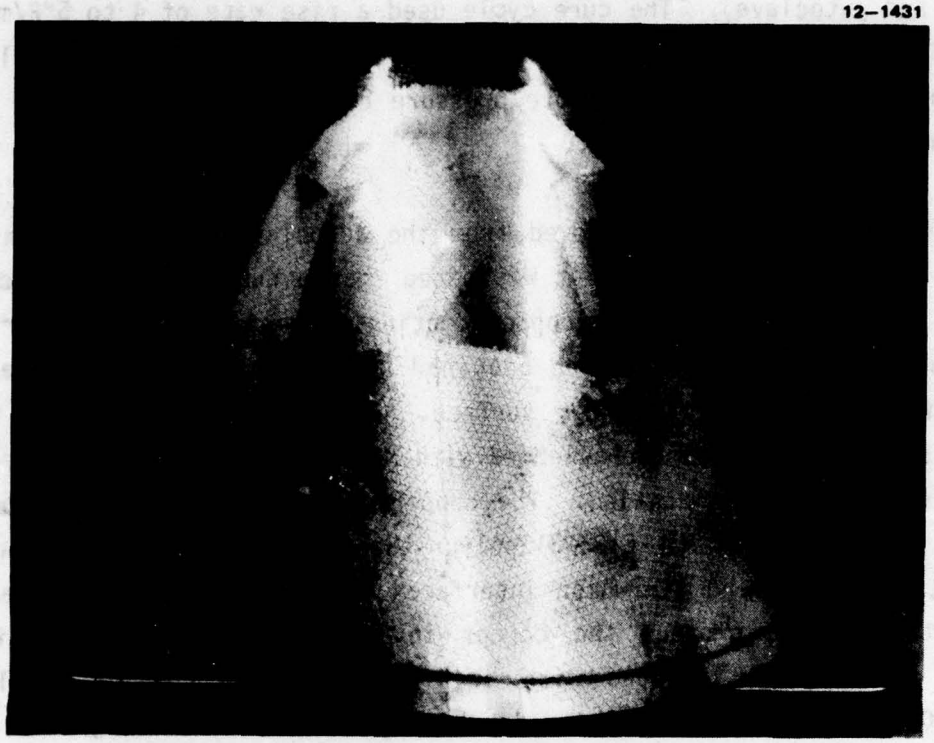

Figure 68A Demonstration radome completely metallized

12–1460

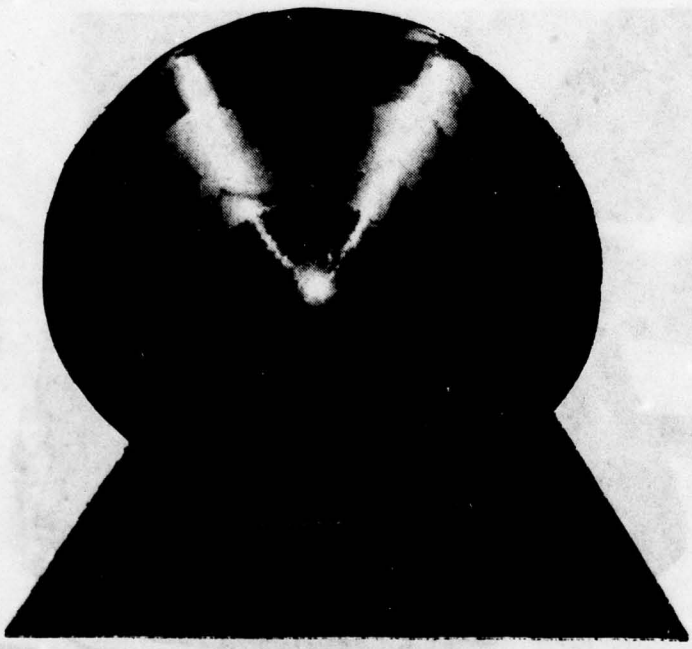

Figure 68B Nose on view of metallized Jestar radome

vacuum and autoclave). The cure cycle used a rise rate of 4 to 5°F/minute to 350°F followed by a one-hour hold at 350° ±5°F. The part was then allowed to cool to approximately 150°F before pressure release. After cooling, the part was removed from the autoclave.

After the radome was removed from the autoclave and the vacuum bag and rubber and boot were removed, it was noted that a number of resin pockets had formed on the exterior of the copper coating. These were due in part to the fact that the conformal silicone boot had bubbles within its thickness which could not be seen on its inner surface. This residue was sanded from the copper surface which was then cleaned with MEK prior to the application of the rain erosion resistant coating. The copper coated demonstration radomes were primed, and 20 mils of MIL-C-83231 polyurethane rain erosion coating was spray applied. The mounting lip which interfaces the aircraft was not covered with polyurethane. To protect the copper in this area against corrosion, the exposed surface was treated with Iridite conversion coating (applied per MIL-B-5087B) which is a corrosion inhibiting coating that has good electrical conductivity and which is commonly used for protecting electrical bonds in aircraft. The completed radome is shown in Figure 69.

12-1430

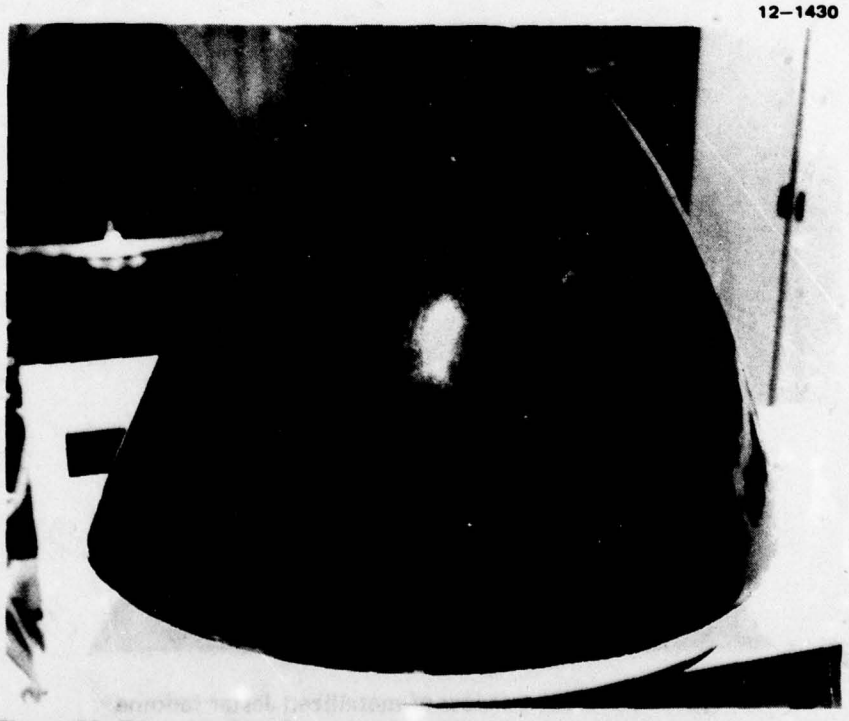

Figure 69 The completed resonant metal radome with rain erosion coating

6.4 TESTING

The radar in with the Jetstar (C-140) aircraft is a Bendix system utilizing the Bendix ANT-1G antenna pictured in Figure 70. Its operational characteristics are given in Table 26.

The production Jetstar radome is tested for transmission efficiency and antenna/radome radiation patterns on a sampling basis in production. Although not of importance in this weather radar, the directional accuracy (beam deflection, or boresight error) is often critical in military radar. Therefore, such tests were conducted for the demonstration units.

Electrical evaluation measurements of the demonstration radomes were conducted at one of Brunswick's outdoor test ranges. The test range is elevated approximately 25 ft. above ground and consists of (1) a primary tower which has a radome positioning fixture with an integral system antenna mount and the

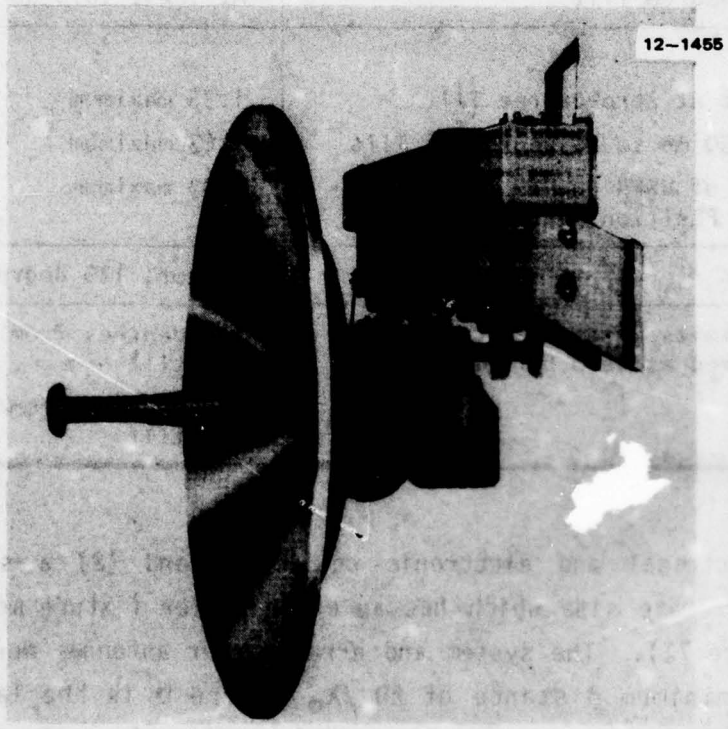

Figure 70 ANT-1G (X-band) sector scanning antenna

TABLE 26
SYSTEM ANTENNA SPECIFICATIONS

12-1438

Reflector Diameter	18 inches
Focal Length	8 inches
Operating Frequency	9375 ±30 mc (X_s band)
Wavelength	3.2 cm
Beam Shape	Symmetrical pencil
Polarization	Vertical
Beam Width	5.3 degrees maximum in E & H Planes
Gain at Zero-Degree Tilt	29.5 db maximum
Side Lobes:	
At Zero-Degree Tilt	At least 18.5 db down
At 10 Degree Tilt	At least 16.0 db down
At 20 Degree Tilt	At least 10.0 db down
VSWR:	
9375 mc at Zero-Degree Tilt	1.35 maximum
9375 ±50 mc to 20 Degree of Tilt	1.63 maximum
Change of VSWR due to Antenna Scan Position	0.03 maximum
Type of Scan	Sector, 120 degrees total
Beam Tilt Limits (Radome tests will be performed at Zero Degree Tilt)	±15 degrees from zero-degree tilt ±20 degrees from zero-degree tilt

necessary electrical and electronic equipment, and (2) a secondary tower located at a remote site which has an error seeker fixture mounting another antenna (Figure 71). The system and error seeker antennas were separated by more than a minimum distance of $2D^2/\lambda_o$, where D is the largest antenna aperture diameter and λ_o is the free-space wavelength at the test frequency.

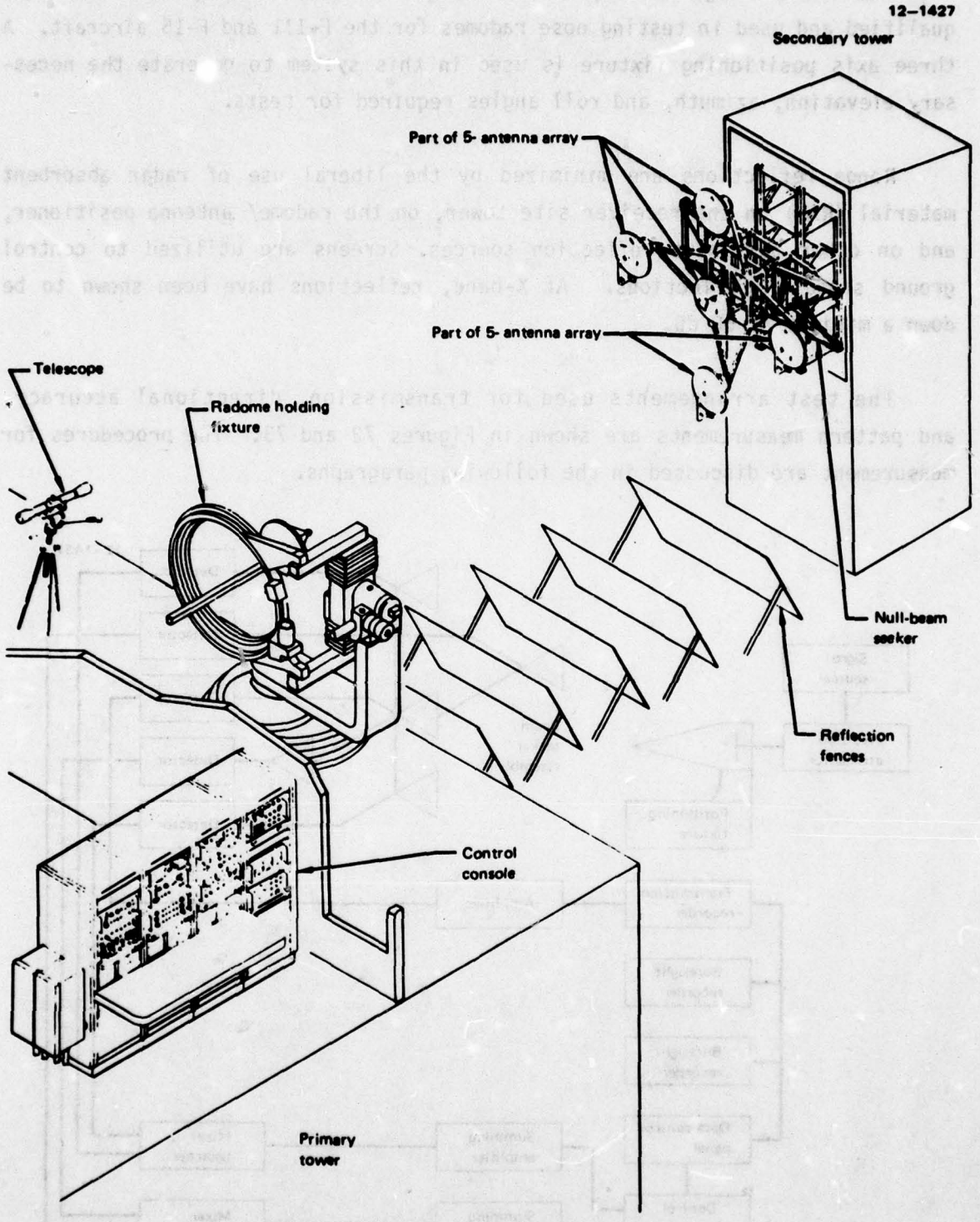

Figure 71 Brunswick radome test range

The basic range and equipment is of the latest design and has been qualified and used in testing nose radomes for the F-111 and F-15 aircraft. A three axis positioning fixture is used in this system to generate the necessary elevation, azimuth, and roll angles required for tests.

Range reflections are minimized by the liberal use of radar absorbent material (RAM) on the receiver site tower, on the radome/ antenna positioner, and on other pertinent reflection sources. Screens are utilized to control ground specular reflections. At X-band, reflections have been shown to be down a minimum of 50 dB.

The test arrangements used for transmission, directional accuracy, and pattern measurements are shown in Figures 72 and 73. The procedures for measurement are discussed in the following paragraphs.

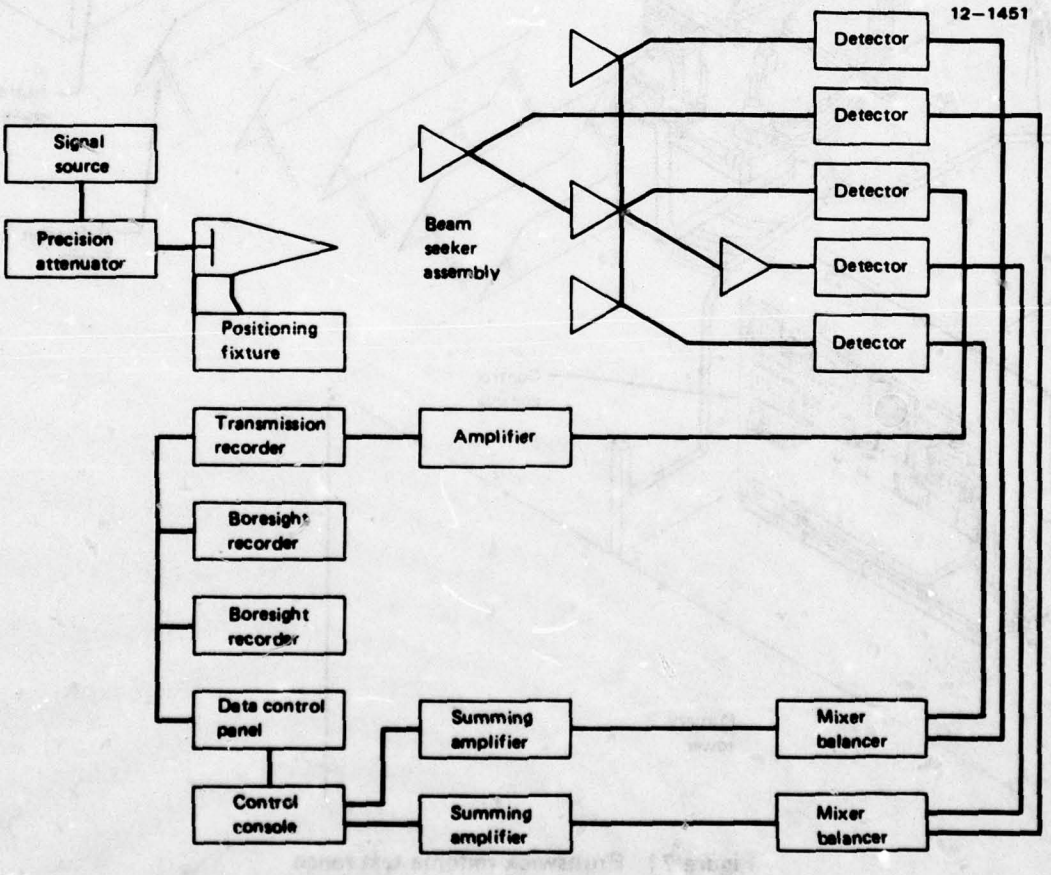

Figure 72 Test arrangement, transmission and directional accuracy

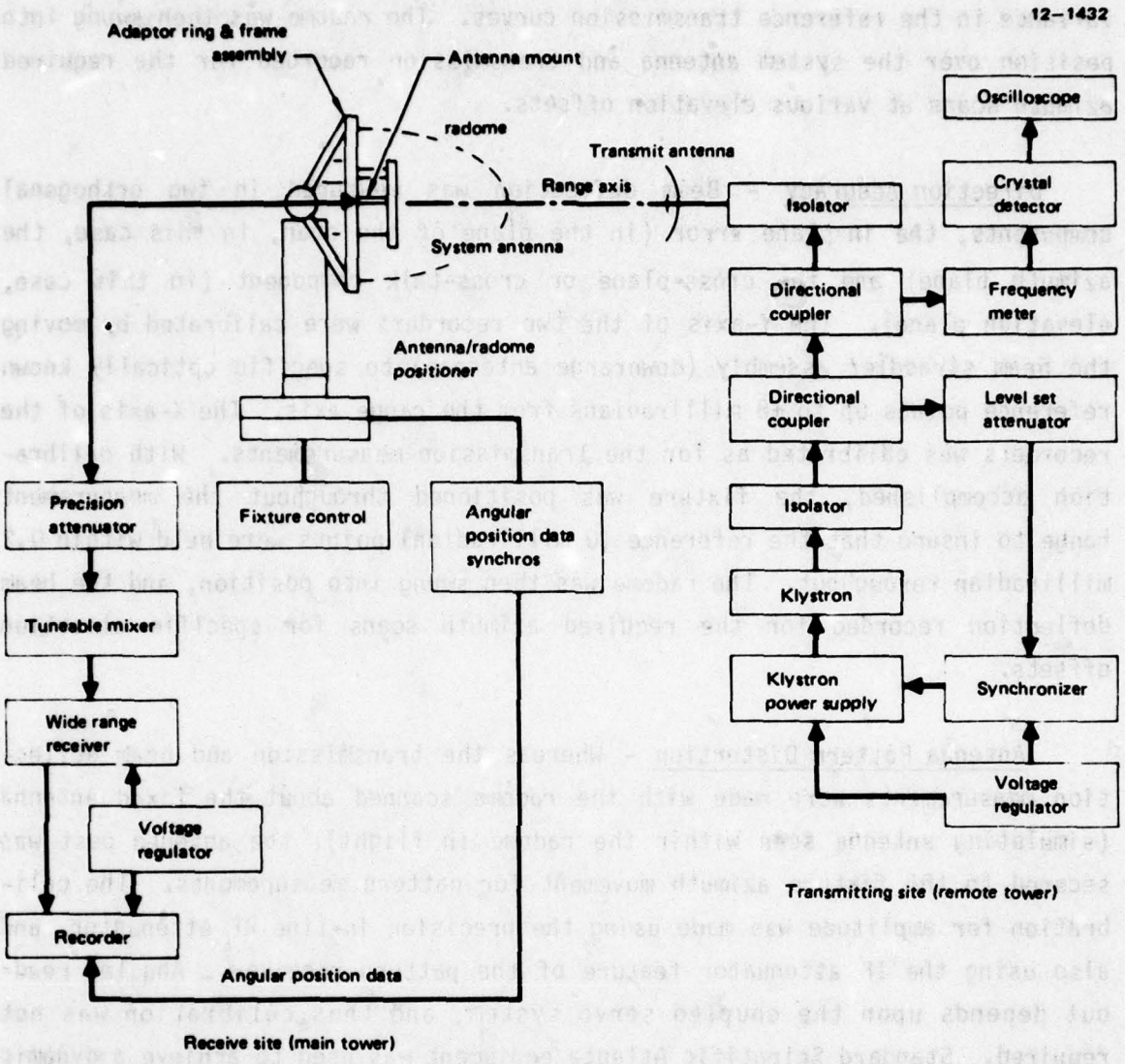

Figure 73 Block diagram of instrumentation for radar antenna/ radome pattern measurements

Power Transmission Efficiency - The test system was initially tuned and the antennas aligned in azimuth, elevation, and roll for maximum received power. The X-Y recorder used for continuous transmission versus scan angle data was calibrated in the Y-axis (using the in-line precision RF attenuator, nonlinearity not exceeding 1%) and the X-axis (using the positioner azimuth movement dial, nonlinearity not exceeding 1%) movements. The positioner was moved throughout the measurement sector without the radome in place to insure that residual reflections from the range or test jig caused no more than ±1%

variance in the reference transmission curves. The radome was then swung into position over the system antenna and transmission recorded for the required azimuth scans at various elevation offsets.

Direction Accuracy - Beam deflection was measured in two orthogonal components, the in-plane error (in the plane of the scan, in this case, the azimuth plane) and the cross-plane or cross-talk component (in this case, elevation plane). The Y-axis of the two recorders were calibrated by moving the beam straddler assembly (downrange antennas) to specific optically known reference points up to ±8 milliradians from the range axis. The X-axis of the recorders was calibrated as for the transmission measurements. With calibration accomplished, the fixture was positioned throughout the measurement range to insure that the reference (0 milliradian) points were held within 0.2 milliradian throughout. The radome was then swung into position, and the beam deflection recorded for the required azimuth scans for specific elevation offsets.

Antenna Pattern Distortion - Whereas the transmission and beam deflection measurements were made with the radome scanned about the fixed antenna (simulating antenna scan within the radome in flight), the antenna post was secured to the fixture azimuth movement for pattern measurements. The calibration for amplitude was made using the precision in-line RF attenuator, and also using the IF attenuator feature of the pattern receiver. Angular readout depends upon the coupled servo system, and thus calibration was not required. Standard Scientific Atlanta equipment was used to achieve a dynamic range of 60 dB and the pattern chart was used so that one chart cycle represented a 360° scan segment. The 0° angular chart position represented the antenna pointed directly through the nose of the radome; i.e., the dead ahead position. Any antenna azimuth offsets within the radome moved the beam peak and the magnitude of this shift could be read from the pattern chart. The antenna and radome were rolled so that the plane of measurement was always physically in azimuth, i.e., the alignment was as in flight for azimuth (H-plane) patterns and was to the on-side position for elevation (E-plane) patterns.

Electrical Tests - The electrical tests comprised a frequency search using radome S/N 2, detailed record tests, and finally tests for auxiliary data. The frequency search was conducted using the azimuth transmission scan (±40°) at 0° elevation at sufficient points to determine the resonant frequency and choose three appropriate frequencies for the record tests. Record tests included transmission scans and pattern recordings per the production test for the Jetstar (C-140) radome, beam deflection scans at the same angles used for transmission, and finally, included tests at three frequencies for all parameters in lieu of the single frequency test for C-140 production units. Auxiliary studies included investigating the effects of antenna polarization, radome cross polarization response, and measuring the effects of building up the inner skin of the radome (using standard glass tape customarily used for electrical wall correction).

As noted in earlier paragraphs, the radome slot design had been scaled using data from several flat panels to achieve resonance at 9.375 GHz, the operating frequency of the C-140 weather radar. It was quickly evident that the resonance achieved was lower than 9.375 GHz. Transmission data was taken at six frequencies and the data showed that the transmission versus frequency response curve had relatively moderate, slowly changing, characteristics and that optimum transmission was near 8.7 GHz. There was some variance between resonance for angles away from the nose (≥20°) and angles near the nose (<20°). Figure 74 shows the transmission versus frequency response for three azimuth angles (each with 0° elevation). Note that the 20° and 40° points (averaged for left and right offsets), each peak between 8.7 and 8.8 GHz, whereas the 0° azimuth plot was showing continually increasing transmission on down to 8.5 GHz or lower. The test frequencies chosen were: (1) 9.375 GHz, the operating frequency of the Jetstar radar, (2) 8.570 GHz, the lowest frequency available with Brunswick's range source, and (3) 8.875 GHz, which is near the radome's resonance for the higher offset angles.

The variation of transmission response and beam deflection with both angle and frequency is indicated by the 0° elevation scans shown in Figure 75. Note that the transmission curve shows essentially flat response versus azimuth angle for 8.570 GHz; whereas the higher frequency curves showed decided trends to higher transmission at the higher angles and a dip near 0°.

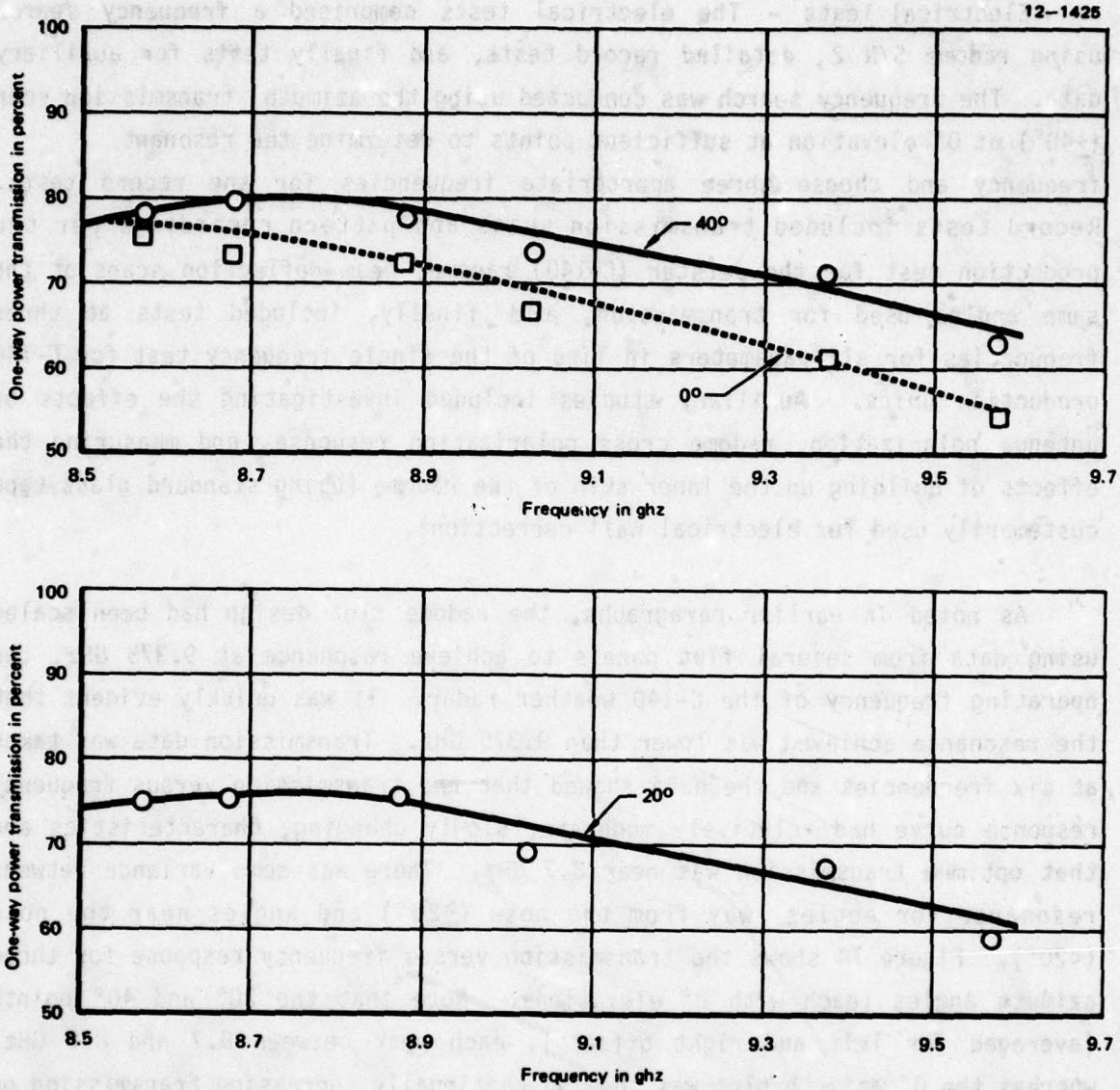

Figure 74 Transmission vs. frequency, RMR S/N 2, three asimuth angles

This fact indicates that the radome construction gave actual variances in resonant frequency in different areas. It was demonstrated in the flat panel investigations that resonant frequency is sensitive to the thickness of the dielectric skin adjacent to the slotted metal. It is believed that excess adhesive flowed towards the nose region during cure because the radomes were cured nose down in the mold. The gravitational effects on the adhesive could cause the substrate skin next to the metal to be thicker near the nose than elsewhere on the radome. This extra thickness may shift the resonant frequency in the nose region.

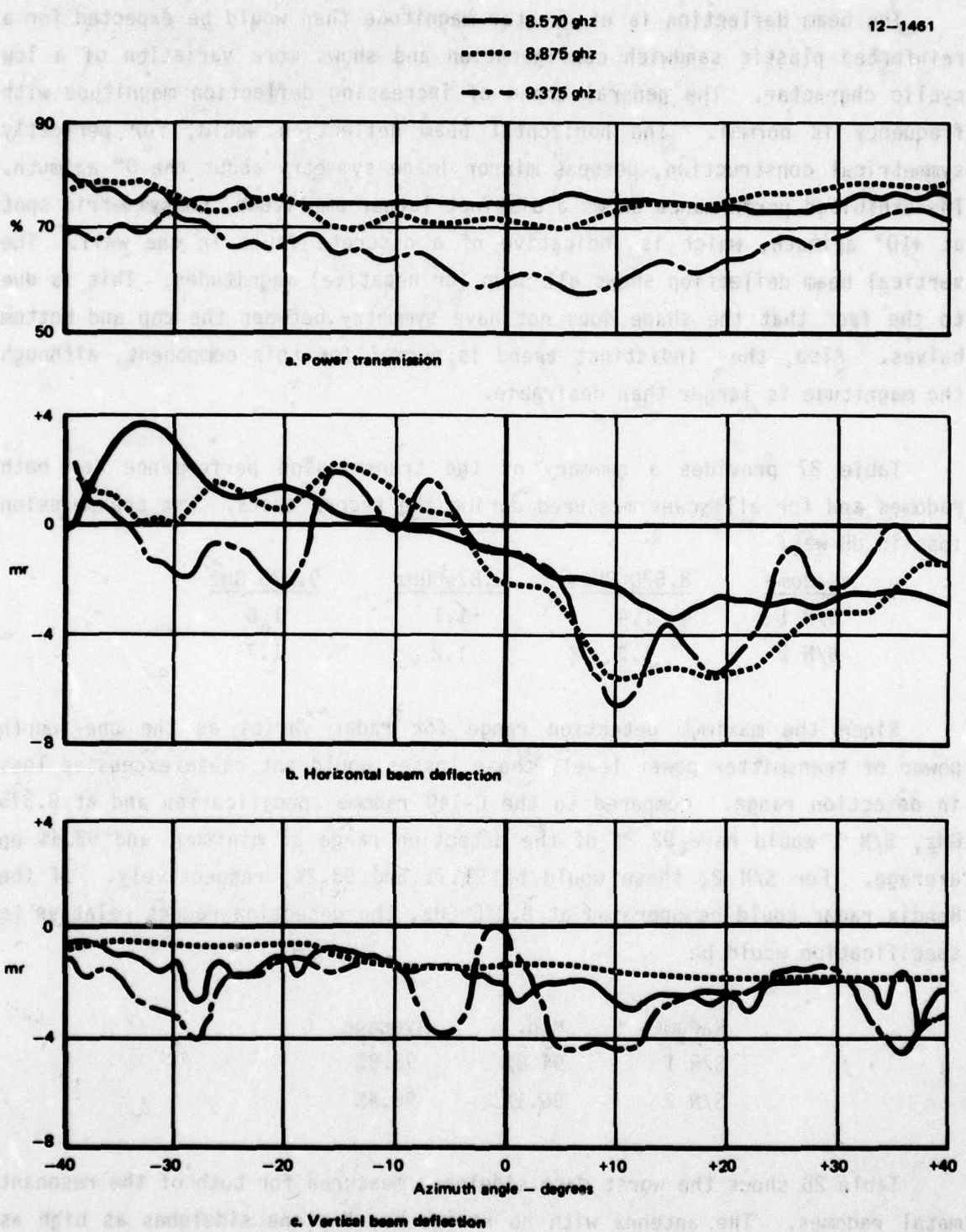

Figure 75 Resonant metal radome S/N 2, performance for azimuth scans at 0° elevation, three frequencies

The beam deflection is of greater magnitude than would be expected for a reinforced plastic sandwich configuration and shows more variation of a low cyclic character. The general trend of increasing deflection magnitude with frequency is normal. The horizontal beam deflection would, for perfectly symmetrical construction, possess mirror image symmetry about the 0° azimuth. The exhibited performance shows a distinct larger amplitude, nonsymmetric spot at +10° azimuth, which is indicative of a discrete fault in the wall. The vertical beam deflection shows all down (or negative) magnitudes. This is due to the fact that the shape does not have symmetry between the top and bottom halves. Also, the indistinct trend is normal for this component, although the magnitude is larger than desirable.

Table 27 provides a summary of the transmission performance for both radomes and for all scans measured during the record tests. Net transmission loss in dB was:

Radome	8.570 GHz	8.875 GHz	9.375 GHz
S/N 1	1.4	1.1	1.6
S/N 2	1.3	1.2	1.7

Since the maximum detection range for radar varies as the one-fourth power of transmitter power level, these losses would not cause excessive loss in detection range. Compared to the C-140 radome specification and at 9.375 GHz, S/N 1 would have 92.2% of the detection range at minimum, and 93.4% on average. For S/N 2, these would be 91.3% and 93.2%, respectively. If the Bendix radar could be operated at 8.875 GHz, the detection ranges relative to specification would be

Radome	Min.	Average
S/N 1	94.8%	95.8%
S/N 2	96.1%	96.4%

Table 28 shows the worst case sidelobes measured for both of the resonant metal radomes. The antenna with no radome has H-plane sidelobes as high as the -20.8 dB level. With the resonant metal radome, the H-plane levels do not exceed -19.1 dB for either radome at any of the three frequencies investi-

TABLE 27

MEASURED TRANSMISSION RESULTS SUMMARY FOR RESONANT METAL RADOMES

12-1493

Freq. (GHz)	Dome I.D.		Measured Transmission, %, Az Scans at Elev Offsets of:									Total All Scans
			-20°	-15°	-10°	-5°	0°	+ 5°	+10°	+15°	+20°	
8.570	S/N 1	Av.	72.0	73.0	72.6	73.5	73.0	73.2	72.0	72.6	71.8	72.6
		Min.	68.5	70.0	70.0	71.5	71.5	71.0	70.0	70.0	69.0	68.5
	S/N 2	Av.	76.3	73.4	74.0	74.5	75.2	75.0	74.1	72.1	72.3	74.1
		Min.	73.0	69.5	71.5	72.0	73.5	72.0	71.0	69.0	68.5	68.5
8.875	S/N 1	Av.	78.2	78.3	78.7	78.0	77.6	76.4	76.5	77.2	77.2	77.6
		Min.	75.5	75.0	75.0	75.0	74.0	73.5	72.5	74.5	74.0	72.5
	S/N 2	Av.	76.3	75.9	76.9	76.9	75.0	74.3	77.7	77.9	72.9	76.0
		Min.	74.0	72.5	72.5	72.5	70.0	70.0	69.0	68.5	69.0	68.5
9.375	S/N 1	Av.	68.7	67.8	68.9	68.2	69.9	68.8	67.6	68.6	68.7	68.6
		Min.	66.0	63.5	64.0	61.5	62.5	65.0	63.0	64.0	64.0	61.5
	S/N 2	Av.	70.0	69.2	68.7	68.8	67.0	66.7	66.7	67.6	67.6	68.0
		Min.	65.5	64.0	61.5	59.0	59.0	61.5	60.0	61.0	61.5	59.0
8.570	Both	Av.	74.2	73.2	73.3	74.0	74.1	74.1	73.1	72.4	72.1	73.4
		Min.	68.5	69.5	70.0	71.5	71.5	71.0	70.0	69.0	68.5	68.5
8.875	Both	Av.	77.3	77.1	77.8	77.5	76.3	75.4	77.1	77.6	75.1	77.3
		Min.	74.0	72.5	72.5	72.5	70.0	70.0	69.0	68.5	69.0	68.5
9.375	Both	Av.	69.4	68.5	68.8	68.5	68.5	67.8	67.2	68.1	68.2	68.3
		Min.	65.5	63.5	61.5	59.0	59.0	61.5	60.0	61.0	61.5	59.0

Notes: (1). Average Transmission Loss at 8.570/8.875/9.375 GHz
= 1.4/1.1/1.6 db for S/N 1
= 1.3/1.2/1.7 db for S/N 2

(2) Repeat Scans (1-2 days elapsed time) gave average 1.2% differences for eight scans repeated, or 0.1% differences if sign of apparent changes considered and averaged.

gated. For the E-plane case, -19.5 dB is reached at resonance and -15.9 dB at 9.375. The C-140 radome requirement is that increases not exceed 3 dB for sidelobes above the -30 dB level.

TABLE 28

WORST-CASE SIDELOBES, TEST ANTENNA AND TWO RMR DOMES

(ALL VALUES IN dB RELATIVE TO BEAM PEAK)

12-1492

Plane	Freq. (GHz)	Dome S.N.	Level for 0° Az, 0° Roll, & Elev = -30°	-15°	0°	+15°	Worst Angle
H	8.570	No Radome			-21.6		
		Radome #1	-20.8	-21.6	-22.5	-21.7	-20.8
		Radome #2	-20.6	-22.1	-22.0	-21.8	-20.6
		Worst Case	-20.6	-21.6	-22.0	-21.7	-20.6
	8.875	No Radome			-27.8		
		Radome #1	-25.9	-29.0	-28.0	-29.5	-25.9
		Radome #2	-26.7	-29.0	-25.0	-28.5	-25.0
		Worst Case	-25.9	-29.0	-25.0	-28.5	-25.0
	9.375	No Radome			-20.8		
		Radome #1	-21.0	-19.1	-20.0	-22.2	-19.1
		Radome #2	-22.2	-21.4	-20.5	-22.7	-20.5
		Worst Case	-21.0	-19.1	-20.0	-22.2	-19.1
E	8.570	No Radome			-20.8		
		Radome #1	-26.1	-24.1	-19.6	-18.5	-18.5
		Radome #2	-28.3	-25.8	-18.3	-27.0	-18.3
		Worst Case	-26.1	-24.1	-18.3	-18.5	-18.3
	8.875	No Radome			-24.8		
		Radome #1	-22.9	-23.1	-19.8	-23.8	-19.8
		Radome #2	-20.3	-21.1	-19.5	-21.0	-19.5
		Worst Case	-20.3	-21.1	-19.5	-21.0	-19.5
	9.375	No Radome			-23.1		
		Radome #1	-16.8	-22.8	-22.5	-20.3	-16.8
		Radome #2	-15.9	-21.4	-20.8	-17.5	-15.9
		Worst Case	-15.9	-21.4	-20.8	-17.5	-15.9

The electrical performance measurements (averages and worst case) are summarized for the two radomes in Table 29.

Final Lightning Test - In order to evaluate the resistance of the final radome configuration to lightning, witness specimens were made and tested to the MIL-B-5087B requirement. The earlier lightning tests (Section 4.0) indicated that 5 mils of copper provided satisfactory protection without introducing undue weight penalty and fabrication difficulties. Accordingly, the copper thickness chosen for the demonstration radomes was 5 mils. Two 12x12 inch specimens were tested. Both specimens were constructed by bonding 5 mil copper sheets with the slot pattern etched through them to the A-sandwich radome substrate material in the same fashion as the demonstration radomes. The specimen substrates, like the Jetstar radome, were constructed of 0.264 inch thick, 6-pound density nylon-phenolic honeycomb core material with 33 mil

TABLE 29

PERFORMANCE SUMMARY FOR RESONANT METAL RADOMES

12-1491

Radome:	S/N 1			S/N 2			UNMETALLIZED
Freq. (GHz):	8.570	8.875 (RESONANCE)	9.375	8.570	8.875 (RESONANCE)	9.375	9.375 (RESONANCE)
Power Transmission, %							
- Average	72.6	77.6	68.6	74.1	76.0	68.0	90.0
- Minimum	68.5	68.5	59.0	68.5	72.5	61.5	85.0
Beam Deflection, Max., mr							
- Nose Area	6.8	6.9	8.8	9.2	10.2	10.6	NA
- Outside Area	7.4	7.8	10.1	9.0	9.2	12.4	NA
Beam Deflection Rates of Change, Max, mr/deg.	0.50	0.68	1.20	0.76	0.80	1.22	NA
Pattern Beamwidth Increase, Max., %							
- H-Plane	10	*	*	6	6	*	≤10
- E-Plane	15	*	*	15	*	10	≤10
Max. Sidelobe Level with Dome, dB							(8.875 GHz)
- H-Plane	-20.8	-25.9	-19.1	-20.5	-25.0	-20.5	-24.8
- E-Plane	-18.5	-19.8	-16.8	-18.3	-19.5	-19.5	-21.8

Notes: (1) mr - milliradians.
(2) Beam Deflection Rates Averaged over 5 Segments.
(3) * For Beamwidths without change (to test accuracy), or decreases in beamwidth.
(4) Sidelobe Levels for Antenna Alone at the three frequencies:
H-Plane -21.6/-27.8/-20.8 dB
E-Plane -20.8/-24.8/-23.1 dB

thick fiberglass epoxy face sheets. The slotted metal surface was bonded to the substrate with 3M Company's AF147 film adhesive and the metal clad side overcoated with 20 mils of polyurethane rain erosion coating (Figure 76).

12-1276

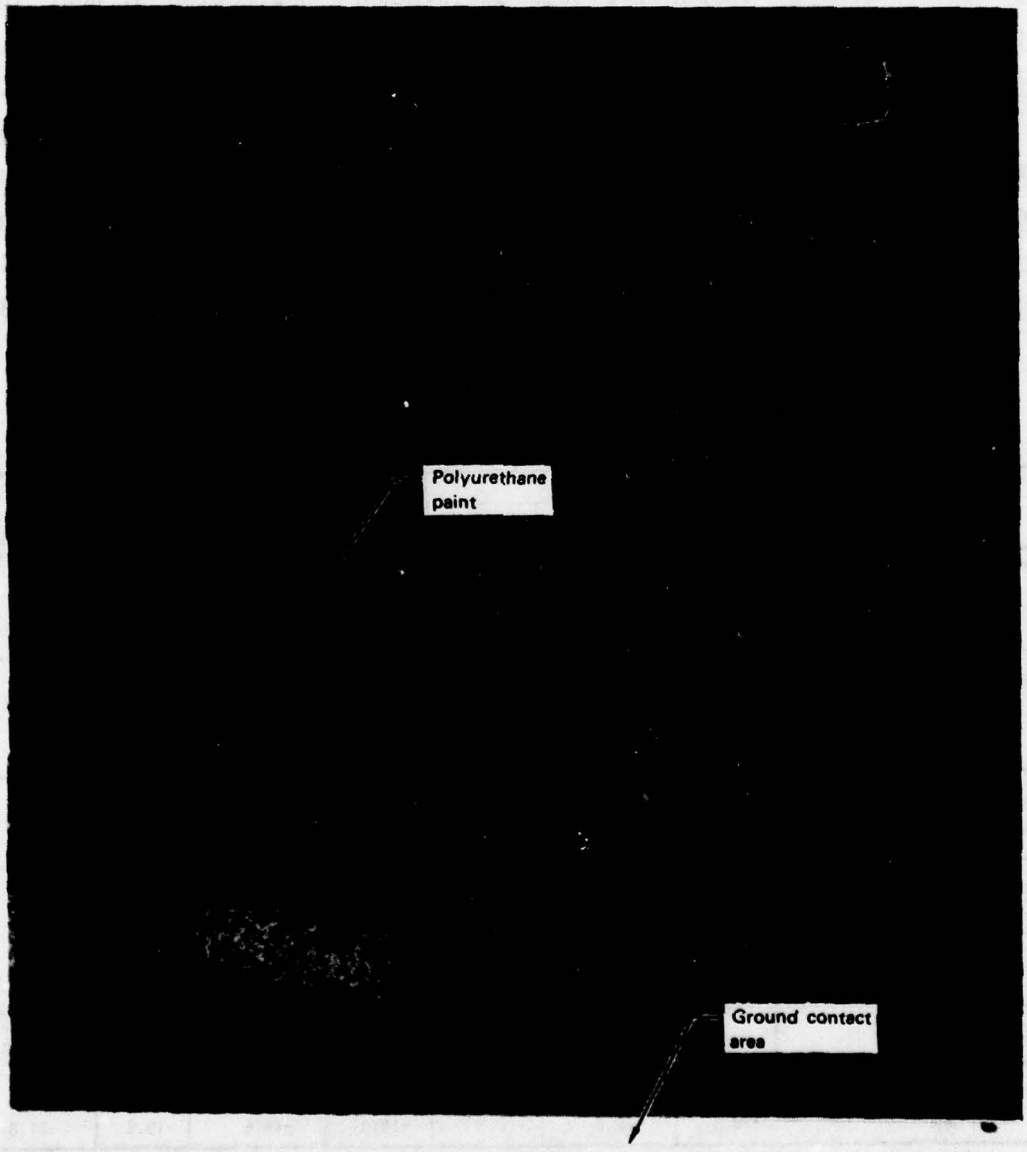

Figure 76 Slotted radome test panel before lightning tests

One of the two specimens had several splice joints in the metal surface like those on the demonstration radomes, while the other was overcoated with a single continuous sheet (no joints). This was to enable us to compare directly the amount of damage done by a lightning strike across a jointed panel versus an unjointed panel.

The specimens were grounded on two opposite edges and the arc discharge probe was positioned approximately one inch above the sample. The specimens were subjected to simulated direct lightning strikes of 200,000 amp peak current per MIL-B-5087B. Figure 77 shows the waveform of the simulated lightning strike. Panel 1, the continuous sheet panel, was struck 3 different times while Panel 2, the jointed panel, was struck only once.

Visual and x-ray inspection revealed most of the damage to be superficial. The primary damage region, or region of direct arc attachment, was 1 inch in diameter (Figures 78 and 79). In this region the metal cover and polyurethane coating had been completely removed. The dielectric substrate

12-1260

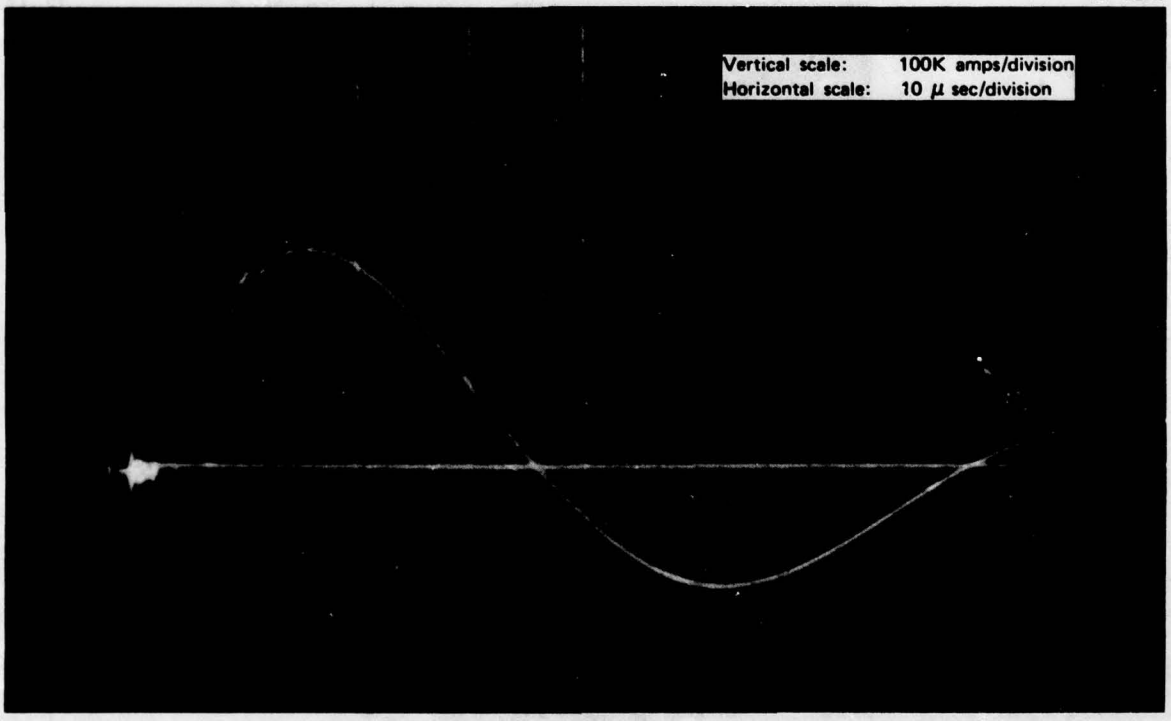

Figure 77 Final configuration lightning test waveform

12-1264

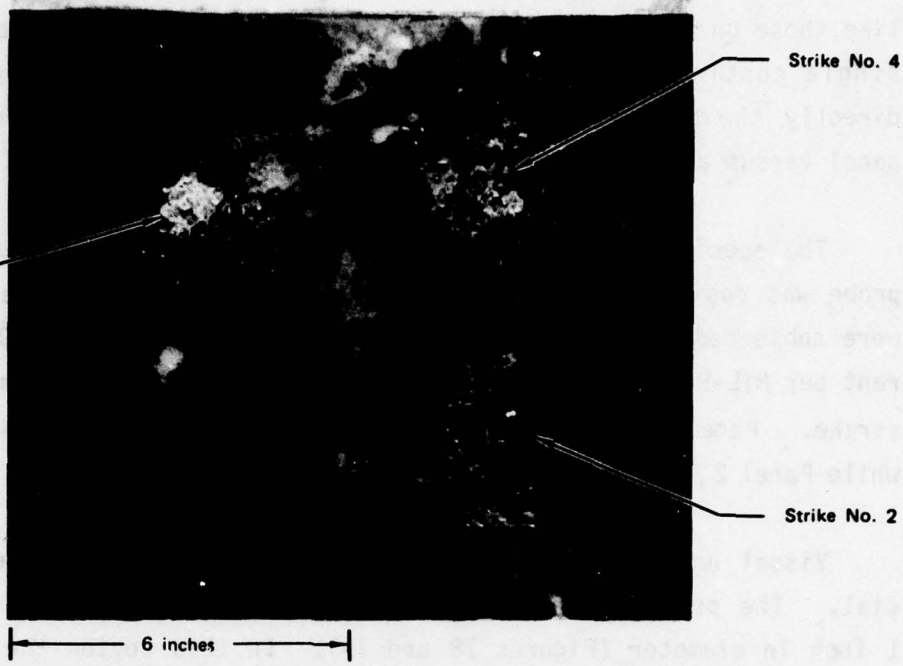

Figure 78 Slotted metal radome test panel no. 1 after lightning testing

12-1265

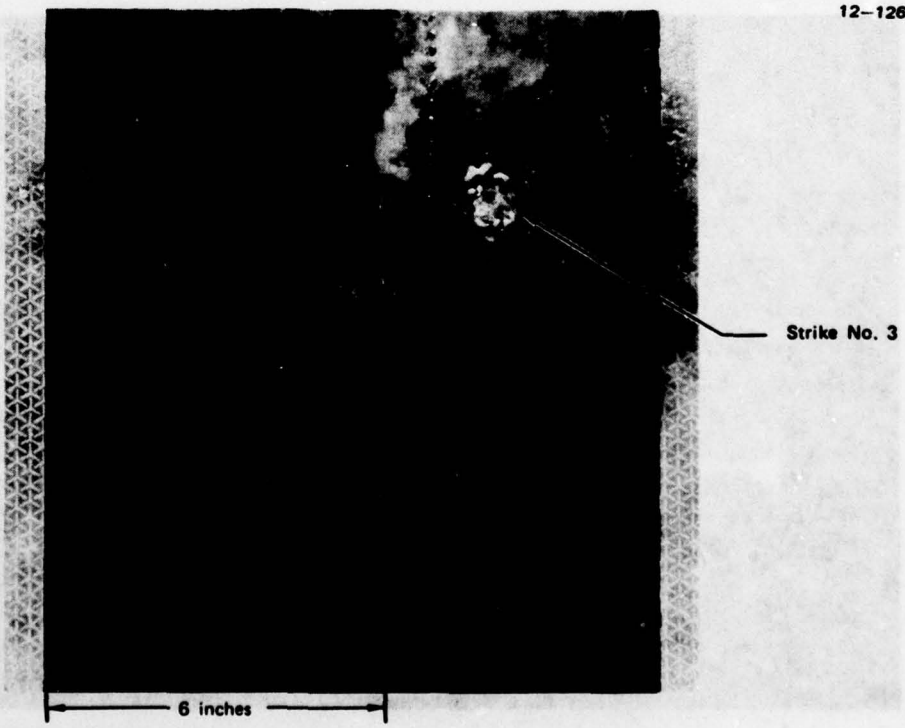

Figure 79 Slotted metal radome test panel no. 2 after lightning testing

had only minor damage to the outermost skin of the "A" sandwich in 2 of the 4 strikes. Figure 80 shows the backside of test panel 1 after the three simulated lightning strikes. A secondary damage region, roughly 3.5 inches in diameter, surrounded the primary area. In this area the rain erosion coating was separated from the substrate. X-ray examination revealed that the tuned slots in this area were enlarged, which indicated that some of the metal cladding had been vaporized in this region as well (Figure 81). In Panel 2, this secondary damage was also observed at points along the joints in the metal cladding. This was not unexpected, for higher current densities are associated with these joints. Figure 82 shows that this secondary damage is very limited.

These tests demonstrate that the demonstration radomes are highly resistant to damage from lightning, especially when it is remembered that the 200,000 amp, 200,000 volt strike simulated in these tests represents the most severe, upper 1 percentile, lightning strike. Damage could be further reduced by making the outer skin of the A-sandwich substrate slightly thicker to improve the local impact resistance of the substrate. Tests performed earlier in the program (Section 4.0) showed that a solid laminate radome substrate does not experience any damage when struck with this level lightning strike.

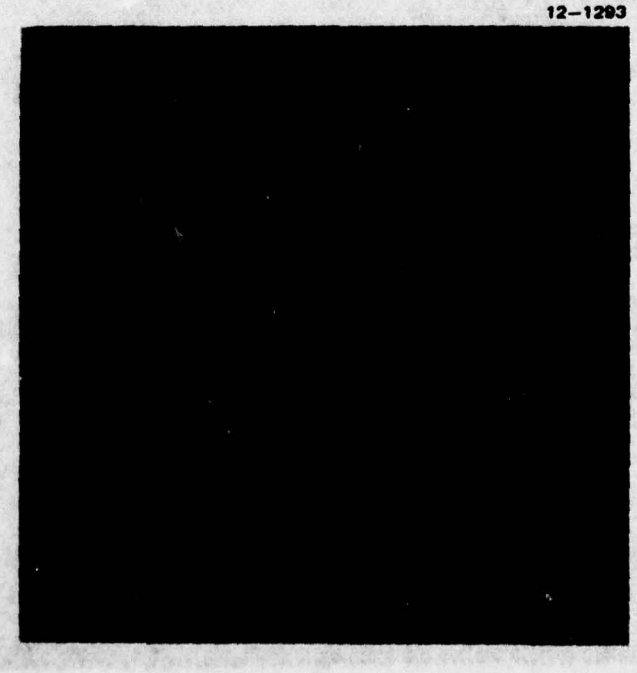

Figure 80 Backside of radome test panel after exposure to 200,000 amp simulated lightning strike.

12–1258

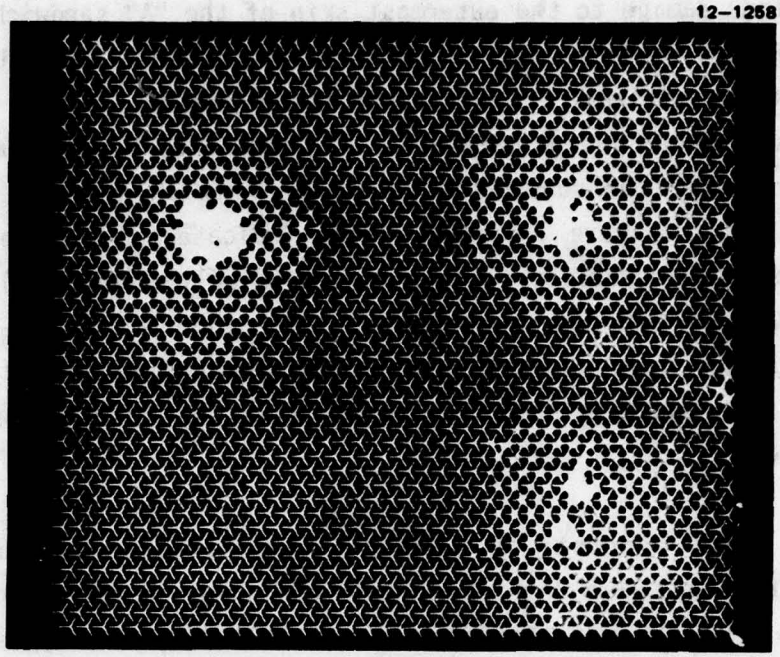

Figure 81 X-ray of slotted metal radome lightning test panel no. 1

12–1259

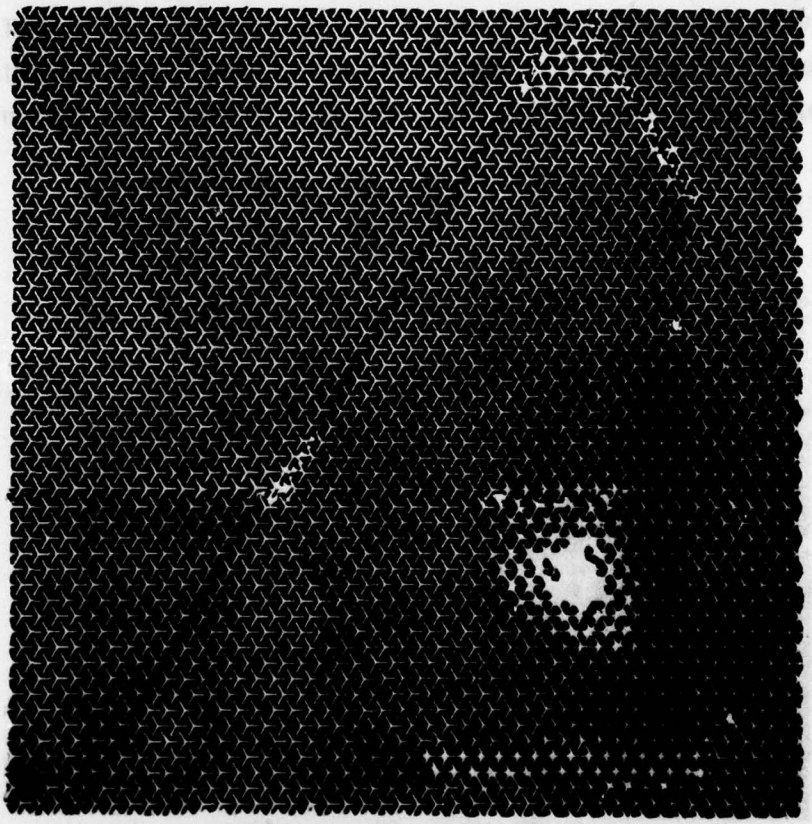

Figure 82 X-ray of slotted metal radome lightning test panel no. 2

6.5 COST ANALYSIS

Assuming an ogive radome shape, a surface area of 25-50 square feet and a production quantity of 100 units, the cost to the customer of a typical high performance military radome, including testing, is on the order of $120.00 per square foot. Metallizing that radome by the method used for these demonstration radomes would add about $36.00 per square foot in labor, and $31.00 per square foot in slotted metal and other materials to that cost. That labor and materials cost could be significantly reduced by using the electroform method described in Section 2.1. It is estimated that the cost of metallizing a radome could be reduced to $34.00 per square foot, including tooling costs, through use of the electroform approach and female radome tooling.

6.6 ENVIRONMENTAL IMPACT STATEMENT

Processes for the manufacture of printed wiring boards which have well-known and documented environmental effects, were used in the manufacture of the slotted skins. These processes at our facility are carefully controlled and meet all current Environmental Protection Agency standards. No new processes were developed in this program which could be expected to have adverse environmental effects.

SECTION VII

CONCLUSIONS

The primary objective of this program, the successful fabrication of a flightworthy, resonant metal radome, was met. Four fabrication approaches were investigated during the initial stages of the program and these included: (1) electroform, (2) wall paper, (3) raised slot, and (4) plate and etch. It was concluded that a combination of the electroform and wall paper approaches would be the most efficient method of fabricating the demonstration radomes and that the electroform technique would provide the best fabrication approach for production radomes. In the latter case, the nonrecurring costs associated with a full-scale radome mandrel could be amortized over an entire production run.

Based on electrical performance test results obtained with full-scale demonstration radomes, the following conclusions can be reached:

- Electrical performance of full-scale, doubly curved radomes and flat panels with slot patterns similar to the patterns used on the radomes is nearly identical (i.e., within 3% at all three test frequencies investigated). This indicates strongly that the inevitable compromises necessary to adapt a periodic array to a doubly curved radome can be tolerated.
- RF transmission efficiency associated with the resonant metal radome is approximately 87 percent of the conventional Jetstar radome efficiency. This corresponds to a decrease in range of 4 percent with the use of the resonant metal radome at resonant frequency, because of the power-range relationship (see Section 6.0).
- To realize the full potential of the resonant metal radome with respect to electrical performance, the entire radome configuration, including the substrate, should be designed as a unit rather than attempting to metallize an existing radome design.

As a result of the various environmental exposure tests conducted during the program, it can be concluded that aircraft radome environmental requirements can be met with a resonant metal radome. Specifically, it was demonstrated that resonant metal radomes:

- o provide better lightning strike protection than conventional radomes
- o reduce static charge build-up on the radome and the associated P-static RF interference
- o provide significant out-of-band attenuation for EMP/EMI attenuation
- o provide adequate environmental and rain erosion resistance.

Comparison of the weight of a resonant metal radome with a conventional metal radome demonstrated that there is a negligible weight penalty associated with the use of the metallic configuration.

SECTION VIII

RECOMMENDATIONS

As a result of this program, recommendations can be made relative to the continued development and use of resonant metal radomes for aircraft and missile applications. Nine specific recommendations follow:

1. Results of testing done in this program should be compared with results predicted by the computer model used by OSU for estimating metallic radome performance. Discrepancies between predicted performance and actual performance should be resolved by continued analytical and experimental efforts. The OSU computer model should be modified to include consideration of the dissipation factor of the dielectric substrate material.

2. Additional work in manufacturing technology is required to scale-up the electroform method of fabrication for possible production radome manufacture.

3. More work is required in the area of higher temperature dielectric materials for resonant metal radomes for supersonic vehicle applications.

4. Additional theoretical work must be accomplished in the area of electrical design, and the work should be closely tied to a hardware program rather than be a parallel effort.

5. Subsequent programs should address designing a resonant metal radome from the beginning rather than adapting existing designs. This would allow optimization of electrical and mechanical properties.

6. Fabrication methods and electrical designs for biplanar radome walls should be developed to improve narrow bandpass characteristics.

7. Investigations into the feasibility of resonant metal radomes which have metal surfaces sufficiently thick to carry structural loads should be conducted. In addition, the feasibility of this type of radome should be explored for application to hypersonic flight vehicles.

8. Studies should be conducted to investigate the possibilities of operating a metallic radome at more than one discrete frequency. Approaches which permit multifrequency operation over the entire radome, or, alternately, which utilize separate regions of the radome, each having its own resonant frequency (e.g., radar, IFF, and ILS frequencies) should be explored.

9. The study of resonant metal radomes should be extended into the millimeter wave regime.

APPENDIX A

SOLUTION MAKE-UP AND OPERATING PARAMETERS

Solution A: Solution A is Conditioner 1200, a proprietary bath manufactured by Shipley Company. It is a solvent which swells the substrate. It is used as supplied at room temperature.

Solution B: Solution B is an etch bath made up by the prototype lab. It was made of 350 ml per liter of water, 25 grams per liter of chromium trioxide, 450 ml per liter of reagent grade sulfuric acid, and 200 ml per liter of 85% phosphoric acid. The bath is maintained at 160°F.

Solution C: Solution C is PM-950. It is a two-part solution made from proprietary solutions PM-950 and Cuposit Z. Both are manufactured by Shipley Company. The bath is made up as follows: PM-950 4% by volume, Cuposit Z 4% by volume, and the remainder deionized water. The PH should be maintained above 12.5 and the temperature at 120°F.

Solution D: Solution D is Hydrochloric acid 25% by volume, operated at room temperature.

Solution E: Solution E is Catalyst 9F, a three-part bath made up of two parts deionized water, one part hydrochloric acid, and one part Catalyst 9F, which is a proprietary solution manufactured by Shipley Company. It is operated at room temperature.

Solution F: Solution F is Accelerator 19, a proprietary Shipley solution made up as follows: One part Accelerator 19 and five parts deionized water. It is maintained at room temperature.

Solution G: Solution G is CP-74 electroless copper, a three-part proprietary Shipley plating bath. It is made up as follows: 80% by volume deionized water, 10% by volume CP-74M, 5% by volume CP-74A, and

5% by volume CP-74B. It is extremely important to mix this bath in the aforementioned order and not to allow any delays between Step No. 1 and Step No. 4. The bath is operated at 120°F.

PROCEDURE:

1) Scrub parts to be plated with pumice and water, rinse thoroughly, and dry completely with compressed air.

2) Immerse the parts in conditioner 1200 (Solution A) for a total of nine minutes. Dry thoroughly with compressed air, then rinse thoroughly in tap water and deionized water.

3) Parts are immersed in Solution B (Sulfuric Acid Etch) for sixteen minutes. Allow the parts to air dry for approximately two minutes. Rinse thoroughly in tap water and deionized water.

4) Immerse parts in Solution C (PM-950) for three minutes. This solution neutralizes the acid etch. Rinse parts thoroughly in tap water and deionized water.

5) Immerse in Solution D (Hydrochloric Acid) for three minutes. Do not rinse.

6) Immerse parts in Solution E (Catalyst 9F) for three minutes and rinse very thoroughly in tap and deionized water.

7) Immerse parts in Solution F (Accelerator 19) for six minutes and rinse thoroughly in tap and deionized water.

8) Plate parts in Solution G (CP-74 Electroless Copper) for thirty minutes and rinse thoroughly in tap and deionized water.

9) Immediately after electroless plating, parts are copper plated for twenty minutes, rinsed thoroughly, and dried with compressed air.

10) Bake the parts at 250°F for two hours.

11) Final plate parts for forty minutes. Rinse thoroughly and air dry.

12) The parts were cleaned and imaged with Dupont dry film resist.

APPENDIX B

LIGHTNING DAMAGE TEST DATA

These tests were conducted at the McDonnell Aircraft Company Lightning Simulation Facility at St. Louis, MO. The data collected here is discussed in Section 4.1 of this report.

A. Intermediate current
(2.7 kA peak)

B. Intermediate plus continuing
current (3.0 kA peak, 50 m sec)

Figure B–1 Lightning damage to copper coated fiberglass panels Copper thickness – 0.0014 inches

12–1454

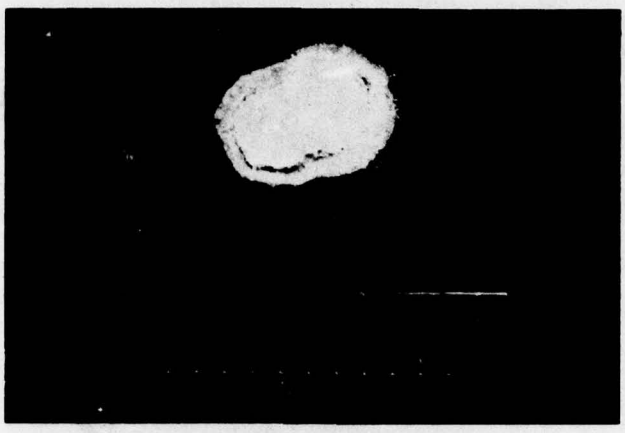

A. High peak current (145 kA)

B. Intermediate current (3 kA peak)

C. Intermediate plus continuing current (3 kA peak, 50 m sec)

Figure B–2 Lightning damage to copper coated fiberglass panels Copper thickness – 0.0028 inches

12–1424

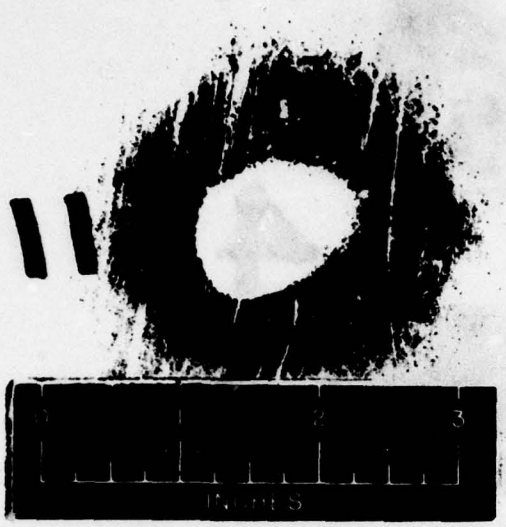

A. High peak current (145 kA)

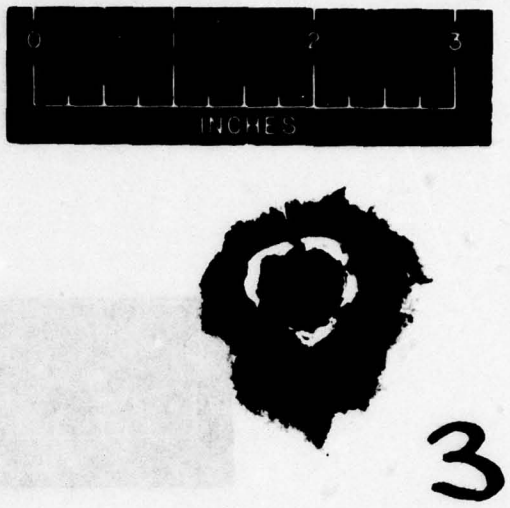

B. Intermediate current (3 kA peak)

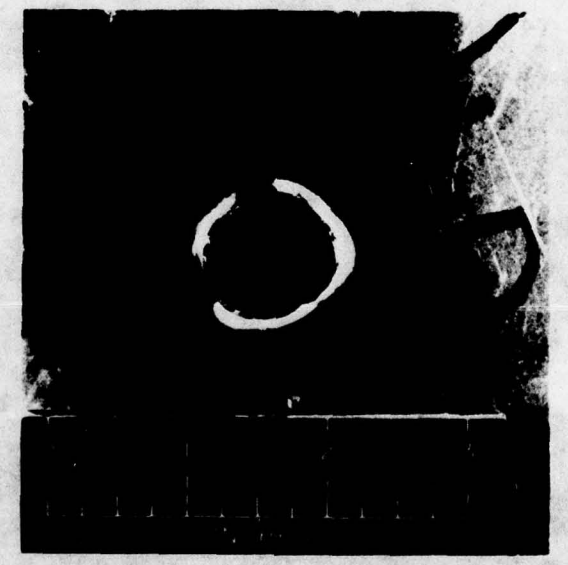

C. Intermediate plus continuing current (3 kA peak, 50 m sec)

Figure B–3 Lightning damage to copper coated fiberglass panels Copper thickness – 0.0067 inches

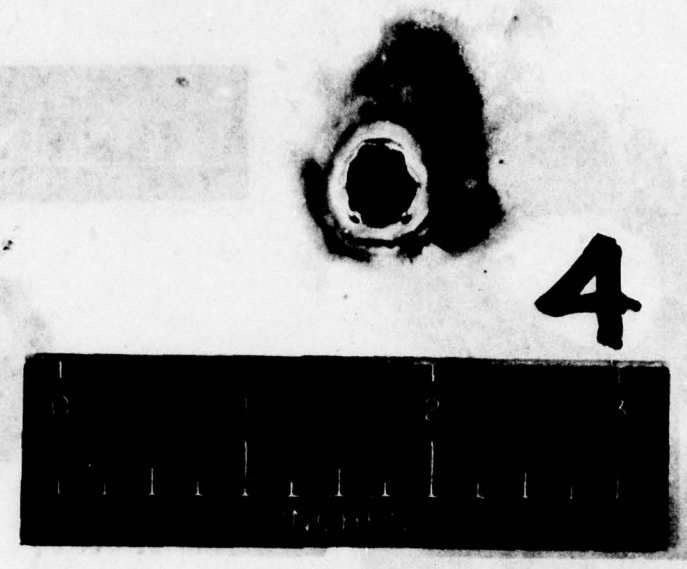

A. Intermediate current
(3 kA peak)

B. Intermediate plus continuing
current (2.85 kA, 50 m sec)

Figure B–4 Lightning damage to copper coated fiberglass panels Copper thickness – 0.0098 inches

LIGHTNING DAMAGE EVALUATION

TESTED AT MCDONNELL AIRCRAFT COMPANY LIGHTNING SIMULATION FACILITY IN ST. LOUIS, MISSOURI

TEST SETUP	MCAIR 600 kilojoule lightning generator
PANEL NUMBER	#1
PANEL DESCRIPTION	4 mils Electroplated Cu/10 mils MIL-C-83231 Polyurethane

TEST NUMBER 1
CURRENT LEVEL 1.98 kA
DAMAGE TO EROSION COAT (∿dia) 3.0 in.
DAMAGE TO METAL (∿dia)
METAL REMOVED 1.6 in.
METAL DELAMINATED 1.6 in.

TEST NUMBER 2
CURRENT LEVEL 1.98 kA
DAMAGE TO EROSION COAT (∿dia) 3.1 in.
DAMAGE TO METAL (∿dia)
METAL REMOVED 1.5 in.
METAL DELAMINATED 1.5 in.

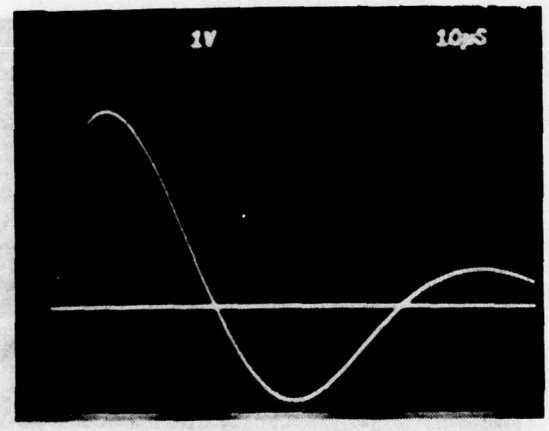

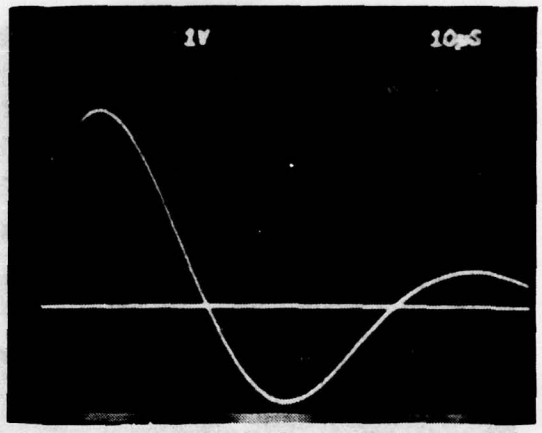

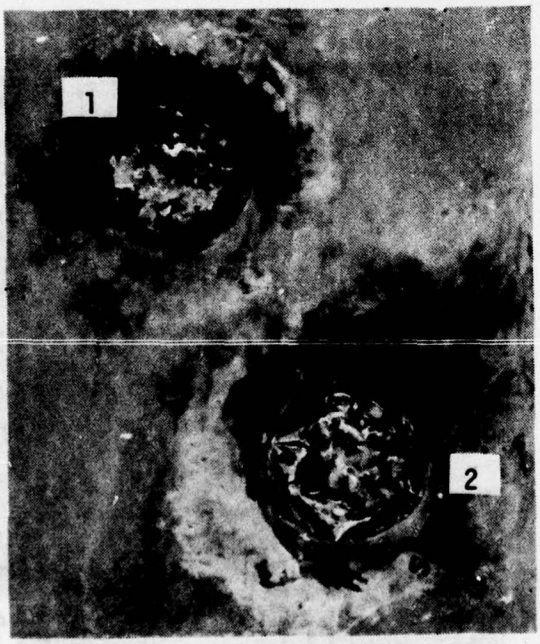

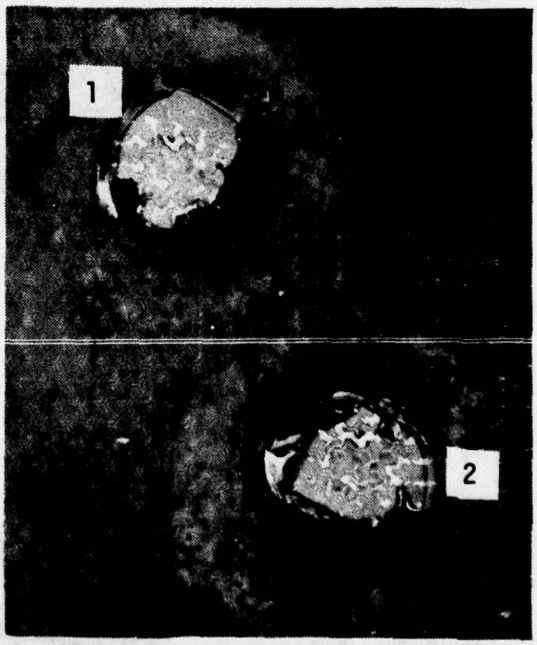

LIGHTNING DAMAGE EVALUATION

TESTED AT MCDONNELL AIRCRAFT COMPANY LIGHTNING SIMULATION FACILITY IN ST. LOUIS, MISSOURI

TEST SETUP 600 kilojoule lightning generator
PANEL NUMBER 3
PANEL DESCRIPTION 4 mils Electroplated Cu/No Rain Erosion Coating

TEST NUMBER 3
CURRENT LEVEL 200 kA
DAMAGE TO METAL (~dia)
METAL REMOVED 1.4 in.
METAL DELAMINATED 2.0 in.

TEST NUMBER 4
CURRENT LEVEL 200 kA
DAMAGE TO METAL (~dia)
METAL REMOVED 1.0 in.
METAL DELAMINATED 1.6 in.

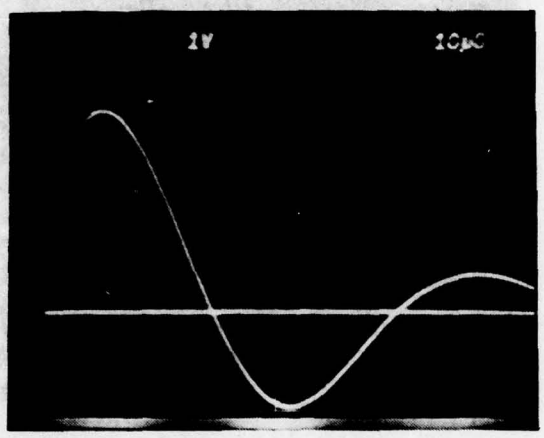

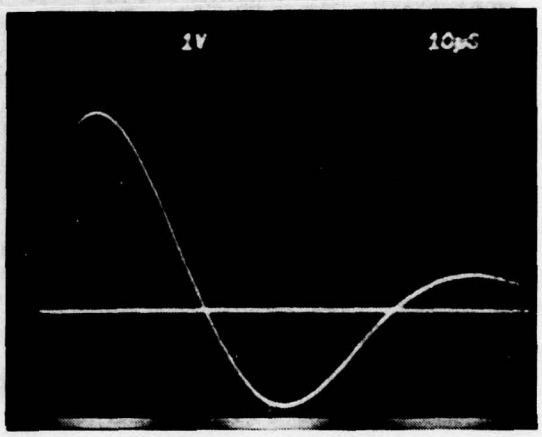

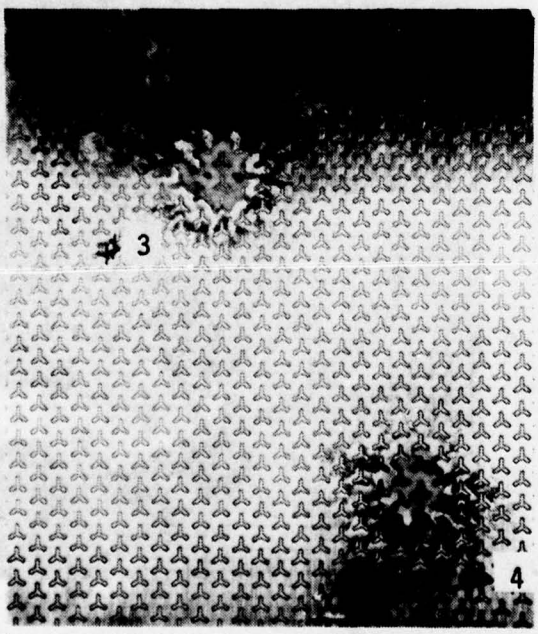

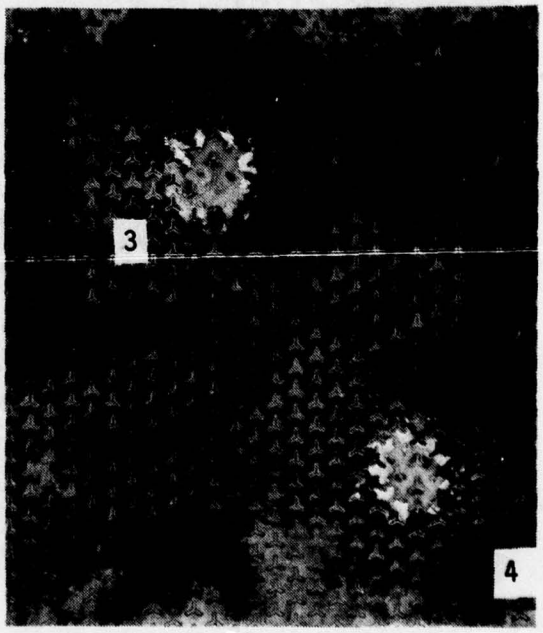

LIGHTNING DAMAGE EVALUATION

TESTED AT MCDONNELL AIRCRAFT COMPANY LIGHTNING SIMULATION FACILITY IN ST. LOUIS, MISSOURI

TEST SETUP MCAIR 600 kilojoule lightning generator
PANEL NUMBER *10*
PANEL DESCRIPTION 4 mils Electroplated Ni/No Rain Erosion Coating

TEST NUMBER 5
CURRENT LEVEL 200 kA
DAMAGE TO METAL (∿dia)
METAL REMOVED 0.0 in.
METAL DELAMINATED 2.0 in.

TEST NUMBER 6
CURRENT LEVEL 205 kA
DAMAGE TO METAL (∿dia)
METAL REMOVED 0.7 in.
METAL DELAMINATED 2.2 in.

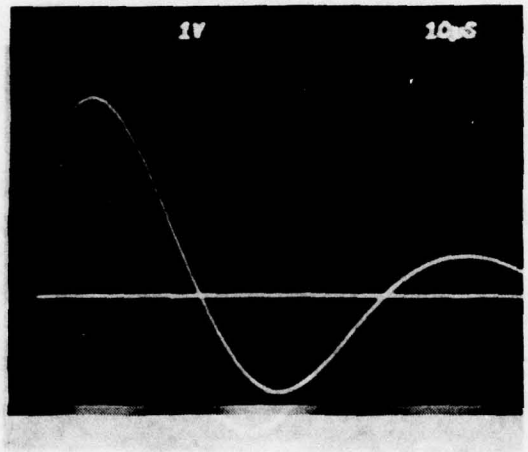

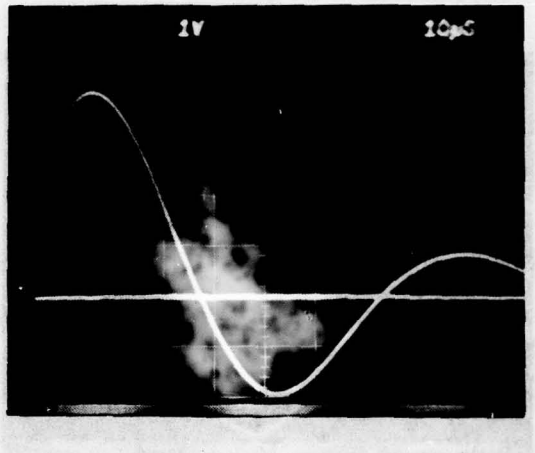

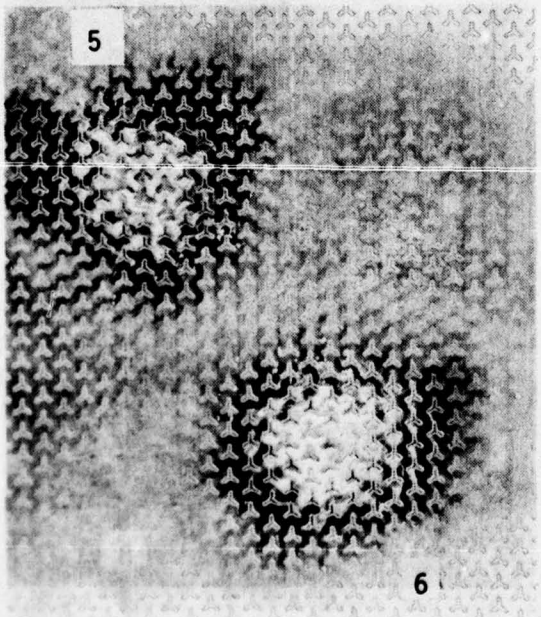

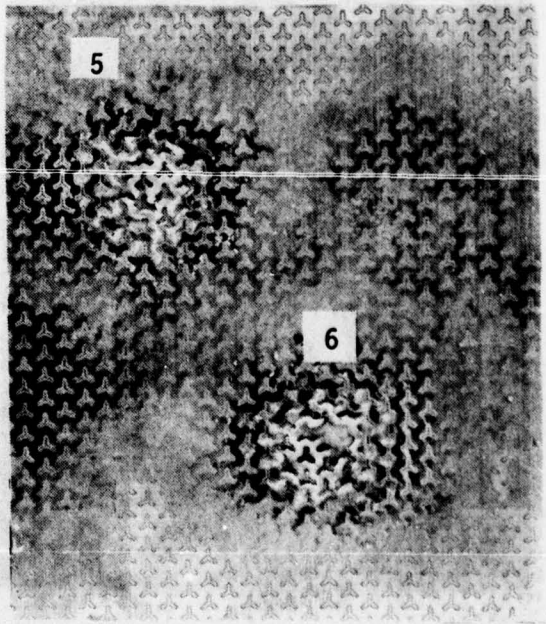

LIGHTNING DAMAGE EVALUATION

TESTED AT MCDONNELL AIRCRAFT COMPANY LIGHTNING SIMULATION FACILITY IN ST. LOUIS, MISSOURI

TEST SETUP MCAIR 600 kilojoule lightning generator
PANEL NUMBER 5
PANEL DESCRIPTION 8 mils Electroplated Cu/7 mils MIL-C-83231 Polyurethane

TEST NUMBER	7
CURRENT LEVEL	205 kA
DAMAGE TO EROSION COAT (∿dia.)	2.4 in.
DAMAGE TO METAL (∿dia)	
METAL REMOVED	0.5 in.
METAL DELAMINATED	0.7 in.

TEST NUMBER	8
CURRENT LEVEL	205 kA
DAMAGE TO EROSION COAT (∿dia)	2.3 in.
DAMAGE TO METAL (∿dia)	
METAL REMOVED	0.5 in.
METAL DELAMINATED	0.7 in.

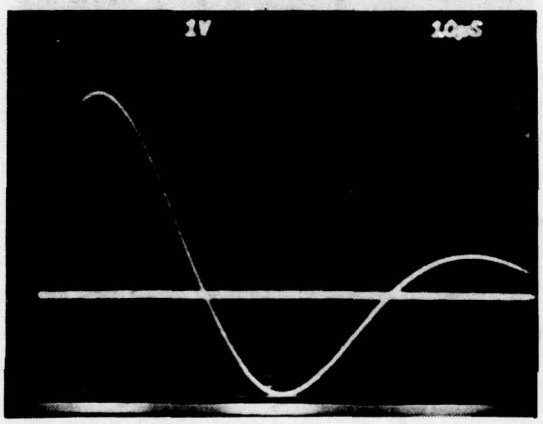

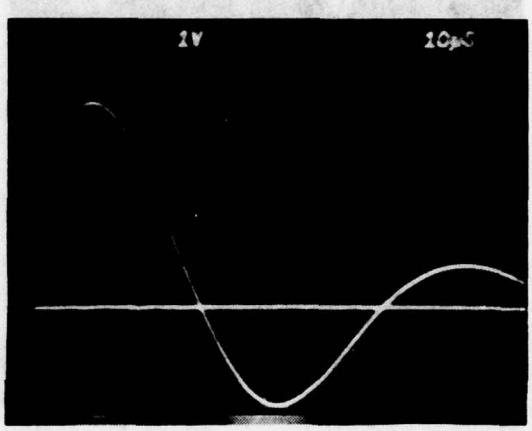

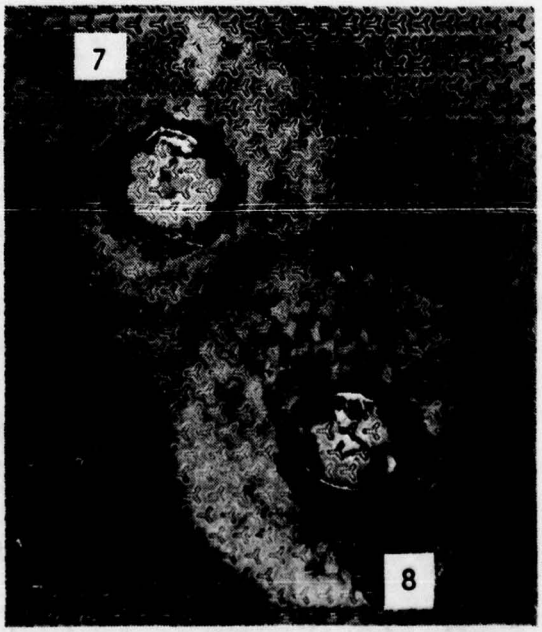

LIGHTNING DAMAGE EVALUATION

TESTED AT MCDONNELL AIRCRAFT COMPANY LIGHTNING SIMULATION FACILITY IN ST. LOUIS, MISSOURI

TEST SETUP MCAIR 600 kilojoule lightning generator
PANEL NUMBER 4
PANEL DESCRIPTION 8 mils Electroplated Cu/15 mils MIL-C-83231 Polyurethane

TEST NUMBER 9
CURRENT LEVEL 205 kA
DAMAGE TO EROSION COAT (~dia) 2.8 in.
DAMAGE TO METAL (~dia)
METAL REMOVED 1.0 in.
METAL DELAMINATED 1.0 in.

TEST NUMBER 10
CURRENT LEVEL 200 kA
DAMAGE TO EROSION COAT (~dia) 2.6 in.
DAMAGE TO METAL (~dia)
METAL REMOVED 1.0 in.
METAL DELAMINATED 1.0 in.

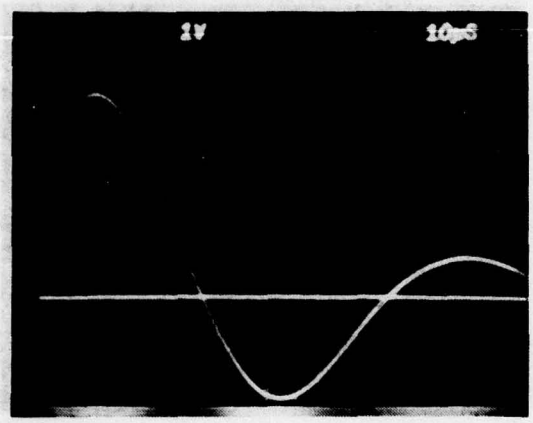

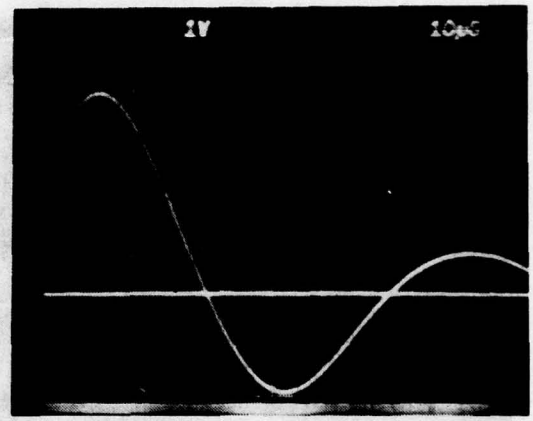

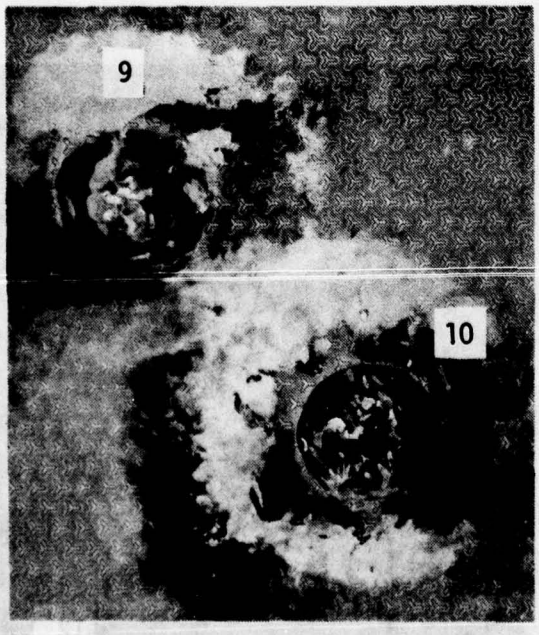

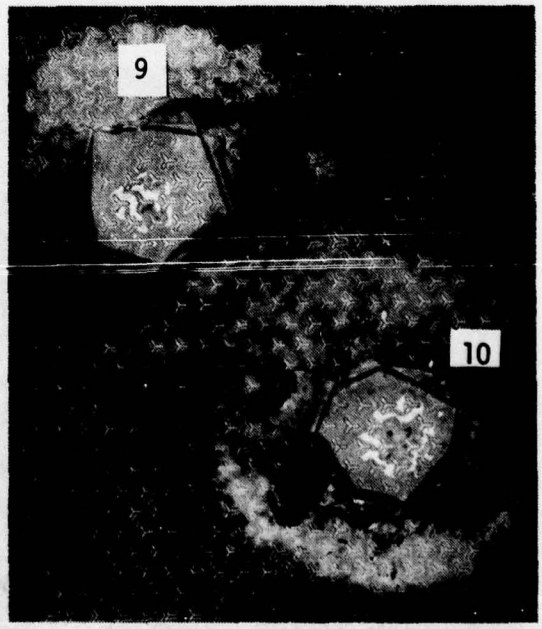

LIGHTNING DAMAGE EVALUATION

TESTED AT MCDONNELL AIRCRAFT COMPANY LIGHTNING SIMULATION FACILITY IN ST. LOUIS, MISSOURI

TEST SETUP MCAIR 600 kilojoule lightning generator
PANEL NUMBER 7
PANEL DESCRIPTION 12 mils Electroplated Cu/15 mils MIL-C-83231 Polyurethane

TEST NUMBER 11
CURRENT LEVEL 200 kA
DAMAGE TO EROSION COAT (~dia) 2.7 in.
DAMAGE TO METAL (~dia)
METAL REMOVED 0.7 in.
METAL DELAMINATED 0.7 in.

TEST NUMBER 12
CURRENT LEVEL 200 kA
DAMAGE TO EROSION COAT (~dia) 2.5 in.
DAMAGE TO METAL (~dia)
METAL REMOVED 0.6 in.
METAL DELAMINATED 0.6 in.

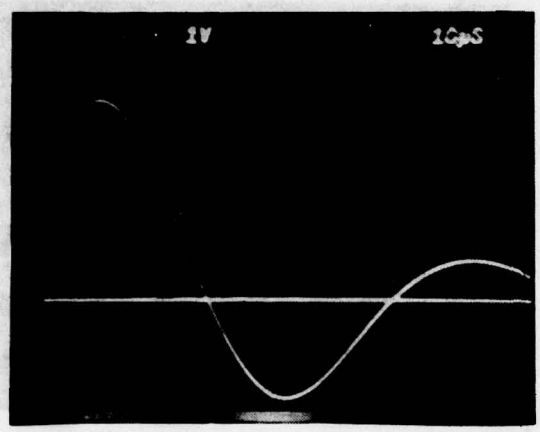

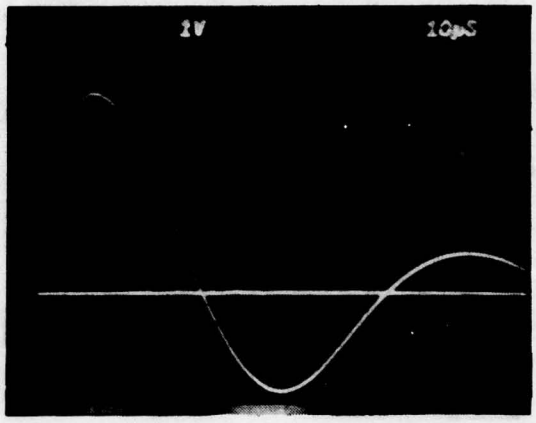

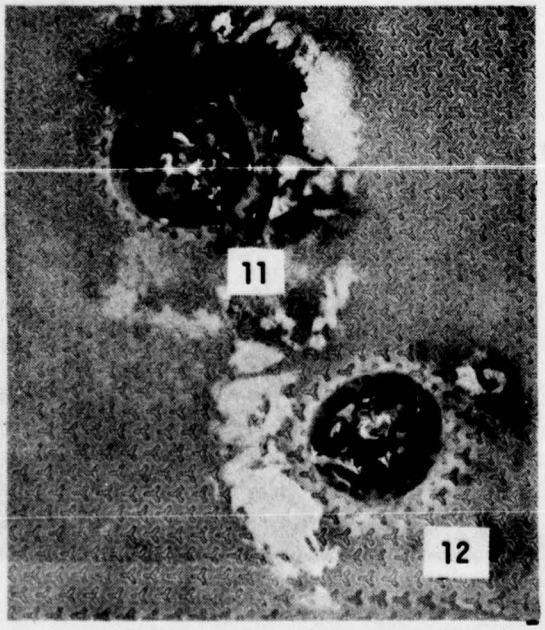

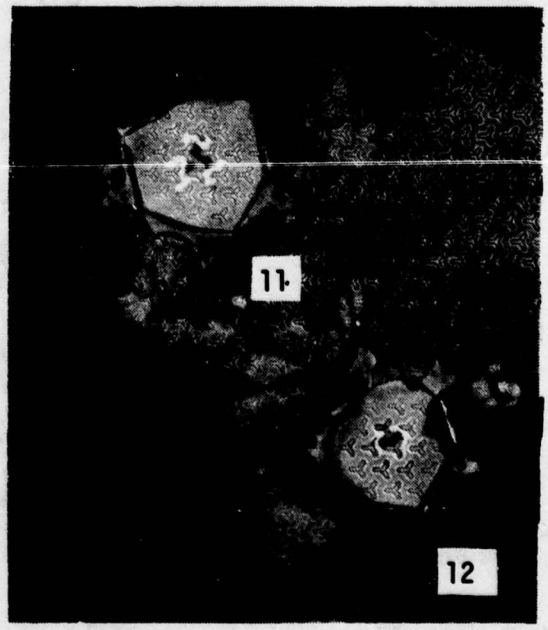

LIGHTNING DAMAGE EVALUATION

TESTED AT MCDONNELL AIRCRAFT COMPANY LIGHTNING SIMULATION FACILITY IN ST. LOUIS, MISSOURI

TEST SETUP MCAIR 600 kilojoule lightning generator
PANEL NUMBER 8
PANEL DESCRIPTION 12 mils Electroplated Cu/6 mils MIL-C-83231 Polyurethane

TEST NUMBER 13
CURRENT LEVEL 205 kA
DAMAGE TO EROSION COAT (∿dia) 2.6 in.
DAMAGE TO METAL (∿dia)
METAL REMOVED 0.6 in.
METAL DELAMINATED 0.6 in.

TEST NUMBER 14
CURRENT LEVEL 200 kA
DAMAGE TO EROSION COAT (∿dia) 2.3 in.
DAMAGE TO METAL (∿dia)
METAL REMOVED 0.5 in.
METAL DELAMINATED 0.5 in.

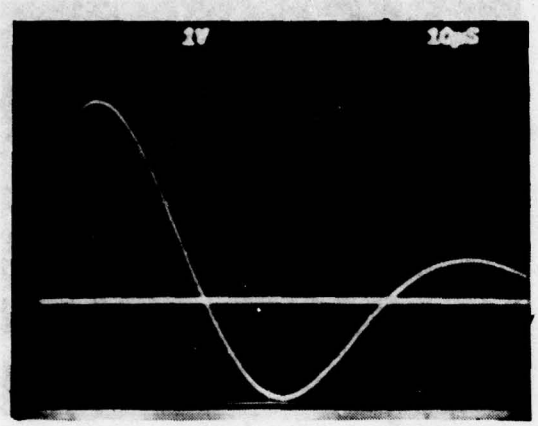

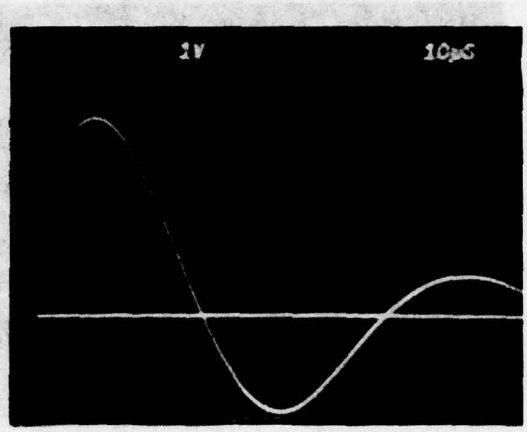

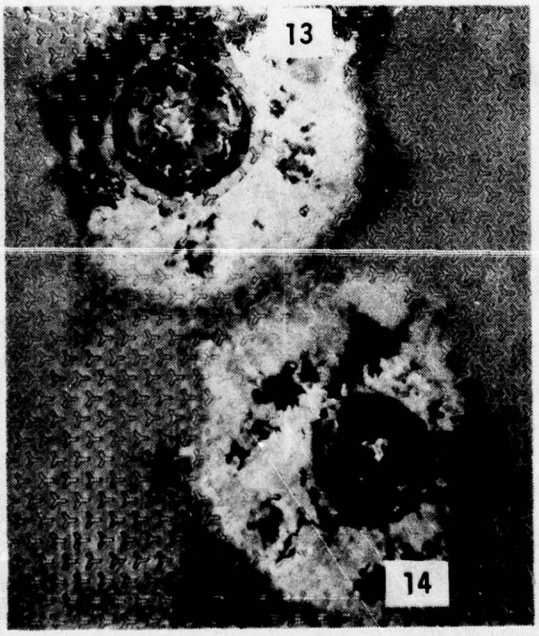

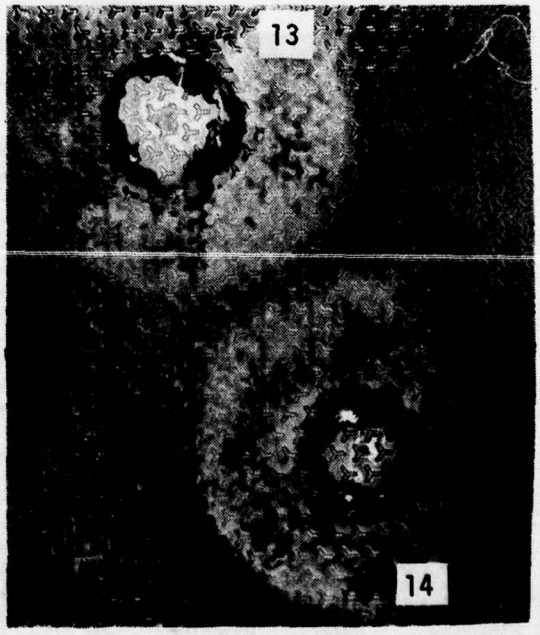

LIGHTNING DAMAGE EVALUATION

TESTED AT MCDONNELL AIRCRAFT COMPANY LIGHTNING SIMULATION FACILITY IN ST. LOUIS, MISSOURI

TEST SETUP MCAIR 600 kilojoule lightning generator
PANEL NUMBER 11
PANEL DESCRIPTION 8 mils Electroplated Ni/No Rain Erosion Coating

TEST NUMBER	15
CURRENT LEVEL	205 kA
DAMAGE TO METAL (∿dia)	
METAL REMOVED	0.0 in.
METAL DELAMINATED	1.0 in.

TEST NUMBER	16
CURRENT LEVEL	205 kA
DAMAGE TO METAL (∿dia)	
METAL REMOVED	0.0 in.
METAL DELAMINATED	0.7 in.

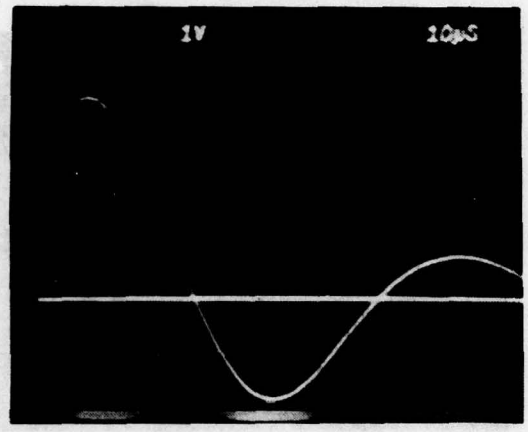

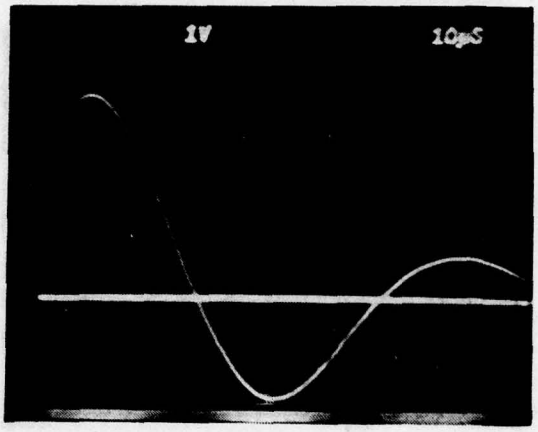

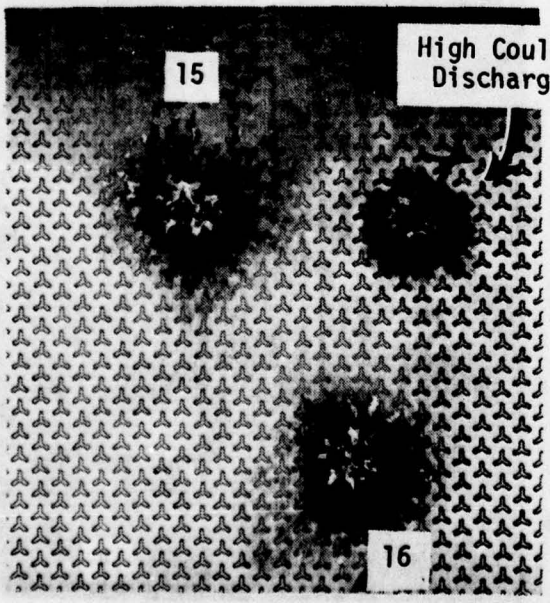

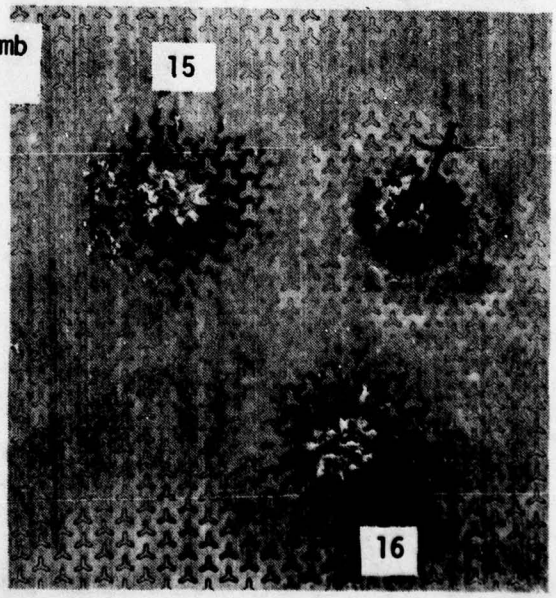

LIGHTNING DAMAGE EVALUATION

TESTED AT MCDONNELL AIRCRAFT COMPANY LIGHTNING SIMULATION FACILITY IN ST. LOUIS, MISSOURI

TEST SETUP *600 kilojoule lightning generator*
PANEL NUMBER 6
PANEL DESCRIPTION 8 mils Electroplated Cu/No Rain Erosion Coating

TEST NUMBER 17
CURRENT LEVEL 190 kA
DAMAGE TO METAL (~dia)
METAL REMOVED Center pieces were removed
METAL DELAMINATED 1.0 in.
REMARKS Localized erosion of surface metal

TEST NUMBER 18
CURRENT LEVEL 195 kA
DAMAGE TO METAL (~dia)
METAL REMOVED Center pieces were removed
METAL DELAMINATED 0.9 in.
REMARKS Localized erosion of surface metal

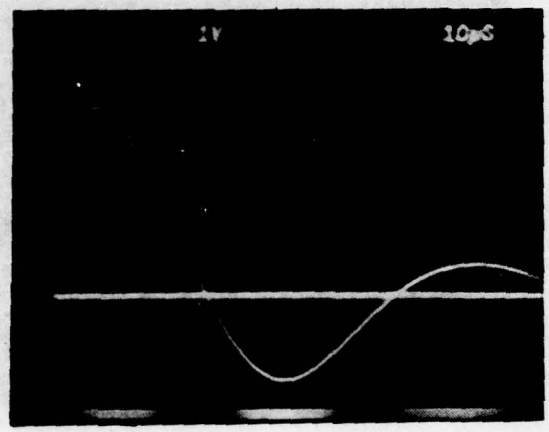

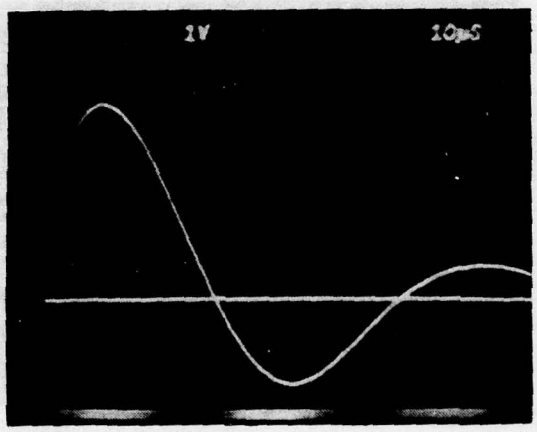

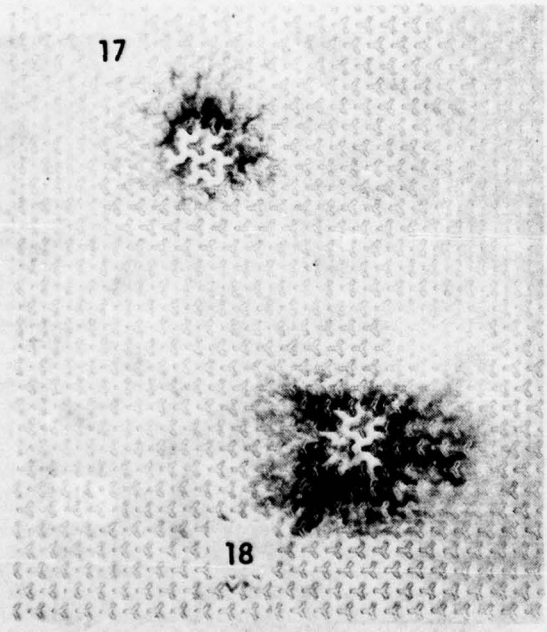

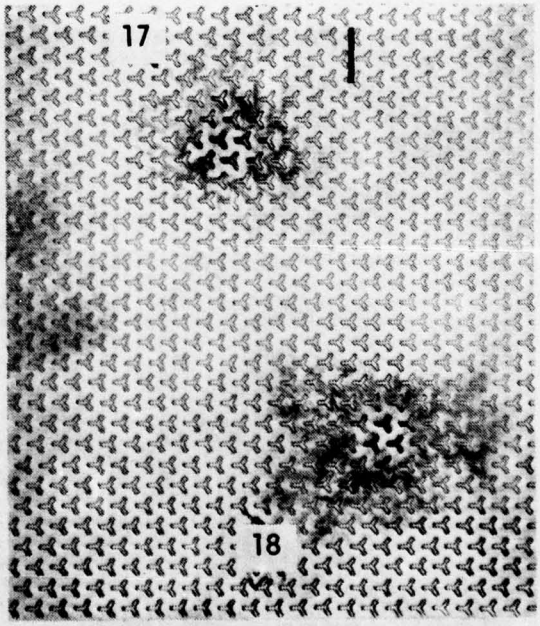

LIGHTNING DAMAGE EVALUATION

TESTED AT MCDONNELL AIRCRAFT COMPANY LIGHTNING SIMULATION FACILITY IN ST. LOUIS, MISSOURI

TEST SETUP MCAIR 600 kilojoule lightning generator
PANEL NUMBER 9
PANEL DESCRIPTION 12 mils Electroplated Cu/No Rain Erosion Coating

TEST NUMBER	19
CURRENT LEVEL	195 kA
DAMAGE TO METAL (~dia)	
METAL REMOVED	Center pieces were removed
METAL DELAMINATED	1.2 in.

TEST NUMBER	20
CURRENT LEVEL	190 kA
DAMAGE TO METAL (~dia)	
METAL REMOVED	Center pieces were removed
METAL DELAMINATED	0.9 in.

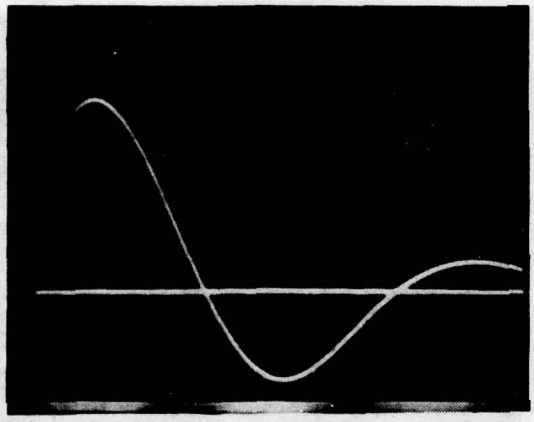

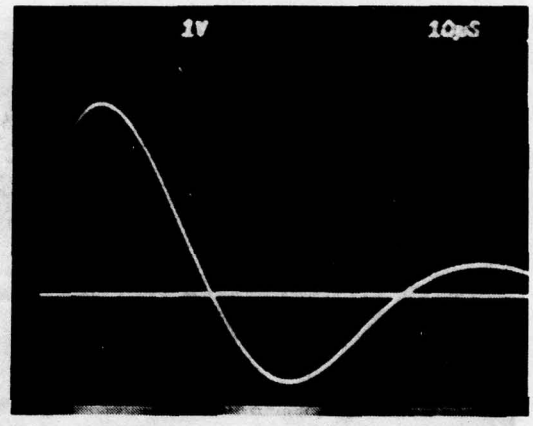

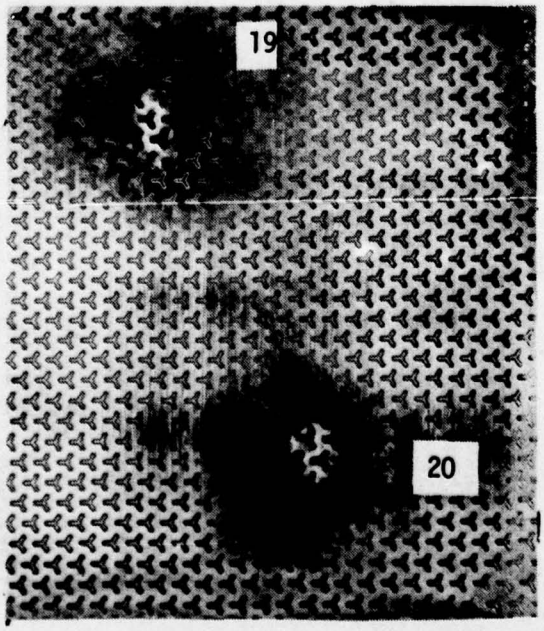

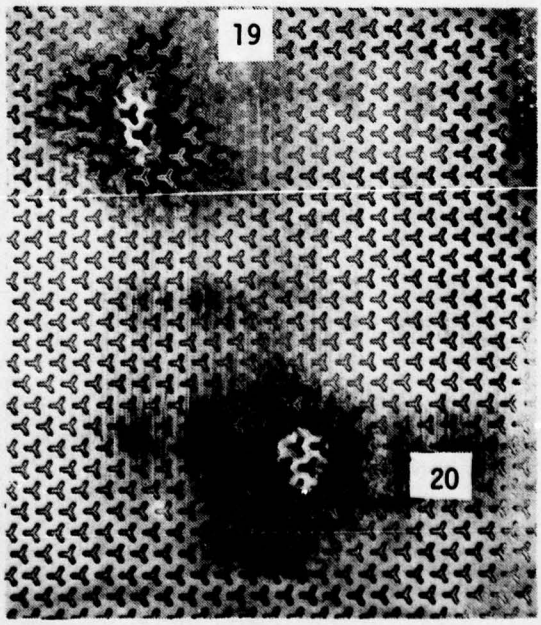

LIGHTNING DAMAGE EVALUATION

TESTED AT MCDONNELL AIRCRAFT COMPANY LIGHTNING SIMULATION FACILITY IN ST. LOUIS, MISSOURI

TEST SETUP	MCAIR 600 kilojoule lightning generator
PANEL NUMBER	#2
PANEL DESCRIPTION	4 mils Electroplated Cu/5 mils MIL-C-83231 Polyurethane

TEST NUMBER 21
CURRENT LEVEL 195 kA
DAMAGE TO EROSION COAT (~dia.) 2.9 in.
DAMAGE TO METAL (~dia)
METAL REMOVED 1.1 in.
METAL DELAMINATED 1.1 in.

TEST NUMBER 22
CURRENT LEVEL 195 kA
DAMAGE TO EROSION COAT (~dia) 2.8 in.
DAMAGE TO METAL (~dia)
METAL REMOVED 1.3 in.
METAL DELAMINATED 1.3 in.

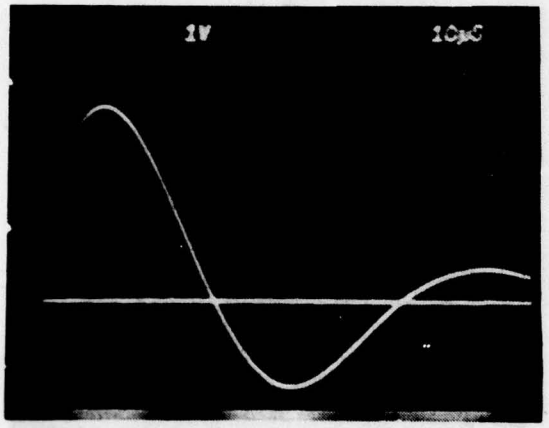

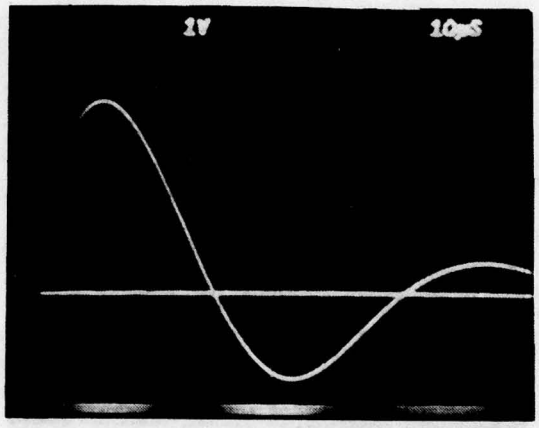

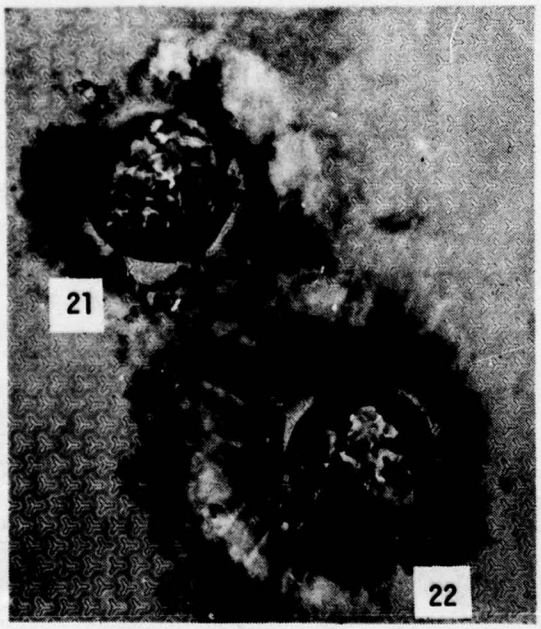

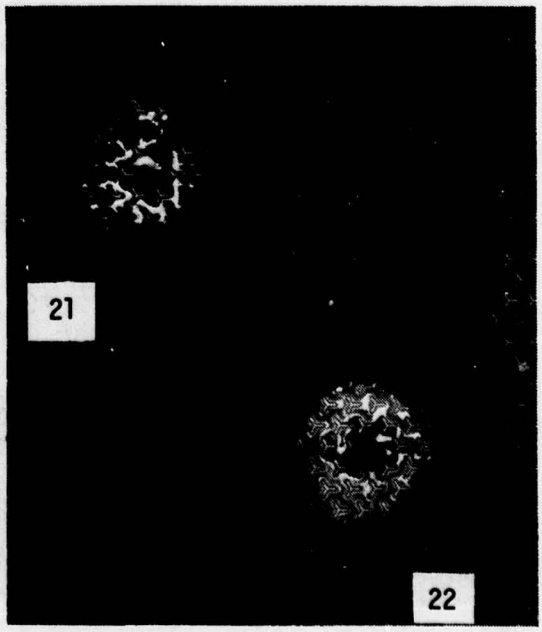

LIGHTNING DAMAGE EVALUATION

TESTED AT MCDONNELL AIRCRAFT COMPANY LIGHTNING SIMULATION FACILITY IN ST. LOUIS, MISSOURI

TEST SETUP MCAIR 600 kilojoule lightning generator
PANEL NUMBER 12
PANEL DESCRIPTION 12 mils Electroplated Ni/No Rain Erosion Coating

TEST NUMBER	23
CURRENT LEVEL	190 kA
DAMAGE TO METAL (∿dia)	
METAL REMOVED	0.0 in.
METAL DELAMINATED	0.0 in.
REMARKS	Minor surface erosion

TEST NUMBER	24
CURRENT LEVEL	195 kA
DAMAGE TO METAL (∿dia)	
METAL REMOVED	0.0 in.
METAL DELAMINATED	0.0 in.
REMARKS	Minor surface erosion

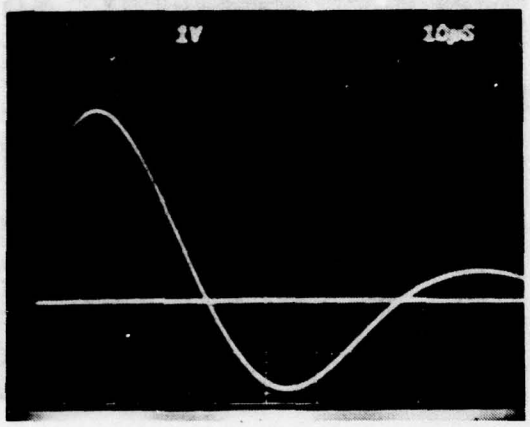

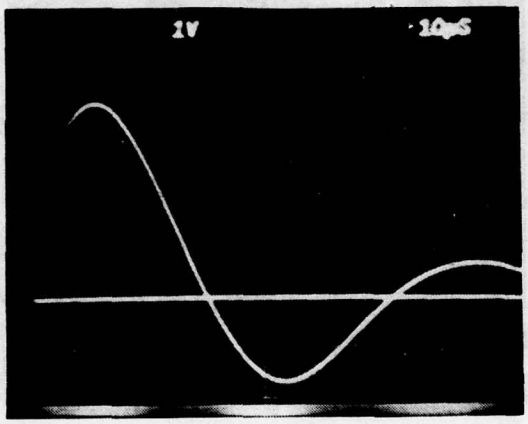

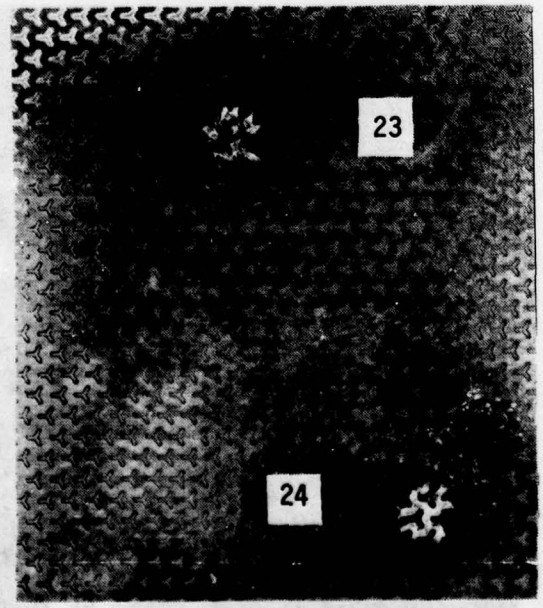

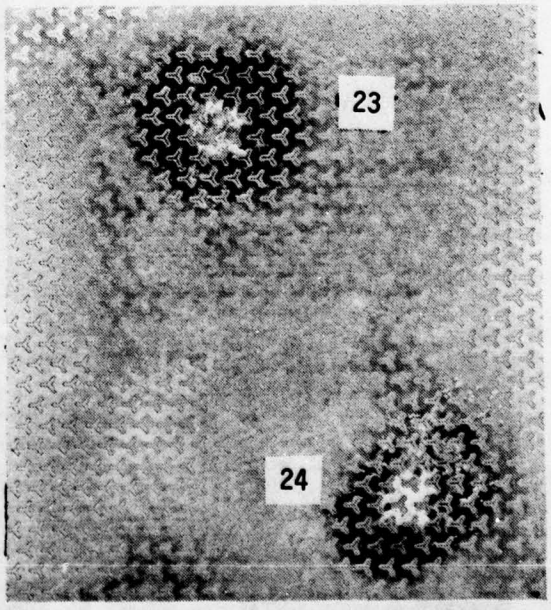

LIGHTNING DAMAGE EVALUATION

TESTED AT MCDONNELL AIRCRAFT COMPANY LIGHTNING SIMULATION FACILITY IN ST. LOUIS, MISSOURI

TEST SETUP MCAIR 600 kilojoule lightning generator
PANEL NUMBER 14
PANEL DESCRIPTION 0.35 mils Electroplated Cu/12 mils MIL-C-83231 Polyurethane

CURRENT LEVEL 200 kA
DAMAGE TO EROSION COAT (~dia) *
DAMAGE TO METAL (~dia)
METAL REMOVED *
METAL DELAMINATED *
REMARKS * Extensive damage to metal along with noticeable edge effects

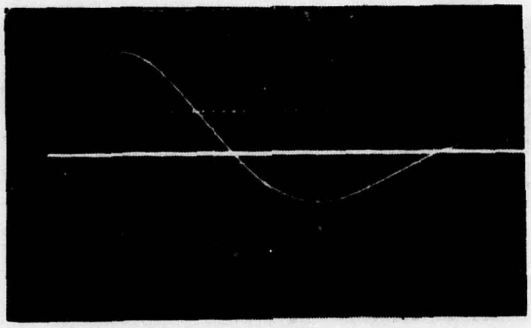

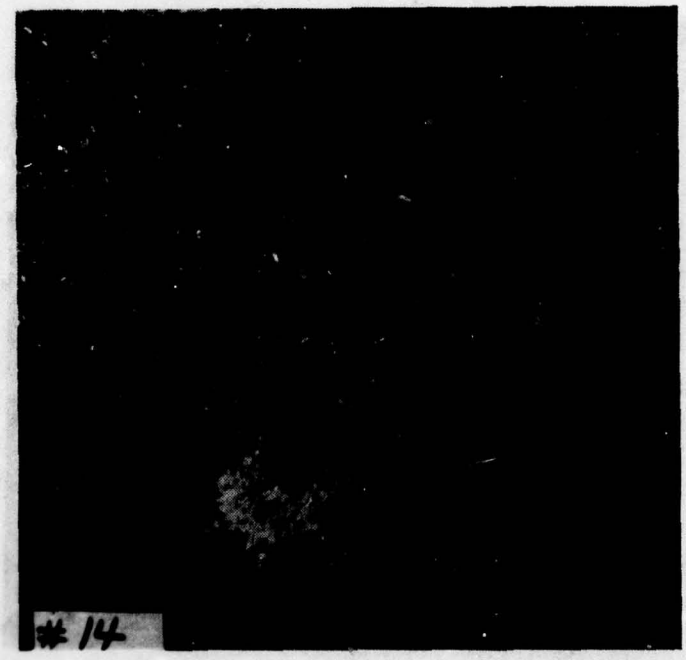

LIGHTNING DAMAGE EVALUATION

TESTED AT MCDONNELL AIRCRAFT COMPANY LIGHTNING SIMULATION FACILITY IN ST. LOUIS, MISSOURI

TEST SETUP MCAIR 600 kilojoule lightning generator
PANEL NUMBER 15
PANEL DESCRIPTION 0.35 mils Electroplated Cu/12 mils MIL-C-83231 Polyurethane

CURRENT LEVEL 200 kA
DAMAGE TO EROSION COAT (~dia) *
DAMAGE TO METAL (~dia)
METAL REMOVED *
METAL DELAMINATED *
REMARKS *Extensive damage to metal along with noticeable edge effects

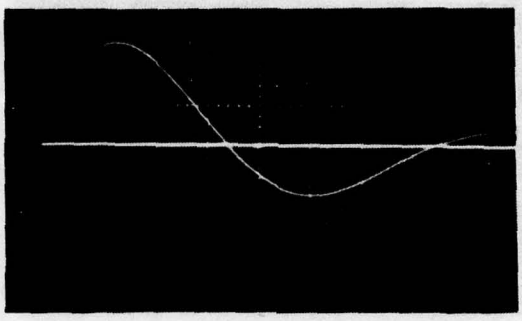

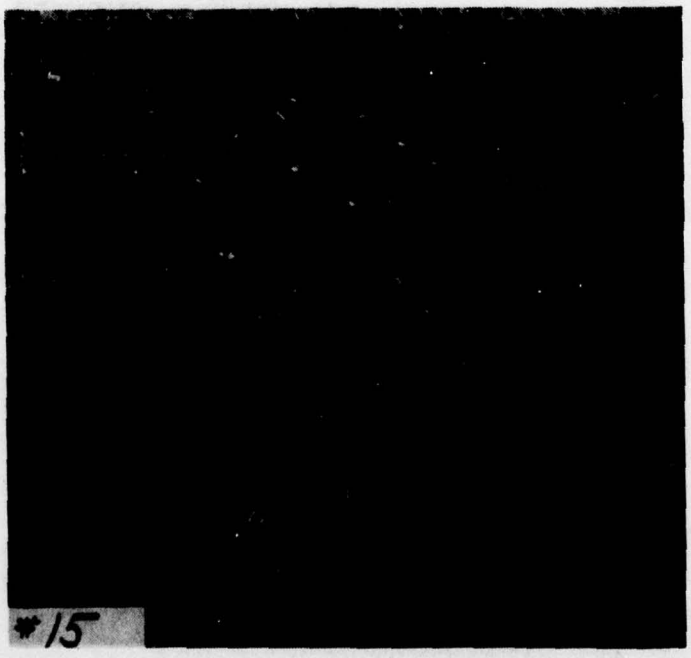

LIGHTNING DAMAGE EVALUATION

TESTED AT MCDONNELL AIRCRAFT COMPANY LIGHTNING SIMULATION FACILITY IN ST. LOUIS, MISSOURI

TEST SETUP MCAIR 600 kilojoule lightning generator
PANEL NUMBER 16
PANEL DESCRIPTION 0.35 mils Electroplated Cu/12 mils MIL-C-83231 Polyurethane

CURRENT LEVEL 205 kA
DAMAGE TO EROSION COAT (~dia) 7.50 in.
DAMAGE TO METAL (~dia)
METAL REMOVED 7.50 in.
METAL DELAMINATED 9.0 in.

REMARKS Slight edge effects

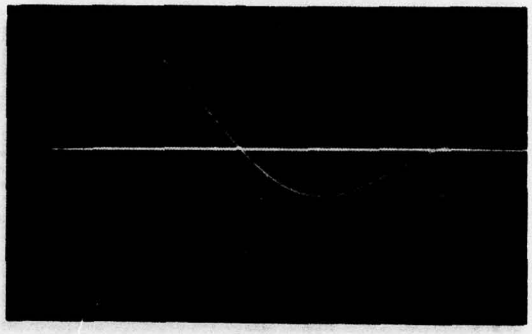

LIGHTNING DAMAGE EVALUATION

TESTED AT MCDONNELL AIRCRAFT COMPANY LIGHTNING SIMULATION FACILITY IN ST. LOUIS, MISSOURI

TEST SETUP MCAIR 600 kilojoule lightning generator
PANEL NUMBER 17
PANEL DESCRIPTION 0.7 mils Electroplated Cu/12 mils MIL-C-83231 Polyurethane

CURRENT LEVEL 200 kA
DAMAGE TO EROSION COAT (~dia) *
DAMAGE TO METAL (~dia)
METAL REMOVED *
METAL DELAMINATED *

REMARKS * Extensive damage to metal along with noticeable edge effects

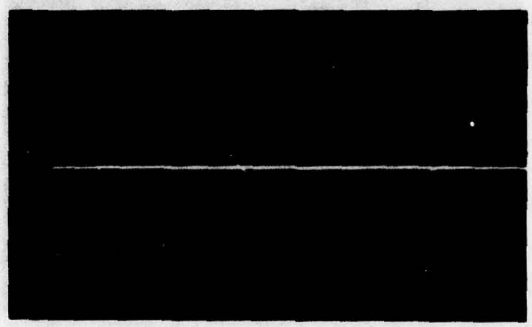

LIGHTNING DAMAGE EVALUATION

TESTED AT MCDONNELL AIRCRAFT COMPANY LIGHTNING SIMULATION FACILITY IN ST. LOUIS, MISSOURI

TEST SETUP MCAIR 600 kilojoule lightning generator
PANEL NUMBER 18
PANEL DESCRIPTION 0.7 mils Electroplated Cu/12 mils MIL-C-83231 Polyurethane

CURRENT LEVEL 205 kA
DAMAGE TO EROSION COAT (~dia) 4.50 in.
DAMAGE TO METAL (~dia)
METAL REMOVED 4.75 in.
METAL DELAMINATED 6.0 in.

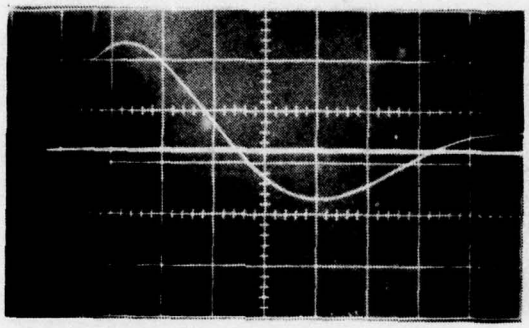

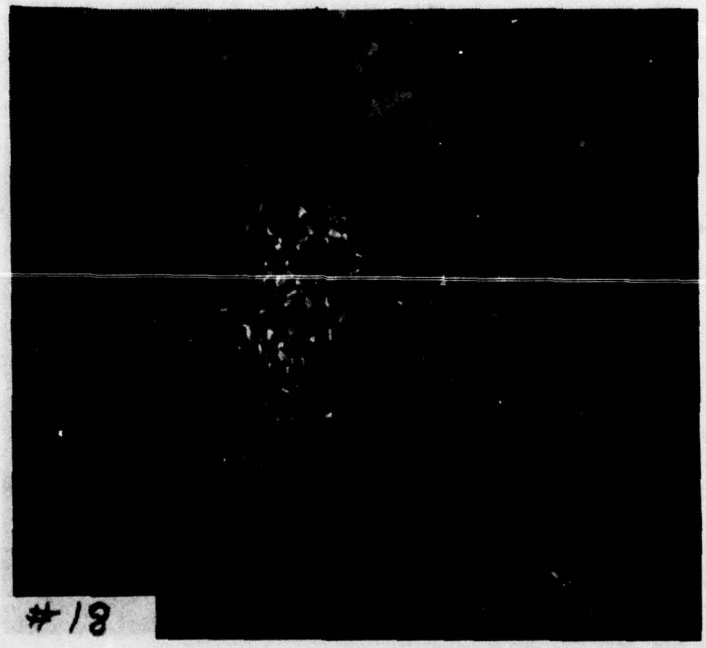

LIGHTNING DAMAGE EVALUATION

TESTED AT MCDONNELL AIRCRAFT COMPANY LIGHTNING SIMULATION FACILITY IN ST. LOUIS, MISSOURI

TEST SETUP MCAIR 600 kilojoule lightning generator
PANEL NUMBER 19
PANEL DESCRIPTION 0.7 mils Electroplated Cu/12 mils MIL-C-83231 Polyurethane

CURRENT LEVEL 200 kA
DAMAGE TO EROSION COAT (~dia) 4.50 in.
DAMAGE TO METAL (~dia)
METAL REMOVED 4.50 in.
METAL DELAMINATED 6.0 in.

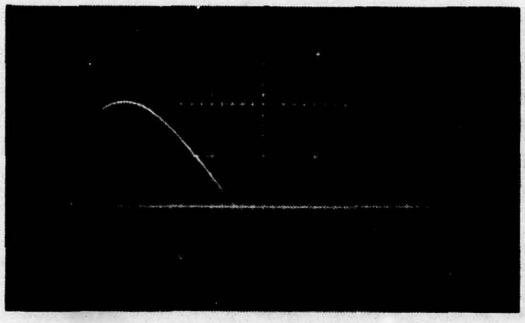

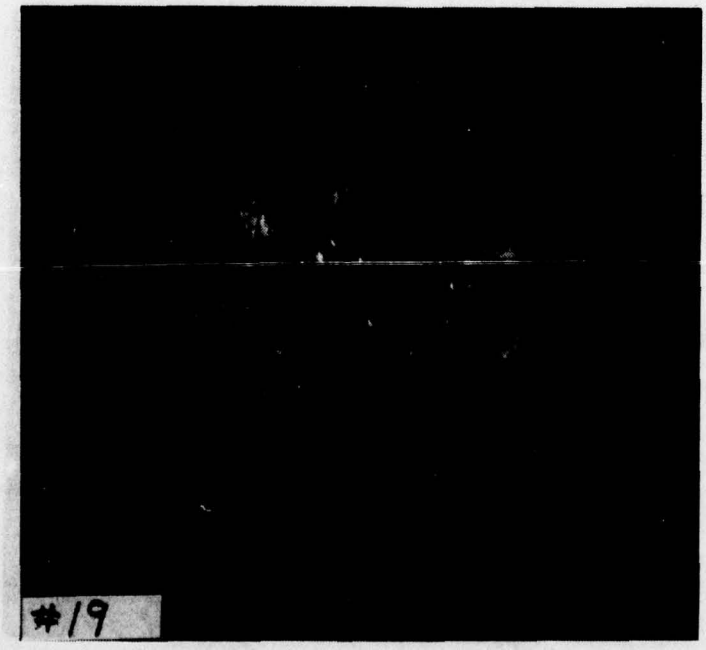

LIGHTNING DAMAGE EVALUATION

TESTED AT MCDONNELL AIRCRAFT COMPANY LIGHTNING SIMULATION FACILITY IN ST. LOUIS, MISSOURI

TEST SETUP MCAIR 600 kilojoule lightning generator
PANEL NUMBER 20
PANEL DESCRIPTION 1.4 mils Electroplated Cu/12 mils MIL-C-83231 Polyurethane

CURRENT LEVEL 200 kA
DAMAGE TO EROSION COAT (~dia) 2.50 in.
DAMAGE TO METAL (~dia)
METAL REMOVED 2.50 in.
METAL DELAMINATED 3.5 in.

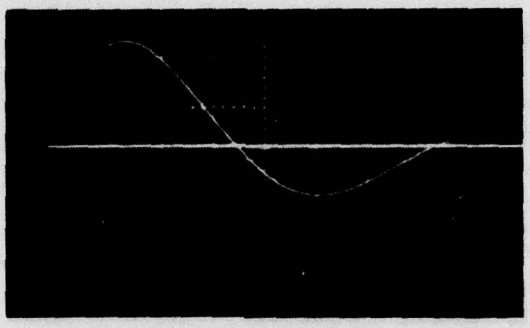

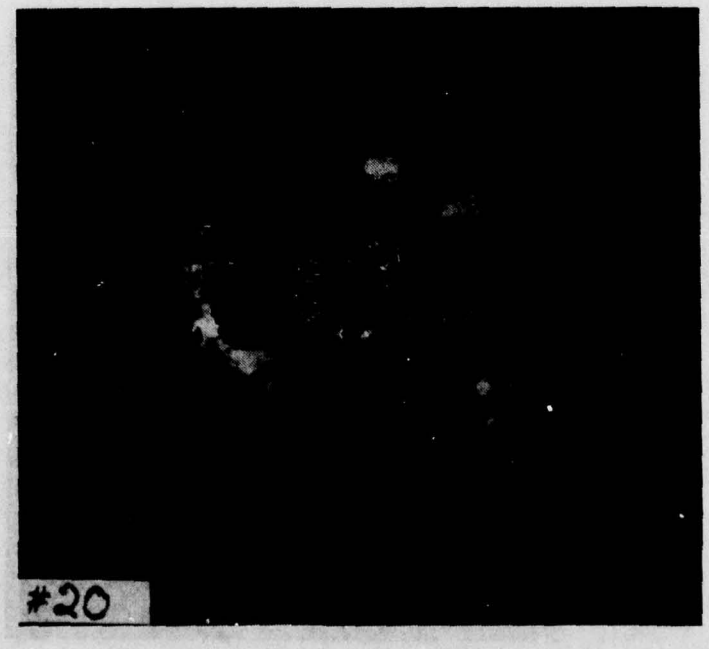

LIGHTNING DAMAGE EVALUATION

TESTED AT MCDONNELL AIRCRAFT COMPANY LIGHTNING SIMULATION FACILITY IN ST. LOUIS, MISSOURI

TEST SETUP MCAIR 600 kilojoule lightning generator
PANEL NUMBER 21
PANEL DESCRIPTION 1.4 mils Electroplated Cu/12 mils MIL-C-83231 Polyurethane

CURRENT LEVEL 200 kA
DAMAGE TO EROSION COAT (∿dia) 2.75 in.
DAMAGE TO METAL (∿dia)
METAL REMOVED 2.75 in.
METAL DELAMINATED 3.25 in.

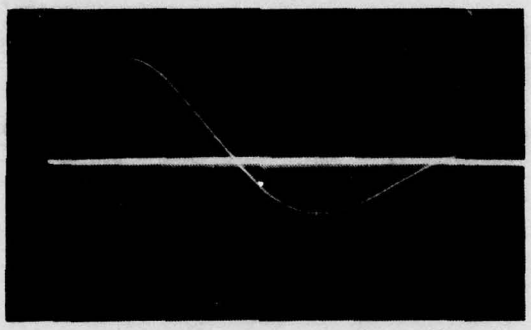

LIGHTNING DAMAGE EVALUATION

TESTED AT MCDONNELL AIRCRAFT COMPANY LIGHTNING SIMULATION FACILITY IN ST. LOUIS, MISSOURI

TEST SETUP MCAIR 600 kilojoule lightning generator
PANEL NUMBER 23
PANEL DESCRIPTION 2.8 mils Electroplated Cu/12 mils MIL-C-83231 Polyurethane

CURRENT LEVEL 200 kA
DAMAGE TO EROSION COAT (~dia) 1.75 in.
DAMAGE TO METAL (~dia)
METAL REMOVED 1.75 in.
METAL DELAMINATED 2.5 in.

LIGHTNING DAMAGE EVALUATION

TESTED AT MCDONNELL AIRCRAFT COMPANY LIGHTNING SIMULATION FACILITY IN ST. LOUIS, MISSOURI

TEST SETUP MCAIR 600 kilojoule lightning generator
PANEL NUMBER 24
PANEL DESCRIPTION 2.8 mils Electroplated Cu/12 mils MIL-C-83231 Polyurethane

CURRENT LEVEL 200 kA
DAMAGE TO EROSION COAT (~dia) 1.50 in.
DAMAGE TO METAL (~dia)
METAL REMOVED 1.50 in.
METAL DELAMINATED 2.5 in.

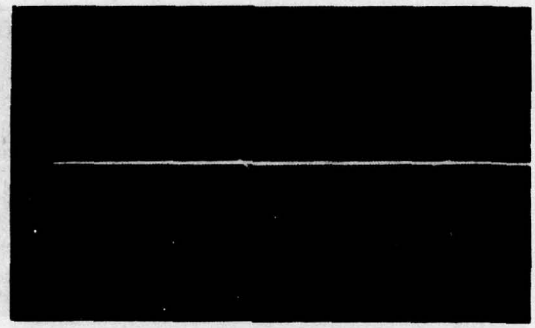

LIGHTNING DAMAGE EVALUATION

TESTED AT MCDONNELL AIRCRAFT COMPANY LIGHTNING SIMULATION FACILITY IN ST. LOUIS, MISSOURI

TEST SETUP MCAIR 600 kilojoule lightning generator
PANEL NUMBER 26
PANEL DESCRIPTION 0.7 mils Electroplated Ni/12 mils MIL-C-83231 Polyurethane

CURRENT LEVEL 200 kA
DAMAGE TO EROSION COAT (~dia) 7.0 in.
DAMAGE TO METAL (~dia)
METAL REMOVED 6.50 in.
METAL DELAMINATED 8.0 in.

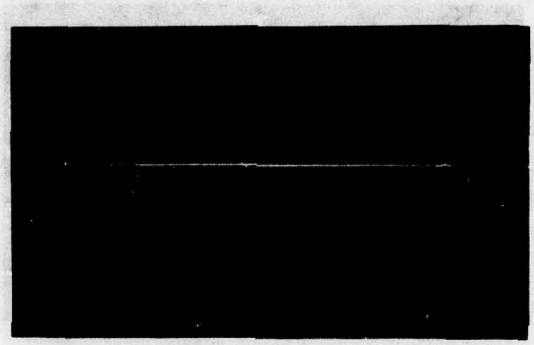

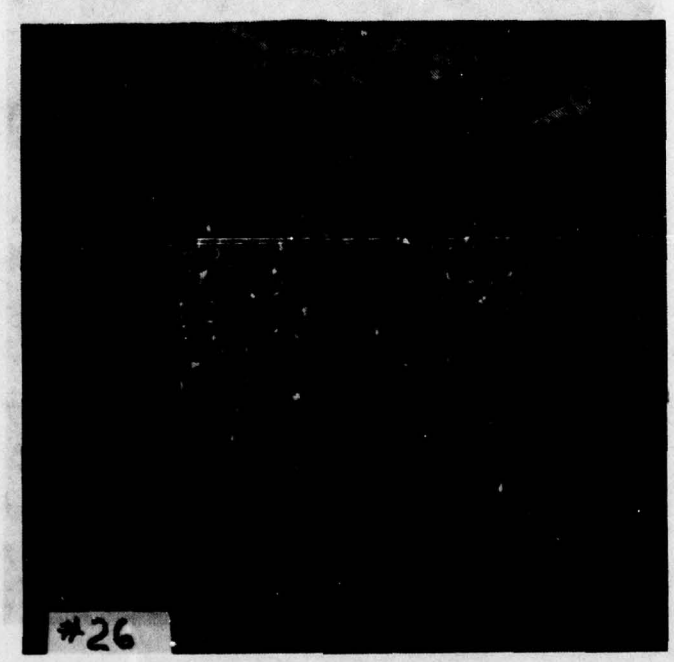

LIGHTNING DAMAGE EVALUATION

TESTED AT MCDONNELL AIRCRAFT COMPANY LIGHTNING SIMULATION FACILITY IN ST. LOUIS, MISSOURI

TEST SETUP MCAIR 600 kilojoule lightning generator
PANEL NUMBER 27
PANEL DESCRIPTION 0.7 mils Electroplated Ni/12 mils MIL-C-83231 Polyurethane

CURRENT LEVEL 200 kA
DAMAGE TO EROSION COAT (~dia) 8.0 in.
DAMAGE TO METAL (~dia)
METAL REMOVED 7.0 in.
METAL DELAMINATED 8.5 in.

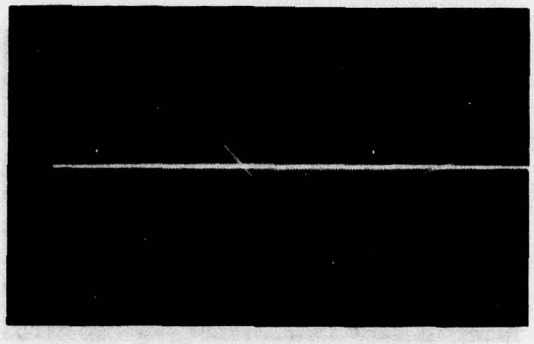

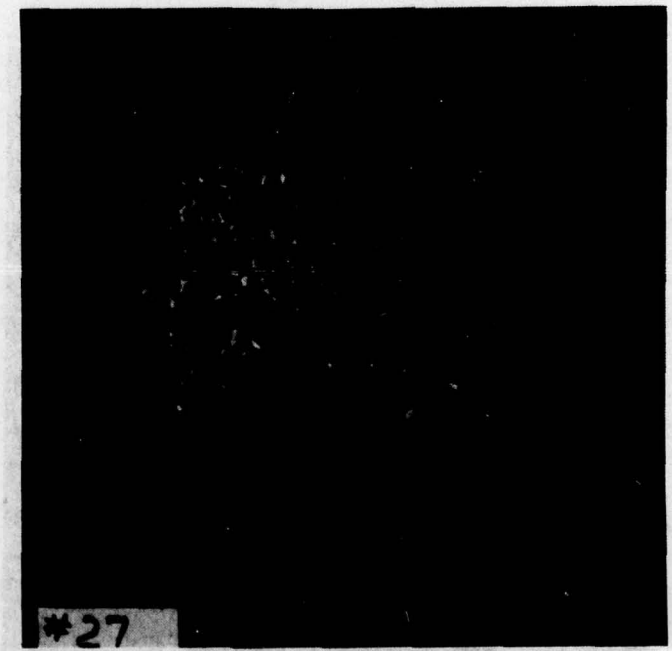

LIGHTNING DAMAGE EVALUATION

TESTED AT MCDONNELL AIRCRAFT COMPANY LIGHTNING SIMULATION FACILITY IN ST. LOUIS, MISSOURI

TEST SETUP MCAIR 600 kilojoule lightning generator
PANEL NUMBER 29
PANEL DESCRIPTION *1.4 mils Electroplated Ni/12 mils MIL-C-8323) Polyurethane*

CURRENT LEVEL 200 kA
DAMAGE TO EROSION COAT (~dia) 7.0 in.
DAMAGE TO METAL (~dia)
METAL REMOVED 6.0 in.
METAL DELAMINATED 7.5 in.

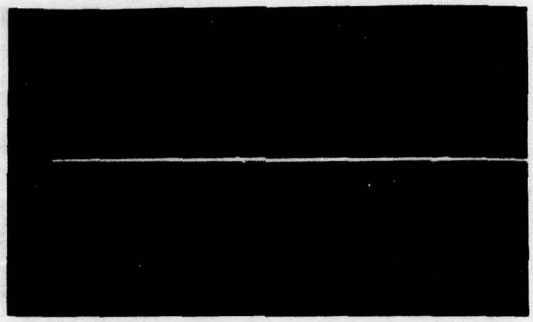

LIGHTNING DAMAGE EVALUATION

TESTED AT MCDONNELL AIRCRAFT COMPANY LIGHTNING SIMULATION FACILITY IN ST. LOUIS, MISSOURI

TEST SETUP MCAIR 600 kilojoule lightning generator
PANEL NUMBER 31
PANEL DESCRIPTION 1.4 mils Electroplated Ni/12 mils MIL-C-83231 Polyurethane

CURRENT LEVEL 200 kA
DAMAGE TO EROSION COAT (~dia) 6.25 in.
DAMAGE TO METAL (~dia)
METAL REMOVED 5.25 in.
METAL DELAMINATED 7.5 in.

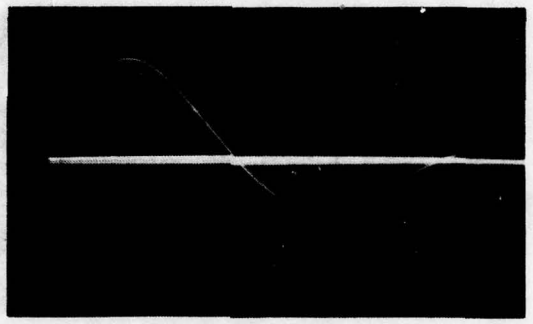

AD-A067 547 MCDONNELL DOUGLAS ASTRONAUTICS CO ST LOUIS MO F/G 17/9
EXPLORATORY DEVELOPMENT OF RESONANT METAL RADOMES.(U)
JUL 78 W R BUSHELLE, L C HOOTS F33615-76-C-5157
UNCLASSIFIED AFML-TR-78-106 NL

3 OF 3
ADA
067547

END
DATE
FILMED
6-79
DDC

LIGHTNING DAMAGE EVALUATION

TESTED AT MCDONNELL AIRCRAFT COMPANY LIGHTNING SIMULATION FACILITY IN ST. LOUIS, MISSOURI

TEST SETUP MCAIR 600 kilojoule lightning generator
PANEL NUMBER 32
PANEL DESCRIPTION 2.8 mils Electroplated Ni/12 mils MIL-C-83231 Polyurethane

CURRENT LEVEL 200 kA
DAMAGE TO EROSION COAT (~dia) 5.0 in.
DAMAGE TO METAL (~dia)
METAL REMOVED 5.0 in.
METAL DELAMINATED 7.0 in .

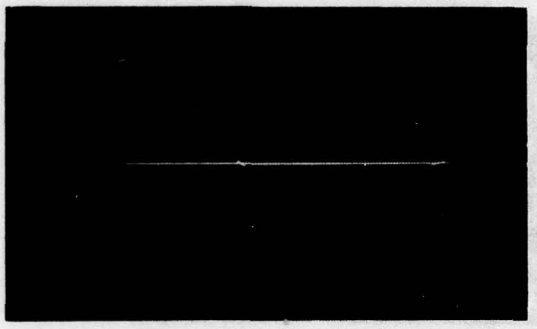

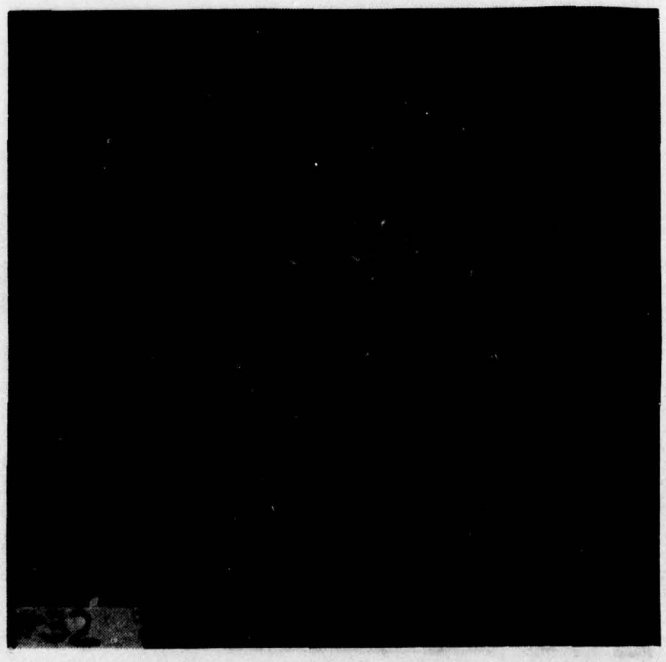

LIGHTNING DAMAGE EVALUATION

TESTED AT MCDONNELL AIRCRAFT COMPANY LIGHTNING SIMULATION FACILITY IN ST. LOUIS, MISSOURI

TEST SETUP MCAIR 600 kilojoule lightning generator
PANEL NUMBER 33
PANEL DESCRIPTION 2.8 mils Electroplated Ni/12 mils MIL-C-83231 Polyurethane

CURRENT LEVEL 200 kA
DAMAGE TO EROSION COAT (~dia) 5.0 in.
DAMAGE TO METAL (~dia)
METAL REMOVED 5.0 in.
METAL DELAMINATED 7.0 in.

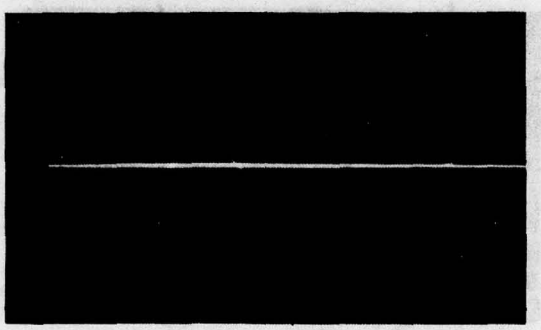

LIGHTNING DAMAGE EVALUATION

TESTED AT MCDONNELL AIRCRAFT COMPANY LIGHTNING SIMULATION FACILITY IN ST. LOUIS, MISSOURI

TEST SETUP	MCAIR 600 kilojoule lightning generator
PANEL NUMBER	#1
PANEL DESCRIPTION	4 mils Electroplated Cu/10 mils MIL-C-83231 Polyurethane

TEST NUMBER #A
CURRENT LEVEL 50 kA
DAMAGE TO EROSION COAT (~dia) 0.6 in.
DAMAGE TO METAL (~dia)
- METAL REMOVED 0.25 in.
- METAL DELAMINATED 0.25 in.

TEST NUMBER #B
CURRENT LEVEL 50 kA
DAMAGE TO EROSION COAT (~dia) 0.9 in.
DAMAGE TO METAL (~dia)
- METAL REMOVED 0.25 in.
- METAL DELAMINATED 0.25 in.

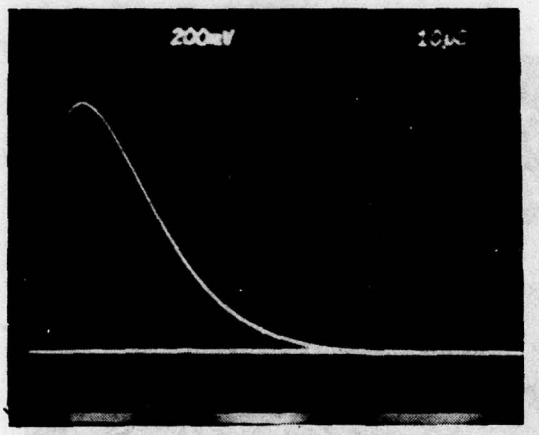

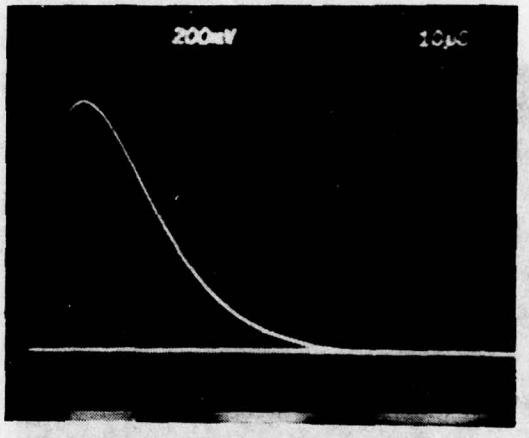

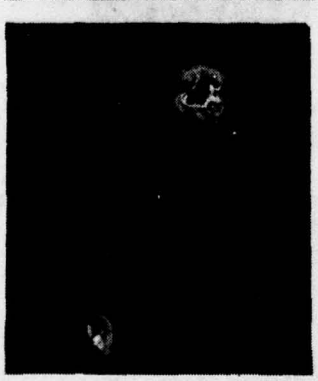

LIGHTNING DAMAGE EVALUATION

TESTED AT MCDONNELL AIRCRAFT COMPANY LIGHTNING SIMULATION FACILITY IN ST. LOUIS, MISSOURI

TEST SETUP MCAIR 600 kilojoule lightning generator
PANEL NUMBER 5
PANEL DESCRIPTION 8 mils Electroplated Cu/7 mils MIL-C-83231 Polyurethane

TEST NUMBER C
CURRENT LEVEL 52 kA
DAMAGE TO EROSION COAT (∿dia) 0.5 in.
DAMAGE TO METAL (∿dia)
METAL REMOVED 0 in.
METAL DELAMINATED Minor erosion

TEST NUMBER D
CURRENT LEVEL 51 kA
DAMAGE TO EROSION COAT (∿dia) 0.5 in.
DAMAGE TO METAL (∿dia)
METAL REMOVED 0 in.
METAL DELAMINATED Minor erosion

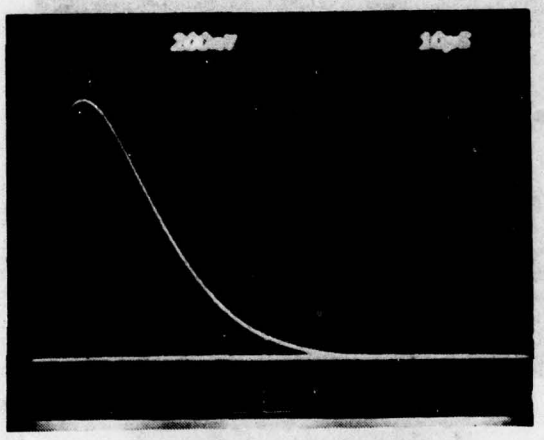

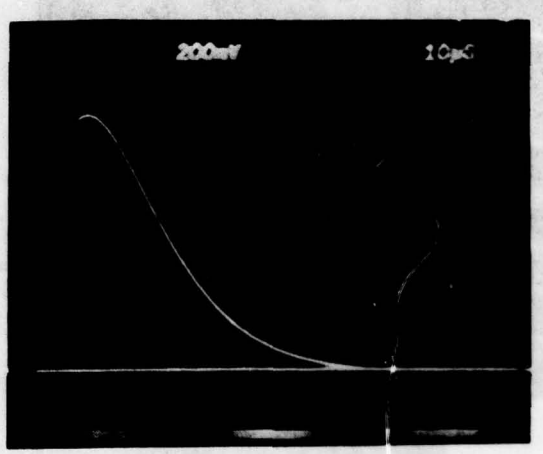

LIGHTNING DAMAGE EVALUATION

TESTED AT MCDONNELL AIRCRAFT COMPANY LIGHTNING SIMULATION FACILITY IN ST. LOUIS, MISSOURI

TEST SETUP 600 kilojoule lightning generator
PANEL NUMBER 3
PANEL DESCRIPTION 4 mils Electroplated Cu/No Rain Erosion Coating

TEST NUMBER	E
CURRENT LEVEL	52 kA
DAMAGE TO METAL (~dia)	
METAL REMOVED	0 in.
METAL DELAMINATED	Very slight

TEST NUMBER	F
CURRENT LEVEL	51 kA
DAMAGE TO METAL (~dia)	
METAL REMOVED	0 in.
METAL DELAMINATED	Very slight

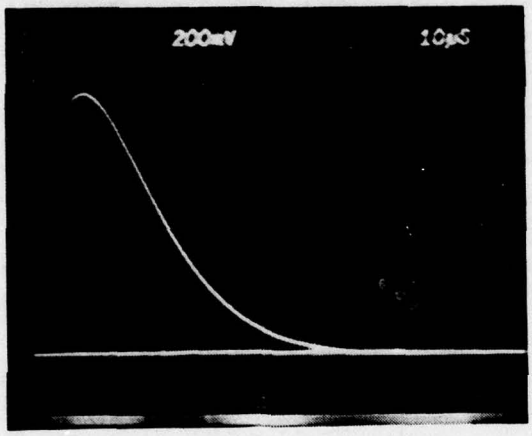

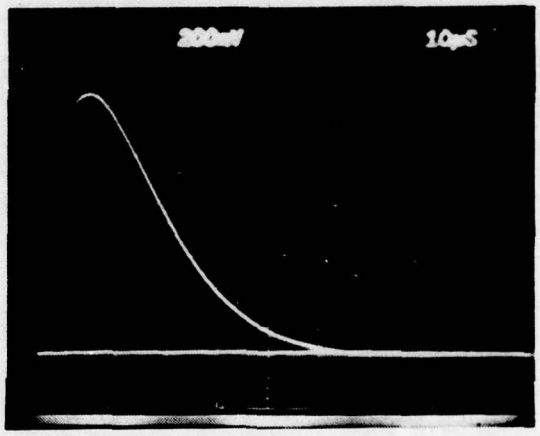

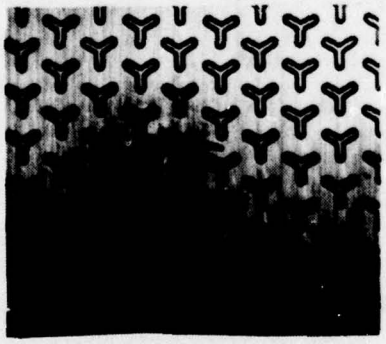

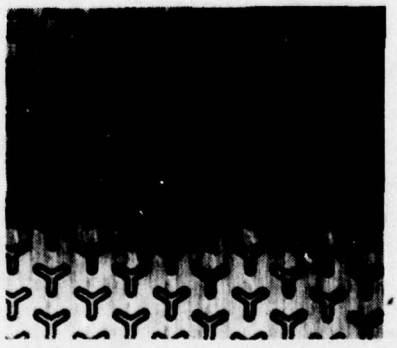

APPENDIX C

RAIN EROSION TEST DATA

These tests were conducted under the direction of G. F. Schmitt at the Air Force Materials Laboratory Whirling Arm Rain Erosion Test Facility, WPAFB, Ohio.

The data is in sequence according to AFML specimen number.

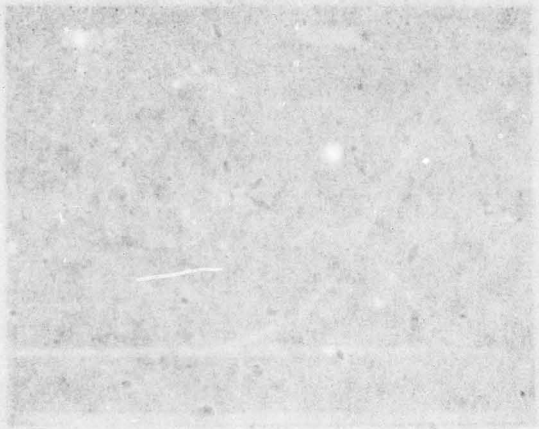

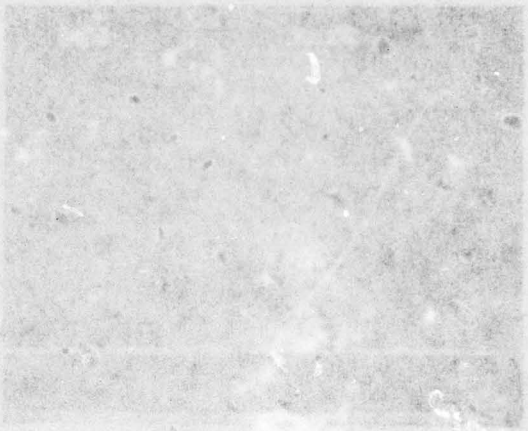

RAIN EROSION EVALUATION

TESTED AT WRIGHT PATTERSON AFB ON AFML WHIRLING ARM RAIN EROSION TEST FACILITY

DATE:	21 December 1976		
SPECIMEN NUMBER	AFML No. 7755 MDAC No. 1		
SPECIMEN DESCRIPTION	8 mils Plated Copper/12 mils MIL-C-83231 Polyurethane		
TEST	AFML Mach 1.2 Rain Erosion Test		
MEAN DROP SIZE	1.8 mm Diameter	TIME TO FAILURE	25.0 min
RAIN RATE	1 in/hr	COMMENTS	Erosion failure
AVERAGE VELOCITY	900 mph		

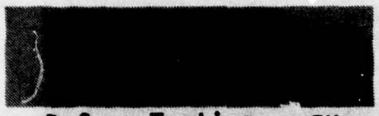

Before Testing .5X

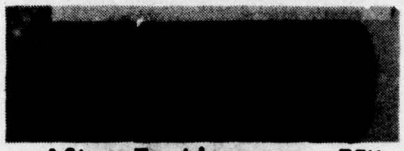

After Testing .75X

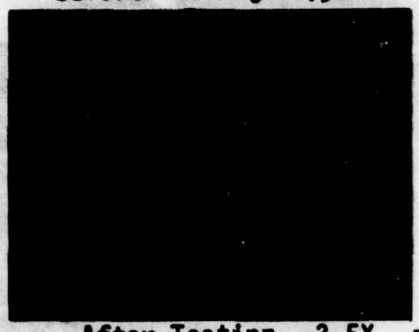

After Testing 2.5X

7755

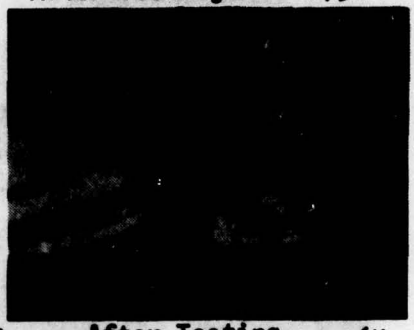

After Testing 6X

RAIN EROSION EVALUATION

TESTED AT WRIGHT PATTERSON AFB ON AFML WHIRLING ARM RAIN EROSION TEST FACILITY

DATE:	21 December 1976		
SPECIMEN NUMBER	AFML No. 7757 MDAC No. 2		
SPECIMEN DESCRIPTION	8 mils Plated Copper/20 mils MIL-C-83231 Polyurethane		
TEST	AFML Mach 1.2 Rain Erosion Test		
MEAN DROP SIZE	1.8 mm Diameter	TIME TO FAILURE	90.0 min
RAIN RATE	1 in/hr	COMMENTS	Erosion failure
AVERAGE VELOCITY	900 mph		

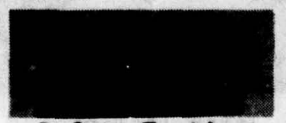

Before Testing .5X

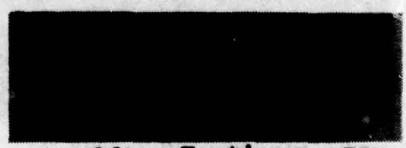

After Testing .75X

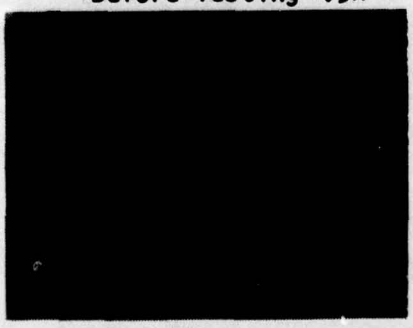

After Testing 2.5X

7757

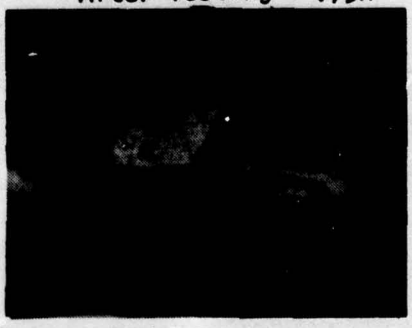

After Testing 6X

RAIN EROSION EVALUATION

TESTED AT WRIGHT PATTERSON AFB ON AFML WHIRLING ARM RAIN EROSION TEST FACILITY

DATE:	21 December 1976		
SPECIMEN NUMBER	AFML No. 7756 MDAC No. 3		
SPECIMEN DESCRIPTION	7 mils Plated Copper/12 mils MIL-C-83231 Polyurethane		
TEST	AFML Mach 1.2 Rain Erosion Test		
MEAN DROP SIZE	1.0 mm Diameter	TIME TO FAILURE	60.0 min
RAIN RATE	1 in/hr	COMMENTS	Erosion Failure
AVERAGE VELOCITY	800 mph		

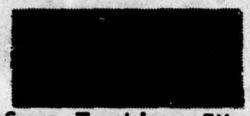

Before Testing .5X

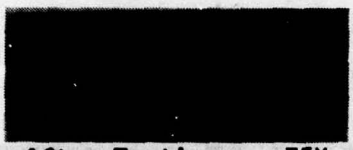

After Testing .75X

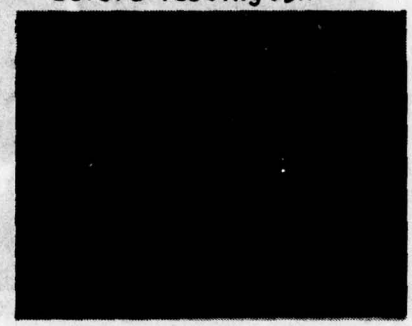

After Testing 2.5X

After Testing 6X

After Testing 6X

7756

After Testing 6X

RAIN EROSION EVALUATION

TESTED AT WRIGHT PATTERSON AFB ON AFML WHIRLING ARM RAIN EROSION TEST FACILITY

DATE:	21 December 1976		
SPECIMEN NUMBER	AFML No. 7758 MDAC No. 4		
SPECIMEN DESCRIPTION	7 mils Plated Copper/30 mils MIL-C-83231 Polyurethane		
TEST	AFML Mach 1.2 Rain Erosion Test		
MEAN DROP SIZE	1.8 mm Diameter	TIME TO FAILURE	75.0 min
RAIN RATE	1 in/hr	COMMENTS	Erosion failure
AVERAGE VELOCITY	800 mph		

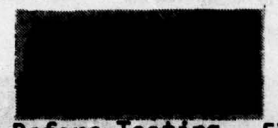

Before Testing .5X

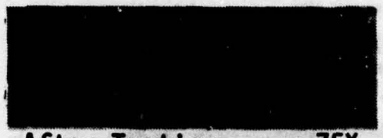

After Testing .75X

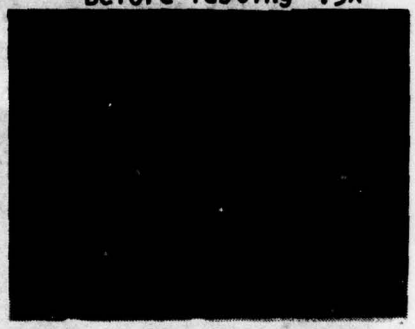

After Testing 2.5X 7758

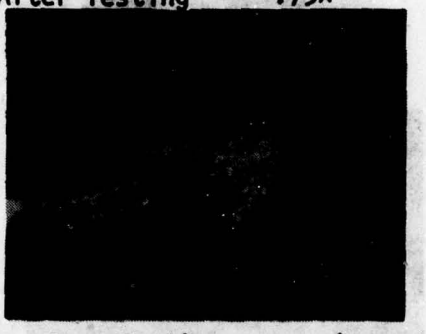

After Testing 6X

RAIN EROSION EVALUATION

TESTED AT WRIGHT PATTERSON AFB ON AFML WHIRLING ARM RAIN EROSION TEST FACILITY

DATE:	21 December 1976		
SPECIMEN NUMBER	AFML No. 7760 MDAC No. 6		
SPECIMEN DESCRIPTION	9 mils Plated Nickel/12 mils MIL-C-83231 Polyurethane		
TEST	AFML Mach 1.2 Rain Erosion Test		
MEAN DROP SIZE	1.8 mm Diameter	TIME TO FAILURE	40.0 min
RAIN RATE	1 in/hr	COMMENTS	Erosion failure
AVERAGE VELOCITY	800 mph		

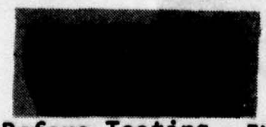

Before Testing .5X

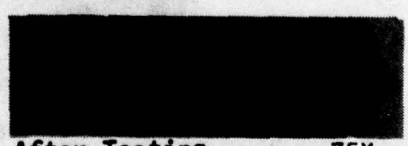

After Testing .75X

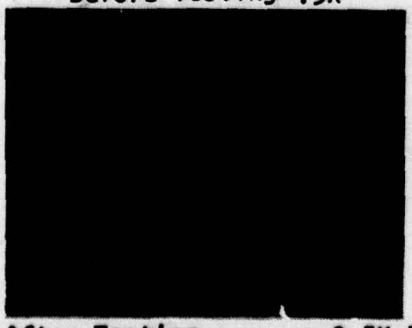

After Testing 2.5X 7760

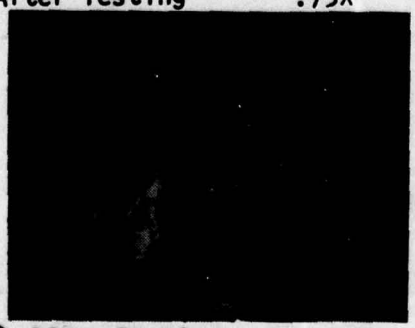

After Testing 6X

RAIN EROSION EVALUATION

TESTED AT WRIGHT PATTERSON AFB ON AFML WHIRLING ARM RAIN EROSION TEST FACILITY

DATE:	21 December 1976		
SPECIMEN NUMBER	AFML No. 7759 MDAC No. 5		
SPECIMEN DESCRIPTION	15 mils Plated Nickel/12 mils MIL-C-83231 Polyurethane		
TEST	AFML Mach 1.2 Rain Erosion Test		
MEAN DROP SIZE	1.0 mm Diameter	TIME TO FAILURE	10.0 min
RAIN RATE	1 in/hr	COMMENTS	Erosion failure
AVERAGE VELOCITY	900 mph		

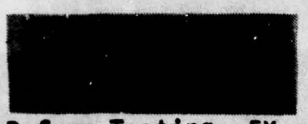

Before Testing .5X

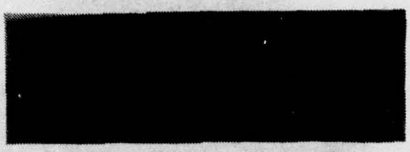

After Testing .75X

After Testing 2.5X

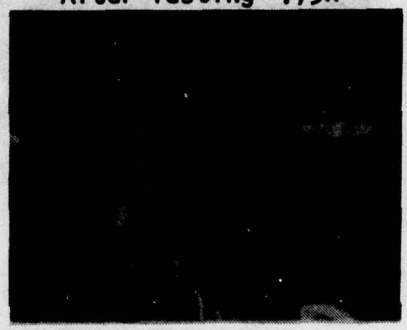

After Testing 6X

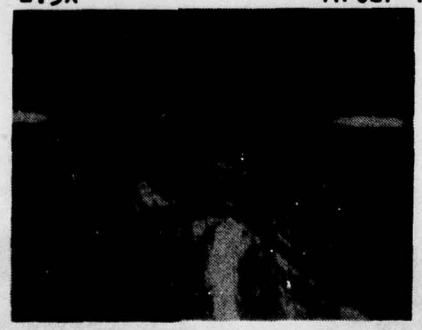

After Testing 6X

7759

RAIN EROSION EVALUATION

TESTED AT WRIGHT PATTERSON AFB ON AFML WHIRLING ARM RAIN EROSION TEST FACILITY

DATE:	21 December 1976		
SPECIMEN NUMBER	AFML No. 7761 MDAC No. 7		
SPECIMEN DESCRIPTION	13 mils Plated Nickel/12 mils MIL-C-83231 Polyurethane		
TEST	AFML Mach 1.2 Rain Erosion Test		
MEAN DROP SIZE	1.8 mm Diameter	TIME TO FAILURE	7.0 min
RAIN RATE	1 in/hr	COMMENTS	Erosion failure
AVERAGE VELOCITY	800 mph		

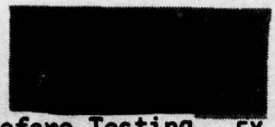

Before Testing .5X

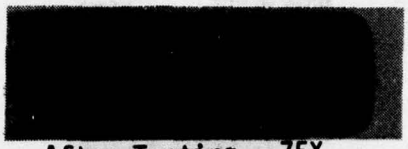

After Testing .75X

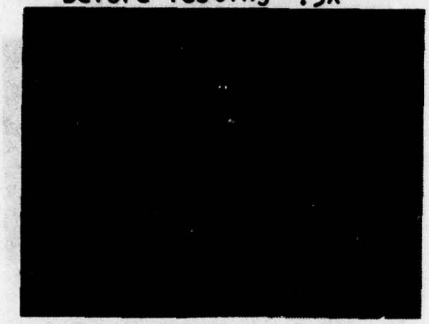

After Testing 2.5X

7761

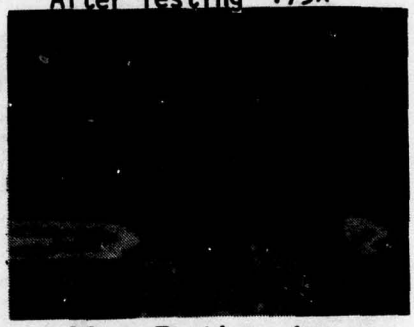

After Testing 6X

RAIN EROSION EVALUATION

TESTED AT WRIGHT PATTERSON AFB ON AFML WHIRLING ARM RAIN EROSION TEST FACILITY

DATE:	21 December 1976		
SPECIMEN NUMBER	AFML No. 7762 MDAC No. 8		
SPECIMEN DESCRIPTION	11 mils Plated Nickel/12 mils MIL-C-83231 Polyurethane		
TEST	AFML Mach 1.2 Rain Erosion Test		
MEAN DROP SIZE	1.8 mm Diameter	TIME TO FAILURE	33.0 min
RAIN RATE	1 in/hr	COMMENTS	Erosion failure
AVERAGE VELOCITY	800 mph		

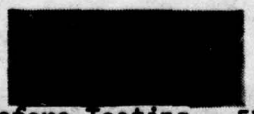

Before Testing .5X

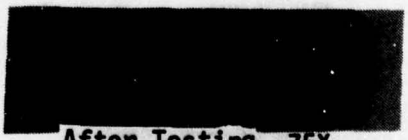

After Testing .75X

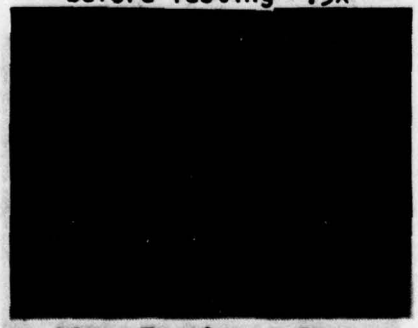

After Testing 2.5X

7762

After Testing 6X

RAIN EROSION EVALUATION

TESTED AT WRIGHT PATTERSON AFB ON AFML WHIRLING ARM RAIN EROSION TEST FACILITY

DATE:	21 December 1976		
SPECIMEN NUMBER	AFML No. 7763 MDAC No. 9		
SPECIMEN DESCRIPTION	10 mils Plated Nickel (no slots)/12 mils MIL-C-83231 Polyurethane		
TEST	AFML Mach 1.2 Rain Erosion Test		
MEAN DROP SIZE	1.8 mm Diameter	TIME TO FAILURE	170.8 min
RAIN RATE	1 in/hr	COMMENTS	Erosion pit
AVERAGE VELOCITY	500 mph		

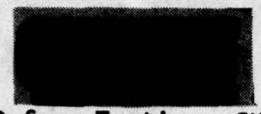

Before Testing .5X

After Testing .75X

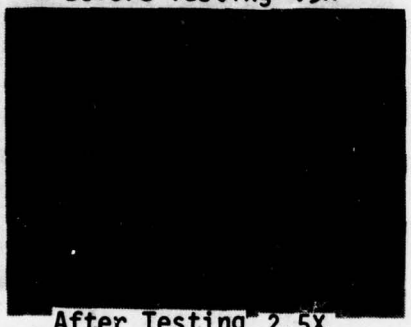

After Testing 2.5X

7763

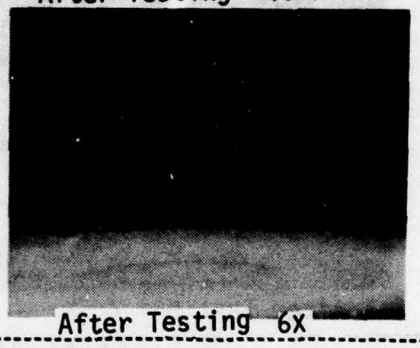

After Testing 6X

RAIN EROSION EVALUATION

TESTED AT WRIGHT PATTERSON AFB ON AFML WHIRLING ARM RAIN EROSION TEST FACILITY

DATE:	21 December 1976		
SPECIMEN NUMBER	AFML No. 7764 MDAC No. 10		
SPECIMEN DESCRIPTION	2 mils Bonded Nickel/12 mils MIL-C-83231 Polyurethane		
TEST	AFML Mach 1.2 Rain Erosion Test		
MEAN DROP SIZE	1.8 mm Diameter	TIME TO FAILURE	87.1 min
RAIN RATE	1 in/hr	COMMENTS	Erosion failure
AVERAGE VELOCITY	800 mph		

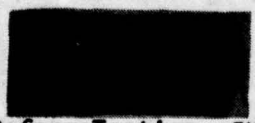

Before Testing .5X

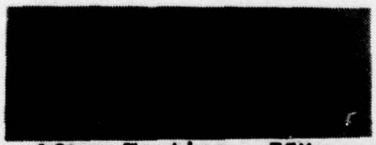

After Testing .75X

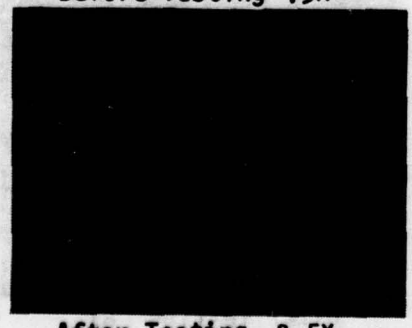

After Testing 2.5X

7764

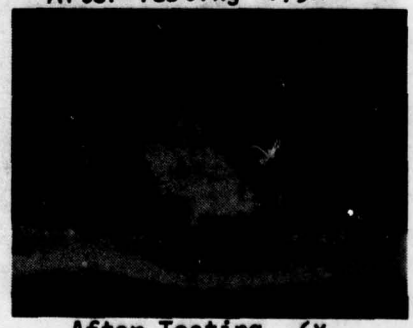

After Testing 6X

RAIN EROSION EVALUATION

TESTED AT WRIGHT PATTERSON AFB ON AFML WHIRLING ARM RAIN EROSION TEST FACILITY

DATE:	21 December 1976		
SPECIMEN NUMBER	AFML No. 7765 MDAC No. 11		
SPECIMEN DESCRIPTION	2 mils Bonded Nickel/12 mils MIL-C-83231 Ployurethane		
TEST	AFML Mach 1.2 Rain Erosion Test		
MEAN DROP SIZE	1.8 mm Diameter	TIME TO FAILURE	83.7 min
RAIN RATE	1 in/hr	COMMENTS	Erosion failure
AVERAGE VELOCITY	800 mph		

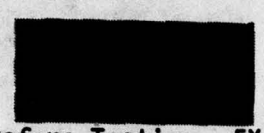

Before Testing .5X

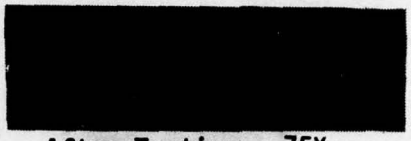

After Testing .75X

After Testing 2.5X

7765

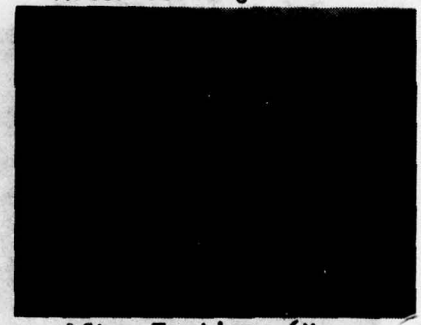

After Testing 6X

RAIN EROSION EVALUATION

TESTED AT WRIGHT PATTERSON AFB ON AFML WHIRLING ARM RAIN EROSION TEST FACILITY

DATE:	21 December 1976		
SPECIMEN NUMBER	AFML No. 7766 MDAC No. 12		
SPECIMEN DESCRIPTION	5 mils Bonded Copper/12 mils MIL-C-83231 Polyurethane		
TEST	AFML Mach 1.2 Rain Erosion Test		
MEAN DROP SIZE	1.8 mm Diameter	TIME TO FAILURE	90.0 min
RAIN RATE	1 in/hr	COMMENTS	Erosion failure
AVERAGE VELOCITY	800 mph		

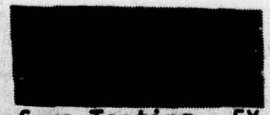

Before Testing .5X

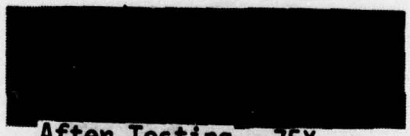

After Testing .75X

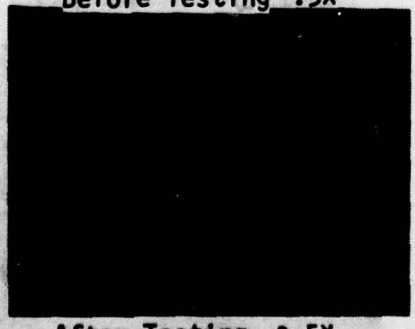

After Testing 2.5X

7766

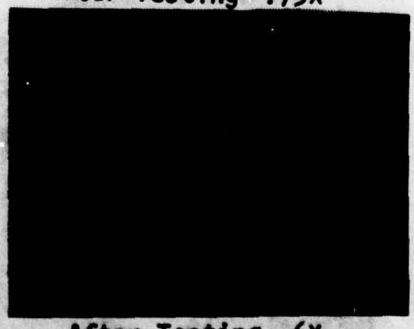

After Testing 6X

RAIN EROSION EVALUATION

TESTED AT WRIGHT PATTERSON AFB ON AFML WHIRLING ARM RAIN EROSION TEST FACILITY

DATE:	21 December 1976		
SPECIMEN NUMBER	AFML No. 7767 MDAC No. 13		
SPECIMEN DESCRIPTION	5 mils Bonded Copper/17 mils MIL-C-83231 Polyurethane		
TEST	AFML Mach 1.2 Rain Erosion Test		
MEAN DROP SIZE	1.8 mm Diameter	TIME TO FAILURE	95.4 min
RAIN RATE	1 in/hr	COMMENTS	Erosion failure
AVERAGE VELOCITY	800 mph		

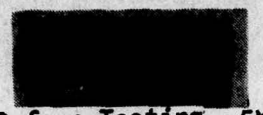

Before Testing .5X

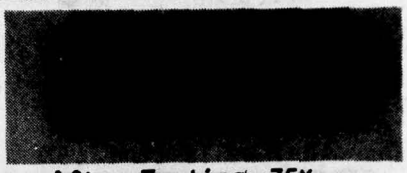

After Testing .75X

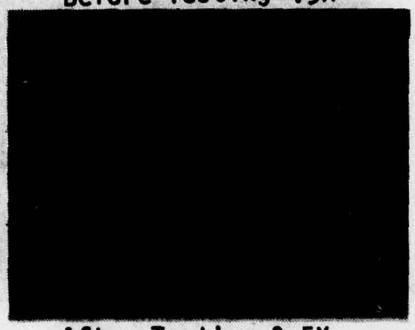

After Testing 2.5X

7767

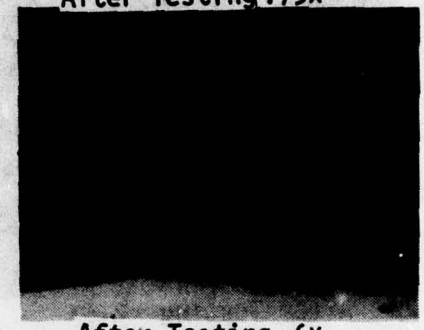

After Testing 6X

RAIN EROSION EVALUATION

TESTED AT WRIGHT PATTERSON AFB ON AFML WHIRLING ARM RAIN EROSION TEST FACILITY

DATE:	21 December 1976		
SPECIMEN NUMBER	AFML No. 7768 MDAC No. 14		
SPECIMEN DESCRIPTION	2 mils Electroformed Nickel (with centerloaded slot)/12 mils MIL-C-83231 Polyurethane		
TEST	AFML Mach 1.2 Rain Erosion Test		
MEAN DROP SIZE	1.8 mm Diameter	TIME TO FAILURE	6.6 min
RAIN RATE	1 in/hr	COMMENTS	Erosion failure
AVERAGE VELOCITY	800 mph		

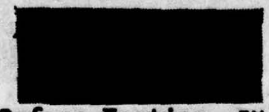

Before Testing .5X

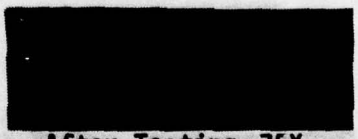

After Testing .75X

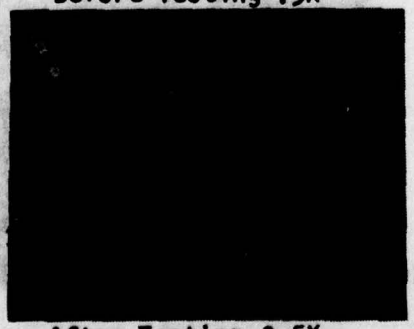

After Testing 2.5X

7768

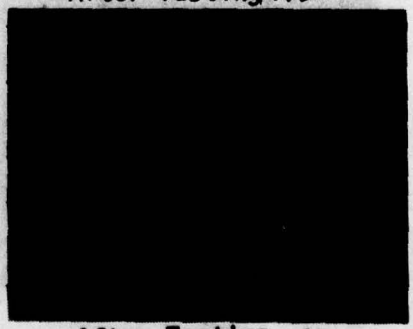

After Testing 6X

RAIN EROSION EVALUATION

TESTED AT WRIGHT PATTERSON AFB ON AFML WHIRLING ARM RAIN EROSION TEST FACILITY

DATE:	21 December 1976		
SPECIMEN NUMBER	AFML No. 7769 NDAC No. 16		
SPECIMEN DESCRIPTION	2 mils Electroformed Nickel (with centerloaded slot)/12 mils MIL-C-83231 Polyurethane		
TEST	AFML Mach 1.2 Rain Erosion Test		
MEAN DROP SIZE	1.8 mm Diameter	TIME TO FAILURE	12.0 min
RAIN RATE	1 in/hr	COMMENTS	Erosion failure
AVERAGE VELOCITY	800 mph		

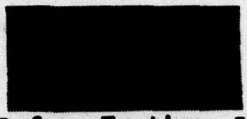

Before Testing .5X

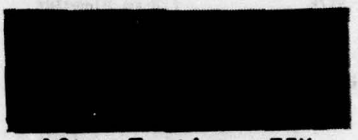

After Testing .75X

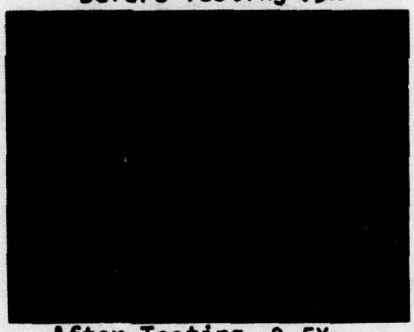

After Testing 2.5X

7769

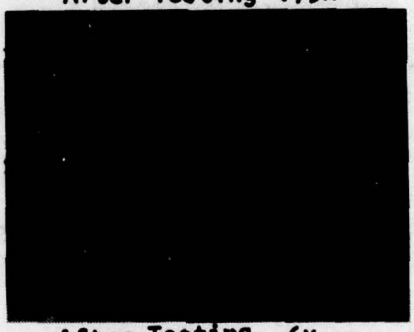

After Testing 6X

RAIN EROSION EVALUATION

TESTED AT WRIGHT PATTERSON AFB ON AFML WHIRLING ARM RAIN EROSION TEST FACILITY

DATE:	11 November 1976		
SPECIMEN NUMBER	AFML No. 7556 MDAC No. 1		
SPECIMEN DESCRIPTION	14 mils Plated Nickel		
TEST	AFML Mach 1.2 Rain Erosion Test		
MEAN DROP SIZE	1.8 mm Diameter	TIME TO FAILURE	5.0 min
RAIN RATE	1 in/hr	COMMENTS	Y-elements gone, Slight laminate erosion.
AVERAGE VELOCITY	500 mph		

RAIN EROSION EVALUATION

TESTED AT WRIGHT PATTERSON AFB ON AFML WHIRLING ARM RAIN EROSION TEST FACILITY

DATE:	11 November 1976		
SPECIMEN NUMBER	AFML No. 7557 MDAC No. 2		
SPECIMEN DESCRIPTION	11 mils Plated Nickel		
TEST	AFML Mach 1.2 Rain Erosion Test		
MEAN DROP SIZE	1.8 mm Diameter	TIME TO FAILURE	5.0 min
RAIN RATE	1 in/hr	COMMENTS	Y-elements gone, Laminate erosion, Layering off of top coat of nickel
AVERAGE VELOCITY	500 mph		

7557

After Testing .96X

7557

After Testing 3.2X

RAIN EROSION EVALUATION

TESTED AT WRIGHT PATTERSON AFB ON AFML WHIRLING ARM RAIN EROSION TEST FACILITY

DATE:	11 November 1976		
SPECIMEN NUMBER	AFML No. 7558 MDAC No. 3		
SPECIMEN DESCRIPTION	12 mils Plated Nickel/12 mils MIL-C-83231 Polyurethane		
TEST	AFML Mach 1.2 Rain Erosion Test		
MEAN DROP SIZE	1.8 mm Diameter	TIME TO FAILURE	5.0 min
RAIN RATE	1 in/hr	COMMENTS	Erosion failure of urethane at Y-element, Metal wire protruding from coating
AVERAGE VELOCITY	500 mph		

7558

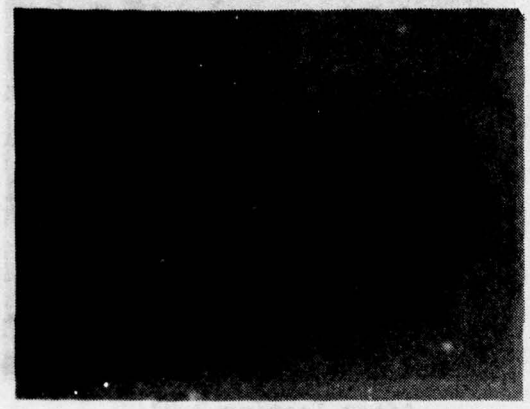

After Testing .96X

7558

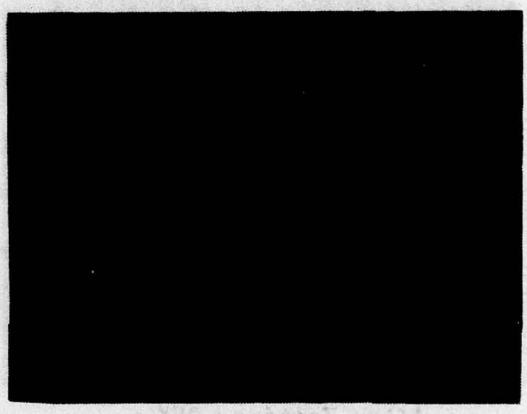

After Testing 3.2X

RAIN EROSION EVALUATION

TESTED AT WRIGHT PATTERSON AFB ON AFML WHIRLING ARM RAIN EROSION TEST FACILITY

DATE:	11 November 1976		
SPECIMEN NUMBER	AFML No. 7559 MDAC No. 4		
SPECIMEN DESCRIPTION	12 mils Plated Nickel/12 mils MIL-C-83231 Polyurethane		
TEST	AFML Mach 1.2 Rain Erosion Test		
MEAN DROP SIZE	1.8 mm Diameter	TIME TO FAILURE	5.0 min
RAIN RATE	1 in/hr	COMMENTS	Erosion failure of urethane at Y-element
AVERAGE VELOCITY	500 mph		

RAIN EROSION EVALUATION

TESTED AT WRIGHT PATTERSON AFB ON AFML WHIRLING ARM RAIN EROSION TEST FACILITY

DATE:	11 November 1976
SPECIMEN NUMBER	AFML No. 7564 MDAC No. 5
SPECIMEN DESCRIPTION	5 mils Bonded Copper/12 mils MIL-C-83231 Polyurethane
TEST	AFML Mach 1.2 Rain Erosion Test
MEAN DROP SIZE	1.8 mm Diameter
RAIN RATE	1 in/hr
AVERAGE VELOCITY	500 mph
TIME TO FAILURE	5.3 min
COMMENTS	Erosion failure of urethane at Y-elements, Copper foil peened beneath coating

7564

After Testing .96X

7564

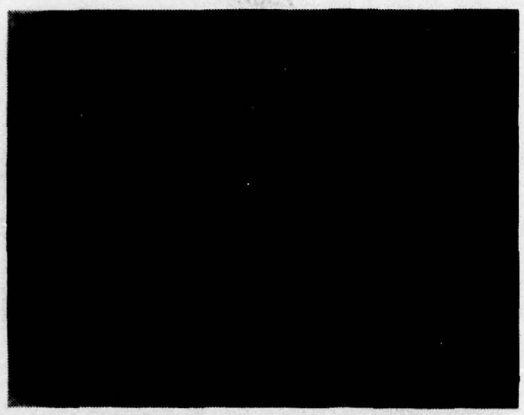

After Testing 3.2X

7564

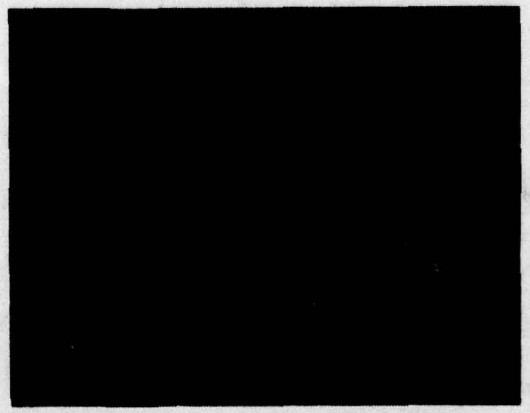

After Testing 3.2X

7564

After Testing 7.7X

7564

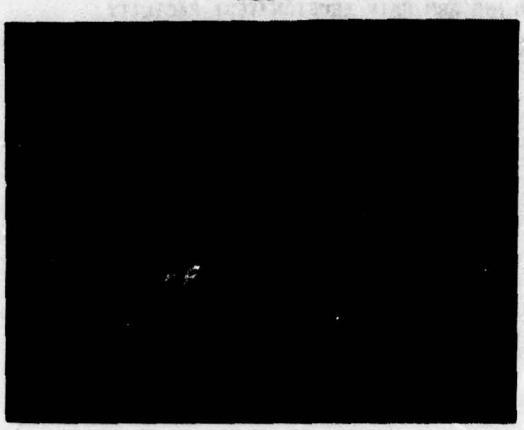

After Testing 7.7X

7564

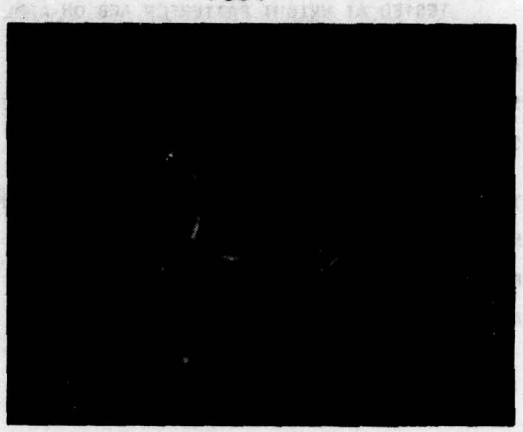

After Testing 9.6X

RAIN EROSION EVALUATION

TESTED AT WRIGHT PATTERSON AFB ON AFML WHIRLING ARM RAIN EROSION TEST FACILITY

DATE:	11 November 1976
SPECIMEN NUMBER	AFML No. 7560 MDAC No. 6
SPECIMEN DESCRIPTION	3 mils Plated Copper/12 mils MIL-C-83231 Polyurethane
TEST	AFML Mach 1.2 Rain Erosion Test
MEAN DROP SIZE	1.8 mm Diameter
RAIN RATE	1 in/hr
AVERAGE VELOCITY	500 mph
TIME TO FAILURE	5.0 min
COMMENTS	Erosion failure initiated at Y-element

RAIN EROSION EVALUATION

TESTED AT WRIGHT PATTERSON AFB ON AFML WHIRLING ARM RAIN EROSION TEST FACILITY

DATE:	11 November 1976		
SPECIMEN NUMBER	AFML No. 7562 MDAC No. 7		
SPECIMEN DESCRIPTION	13 mils Plated Copper		
TEST	AFML Mach 1.2 Rain Erosion Test		
MEAN DROP SIZE	1.8 mm Diameter	TIME TO FAILURE	5.0 min
RAIN RATE	1 in/hr	COMMENTS	Y-elements gone at 2.0 min, Laminate erosion
AVERAGE VELOCITY	500 mph		

RAIN EROSION EVALUATION

TESTED AT WRIGHT PATTERSON AFB ON AFML WHIPLING ARM RAIN EROSION TEST FACILITY

DATE:	11 November 1976		
SPECIMEN NUMBER	AFML No. 7561 MDAC No. 8		
SPECIMEN DESCRIPTION	12 mils Plated Copper/12 mils MIL-C-83231 Polyurethane		
TEST	AFML Mach 1.2 Rain Erosion Test		
MEAN DROP SIZE	1.8 mm Diameter	TIME TO FAILURE	5.0 min
RAIN RATE	1 in/hr	COMMENTS	Erosion failure initiated at Y-element
AVERAGE VELOCITY	500 mph		

7561

After Testing .96X

7561

After Testing 3.2X

RAIN EROSION EVALUATION

TESTED AT WRIGHT PATTERSON AFB ON AFML WHIRLING ARM RAIN EROSION TEST FACILITY

DATE:	11 November 1976
SPECIMEN NUMBER	AFML No. 7563 MDAC No. 9
SPECIMEN DESCRIPTION	8 mils Plated Copper
TEST	AFML Mach 1.2 Rain Erosion Test
MEAN DROP SIZE	1.8 mm Diameter
RAIN RATE	1 in/hr
AVERAGE VELOCITY	500 mph
TIME TO FAILURE	5.0 min
COMMENTS	Y-elements gone at 1.5 min, Laminate erosion, Adhesion loss of copper

7563

After Testing .96X

7563

After Testing 3.2X

RAIN EROSION EVALUATION

TESTED AT WRIGHT PATTERSON AFB ON AFML WHIRLING ARM RAIN EROSION TEST FACILITY

DATE:	11 November 1976
SPECIMEN NUMBER	AFML No. 7565 MDAC No.10
SPECIMEN DESCRIPTION	5 mils Bonded Copper/12 mils MIL-C-83231
TEST	AFML Mach 1.2 Rain Erosion Test
MEAN DROP SIZE	1.8 mm Diameter
RAIN RATE	1 in/hr
AVERAGE VELOCITY	500 mph
TIME TO FAILURE	5.0 min
COMMENTS	No coating failures, Peening of copper beneath

RAIN EROSION EVALUATION

TESTED AT WRIGHT PATTERSON AFB ON AFML WHIRLING ARM RAIN EROSION TEST FACILITY

DATE:	11 November 1976
SPECIMEN NUMBER	AFML No. 7566 MDAC No.11
SPECIMEN DESCRIPTION	5 mils Bonded Copper
TEST	AFML Mach 1.2 Rain Erosion Test
MEAN DROP SIZE	1.8 mm Diameter
RAIN RATE	1 in/hr
AVERAGE VELOCITY	500 mph
TIME TO FAILURE	5.3 min
COMMENTS	Peening of leading edge area, Erosion of slots, Laminate erosion, Incipient adhesion loss

7566

After Testing .96X

7566

After Testing 3.2X

7566

After Testing 3.2X

RAIN EROSION EVALUATION

TESTED AT WRIGHT PATTERSON AFB ON AFML WHIRLING ARM RAIN EROSION TEST FACILITY

DATE:	11 November 1976		
SPECIMEN NUMBER	AFML No. 7567 MDAC No. 12		
SPECIMEN DESCRIPTION	5 mils Bonded Copper		
TEST	AFML Mach 1.2 Rain Erosion Test		
MEAN DROP SIZE	1.8 mm Diameter	**TIME TO FAILURE**	5.0 min
RAIN RATE	1 in/hr	**COMMENTS**	Peening of leading edge area, Erosion of slots, Laminate erosion, Incipient adhesion loss
AVERAGE VELOCITY	500 mph		

REFERENCES

1. Pelton, E. L., "A Streamlined Metallic Radome with High Transmission Performance," Report AFAL-TR-73-100, Air Force Avionics Laboratory, March 1973.

2. Munk, B.A., "Resonant Frequency of Periodic Surfaces for Oblique Incidence," Report 2148-5, Ohio State University, January 1967.

3. Munk, B. A., "The Backscattering from a Tuned Resonant Surface Mode on an Array of Short Loaded Dipoles," Report 2148-6, Ohio State University, March 1967.

4. Mentzer, C. A., "Transmission Properties of Tuned Resonant Windows," Report 2383-8, Ohio State University, January 1969.

5. Munk, B. A., Kouyomjian, R. G., and Peters, L., "Reflection Properties of Periodic Surfaces of Loaded Dipoles," Vol. AP-19, pp 612-617, IEEE Trans. Antennas. Propagat., September 1971.

6. Weaver, J. H., "Nickel Electroplated Non-Conductive Materials for Rain Erosion Protection," Report AFML-TR-66-398, Air Force Materials Laboratory, May 1968.

7. Shenk, R. F., "Photoforming Thin Metal Plates," Metal Progress, March 1971.

8. Mock, J. A., "Take a Look at Vacuum Metallizing for Low Cost Bright Metallic Finishes," Vol. 87, No. 4, Materials Engineering, April 1978.

9. Schulte, E. H. and Clifford, D. W., "Experimental Evaluation of Lightning Protective Coatings for Boron/Epoxy Composites," Third National Technical Conference, Society of Aerospace Material and Process Engineers, Huntsville, AL, 5-7 Oct 1971.

10. Clifford, D. W., "Lightning Simulation Testing of Composites," presented at the 22nd Annual Meeting of the Institute of Environmental Sciences, Philadelphia, PA, 25-28 April 1976.

11. Weaver, J. H., "Electroplated Nickel Rain Erosion Resistant Coating," Report AFML-TR-67-358, Air Force Materials Laboratory, January 1968.

12. Schmitt, G. F., "Materials Parameters that Govern the Rain Erosion Behavior of Polymeric Coatings and Composites at Subsonic Velocities," Report AFML-TR-71-197, Air Force Materials Laboratory, December 1971.

13. Technical Proposal, "Exploratory Development of Resonant Metal Radomes," Report 1457, Vol. I, McDonnell Douglas Corporation, March 1976.

14. Munsell, M. B. and Clifford, D. W., "RF Measurements of Electrostatic Discharges Produced by Triboelectric Charging of Nonmetallic Structure," presented at the 1977 IEEE International Symposium of Electromagnetic Compatibility, Seattle, Washington, 2-4 August 1977.

15. Kornbau, T. W. and Munk, M. A., "Design of a Metallized Radome for the C-140 Aircraft," Report 4346-4, Ohio State University, August 1977.

16. Munk, B. A., Luebbers, R. J., and Fulton, R. D., "Transmission through a Two-Layer Array of Loaded Slots," Vol. AP, IEEE Transactions on Antennas and Propagation, November 1974.

17. Munk, B. A. and Kornbau, T. W., "Mono-Planar Arrays of Generalized Three-Legged Elements in a Stratified Dielectric Medium," AFAL-TR-78-43, Air Force Avionics Laboratory, May 1978.

GLOSSARY

Azimuth - An arc in the horizontal plane, measured in degrees.

Dielectric Constant - As used in this work this is actually the relative dielectric constant, which is the ratio of the absolute dielectric constant of a material to that of a vacuum. It is a measure of a material's ability to store energy, or its inductive capacity.

Fineness Ratio - In the case of a radome, it is the ratio of length to base diameter.

Incidence Angle - The angle between the normal radome wall (at a point of impingement of a ray) and the incident plane.

Mil - A unit of length equal to 1/1000 of an inch (0.001 in.).

Parallel Polarization - When the angle between the electric field (E) vector and the incident plant is 0° or parallel ($\theta_{\parallel}$ Pol.).

Perpendicular Polarization - When the angle between the electric field (E) vector and the incident plane is 90°, or perpendicular ($\theta_{\perp}$Pol.).

Polarizing Angle - The angle between the electric field (E) vector and the incident plane.

Prepreg - In plastics fabrication, a material consisting of an uncured resin impregnated on a reinforcement carrier, such as polyimide precursor on quartz or glass fabric.

Transmission Efficiency - A relative number determined by the ratio of energy transmitted through a radome to the incident energy, usually expressed in % power.

*U.S.Government Printing Office: 1979 — 657-002/468